

T.C.
HACETTEPE UNIVERSITY
INSTITUTE OF HEALTH SCIENCES

**SELECTION AND CHARACTERIZATION OF IMMUNE-
RESISTANT ACUTE MYELOID LEUKEMIA CELLS**

Ph.D. Mubaida PARVEEN

Tumor Biology and Immunology Program
DOCTOR OF PHILOSOPHY (PH.D.) THESIS

ANKARA

2024

T.C.
HACETTEPE UNIVERSITY
INSTITUTE OF HEALTH SCIENCES

**SELECTION AND CHARACTERIZATION OF IMMUNE-
RESISTANT ACUTE MYELOID LEUKEMIA CELLS**

Ph.D. Mubaida PARVEEN

Tumor Biology and Immunology Program
DOCTOR OF PHILOSOPHY (PH.D.) THESIS

THESIS SUPERVISOR
Prof. Dr. Güneş ESENDAĞLI

ANKARA

2024

**SELECTION AND CHARACTERIZATION OF IMMUNE RESISTANT
ACUTE MYELOID LEUKEMIA CELLS**

Mubaida Parveen

Supervisor: Prof. Dr. Güneş Esendağlı

This thesis study has been approved and accepted as a Ph.D dissertation in “Tumor Biology and Immunology Program by the assesment committee, whose members are listed below, on 18.01.2023.

- Chairman of the
Committee:** *Prof. Dr. Ayşegül Üner
Hacettepe University, Faculty of Medicine*
- Member:** *Assoc. Prof. Dr. Zihni Ekim Taşkıran
Hacettepe University, Faculty of Medicine*
- Member:** *Assoc. Prof. Dr. Neşe Ünver
Hacettepe University, Cancer Institute*
- Member:** *Assist. Prof. Dr. Serkan Belkaya
Ihsan Doğramacı Bilkent University, Ankara*
- Member:** *Assist. Prof. Dr. Diğdem Yöyen Ermiş
Bursa Uludağ University, Faculty of
Medicine*

1.3 Subat 2024

This dissertation has been approved by the above committee in conformity to the related issues of Hacettepe University Graduate Education and Examination Regulation.

Prof. Müge YEMİŞCİ ÖZKAN, MD, PhD

Director

YAYIMLAMA VE FİKRİ MÜLKİYET HAKLARI BEYANI

Enstitü tarafından onaylanan lisansüstü tezimin/raporumun tamamını veya herhangi bir kısmını, basılı (kağıt) ve elektronik formatta arşivleme ve aşağıda verilen koşullarla kullanıma açma iznini Hacettepe Üniversitesine verdiğimi bildiririm. Bu izinle Üniversiteye verilen kullanım hakları dışındaki tüm fikri mülkiyet haklarım bende kalacak, tezimin tamamının ya da bir bölümünün gelecekteki çalışmalarda (makale, kitap, lisans ve patent vb.) kullanım hakları bana ait olacaktır.

Tezin kendi orijinal çalışmam olduğunu, başkalarının haklarını ihlal etmediğimi ve tezimin tek yetkili sahibi olduğumu beyan ve taahhüt ederim. Tezimde yer alan telif hakkı bulunan ve sahiplerinden yazılı izin alınarak kullanılması zorunlu metinlerin yazılı izin alınarak kullandığımı ve istenildiğinde suretlerini Üniversiteye teslim etmeyi taahhüt ederim.

Yükseköğretim Kurulu tarafından yayınlanan **“Lisansüstü Tezlerin Elektronik Ortamda Toplanması, Düzenlenmesi ve Erişime Açılmasına İlişkin Yönerge”** kapsamında tezim aşağıda belirtilen koşullar haricince YÖK Ulusal Tez Merkezi / H.Ü. Kütüphaneleri Açık Erişim Sisteminde erişime açılır.

- Enstitü / Fakülte yönetim kurulu kararı ile tezimin erişime açılması mezuniyet tarihimden itibaren 2 yıl ertelenmiştir. ⁽¹⁾
- Enstitü / Fakülte yönetim kurulunun gerekçeli kararı ile tezimin erişime açılması mezuniyet tarihimden itibaren 6 ay ertelenmiştir. ⁽²⁾
- Tezimle ilgili gizlilik kararı verilmiştir. ⁽³⁾

18/01/2023

Mubaida PARVEEN

1

¹“Lisansüstü Tezlerin Elektronik Ortamda Toplanması, Düzenlenmesi ve Erişime Açılmasına İlişkin Yönerge”

- (1) Madde 6. 1. Lisansüstü teze ilgili patent başvurusu yapılması veya patent alma sürecinin devam etmesi durumunda, tez danışmanının önerisi ve enstitü anabilim dalının uygun görüşü üzerine enstitü veya fakülte yönetim kurulu iki yıl süre ile tezin erişime açılmasının ertelenmesine karar verebilir.
- (2) Madde 6. 2. Yeni teknik, materyal ve metotların kullanıldığı, henüz makaleye dönüşmemiş veya patent gibi yöntemlerle korunmamış ve internetten paylaşılması durumunda 3. şahıslara veya kurumlara haksız kazanç imkanı oluşturabilecek bilgi ve bulguları içeren tezler hakkında tez danışmanının önerisi ve enstitü anabilim dalının uygun görüşü üzerine enstitü veya fakülte yönetim kurulunun gerekçeli kararı ile altı ayı aşmamak üzere tezin erişime açılması engellenebilir.
- (3) Madde 7. 1. Ulusal çıkarları veya güvenliği ilgilendiren, emniyet, istihbarat, savunma ve güvenlik, sağlık vb. konulara ilişkin lisansüstü tezlerle ilgili gizlilik kararı, tezin yapıldığı kurum tarafından verilir *. Kurum ve kuruluşlarla yapılan işbirliği protokolü çerçevesinde hazırlanan lisansüstü tezlere ilişkin gizlilik kararı ise, ilgili kurum ve kuruluşun önerisi ile enstitü veya fakültenin uygun görüşü üzerine üniversite yönetim kurulu tarafından verilir. Gizlilik kararı verilen tezler Yükseköğretim Kuruluna bildirilir.
Madde 7.2. Gizlilik kararı verilen tezler gizlilik süresince enstitü veya fakülte tarafından gizlilik kuralları çerçevesinde muhafaza edilir, gizlilik kararının kaldırılması halinde Tez Otomasyon Sistemine yüklenir
* Tez danışmanının önerisi ve enstitü anabilim dalının uygun görüşü üzerine enstitü veya fakülte yönetim kurulu tarafından karar verilir.

ETHICAL DECLARATION

In this thesis study, I declare that all the information and documents have been obtained in the base of the academic rules and all audio-visual and written information and results have been presented according to the rules of scientific ethics. I did not do any distortion in data set. In case of using other works, related studies have been fully cited in accordance with the scientific standards. I also declare that my thesis study is original except cited references. It was produced by myself in consultation with supervisor (Prof. Dr. Güneş ESENDAĞLI) and written according to the rules of thesis writing of Hacettepe University Institute of Health Sciences.

Mubaida PARVEEN

ACKNOWLEDGEMENTS

I would like to express my profound appreciation to my mentor, Prof. Dr. Güneş Esendağlı, for guiding me through my thesis studies with his vast expertise, valuable counsel, boundless patience, and meticulous assessment. Beyond being an advisor, he has truly become a role model, exemplifying a deep passion for science, and the significance of contemplating uncommon observations in our everyday lives.

I want to express my gratitude to the faculty members of the Department of Basic Oncology for their ongoing support throughout my doctoral studies. Special thanks to Assoc. Prof. Dr. Hande Canpınar, Assoc. Prof. Dr. Füsün Özmen, Assoc. Prof. Dr. Neşe Ünver, and Assoc. Prof. Dr. Begüm Kocatürk. Additionally, I extend my appreciation to the technicians and staff for their generous support.

I want to express my deep appreciation to the members of the Esendağlı lab for their invaluable friendship, and unwavering support. I extend special thanks to Dr. Utku Horzum, Dr. Diğdem Yöyen Ermiş, Dr. Süleyman Can Öztürk, Dr. Ece Tavukçuoğlu, Dr. Saniye Elvan Öztürk, Sibel Gökşen, Hamdullah Yanık, Sakine Ulusoy, Sıla Ulutürk, Gizem Akça, Tuğçe Temel, Onurcan Sezginer, Gözde Bilir, Pınar Acar, Kerim Bora Yılmaz, Anıl Işık and Ali Mert Sencar for fostering a fantastic and productive atmosphere. My sincere gratitude goes to Prof. Dr. Ayşegül Üner, Assoc. Prof. Dr. Zihni Ekim Taşkiran, Assist. Prof. Dr. Beren Karaosmanoğlu, Assist. Prof. Dr. Ceren Sucularli, Assist. Prof. Dr. Güneş Dinç, for their scientific contributions and invaluable support towards this thesis.

Finally, I express immense gratitude to my dear family and friends. I extend endless thanks to my parents, Mohd Anwar and Nigar Uzma, along with my siblings for their dedicated efforts and sacrifices, for creating opportunities and possibilities, for respecting my goals and my life, and for consistently being by my side throughout my education and training. Their unwavering support made this work possible. Lastly, this journey would not have been achievable without the constant encouragement and motivation from my life partner, Mohd Minhaj. He helped me navigate and stay resilient during the most challenging or disheartening days, bringing new meaning to my life and altering the course of my time throughout my doctoral education years.

ABSTRACT

Parveen, M., Selection and Characterization of Immune Resistant Acute Myeloid Leukemia cells. Hacettepe University Graduate School of Health Sciences, Tumor Biology and Immunology Doctor of Philosophy Program, Ankara, 2024.

Resistance to immunity is associated with the selection of cancer cells with superior capacities to survive inflammatory reactions. In the case of AML, immune reactions induce dynamic changes at genetic and epigenetic levels, resulting in unique morphological, phenotypic, and genetic characteristics. To investigate this phenomenon, we developed an ex-vivo immune selection model, isolating residual subpopulations termed "immune-experienced" AML (ieAML) cells. Upon surviving immune reactions, these malignant blasts exhibited reduced proliferation, signs of myeloid differentiation and activation, and decreased immunogenicity. The observed low-pace proliferation, differentiation, and decreased immunogenicity were associated with immune resistance in myeloid leukemia. Furthermore, in the context of immune experience, ieAML cells displayed variations in behavior, including adhesion, migration, and polarization capacities. These immune-experienced AML subpopulations were found to impede T cell responses, resulting in reduced secretion of key anti-tumor immune response mediators. Transcriptomic analyses identified a limited set of commonly altered pathways and differentially expressed genes (DEGs) in all ieAML cells derived from various parental cell lines. Molecular signatures associated with interferon (IFN) and inflammatory cytokine signaling were enriched in AML cells resistant to T cell-mediated immune reactions. Individual ieAML lines exhibited diverse cellular responses upon subjecting them to mixed leukocyte-leukemia cell reactions (MLLRs), highlighting the variation in the regulation of similar pathways across different ieAML cell lines. Notably, distinctive traits of inflammatory pathways, such as IFN- γ , IFN- α , TNF- α , TGF- β , apoptosis, IL-6, and IL-2 signaling, were enriched. Transcription factors c-MYB and KLF6 emerged as potential markers for ieAML cells, with their expression and nuclear localization observed in subpopulations of blasts in AML patients' bone marrow aspirates. The nuclear localization of KLF6 and c-MYB transcription factors served as potential indicators of immune encounter status. Interestingly, the immune modulatory capacities of ieAML cells were transient and waned when immune selection pressure was removed. Despite this, our findings suggest that myeloid leukemia cells harbor subpopulations capable of adapting to the challenging conditions imposed by immune reactions. The prior "immune experience" of these cells may contribute to secondary resistance to immune intervention therapies. This study sheds light on the dynamics of immune interactions in AML and underscores the importance of understanding the adaptive mechanisms that cancer cells employ to escape immune surveillance.

Keywords: AML, Immune response, inflammation, interferon, immunotherapy, T cell, costimulation.

This project is partially supported by The Scientific and Technological Research Council of Turkey (TUBITAK), project number 120S909

ÖZET

Parveen, M., İmmün-Dirençli Akut Miyeloid Lösemi Hücrelerinin Seçilimi ve Karakterizasyonu. Hacettepe Üniversitesi Sağlık Bilimleri Enstitüsü, Tümör Biyolojisi ve İmmünolojisi Doktora Programı, Ankara, 2024. Bağışıklık direnci, inflamatuvar reaksiyonlarda hayatta kalmak için üstün kapasiteye sahip kanser hücrelerinin seçilmesiyle ilişkilidir. AML vakasında, bağışıklık reaksiyonları genetik ve epigenetik seviyelerde dinamik değişikliklere neden olarak benzersiz morfolojik, fenotipik ve genetik özelliklere yol açmaktadır. Bu fenomeni araştırmak için, "immün-deneyimli" AML (ieAML) hücreleri olarak adlandırılan kalıntı alt popülasyonları izole eden bir ex-vivo immün seçim modeli geliştirdik. İmmün reaksiyonlar sonrası sağ kalan bu malign blastlar azalmış proliferasyon, miyeloid farklılaşma ve aktivasyon belirtileri ve azalmış immünojenite sergilemiştir. Çoğalmanın yavaşlaması, farklılaşma ve azalmış immünojenitenin gözlemlenmesi miyeloid lösemide immün direnç ile ilişkilendirilmiştir. Ayrıca, bağışıklık deneyimi bağlamında, ieAML hücreleri yapışma, göç ve polarizasyon kapasiteleri bakımından davranış değişiklikleri sergilemiştir. Bağışıklık deneyimi olan bu AML alt popülasyonlarının T hücre yanıtlarını engellediği ve bunun sonucunda temel anti-tümör bağışıklık yanıtı mediatörlerinin salgılanmasının azalmasına neden olduğu bulunmuştur. Transkriptomik analizlerle, çeşitli parental hücre hatlarından türetilen tüm ieAML hücrelerinde yaygın olarak değiştirilmiş sınırlı sayıda yolak ve farklı şekilde ifade edilen genler (DEG'ler) tanımlanmıştır. İnterferon (IFN) ve inflamatuvar sitokin sinyalleri ile ilişkili moleküler belirteçler, T hücresi aracılı bağışıklık reaksiyonlarına dirençli AML hücrelerini zenginleştirmiştir. Bireysel ieAML hatları karışık lökosit-lösemi hücre reaksiyonları (MLLR) 'ye maruz bırakıldığında farklı hücrel tepkiler göstermiştir ve farklı ieAML hücre hatları arasında benzer yolakların düzenlenmesindeki çeşitliliği vurgulamıştır. Özellikle, IFN- γ , IFN- α , TNF- α , TGF- β , apoptoz, IL-6 ve IL-2 sinyali gibi inflamatuvar yolakların ayırt edici özelliklerini zenginleştirmiştir. c-MYB ve KLF6 transkripsiyon faktörleri, AML hastalarının kemik iliği aspiratlarındaki blast alt popülasyonlarındaki ekspresyonları ve nükleer lokalizasyonları açısından ieAML hücreleri için potansiyel bir belirteçler olduğu tespit edilmiştir. KLF6 ve c-MYB transkripsiyon faktörlerinin nükleer lokalizasyonu, immün etkileşim durumunun potansiyel göstergeleri olduğu tespit edilmiştir. İlginç bir şekilde, ieAML hücrelerinin immün modülatör kapasiteleri geçici olduğu ve immün seçim baskısı kaldırıldığında azaldığı görülmüştür. Buna rağmen, bulgularımız miyeloid lösemi hücrelerinin bağışıklık reaksiyonların oluşturduğu zorlu koşullara uyum sağlayabilen alt popülasyonlar barındırdığını göstermektedir. Bu hücrelerin önceki "immün deneyimi" immün müdahale tedavilerine karşı ikincil dirence katkıda bulunmuş olabilir. Bu çalışma AML'deki immün etkileşimlerin dinamiklerine ışık tutmakta ve kanser hücrelerinin immün gözetimden kaçmak için kullandıkları adaptif mekanizmaları anlamının önemini vurgulamaktadır.

Anahtar kelimeler: AML , immün yanıt, inflamasyon, interferon, immünoterapi, T hücresi, kostimülasyon.

Bu proje TÜBİTAK tarafından 120S909 numaralı proje desteği ile desteklenmiştir.

CONTENTS

APPROVAL	III
YAYIMLAMA VE FİKRİ MÜLKİYET HAKLARI BEYANI	IV
ETHICAL DECLARATION	V
ACKNOWLEDGEMENTS	VI
ABSTRACT	VII
ÖZET	VIII
CONTENTS	IX
LIST OF ABBREVIATIONS	XII
LIST OF FIGURES	XVIII
LIST OF TABLES	XXIII
1. INTRODUCTION	1
2. LITERATURE REVIEW	3
2.1. Overview and Classification of Acute Myeloid Leukemia	3
2.2. AML Classification	4
2.3. Prognosis of AML	6
2.4. Challenges and Limitations in Current Treatment Strategies	6
2.5. Dynamics and Heterogeneity of Leukemia Stem Cells	7
2.6. Dysregulated Inflammatory Pathways and Heterogeneity in AML	10
2.7. Myeloid Maturation in Acute Myeloid Leukemia	15
2.8. Allogeneic Transplantation: Addressing Relapse Dynamics in AML	16
2.9. The Immunogenicity of AML Blasts	18
2.10. The Immunological Shaping of Cancer	19
3. MATERIALS AND METHODS	25
3.1. Materials	25
3.2. Buffers and Solutions	26
3.3. Cell Culture	27
3.3.1 Thawing and Culturing of Acute Myeloid Leukemia Cell Lines	27
3.3.2 Cell Counting	28
3.4. Isolation of Peripheral Blood Mononuclear Cells	29

3.5.	Optimization of Co-Culture Ratio and Time Interval through Mixed-Leukocyte-Leukemia Cell Reactions (MLLR)	30
3.6.	Selection and Purification of the AML Cell Population from the MLLRs	31
3.7.	Purification of CD4 ⁺ and CD8 ⁺ T-cells by FACS	33
3.8.	Re co-culturing of ieAML Cells with T Cells and PBMCs	34
3.9.	Analysis of Cell Death by Annexin PI Labeling	35
3.10.	Cell Cycle Analysis	35
3.11.	Studies on Adhesion and Migration Dynamics of ieAML and wtAML Cells	36
3.11.1.	Polarization Capacity of ieAML and wtAML Cells on Coated Surfaces	36
3.11.2.	Real-time Analysis of Cell Adhesion Dynamics	37
3.11.3.	Migration Assay with the Boyden Chamber Reservoir	38
3.12.	May-Grünwald – Giemsa Staining for Morphological Analysis of the Cells	39
3.13.	Immunophenotyping	40
3.14.	Molecular Analyses	41
3.14.1.	Total RNA Isolation for Next Generation Sequencing (NGS)	41
3.14.2.	Concentration and Cleaning of Isolated Total RNA Samples	42
3.14.3.	Next Generation Sequencing (NGS)	42
3.14.4.	Transcriptomic Analysis	42
3.14.5.	RNA Isolation for Real-time PCR (RT-PCR)	44
3.14.6.	cDNA Synthesis	45
3.14.7.	Polymerase Chain Reaction (PCR)	45
3.14.8.	Semiquantitative Real-time PCR	47
3.14.9.	Gel Electrophoresis	48
3.15.	Immunofluorescence Microscopy	49
3.16.	Multiplex Cytometric Bead-Based Assay	50
3.17.	Reactive Oxygen Species and Nitric Oxide Analysis	52
3.18.	Statistical Analysis	53
4.	RESULTS	54
4.1.	A subpopulation of AML cells withstands immune responses, slows down their growth, and exhibits immunomodulatory characteristics	54
4.2.	Expression of Surface Markers Associated with Myeloid Activation and Differentiation	62

4.3.	Assessment of ROS and NO Production	65
4.4.	The Impact of ieAML Cells on T Cell Responses	66
4.5.	Transience and Heterogeneity of Immune Modulatory Capacities of ieAML Cells	68
4.6.	Limited Number of Genes were Expressed as Common Indicators of the Immune Pressure on Myeloid Leukemia Cells	72
4.7.	KLF6 and c-MYB as Transcription Factors Marking the Immune-Experienced AML Cells.	83
4.8.	KLF6 and c-MYB Expression in Primary AML Blasts from Bone Marrow Aspirates of Patients	87
5.	DISCUSSION	89
6.	CONCLUSION AND RECOMMENDATIONS	99
7.	GENİŞ ÖZET	102
7.1.	Metodoloji	103
7.2.	Sonuçlar	105
7.3.	Tartışma	114
7.4.	Sonuç ve Öneriler	124
8.	REFERENCES	127
9.	APPENDICES	146
	Appendix 1: Ethics Committee Approval	146
	Appendix 2: Scientific meetings where the data of this thesis were presented	148
	Appendix 3: Thesis Originality Report	149
	Appendix 4: Digital Receipt	150
10.	CURRICULAM VITAE	151

LIST OF ABBREVIATIONS

AlloSCT	Allogeneic stem cell transplantation
AML	Acute myeloid leukemia
APCs	Antigen presenting cells
APL	Acute promyelocytic leukemia
ASXL1	Additional sex comb-like 1
ATCC	American type cell culture
ATM	Ataxia telangiectasia mutated
ATRA	All-trans retinoic acid
B2M	Beta-2 microglobulin
Bcl-2	B-cell lymphoma 2
BCOR	BCL6 corepressor
BET	Bromodomain and extraterminal domain
BSA	Bovine serum albumin
bZip	Basic leucine zipper domain
CD	Cluster of differentiation
cDNA	Complementary DNA
CEBPA	CCAAT/enhancer-binding protein alpha
CFSE	Carboxyfluorescein succinimidyl ester
CREBBP	CREB-binding protein
CSC	Cancer stem cell
CTLA-4	Cytotoxic T-lymphocyte-associated antigen 4
CTLs	Cytotoxic T lymphocytes
CXCL2	Chemokine (C-X-C motif) ligand 2
CXCR3	C-X-C Motif Chemokine Receptor 3
DAF₂DA	4,5-diaminofluorescent diacetate
DC	Dendritic cell
DDX41	DEAD-box RNA helicase 41 gene

DEG	Differential expressed genes
DMSO	Dimethyl sulfoxide
DNMT	DNA methyltransferase
ECOG	Eastern Cooperative Oncology Group
ELN	European Leukemia Network
EmPCR	Emulsion polymerase chain reaction
FAB	French-American-British
FACS	Fluorescence-activated cell sorting
FBS	Fetal bovine serum
FDA	Food and Drug Administration
FLIP	Flice inhibitory protein
FLT3-ITD	FMS-like tyrosine kinase receptor 3 internal tandem duplication
GATA-2	GATA-binding factor 2
G-CSFR	Granulocyte colony-stimulating factor
GM-CSF	Granulocyte macrophage colony-stimulating factor
GM-CSFR	Granulocyte macrophage colony-stimulating factor receptor
GMP	Granulocyte-macrophage progenitors
GSEA	Gene set enrichment analysis
GvHD	Graft vs host disease
GvL	Graft vs Leukemia
H₂DCFDA	Carboxy-dichlorodihydrofluorescent diacetate
HDAC	Histone deacetylase
HLA	Human leukocyte antigens
HMA	Hypomethylating agents
HMGB1	High mobility group box protein 1
HO-1	Heme oxygenase-1
HSC	Hematopoietic stem cell
ICAM	Intercellular adhesion molecule 1

ICC	International consensus commission
ICOS-LG	Inducible T cell costimulator ligand
iDEP	Integrated differential expression and pathway analysis
IDH1	Isocitrate dehydrogenase 1
IDH2	Isocitrate dehydrogenase 2
IDO	Indoleamine 2,3-dioxygenase
ieAML	Immune experienced acute myeloid leukemia
IFN-γ	Interferon gamma
IL-10	Interleukin 10
IL-1RA	Interleukin-1 receptor antagonist
IL1RAP	Interleukin-1 receptor accessory protein
IL-1β	Interleukin 1 beta
IL-3R	Interleukin 3 receptor
JAK-STAT	Janus kinase/signal transducers and activators of transcription
KAT6A	K(lysine) acetyltransferase 6A
KIRs	Killer Ig-like receptors
KLF2	Krüppel-like Factor 2
KLF6	Krüppel-like Factor 6
LAG3	Lymphocyte-activation gene 3
LMPP	Lymphoid-primed multipotential progenitors
LSCs	Leukemia stem cells
LSD1	Lysine specific demethylase 1
MCL1	Myeloid cell leukemia-1
M-CSFR	Macrophage colony-stimulating factor receptor
MDB	Membrane desalting buffer
MDR	Multi drug resistance
MDS	Myelodysplastic syndromes
MDSC s	Myeloid derived suppressor cells

MFI	Mean fluorescence intensities
MgCl₂	Magnesium chloride
MHC	Major histocompatibility complex
MICA/B	MHC class I chain-related protein A/B
MLLR	Mixed leukocyte leukemia reaction
MPP	Multipotent progenitor cell
MRC	Myelodysplasia-related changes
MRD	Minimal residual disease
MYB	Myeloblastosis
NaCl	Sodium chloride
NED	No evidence of disease
NEMO	NF- κ B essential modulator
NF-$\kappa$$\beta$	Nuclear factor kappa B
NGS	Next generation sequencing
NIH	National Institutes of Health
NK	Natural killer
NKG2D	Natural killer group 2 member D
NLRP3	NLR family pyrin domain containing 3
NO	Nitric oxide
NPM	Nucleophosmin
NR4A	Nuclear receptor 4 A
OS	Overall survival
p38 MAPK	p38 mitogen-activated protein kinases
PBMC	Peripheral blood mononuclear cell
PBS	Phosphate buffer saline
PCR	Polymerase chain reaction
PD-1	Programmed cell death protein 1
PD-L1	Programmed cell death ligand 1
PD-L2	Programmed cell death ligand 2

PI	Propidium iodide
PI3	Phosphoinositide-3-kinase
PI3K/AKT	Phosphoinositide 3-kinase (PI3K)/protein kinase B
PKB	Protein kinase B
PMA	Phorbol 12-myristate 13-acetate
PML	Promyelocytic leukemia protein
PRR	Pattern recognition receptor
PS	Polystyrene
PVLR2	PVR-related 2
PVR	Poliovirus receptor
ROS	Reactive oxygen species
RPM	Revolutions per minute
RPMI	Roswell Park Memorial Institute
RT	Reverse transcriptase
RTCA	Real time cell analysis
RT-PCR	Real-time Polymerase chain reaction
RUNX1	Runt-related transcription factor 1
RxRα	Retinoid X receptor alpha
SA-PE	Streptavidin-phycoerythrin
SCF	Stem cell factor
SCT	Stem cell transplantation
sFASL	Soluble FAS ligand
STAT	Signal transducer and activator of transcription
STAT5B	Signal transducer and activator of transcription 5 B
STRING	Search Tool for the Retrieval of Interacting Genes/Protein
TAA	Tumor associated antigen
TAM	Tumor associated macrophage
TBE	Tris borate EDTA
TCGA	The Cancer Genome Atlas

TCR	T cell receptor
TET2	Tet methylcytosine dioxygenase 2
TGF-β	Transforming growth factor-beta
Th1	T helper 1
TIM3	T-cell Ig and mucin domain 3
TLR	Toll like receptor
TME	Tumor microenvironment
TNF-α	Tumour Necrosis Factor alpha
TPM	Transcript per million
Treg	Regulatory T
TSA	Tumor surface antigen
ULBP	UL16 binding protein
VCAM	Vascular cell adhesion molecule-1
VEGF	Vascular endothelial growth factor
WHO	World Health Organization
Wnt	Wingless-related integration site
wtAML	wild type acute myeloid leukemia

LIST OF FIGURES

Figure	Page
2.1 Evolution, development and relapse of acute myeloid leukemia (AML). Illustrating therapy resistance mediated by leukemic stem cells (LSC).	9
2.2 Signaling pathways and mutations sustaining stem like features and heterogeneity in AML.	15
2.3 Immunotherapies targeting minimal residual disease (MRD) after allogeneic hematopoietic stem cell transplantation (allo-HSCT) in AML aim to prevent relapse.	17
2.4 The strategies applied by AML cells to dodge immunological responses.	18
2.5 The cancer immune cycle depicting three major stages: 1) Recognition of tumor antigens followed by immune activation. 2) Trafficking and tumor infiltration of immune cells. 3) Killing of cancer cells by immune response.	23
3.1 A schematic diagram for Fuchs Rosenthal Counting chamber	29
3.2 Schematic representation of the cell separation using the gradient centrifugation method. At the end of the centrifugation, the PBMC population can be isolated as a buffy layer.	30
3.3 Schematic diagram of the experimental setup for MLLRs.	31
3.4 Experimental setup to purify and sort viable AML cells from the co-cultures.	33
3.5 Gating strategy for the selection and isolation of immune-experienced AML sub-population from co-cultures.	33
3.6 Gating strategy for cell cycle analysis.	36
3.7 Gating strategy for immunophenotyping AML cells	40
3.8 Distribution of 13 different microbeads used in cytokine determination, depending on size and internal fluorescence intensity. Microbeads are divided into 2 populations with SSC and FSC parameters and 13 populations with FL4 parameters. The amount of cytokines that each population specifically binds is measured by the FL2 parameter.	52
4.1. A) Allogenic PBMCs and AML cells were labelled with eFluor670 and CFSE proliferation tracer fluorescent dyes, respectively, and the mixed-leukocyte-leukemia cell reactions (MLLRs) were established for 72h in the presence of T cell	55

- stimulating CD3 mAbs. Representative flow cytometry plots for proliferation responses of the co-cultured PBMCs and THP-1 cells are shown. **B)** The change in viability of THP-1 cells in the MLLRs with increasing ratios of PBMCs was assayed at 24h, 48h and 72h by flow cytometry following staining with PI.
- 4.2.** In the MLLRs (0.25:1 co-culture ratio, 48h) established for the isolation of surviving AML cells, PBMCs were labelled with CFSE and AML cells left unstained. **A)** A representative gating strategy used for FACS of the DRAQ7-negative viable CD13⁺ AML cells (CFSE-negative) and a purity analysis of the ieAML cells obtained after the sorting are given. **B)** May-Grünwald Giemsa (MGG) staining was done for comparing the cytological features of wtAML and ieAML cells. Representative images out of three independent staining are given. **56**
- 4.3** Proliferation capacities of wtAML and ieAML cells were determined by Ki67 staining. **A)** Immunofluorescence images of wtTHP-1, wtU937, wtHL-60 and ieTHP-1, ieU937, ieHL-60 are shown. **B)** Bar graphs display the mean percentage (\pm SEM) of Ki67-positive cells for each AML cell line that underwent the selection process. Scale bars, 10 μ m. **57**
- 4.4** Cell cycle analysis of wtAML and ieAML cells after 48 hours and 72 hours resting in full media. **A)** Percentage distribution of the cells at G2/M, S and G1/G0 phases are shown for each cell line. **B)** A representative flow cytometry histogram showing the DNA content stained with PI in wtTHP-1 and ieTHP-1 cells. **58**
- 4.5** ieAML isolated and purified after 48 hour of co-culture with PBMCs were assessed for migration capacities compared with wtAML cells using Boyden chamber. **59**
- 4.6** wtAML cells and ie AML isolated and purified after 48 hour of co-culture with PBMCs were assessed for adhesion. **A)** Migration assessed by Boyden chamber and XCELLigence real-time. **B)** Bar graphs showing adhesion capacities on fibronectin coated and matrigel coated surfaces at 24 hours. **C)** At 48 hours. **60**
- 4.7** ieAML cells isolated from 48h of co-culture with PBMCs and wtAML cells were cultured on two different cell surface matrix fibronectin and matrigel for polarization. **A)** Based on cell area, cell perimeter and cell aspect ratio directionality of the actin cytoskeleton on different surfaces were calculated **61**

- based on the polarity index plot. **B)** Immunofluorescence staining showing cell surface representation of actin cytoskeleton orientations showing their polarity (nucleus, DAPI; actin, red). The scale bars are 10 μm .
- 4.8** Immunophenotypic markers associated with myeloid activation and differentiation were analyzed by flow cytometry. **A)** The mean percentage results obtained from three independent analyses presented as a heatmap. **B)** The markers significantly modulated between wtAML and ieAML cells are typed in bold. **64**
- 4.9** ROS and NO levels in wtAML and ieAML cells. **A)** Bar graph showing ROS and NO level between wt and ie AML cells. **B)** Representative histograms depict the fluorescence intensities of H₂DCFDA and DAF₂DA. **65**
- 4.10** Re-exposure to immune reactions reveals functional assets of ieAML cells. **A)** The ieAML cells freshly purified from the MLLRs were co-cultured with increasing amounts of PBMCs under CD3 stimulation for 72h. The MLLRs with wtAML cells were used as controls. The change in viability of AML cells was determined by PI staining. (n=3, the data points are presented as average \pm SEM). Representative flow cytometry histograms are given below. **B)** The ieAML and wtAML cells were co-cultured with increasing ratios of CD4⁺ and CD8⁺ T cells. The percentages of proliferated T cells were calculated and plotted. **67**
- 4.11** In vitro stability of acquired characters by ieAML cells. **A)** Amount of apoptotic cells upon long-term (> 96h) continuous culturing (CC) of the ieAML cells under standard conditions was assessed by annexin V and PI staining by flow cytometry. One representative image out of three independent experiments is shown. **B)** CFSE dilution assay for 72h was performed for determining the proliferation rate of continuously cultured wtAML and ieAML cells. (n=3, the data points are presented as average \pm SEM) **C)** The continuously cultured ieAML cells (CC) were re-exposed to CD3-stimulated CD4⁺ and CD8⁺ T cells. Proliferation of T cells was determined by flow cytometry for 72h. **68-69**
- 4.12** The amount of T cell-associated cytokines secreted in the co-cultures assayed by flow cytometric by multiplex bead-based cytokine assays. **A)** Graph showing major cytokines with decreased secretion in co-culture. **B)** The amount of cytokines secreted by the T cells cultured with the ieAML cells (CC) **71-72**

- were normalized to those cultured with the freshly obtained ieAML cells was plotted as a heatmap
- 4.13** Transcriptomic analysis of the ieAML cells. **A)** RNA-seq heat maps are created and **B)** Hierarchical clustering analyses were performed on purified cells. **C)** Venn diagrams for upregulated and downregulated DEGs in the ieAML cells compared to their wtAML counterparts. **D)** Gene set enrichment heatmaps showing 84 common DEGs for all three ieAML cells. **74**
- 4.14** Network and pathway analyses commonly enriched in all three ieAML cells **75**
- 4.15** Heatmaps of the genes involved in enriched **A)** Major biological pathways from the KEGG database are plotted for the genes regulated commonly in all three cell lines studied. **B)** Enrichment of the pathways involved in biological processes and inflammatory responses are shown in the upper and the lower panels, respectively. The data from commonly regulated DEGs in all three cell lines are used for the analysis. **76**
- 4.16** Gene set enrichment analysis (GSEA) of related gene sets. The most variable genes were ranked, and enrichment scores were calculated and plotted against the position of the genes within the rank ordered dataset using GSEA 3.0 software. The enrichment plots with the highest score are given. **77-78**
- 4.17** Enrichment of the pathways involved in biological processes and inflammatory responses are shown in the upper and the lower panels, respectively, for each cell line studied are given separately. **79-81**
- 4.18** **A)** TCGA bioinformatics on AML patient data are analyzed for DEGs identified in the ieAML cells and presented as a heatmap. **B)** Selected gene expression in favor. Intermediate and poor prognosis group represented as dot plot. **82-83**
- 4.19** The expression dynamics of KLF6 and MYB genes were analyzed by quantitative RT-PCR in ieAML cells cultured alone for 72h. The RNA was pooled from independent experiments (n=6) and the RT-PCR analyses were done as two technical replicates. **84-85**
- 4.20** KLF6 and c-MYB expression in ieAML cells. **A)** The frequency of AML cells with KLF6 and c-MYB proteins in the nuclear region are plotted (n=3). **B)** Bar graph showing KLF6 and c-MYB nuclear MFI **C)** KLF6 and c-MYB immunofluorescence micrographs of wtAML and ieAML cells. Higher magnification of a representative cell is shown **86**

on the right-hand side (scale bar, 1 μm). One representative image out of three independent experiments is shown.

- 4.21** The level of nuclear KLF6 and c-MYB in the primary AML blasts from the bone marrow aspirates of patients (n=11). **A)** The pie charts given on top of the graphs show the percentage of AML blasts with 1.5 times higher levels of nuclear KLF6 or with 1.5 times lower levels of nuclear c-MYB expression than the average of the AML blasts found in each patient sample on the left-hand side and the right-hand side, respectively, each dot represents an AML blast, and the red lines represent the median values. **B)** Representative micrographs of the bone marrow aspirates, which display the heterogeneity of AML cells with nuclear localization of KLF6 and c-MYB, are given below. **88**
- 5.1** A schematical diagram showing the changes in immune experienced AML cells (ieAML) after non-specific T cell-mediated MLLRs. **101**

LIST OF TABLES

Table		Page
2.1	AML Classification according to differentiation stages.	4
3.1	Antibodies used for Immunophenotyping.	41
3.2	Reaction set-up for cDNA synthesis.	45
3.3	Primer sequences for the selected genes along with the sizes in bp.	46
3.4	PCR components and reaction mixture.	46
3.5	Gradient PCR program for KLF6, KLF2, B2M, c-MYB, MCL1, SOD2, β -Actin.	47
3.6	Specific annealing temperatures assessed after gradient PCR.	47
3.7	Semi-quantitative RT-PCR components and associated information.	48
3.8	Program for the Semiquantitative Real Time-PCR.	48
3.9	Clinical properties of AML patients.	50

1. INTRODUCTION

Harnessing the immune system's anti-tumor responses has emerged as a highly promising strategy for cancer therapy (1). In addition to the conventional approaches, interventions such as inhibiting suppressive signals or transferring tumor-specific T lymphocytes demonstrated effectiveness against the disease progression and improved patient survival (2). Allogeneic hematopoietic stem cell transplantation (alloSCT) is a type of non-specific immunotherapy that is generally utilized for the treatment of leukemia (3). Allogeneic SCT is believed to enhance immune responses in individuals with moderate to poor risk AML by triggering the “graft-versus-leukemia (GvL)” effect (4). Although progress has been made in reducing mortality associated with transplants, relapse of leukemia, which usually emerges soon after the treatment or many months after achieving remission, continues to be a significant obstacle in therapy (5, 6). Malignant cells when exposed to the immune system's selection pressure may undergo adaptations favoring their survival. They reduce immunogenic potential therefore become unable to trigger an immune response (7). Decline in immunogenicity is evident in AML post-allogeneic SCT and is associated with relapse (7, 8). HLA-mismatched transplants, under immunological pressure exerted by donor T cells, encounter difficulties arising from the genetic instability of leukemia, resulting in clonal heterogeneity and immune evasion (9). T cell exhaustion can also occur as a result of extended exposure to leukemia antigens or costimulatory signals. This condition is characterized by a decline in T cell proliferation, cytokine release, and cytotoxic abilities (10). The excessive production of inhibitory receptors, such as PD-1 and CTLA-4, further leads to the suppression of T cells (11). Nevertheless, the use of immune checkpoint inhibitor such as CTLA-4 and PD-1 in AML has resulted in less favorable results when compared to other cancers with immunogenic potential (12).

Myeloid leukemia cells can constitutively express costimulatory molecules such as CD80, CD86, and ICOS-LG, which may serve to amplify T cell responses (11). However, a study from our laboratory group showed that leukemia cells can develop a resistance to immunological attacks by upregulating PD-L1 and PD-L2

in response to interferon (IFN)- γ released by activated T cells. This allows AML cells to evade the immune system and acquire immune evasion capabilities (13). AML cells produce excessive amount of costimulatory signals, which have a deleterious influence on the responses of effector T cells. This can potentially result in exhaustion of T cells' functional capacities (10). These data demonstrate similarities to cases of recurrence after transplantation, suggesting the existing of a mechanism by which the immune system can avoid detection and attack following SCT (8). Post-Graft-versus-Leukemia (GvL) periods be followed by relapse due to immune reactions that lead to modification in leukemia cells, which are associated with the development of remaining disease with improved immune modulatory capabilities (14).

In this thesis study, we strategically exerted customized immunological pressure on the AML cell lines, targeting, selecting and analyzing the surviving subpopulation which we referred to as immune-experienced AML cells (ieAML). This deliberate targeting approach unveiled the characteristics of immune resistant myeloid leukemia cells, characterized by slow proliferation, differentiation, and decreased immunogenicity. Furthermore, our study significantly identified two transcription factors, c-MYB and KLF6, as potential biomarkers indicative of AML cells under immunological pressure attempting to navigate and survive the complexities of immune modulation. Hence, our study provides valuable insight into the complex dynamics and resilient behaviour of immunologically modulated myeloid leukemia cells.

2. LITERATURE REVIEW

2.1. Overview and Classification of Acute Myeloid Leukemia

Acute Myeloid Leukemia (AML) is a rapidly progressing complex, and evolving cancer, characterized by the accumulation of immature myeloid progenitor cells known as blasts (15). These cells lack the capacity to mature into functional blood cells due to a hindrance in normal differentiation program, which results in uncontrolled proliferation, impaired normal growth, and decreased vulnerability to programmed cell death (16). AML predominantly affects adults and is a major contributor to leukemia-related deaths (17). AML is notably more frequently observed in the older adults, patients 55 years of age and above account for over two-thirds of all diagnoses with a typical median age of 68 years (18). Every year, AML causes more than 80,000 fatalities worldwide, and for the next 20 years, this figure is predicted to quadruple (19). In the United States, individuals diagnosed with AML currently have a 5-year relative survival of 30%, a significant increase from the 18% reported in 2000 (20). The availability of more innovative and effective treatment regimens had led to a reduction in mortality after transplants, which is associated with age and post-transplant care are all contributing factors to improvements in therapeutic outcomes in AML. According to the recently updated data, projected 5-year overall survival (OS) is 30% and varies significantly by age, 50% OS in younger patients but <10% OS over 60 have been anticipated (21, 22).

While AML is primarily sporadic, individuals who have previously underwent radiation therapy or exposure to cytotoxic agents are more likely to develop myeloid cancers such as AML and myelodysplastic syndrome (MDS) (23). Furthermore, a growing understanding of hereditary haematological cancers has shown that a germline susceptibility accounts for 5–10% of AML cases (24). Reduction in leukemic blast count with chemotherapy using cytarabine and anthracycline is seen, there has been limited improvement in long-term outcomes for over three decades. The median OS remains one year and the five year OS rates for individuals aged 60 years and above range between 35% and 40% (15, 25). AML cells obtained from patient samples generally exhibit a hierarchical cellular

arrangement. At the apex of this hierarchy resides a sub-population of leukemia stem cells (LSCs) that have the ability for continuous regeneration which sustain the disease in immunodeficient animals over a prolonged duration. LSCs are characterized with limited differentiation into non-LSC blasts, which mimic LSCs. Non-LSC blasts are unable to self-renew. Nevertheless, these cells can acquire self-renewal capacity and generate leukemia when consequently transplanted to immunodeficient animals. The initial conceptualization of leukemia as a hierarchically organized disease dates back to in vitro research on AML progenitors (26, 27). Later, Dick and co-workers showed that AML is organized in a similar hierarchy to that of in normal hematopoiesis LSCs act as long-term drivers, like in normal hematopoiesis (28, 29, 30).

2.2. AML Classification

At present, The World Health Organization (WHO) classification system and the International Consensus Classification (ICC) are both widely used for categorizing AML. According to WHO 2022 classification, the patients are analyzed for the genetic constitution of AML blast cells including chromosomal alterations, as well as identifying aberrant cellular development (18, 31). while the ICC emphasizes genetic factors with clinical and prognostic significance (32).

Table 2.1: AML classification according to differentiation stages..

FAB subtype	Name
M0	Undifferentiated acute myeloblastic leukemia
M1	Acute myeloblastic leukemia with minimal maturation
M2	Acute myeloblastic leukemia with maturation
M3	Acute promyelocytic leukemia (APL)
M4	Acute myelomonocytic leukemia
M4 eos	Acute myelomonocytic leukemia with eosinophilia
M5	Acute monocytic leukemia
M6	Acute erythroid leukemia
M7	Acute megakaryoblastic leukemia

Two revised AML classification schemes were unveiled in 2022, taking into account the significance of molecular profiling in diagnosis as well as

improvements in our knowledge of AML pathogenesis (33, 34). The range of genetic anomalies that define AML is now expanded by the new classifications. Nucleophosmin (NPM1) mutations, previously associated with MDS, are now recognized as AML-defining due to their association with rapid progression (35, 36). CCAAT enhancer binding protein (CEBPA) mutated AML is defined differently in the two systems, with the International consensus Commission for myeloid neoplasm (ICC) only requiring a specific mutation, while the WHO classification includes both biallelic mutations and specific basic leucine zipper (bZIP) region mutations, which have distinct clinical characteristics and better outcomes (37, 38, 39).

The classifications also vary in blast percentage thresholds for AML diagnosis, particularly in cases with genetic abnormalities. The ICC mandates a minimum of 10% blasts, whereas the WHO typically maintains a 20% threshold. Additionally, the ICC introduces a new group for (MDS)/AML with 10%-19% blasts, recognizing similarities with $\geq 20\%$ myeloblast patients. The concept of AML with myelodysplasia-related changes (MRC) does not appear in either classification (40, 41, 42, 43).

The importance of genetic analysis in patients with suggestive family history or specific molecular/cytogenetic lesions is emphasized to identify germline predispositions (44), which can modify treatment decisions and family monitoring. The identification of a germline predisposition can change a patient's treatment choices, including the selection of donors for allogeneic SCT and decisions about the appropriate conditioning regimen (45, 46). It can also affect the monitoring and assessment of family members. For instance, DEAD-box Helicase 41 (DDX41) germline mutations, which are the prevailing genetic predispositions in MDS and AML (47, 48), play a role in AML development when coupled with a second "hit" in DDX41 (49). AML patients with DDX41 germline mutations exhibit distinctive clinical characteristics, such as a higher occurrence in males, low levels of peripheral blood leukocytes and bone marrow blast counts, and a strong positive response to chemotherapy, resulting in an overall favorable prognosis in contrast to individuals with wild-type DDX41 (50).

2.3. Prognosis of AML

Long term prognosis of AML depends on the treatment response in terms of duration and effectiveness. In complete remission, the bone marrow shows fewer than 5% blasts, blood cell counts return to normal, and no evidence of disease or symptoms (NED) are noted following treatment. Complete molecular remission is typically declared when no traces of leukemia blasts are detectable in the bone marrow. In minimal residual disease (MRD), standard tests fail to detect leukemia blasts in the bone marrow after treatment; however, sensitive tests such as PCR or flow cytometry can identify the residual AML blasts. Active disease occurs when evidence of leukemia cells is present during the treatment or after the treatment i.e. relapse. A key criterion for identifying relapse is the presence of more than 5% myeloid blasts in the bone marrow.

AML has been classified into three risk categories as: favourable, intermediate and adverse by the European Leukemia Network (ELN). In 2022 ELN released updated guidelines, revising their 2017 risk classification for AML (51). These new guidelines incorporate recent molecular discoveries and clinical trial data, with a focus on assessment of dynamic risk factors such as residual disease negativity. Of note, these guidelines are predominantly based on the data from patients who received intensive treatments.

2.4. Challenges and Limitations in Current Treatment Strategies

Over the last ten years, the primary approach for treating AML has involved a combination of anthracycline antibiotics (such as idarubicin and daunorubicin) that impede DNA replication in dividing cells, along with nucleoside analogs (such as cytosine arabinoside) (52, 53). This initial therapy is most commonly known as “7+3” regimen followed by several months of cytosine arabinoside treatment in multiple cycles. Recently, whole-genome and targeted sequencing studies have identified mutated genes directly linked to abnormal gene expression in AML. These mutations often affect epigenetic regulation of transcription and have become key targets for AML treatment. Among these targets, DNA methyltransferase (DNMT) inhibitors like azacitidine and decitabine, known as hypomethylating

agents (HMAs), are promising. In addition, inhibitors for mutated isocitrate dehydrogenase enzymes (IDH1 and IDH2), such as AG-120, IDH305, FT-210, and enasidenib (Stein et al. 2017), are under clinical development. Histone deacetylases (HDAC) inhibitors (such as panobinostat, vorinostat, mocetinostat, entinostat, and pracinostat) have proven more effective in combination with HMAs. Similarly, inhibitors of bromodomain and extraterminal (BET) proteins (CPI-0610, TEN-010, and GSK525762) have demonstrated anti-leukemia activity in animal models. Another important class of inhibitors targets mutated FMS-like tyrosine kinase receptor 3 (FLT3), which are prevalent in AML. Various inhibitors like sorafenib, quizartinib, midostaurin, crenolanib, and gilteritinib are being explored in combination with other treatments to target this mutation. Venetoclax, a selective B-cell lymphoma 2 (BCL-2) inhibitor, was approved by FDA to be used in combination with HMAs or lower-dose cytarabine for newly diagnosed AML patients who are unfit for standard induction therapy. These advancements reflect a shift toward targeted therapies that are tailored to the genetic and molecular attributes of AML, offering new avenues for more effective and personalized treatment strategies.

Despite these therapeutic advancements, complete remissions are often achieved, but relapse remains a common issue. This can be due to the presence of leukemia stem cells (LSCs), which are less developed than leukemia blasts and are in a dormant phase of the cell cycle. Consequently, conventional drugs are ineffective against LSCs due to their quiescence and other survival mechanisms like drug efflux and multi-drug resistance (54, 55). While allogeneic SCT is considered as a therapeutic choice for high-risk and relapsed AML, its success is limited by transplant-related complications and refractory disease, resulting in significant morbidity and mortality rates. This raises questions about the overall reliability of current therapeutic approaches for AML with poor prognosis.

2.5. Dynamics and Heterogeneity of Leukemia Stem Cells

Conventional chemotherapy for AML, which often induces complete remission has not been changed over the past decade. However, relapse is frequent among patients diagnosed with AML and attributed to the presence of LSCs (56).

LSCs are developmentally more nascent than leukemia blasts and are in a quiescent stage of the cell cycle that restricts the efficiency of conventional anti-cancer therapeutics (57, 58, 59). These cells are proficient at removing toxic molecules by efflux mechanisms and eventually contribute to multidrug resistance (54, 55). The presence of drug-resistant LSCs, which survive the conditioning regimens of intensive chemotherapy (60), may lead to the failure of allogeneic SCT, which is considered as the only medical option in high-risk and relapsed AML. The LSC concept was first introduced as cancer stem cells (CSCs) in AML (29, 30). Since CSCs are considerably heterogeneous and at very low frequency, whether they exist in all types of cancers is still disputed. In contrast, a rather clear hierarchal organization is observed in AML, similar to normal hematopoiesis, where a rare population of self-renewing LSC multiplies and thrives into massive amounts of “mature” leukemic blasts, which are generally devoid of self-renewal capacity (29, 30). LSCs express two major surface antigens, CD34 and CD38, which are also shared by normal hematopoietic stem cells (30). The CD34⁺CD38⁻ population is classically recognized as the lymphoid-primed multipotent progenitor (LMPP)-like LSCs. On the other hand, the CD34⁺CD38⁺ fraction bears similarities with the granulocyte-macrophage progenitors (GMPs). The GMP-like LSCs are identified with IL-3R (CD123), whereas the LMPP-like cells lack CD90, a marker associated with the lymphoid lineage (61). Moreover, a minor subpopulation of LSCs was identified with no CD34 expression but retained tumor-initiating capacity (62). Albeit being shared by normal hematopoietic stem cells or progenitor cells, additional surface molecules which are upregulated on LSCs (such as CD7, CD123, CD32, CD33, CD244, CD44, CD47, CD96, CD99, CD157, IL1RAP, and TIM-3) can be useful for detecting stemness in leukemia (63). Correspondingly, the plethora of LSC-associated surface antigens is a mere indication of heterogeneity in myeloid leukemia. These surface antigens are also potential candidates for the LSC-targeted therapies. For example, a CD33-directed therapy with gemtuzumab ozogamicin not only depletes the leukemia blasts but also reduces the amount of CD34⁺CD38⁻CD33⁺ LSC populations (64).

MINIMAL RESIDUAL DISEASE (MRD)

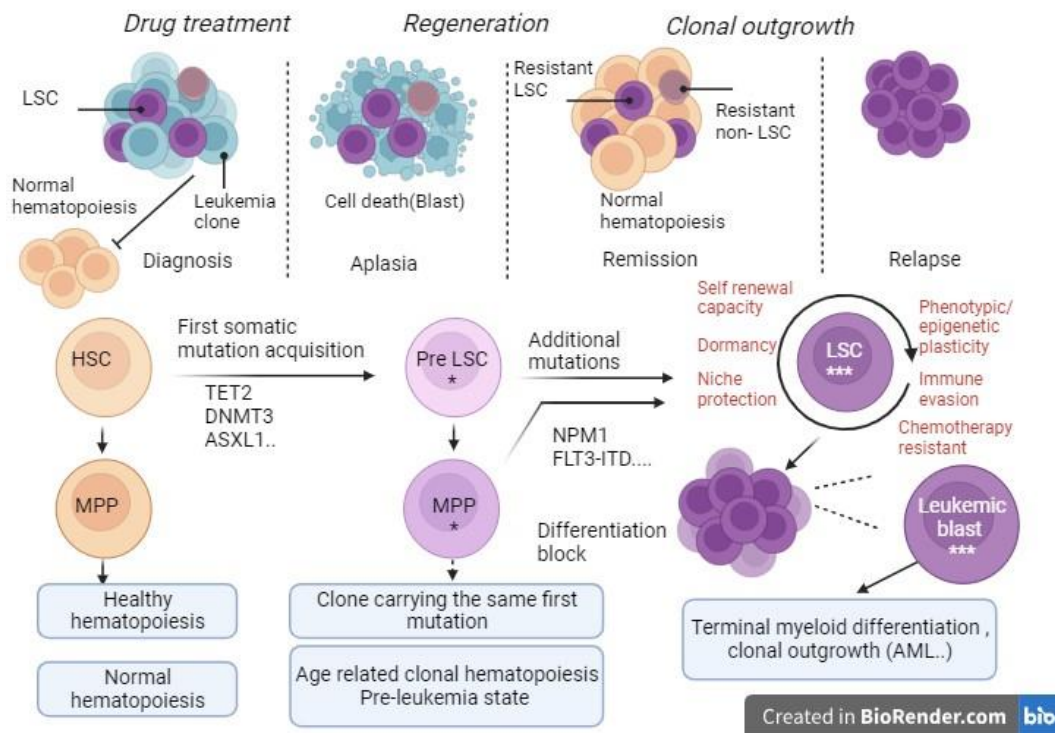


Figure 2.1. Evolution, development and relapse of acute myeloid leukemia (AML). Illustrating therapy resistance mediated by leukemic stem cells (LSC). Adapted from Stelmach & Trumpp, 2023 (65).

The accumulation of distinct genetic abnormalities has been evidenced for the heterogeneity in AML. On the other hand, the impact of the microenvironment should be considered as a confounding factor. AML blasts and LSCs that develop in immune compartments such as bone marrow, peripheral blood, and spleen are frequently exposed to inflammatory mediators. Accordingly, these cells tend to adopt a biological program that favors tumor growth as well as protects them from immune-mediated elimination. As a result, myeloid leukemia develops in close association with immune mediators that leads to the differential expression of many genes. Thus, in every stage of leukemogenesis, not only the immunophenotype but also the biological characteristics of AML cells are altered under the pressure of inflammatory responses (66, 67). Especially during disease progression, stromal cells within the bone marrow environment provide a shelter for LSCs that are exposed to metabolic, immune, and genomic stresses. In this haven, AML blasts replenish and become heterogeneous, acquire resistance and immune evasion capacities (68, 69). Two subpopulations of LSCs have been described according to

mutational signatures; LSC populations enriched in FLT3 and nucleophosmin (NPM1) driver mutations are annotated to the GMP-like LSCs, whereas LSC subpopulations with isocitrate dehydrogenase (IDH)1 and IDH2 mutations are associated with the LMPP-like cells (61). Of note, the CD34⁻ LSCs are also frequently identified with NPM1 (70, 71) and TET2 mutations (72). A fraction of AML blasts bearing in LSC properties can be identified with a high potential to establish tumors in immunocompromised animals (73) however, despite being clonally-related to the LSCs with a common set of mutations, these cells lose their tumor-forming capacity when obtained from older patients (74, 75). Additionally, AML patients aged 60 and above, the long-term prognosis under conventional chemotherapy is not favorable (76). A mutation in the enzyme DNA methyltransferase 3A (DNMT3A) can cause dysregulation in the DNA methylation machinery, which has been described as a pre-leukemia stage in hematopoietic stem cells (77). Epigenetic regulation in leukemia heavily relies on histone alterations. As a result, AML is associated with an overexpression of the lysine-specific demethylase 1 (LSD1) enzyme, which is responsible for removing methyl groups from histones. Inhibiting this enzyme lowers leukemia cell engraftment, a characteristic that is correlated with the LSC population (78, 79, 80). Nevertheless, the epigenetic regulation in AML resides at the crossroads of genetic differences and microenvironmental factors, including many inflammatory mediators, lead to heterogeneity (68, 69, 73).

2.6. Dysregulated Inflammatory Pathways and Heterogeneity in AML

A leukemia blast is prone to many intracellular stresses such as (i) mutations and chromosomal alterations due to genetic instability, (ii) the dysregulated genetic and metabolic processes, and (iii) the functional aberrations because of the truncated proteins. These factors eventually serve as triggers for the pathways connected to the ‘intrinsic’ inflammatory signals. Alternatively, the unrestrained cell proliferation, the abundance of factors and metabolites released by the leukemia cells, and the mediators produced during the immune surveillance create microenvironment-driven stress, which generates the ‘extrinsic’ inflammatory signals (81). Either derived from the intrinsic or extrinsic sources, the inflammatory

signals tend to merge in common pathways (i.e., Hedgehog, Wnt/ β -catenin, Notch, JAK-STAT, PI3K/AKT, NF- κ B, and p38 MAPK) that activate specific transcription factors. Alterations in these pathways contribute not only to leukomogenesis but also to the increase in the diversity of leukemia sub-clones (82, 83). Tumor development can benefit both from anti- and proinflammatory molecules. TGF- β , IL-10, IL-1RA, and IL-35, which are anti-inflammatory mediators such as not only limit anti-tumor immunity but also increase tumor cell survival. Whereas the proinflammatory mediators like IL-1 β , IL-6, TNF- α , GM-CSF, and IL-3 modify the tumor microenvironment in favor of malignant progression and increase the aggressiveness of the disease (84). Nevertheless, a balanced and constitutive expression of these factors, which are usually found at low or moderate levels, maintains a protumorigenic condition that bears the facets of chronic inflammation (84).

In the bone marrow, leukemogenesis is a multistep process mediated by transcription factors and receptors, which are also implicated in inflammatory signaling pathways. The co-existence of *KIT* and *RAS* mutations is a driver of malignant proliferation in patients with AML (85, 86, 87). GATA-2, a regulatory transcription factor involved in hematopoiesis and maintenance of pluripotency (88) can be mutated in MDS (89). The downstream mediator of Ras, p38 mitogen-activated protein kinase (MAPK) phosphorylates and activates the GATA-2 (90). This link between the RAS oncogene and GATA-2 forms positive feedback since the target genes of GATA-2 include IL1B and CXCL2 (91). Alternatively, Fms-like tyrosine kinase 3 (FLT3) and c-KIT (CD117) pathways, which are respective receptors for FLT3 ligand and stem cell factor (SCF) cytokines, are also deregulated in AML. These pathways contribute to cell survival and proliferation.

The nuclear receptor 4A (NR4A) group of transcription factors, which are immediate responders to many stresses and restores the cellular homeostasis, synergistically activate the β -catenin expression in AML blasts. Inflammatory responses are strengthened through the β -catenin signaling and enable crosstalk between Wnt/ β -catenin and nuclear factor kappa-light-chain-enhancer of activated B cells (NF- κ B) pathways (92). Nevertheless, in a context-dependent manner, this interaction might have either anti-tumor or pro-tumor consequences (93). The NF-

κ B family contributes to proliferation, apoptosis, intercellular communication, angiogenesis, and inflammation. Aberrant activation of NF- κ B is commonly detected in many malignancies, including AML (94).

Oncogenic activities in AML lead to oxidative stress and DNA damage, which activate the NF- κ B pathway. This activation occurs through a mechanism that involves the ataxia telangiectasia mutated (ATM) and the NF- κ B essential modulator (NEMO) (95). Besides, a mutation in the runt-related transcription factor 1 (RUNX1), that acts as a suppressor of NF- κ B signaling, leads to abnormal activation of the NF- κ B pathway (96). The canonical NF- κ B signaling is prominent both in AML blasts and LSC and correlates with therapy resistance and escape from apoptosis (97, 98). High levels of nitric oxide (NO) (99), heme oxygenase-1 (HO-1), and proinflammatory molecules including TNF- α and IL-1 β have been acknowledged as markers of enhanced NF- κ B activity in AML (100, 101, 102). Due to continuous activation of NF- κ B, an autocrine TNF- α secretion has been reported in the leukemia-initiating cells or LSCs (102).

The CCAAT/enhancer-binding protein alpha (C/EBP α) controls hematopoietic development and alters many signaling pathways. C/EBP α is responsible for inducing myeloid-specific genes including M-CSFR, G-CSFR, and GM-CSFR (103, 104). Loss-of-function or downregulation in C/EBP α expression results in a differentiation deficit in the myeloid lineage. For example, AML1-ETO or FLT3-ITD mutations can suppress C/EBP α ; therefore, interfere with myeloid differentiation and promote leukemogenesis (105, 106). Furthermore, genetic alterations in the C/EBP α gene have been identified in 10%-15% of individuals diagnosed with AML (106). In addition to controlling myeloid-specific genes, CCAAT/enhancer-binding protein alpha (C/EBP α) and its mutated variant can interact with NF- κ B, supporting prosurvival mechanisms such as Bcl-2 and cellular caspase 8 (FLICE)-like inhibitory protein (FLIP) (107). The Janus kinase (JAK)- signal transducer and activator of transcription (STAT) pathway, which is activated by growth factors like granulocyte-macrophage colony-stimulating factor (GM-CSF) and granulocyte colony-stimulating factor (G-CSF), as well as cytokines like IL-6 and IL-10, has been associated with AML biology (84, 108, 109, 110).

IL-6 is implicated in the acute phase reactions, regulation of hematopoiesis, and expansion of leukemic blasts (111, 112), whereas IL-10 is one of the most immune-suppressive cytokines that can directly impede anti-tumor immunity (113). The intracellular signaling of cytokines depends on the activation of STAT3. Unsurprisingly, the myelopoiesis growth factors G-CSF and GM-CSF enhance the proliferation and viability of AML cells through phosphorylation of STAT3 and STAT5 (109, 111). Especially, aberrant activation of STAT3 has been implicated in AML and myelodysplastic syndrome (MDS) pathogenesis and associated with reduced progression-free survival (114). On the other hand, a splice variant of STAT3, namely, STAT3 β , may interfere with the pro-tumor actions of this pathway (115).

In acute promyelocytic leukemia (APL), a well-recognized fusion occurs between STAT5B and retinoic acid receptor (RAR) due to a deletion on chromosome 17 (116). This fusion protein enhances the STAT3 signaling and hinders myeloid maturation by inhibiting the transcriptional activity of RAR α /retinoid X receptor (RxR) α . In AML, dysregulation in the JAK/STAT pathway may contribute to immune evasion (117). Recently, a study from our group demonstrated that the induction of myeloid maturation through RAR α and RxR α ligands in AML and MDS potentiated atypical IFN- γ signaling through STAT3, while the classical anti-tumor effects of this cytokine are typically mediated through STAT1 (13). Therefore, inhibition of STAT3 has been anticipated as a promising therapeutic approach in myeloid malignancies. In conclusion, the involvement of lymphoid organs in which leukemia develops provides a continuum of factors required for the stimulation of inflammatory pathways; whereas the bone marrow niche supports the signals for stemness. Therefore, the pathways of inflammation and stemness congregate to sustain the leukemogenesis and plasticity of AML blasts. This dynamic process is the main driver of cancer heterogeneity.

IL-1 β , another crucial inflammatory cytokine, linked with unfavourable prognosis in hematological malignancies, including AML. It is produced by multiple cells such as macrophages, dendritic cells, fibroblasts, and endothelial cells, its receptor IL-1R1 expression is upregulated on AML blasts (118), leading to the formation of a potential positive feedback loop. IL-1 β promotes the

advancement of AML by activating p38 mitogen-activated protein kinase (MAPK) and causing abnormal activation of the GATA binding protein-2 (GATA-2) transcription factor (90). It is generated as a reaction to foreign antigens that are identified by pattern recognition receptors (PRRs) such Toll-like receptors (TLR). However, the synthesis of the physiologically active IL-1 β molecule requires a second stimulus through a caspase-1-related enzymatic cascade (119).

The activation of caspase-1 is facilitated by a complex consisting of multiple proteins, known as the inflammasome complex. This complex is widely recognized as a characteristic feature of acute inflammation (120). The inflammasome, which plays a vital role in disorders such as autoimmunity and cancer (121, 122, 123) is responsible for the processing of IL-1 β (120). Activation of the NLRP3 inflammasome and subsequent production of IL-1 β have been observed in solid tumors, including breast, head, and neck (124), stomach, and lung malignancies, affecting metastatic cells (124, 125). Increased serum levels of IL-1 β and IL-18 (126), which promote chemoattraction and dissemination of leukemia cells have been detected in AML. Nevertheless, proliferation of normal myeloid progenitors is suppressed by IL-1 β (127). Increased expression of NOD-like receptor family pyrin domain containing 3 (NLRP3) inflammasome is observed in AML and is controlled by variables such as the PML tumor suppressor protein and the KRAS G12D mutation (128, 129). Upregulation of NLRP3 in AML blasts through the NF- κ B pathway augments the proliferation, survival, and resistance to chemotherapy (130). IL1RAP, which is linked to IL-1R1, FLT3, and c-KIT, is strongly correlated with poor prognosis in AML patients (131). High mobility group box 1 (HMGB1) governs the production of inflammatory cytokines, including tumor necrosis factor alpha (TNF- α), which subsequently promote the expression of IL-1 β in AML (132). TNF- α produced by leukemic stem cells (LSC) promotes the development of leukemia and resistance to therapy (133). Thus, targeting IL-1 β , NF- κ B, caspase-1, or TNF- α exhibits anti-leukemia potential (85). Anakinra, canakinumab, and rilonacept are among the therapeutic compounds undergoing clinical trial evaluation (118).

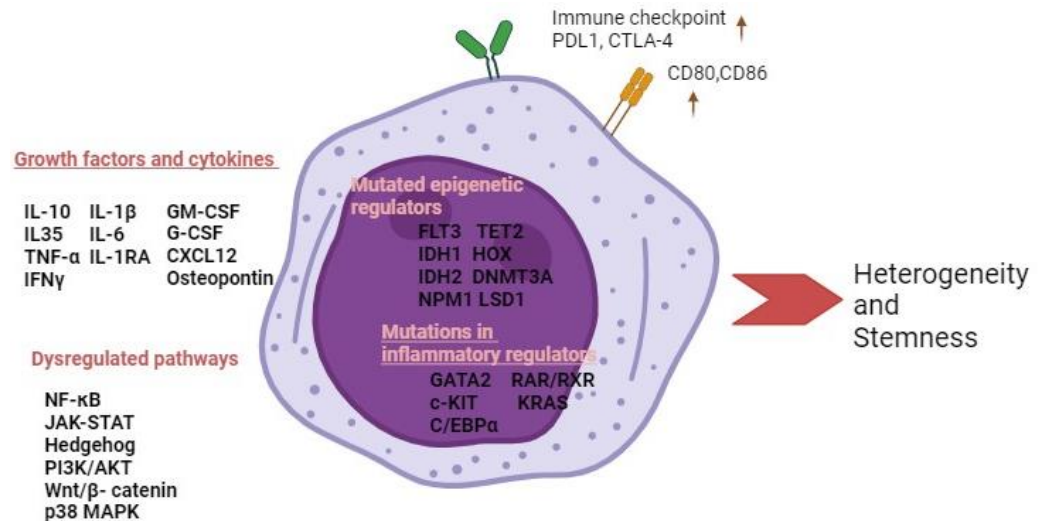


Figure 2.2. Signaling pathways and mutations sustaining stem like features and heterogeneity in AML.

2.7. Myeloid Maturation in Acute Myeloid Leukemia

Immature AML blasts accumulate in the bone marrow due to defects in hematopoiesis and exhibit uncontrolled proliferation and growth (134). These blasts spanning various stages of hematopoiesis, lack the capacity for differentiation or apoptosis. In AML biology, it has been commonly believed that mutations or multiple genetic aberrations lead to a differentiation block and enhanced cell proliferation (135, 136). Many targeted therapies for AML focus on inducing cancer cell differentiation (137, 138, 139). Over the past ten years, differentiation therapies have played a key role in the treatment of APL. These therapies include the use of all-trans retinoic acid (ATRA) (137), isocitrate dehydrogenase inhibitors (IDH) (140, 141), anthracyclines, antibiotics (idarubicin, daunorubicin), nucleoside analogs, DNA methyltransferase (DNMT) inhibitors such as azacytidine and decitabine, histone deacetylases (HDAC) inhibitors, bromodomain and extraterminal (BET) inhibitors, and Flt3-like tyrosine kinase receptor 3 (FLT3) inhibitors.

Although induction chemotherapy leads to high rates of remission among 70-80% of patients younger than 60 years and 50% of patients older than 60 years, relapse within six months is common, particularly in elderly patients, and is associated with a poor prognosis (142, 143). Accordingly, a post-remission therapy

intends to minimize relapse by removing all remaining leukemia cells (144). AML therapies primarily aim elimination or differentiation of LSCs or the promotion of their differentiation. It is believed that LSC maturation follows a unidirectional and non-reversible pathway, similar to the differentiation of normal cells. Thus, relapse is likely to arise from immature leukemia cells that possess mutations and a blockade in differentiation, impeding their maturation in response to therapy (145, 146).

However, recent in vivo data demonstrated that AML progression is driven by a reduced or biased differentiation rather than a repressed differentiation. In addition, the emerging role of many transcription factors (e.g. PU.1) in controlling the equilibrium between leukemogenic and non-leukemogenic states adds complexity to our knowledge on AML development (147, 148). Another intriguing finding showed that triggering AML differentiation in vivo can also result in the formation of two mature myeloid lineages. One of those lineage did not contribute to the disease whereas the other one persisted in extramedullary organs during remission and had potential to relapse (149). Due to the minimal residual disease the initial induction therapy is usually followed by consolidation therapy and allogeneic or autologous hematopoietic SCT. For patients with AML at moderate and poor risk categories, allogeneic SCT is considered as the preferred treatment approach (3) generally attributed to its potent anti-leukemia effects and a robust graft-versus leukemia effects (GvL) (4).

2.8. Allogeneic Transplantation: Addressing Relapse Dynamics in AML

Although transplant-related mortality has declined in recent decades, relapse remains the leading cause of transplant failure. Alloreactivity against healthy tissue, which occurs as graft-versus-host disease (GvHD), is another plausible cause of graft failure (150, 151). GvHD and relapse are the main causes of poor survival (OS) in AML patients treated with allo-SCT, which is still about 50% after 3 years (21).

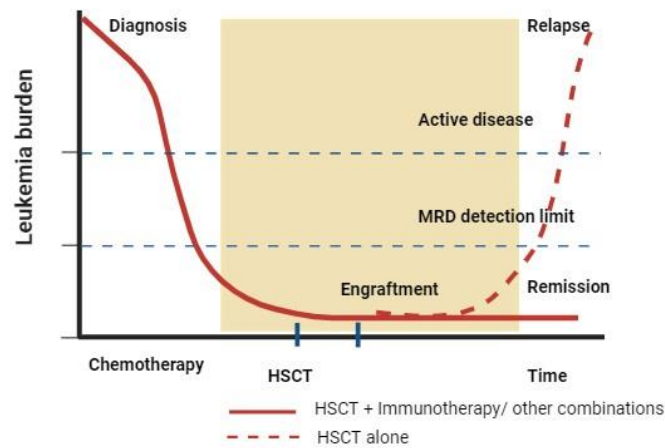


Figure 2.3. Immunotherapies targeting minimal residual disease (MRD) after allogeneic hematopoietic stem cell transplantation (allo-HSCT) in AML aim to prevent relapse. Adapted from Hattori and Nakamaki 2019 (152).

Relapse often occurs months or years after remission and typically after the termination of therapy. Loss of immunogenicity in AML occurs after allogeneic SCT under constant immunological selection pressure, leading to immunological escape and relapse by several possible mechanisms. Firstly, in HLA-incongruent grafts, the strong immunological pressure after transplantation is usually favored by donor T cells together with the genomic instability of tumor cells, resulting in the emergence and selection of mutant variants with genetic loss of part or all of the HLA locus, leading to a reduction in HLA presentation, which hinders the ability of T lymphocytes from the donor to identify and target AML cells. In addition, downregulation of HLA expression caused by abnormalities in transcriptional regulators may also contribute to relapse (9). Secondly, another factor that determines the T-cell response is tumor burden. High leukemia antigen levels lead to T cell exhaustion and simultaneous increase in inhibitory molecules expressions such as PD-1, which upon binding with its ligands PD-L1 and PD-L2 decrease proliferation and cytotoxic potential of reactive T cells (5). Thirdly, expression of anti-inflammatory enzymes and cytokines and reduction of pro-inflammatory cytokines lead to direct immunosuppression in AML. A study by Toffari et al. (8) showed upregulation of co-inhibitory molecules (PD-L1 and B7-H3) in post-transplant relapse and a subsequent increase in corresponding receptors on T cell,

suggesting different mechanisms of immune evasion after transplantation. Thus, relapse may occur after an interval of effective GvL when the immune system becomes tolerant to residual disease and undergoes immune evasion through clonal selection of immunoresistant progenitor cells. AML cells develop mechanisms to evade immune responses as they expand in the primary or secondary immune organs and are exposed to inflammatory immune responses (14).

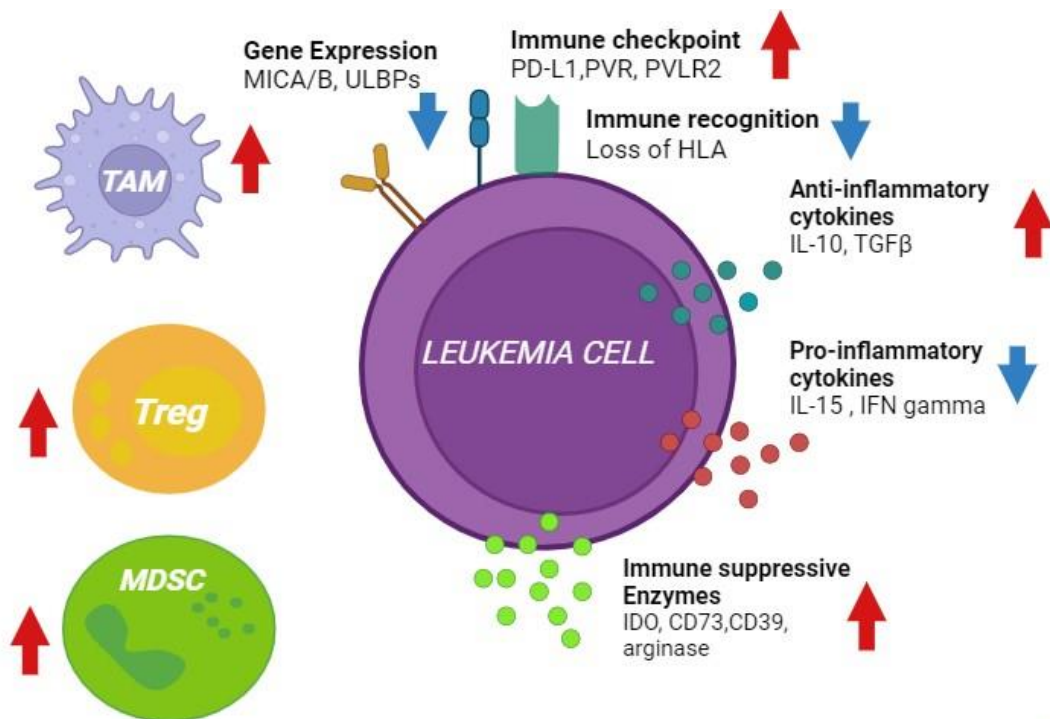


Figure 2.4. The strategies applied by AML cells to dodge immunological responses. Adapted from Hattori and Nakamaki, 2019 (152).

2.9. The Immunogenicity of AML Blasts

AML cells, which were previously thought to engage only in immunosuppression, actually can also co-stimulate T cells by expressing CD80, CD86, and ICOS-LG from the B7 protein family on their surface, just like antigen-presenting cells (10, 11). However, studies have shown that AML cells encountering the cytokine IFN- γ released by activated T cells initiate the expression of PD-L1 and PD-L2 co-inhibitor molecules. This leads to inhibition of T cell

responses by binding to the PD-1 receptor (13) . This mechanism by which AML cells stimulate and then suppress T cell responses is termed "adaptive resistance." Furthermore, another study by our group has shown that co-stimulation by AML cells negatively affects effector T cell responses by causing T cell exhaustion (10).

In this context, immunotherapies have recently come to the forefront as a treatment option for AML, which is in close relation with the immune system. However, compared to solid tumors the outcomes of immunotherapies inhibiting PD-1 and CTLA-4 pathways in AML patients have not been very promising (1, 12). The underlying reason for this is that immunotherapies do not generate immune responses from scratch, but rather reinforce pre-existing immune responses. In addition, heterogeneities in the individual's immune system and differences within tumor microenvironment are other obstacles for an efficient immune therapy in AML (153). The effectiveness of PD-1 blockade therapy in classical Hodgkin lymphoma (cHL) defies expectations based on its low mutational burden compared to solid tumors. While cHL exhibits fewer somatic mutations, whole-exome sequencing of HRS cells from cHL samples indicates a median of only 244 mutations per case, much lower than in solid tumors (154). Similar to other hematological malignancies, AML cells have low mutational burden and are therefore less immunogenic (153). Furthermore, AML cells have a tendency to lose the surface antigens that allow the immune system to recognize them, just like in solid tumors. As a result they are able to dodge T cell response by recruiting immune suppressor cells, including myeloid-derived suppressor cells (MDSCs) and T regulatory (Treg), to the tumor milieu (155). In this context, elucidating the relationship between AML cells and immune escape mechanisms is crucial for designing effective treatment strategies.

2.10. The Immunological Shaping of Cancer

Immune response against tumors requires the activation of "the cancer-immune cycle," a concept derived from the research conducted by Chen et al. (156). The cycle consists of three primary phases: 1) Identification and stimulation of immune cells, 2) movement and penetration into the tumor's interior, and 3) immune-driven elimination of tumor cells. Tumor immune escape is inevitable if

there are any interruptions in these stages. Cancer cells often utilize a series of tactics to evade detection by the immune system, hence limiting treatment efficacy. It is imperative to determine the precise evasion mechanism employed by cancer for each individual patient to ascertain the optimal therapeutic approach (157).

The tumor response entails various crucial pathways that encompass the process of detection and immune activation. For example the UL16 binding protein (ULBP) and MHC class I chain-related polypeptide A (MICA/MICB), which are ligands for the activating NK group 2D (NKG2D) produced in response to cellular stressors, are found in different types of tumor (158, 159). These proteins serve as targets for specific types of T cells ($\gamma\delta$ T cells, $CD8^+\alpha\beta$) and natural killer (NK) cells. Upon activation, these cells facilitate cytotoxic cell-mediated death and secrete IFN- γ . Nevertheless, tumor cells have the ability to evade immune destruction by releasing NKG2D ligands, resulting in a reduction in NKG2D expression on host immune cells (159, 160). T cells predominantly detect malignancies via antigen-specific T-cell receptors (TCR). As cancer cells grow, they accumulate more mutations, resulting in the production of neoantigens and aberrant protein expression (161). Tumor antigens can be broadly grouped into tumor-specific antigens (TSA) and tumor-associated antigens (TAA), which are abundantly produced by malignant cells (161, 162). The process of eliminating tumor cells by cell-mediated killing mechanisms, specifically by NK cells, results in a spread of tumor antigens. Next, dendritic cells (DCs) internalize the tumor antigens, undergo maturation, and relocate to lymph nodes. There, they present antigens to naive T cells, initiating T cell activation, differentiation, and proliferation (159, 163). Sufficient co-stimulation is essential, since its absence results in T cell anergy and tolerance (164).

The tumor microenvironment (TME) is frequently acknowledged with immunosuppressive properties as a result of factors released by malignant cells and immune cells like Tregs, MDSCs, and tumor associated macrophages (TAMs). Interleukin 10 (IL-10), indoleamine 2, 3-deoxygenase (IDO), vascular endothelial growth factor (VEGF), and transforming growth factor beta (TGF- β) hinder the maturation of DCs, hence restricting the expression of co-stimulatory proteins (157, 165, 166, 167, 168, 169). Furthermore, when cytotoxic T lymphocytes (CTLs)

move to tumor site, they eliminate tumor that display antigens on major histocompatibility complex class I (MHC-I). Tumors can evade immune recognition by either losing specific antigens, or gaining alterations in the antigen-presenting machinery, which lead to diminished immunogenicity (157, 158). Tumors become vulnerable to NK cell-induced destruction when MHC-I is lost, as this eliminates inhibitory signals transmitted by HLA class I-binding receptors such as killer Ig-like receptors (KIRs) (160).

The migration of immune cells inside tissues is regulated by molecules promoting chemotaxis and adhesion (170). Chemotactic cytokines, play a crucial role in modulating cell motion especially for immune cells. Different subsets of immune cells express different chemokine receptors, which results in recruitment of a specified immune cell subset proficient for the stress or infection exposed (170). For example, the process of NK cell maturation or naïve T cell differentiation includes alterations in the chemokine receptor's expression, enabling them to migrate to tumor locations. The chemokine receptor CXCR3 and its ligands, CXCL9, CXCL10, and CXCL11, that are triggered by IFN- γ and partially by type I interferon, assist in the tumor influx of leukocytes and promote tumor destruction (157, 158, 170). The aberrant expression of various chemokine receptors and their ligands are linked to an extensive range of human disorders including various inflammatory conditions, malignancies and autoimmune diseases (170).

Tumor cells frequently utilize evasion strategies to impede the invasion of anti-tumor leukocytes. Additionally, they facilitate the influx of tumor promoting leukocytes like immature DCs, MDSCs, TAMs, and Tregs which are linked to adverse outcomes in patients in several malignancies (162, 170). The epigenetic silencing of chemokines such as CXCL10 and CXCL9 leads to abnormalities in the IFN- γ signaling. The mutations causing loss-of-function in Janus kinase (JAK)1/2 lead to IFN- γ unresponsiveness and reduced expression of IFN- γ -related genes. The aforementioned observations highlight the crucial significance of immune cell movement in relation to cancer, as well as the intricate interaction between chemokines, their receptors, and inflammatory responses associated with tumors (157, 170).

Another crucial process known as extravasation, by which leukocytes leave blood vessels and arrive at areas of tissue damage, infection, or tumor, is another critical event for the passage of cells into tissues (171). Adhesion molecules such as intracellular adhesion molecules (ICAM) and vascular adhesion molecules (VCAM) are produced by endothelial cells to promote cell attachment (171). VEGF is secreted in the setting of tumor growth to fulfill the oxygen and nutritional requirements. However, VEGF-A suppresses VCAM and ICAM on endothelial cells and hinders extravasation and impedes immune cells from homing to the tumor location (157). When immune cells arrive at the tumor location, they begin to carry out their effector roles, which include direct or indirect removal of tumor cells (158, 159). T helper 1 cells (Th1), CTLs, and NK cells all produce IFN- γ , which boosts tumor immunogenicity by triggering MHC-I expression, attracting lymphocytes that infiltrate tumors, preventing tumor cell growth via cell cycle inhibitors, and facilitating death (158, 159). On the other hand, IFN- γ also functions as an immune modulatory mediator by causing the production of PD-L1. PD-L1 inhibits functions and/or triggers apoptosis of effector T cells and NK cells resulting in poor prognosis (172). Prolonged phosphoinositide 3-kinase (PI3K)-protein kinase B (PKB or AKT) network activation or constitutive STAT3 pathways activation can also result enhanced PD-L1 expression (173, 174, 175).

To evade the anti-tumor effects of IFN- γ and receive continuous stimulation of PI3K/AKT and STAT3, tumor cells may acquire aberrations in the IFN- γ transduction pathway (176, 177, 178, 179). This enables them to resist immune regulation.

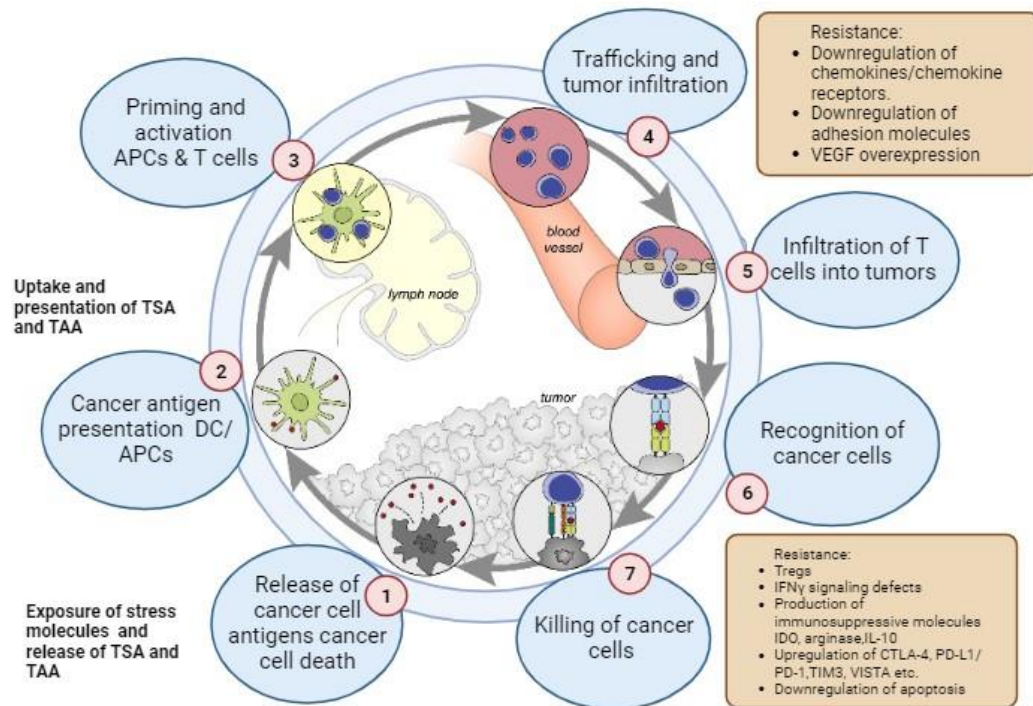


Figure 2.5. The cancer immune cycle depicting three major stages: 1) Recognition of tumor antigens followed by immune activation. 2) Trafficking and tumor infiltration of immune cells. 3) Killing of cancer cells by immune response. Adapted and modified from D. S. Chen & Mellman, 2013 (156).

The mechanisms regulating immune activation or tolerance in hematological malignancies may differ significantly from those reported for solid cancers. Nevertheless, hematological malignancies and solid tumors share several immune escape routes as well (180, 181, 182, 183, 184), while the latter have specific tolerance mechanisms in place (185). Under physiological conditions, the immune system possesses capability to discriminate between endogenous and foreign molecules. While immune system neutralizes the non-self-molecules, it develops a tolerance mechanism to the self-molecules (186). Tumor cells with impaired cellular activities that have undergone mutations display tumor-associated antigens on their surface that allow their recognition and destruction by the immune system. With respect to pro-inflammatory cytokines (for instance IFN- γ), it has long been considered that they are crucial for triggering anti-tumor T-cell responses and facilitating tumor rejection. Nonetheless, chronic antigen exposure coupled with

constitutive IFN- γ signaling triggers a multigenic program driven by STAT1 (which is PD-L1 independent) and imparts resistance to immunotherapy and radiotherapy (187). It is evident that certain tumor cells cannot be eliminated by the immune system, resulting in the emergence of neoplastic disease (188).

To refine the intricate mechanism referred to as immunological control of cancer, elimination, equilibrium, and escape phases of tumor immunology should be considered. During the elimination phase, immune system activated by tumor antigens and proinflammatory factors discharge in the tumor milieu and effectively eradicate the majority of tumor cells. This is followed by the onset of the equilibrium phase, which is a dynamic process involving the remaining tumor cells that manage to survive elimination despite the presence of the immune system. During equilibrium phase, although the immune system can keep tumor cells in check and limit their proliferation; it cannot totally eradicate the tumor cells. However, when this phase ends in favor of the tumor cells, the malignant cells that evade the immune responses become desensitized to apoptotic signals proliferate and spread by suppressing the immune responses (163).

Genomic studies of AML and other malignancies have shown that all tumors are genetically heterogeneous and display characters of additional evolution in response to treatment. This heterogeneity within the tumor is thought to be of clinical importance because it is the substrate for natural selection that drives tumor evolution, immune escape, recurrence, and resistance to therapy. Heterogeneity in gene expression or cell state (189) and maturation plasticity (149) have recently emerged as the major sources of relapse or immune resistance in AML in response to various treatments.

The heterogeneous nature of AML, the mechanisms of immune modulation and the evolution and generation of resistant subpopulation needs to be thoroughly investigated to enhance future immune intervention therapies for hematological malignancies. In this context, elucidating the relationship of AML cells with the immune system and their evasion mechanisms is crucial for the effectiveness of treatment approaches.

3. MATERIALS AND METHODS

The study was conducted at the Department of Basic Oncology, Hacettepe University Cancer Institute, spanning from February 2018 to July 2023. All experiments were conducted in accordance with the local non-interventional clinical research ethics committee (Approval No: GO 19/1142).

3.1. Materials

RPMI-1640 (Biological Industries, USA), 10X trypsin-EDTA (Biological Industries, USA), phosphate buffered saline powder (Advansta, USA), fetal bovine serum (FBS) heat-inactivated, trypan blue, penicillin streptomycin (Biowest, France), propidium iodide, DRAQ7TM (Biolegend, USA), carboxyfluoresceinsuccinimidyl (CFSE) cell tracer, anti-human CD3 mAb (Clone: Hit3 α), cell division dye eFluor670 (eBioscience, USA), LEGENDplex Human CD8/NK Panel (13-plex), PMA (Phorbol 12-Myristate 13-Acetate, Cell Signaling, USA), accudrop beads (BD Biosciences, USA), dimethyl sulfoxide, DNA marker 50 bp (Thermo Fisher Scientific, USA), histopaque 1.077 g/mL, ethidium bromide solution (Sigma-Aldrich, USA), 4',6-diamidino-2-phenylindole dihydrochloride (DAPI), ethanol 96%, (AppliChem, Germany); Seakem® Le agarose (Lonza, USA), isopropanol 98%, cellwash, filter paper, Sodium chloride (NaCl), DNase enzyme (DNase I), Dream Taq buffer solution, Taq polymerase enzyme, 25 mM dNTP solution, oligo(dT) primers, 4x reaction buffer solution, ribonuclease inhibitor (RiboLock), reverse transcriptase (RT) enzyme (Thermo Scientific, USA); 100 bp DNA marker (GeneDirex OneMark 100, USA), β -actin rabbit anti-human monoclonal antibodies, SsoAdvancedTM Universal SYBR® Green Supermix solution (BioRad, USA), RNeasy Mini Kit (Qiagen, USA), RNA purification and concentration kit (Zymo Research, USA); loading dye (6x; Thermo Scientific, USA; BioRad, USA), agarose (Lonza, Switzerland); oligonucleotides used in polymerase chain reactions (PCR) (Sentegen, Turkey), Non-essential amino acids (HyCloneTM, GE Healthcare, UK), Carboxy-dichlorodihydrofluorescent diacetate (H₂DCFDA), 4,5-diaminofluorescent Diacetate (DAF₂DA), Apoptosis assay kit (BioLegend, USA), RNA isolation kit (M&N, USA), RNA cleaning and

concentration kit (Zymo Research, USA), Matrigel™, fibronectin, Boyden chamber (Corning, USA), Glass slides, Lamel (IsoLab, Germany), mounting medium (Abcam, UK), U-bottom 96-well plates, 24-well plates, 6-well plates, serological pipettes (5mL and 20mL), T75, T25 flasks, tubes (1.5 mL, 15 mL, 50 mL), Round base, 5 mL, 75 x 12 mm PS tubes with an integrated ventilation push cap, 5 mL round bottom flow tubes, and other plastic materials (Sarstedt, Germany; Nest, China).

3.2. Buffers and Solutions

Phosphate-buffered Saline (PBS): Commercially available PBS buffer pouches were dissolved in 500mL distilled water (dH₂O) and sterilized by autoclaving to obtain 1X ready to use PBS solution and later stored at 4°C for future use.

Complete RPMI-1640 medium: A culture medium with 10% FBS was prepared by combining 55 mL of heat-inactivated FBS and 5.5 mL (final concentration approximately 1%) of penicillin/streptomycin with 500 mL of RPMI 1640 medium containing stable L-glutamine. The freshly prepared complete RPMI 1640 was then stored at 4°C.

eFluor670 and Carboxyfluorescein succinimidyl ester (CFSE): For preparing a 5 mM stock solution, lyophilized CFSE (100 µg) was dissolved in 36 µL Dimethyl sulfoxide (DMSO) and efluor670 (500 µg) in 126 µL DMSO. Stock solutions were aliquoted and stored at -80°C in dark for later use.

Trypan blue: Trypan blue 40 mg was weighed and dissolved in 1X PBS and passed through a 0.22 µm filter to prepare a 4% (w/v) trypan solution, aliquoted 500 µL in 1 mL eppendorf and stored at room temperature. The shelf life of the solution is 3 years at room temperature.

Anti-human CD3 monoclonal antibody (αCD3): For T cell stimulation assays, a working volume of 5 µg/mL of anti-human CD3 were prepared in serum-free RPMI-1640 from a stock solution of 1 mg/mL and was then aliquoted and refrigerated at a temperature of -20° C.

Propidium iodide solution: PI (5 mg) was weighed and dissolved in 1 mL dH₂O to get a final concentration of 2.5 mM and kept away from light by aliquoting and storing at 4°C. Shelf life of the solution +2-8°c for at least 6 months.

Phorbol 12-myristate 13-acetate: A 200 μ M stock solution was prepared by dissolving PMA powder in DMSO. From this stock, a working solution with a concentration of 80 μ M was made using serum-free RPMI 1640, aliquoted, and kept at -20°C .

Carboxy-dichloro-dihydro fluorescent Diacetate (H_2DCFDA): 100 mg of lyophilized H_2DCFDA was dissolved in DMSO under sterile conditions to prepare a 100 mM solution and stored at -80°C in aliquots.

4, 5-Diaminofluorescent Diacetate (DAF_2DA): DAF_2DA in lyophilized form (100 mM) was dissolved in DMSO under sterile conditions and intermediate stock solutions were prepared at a concentration of 500 μ M. The prepared solutions were stored in aliquots at -80°C .

Primary and Secondary Antibodies: Mouse anti-human mAbs (KLF2, KLF6, β -actin, Ki67), rabbit anti-human c-Myb monoclonal antibody used in immunofluorescence analysis. Secondary antibodies included anti-mouse Alexa 488, anti-mouse Alexa 647, anti-rabbit Alexa 555, and DAPI, all prepared in 1X PBS with 2% BSA at a 1:1000 dilution. Both primary and secondary antibodies were freshly prepared for each sample staining.

3.3. Cell Culture

3.3.1 Thawing and Culturing of Acute Myeloid Leukemia Cell Lines

The cryogenic vials of THP-1, U937, and HL-60 cell lines, which were previously stored by our laboratory members were removed from the nitrogen tank, thawed by gently swirling in a pre-maintained water bath at 37°C . During the thawing process, melting the ice crystals (< 2 minutes) is sufficient. At this stage, the sample was quickly decontaminated with 70% ethanol and placed in the laminar hood. After that, the sample was moved into a 50 mL tube with complete RPMI 1640 medium and subjected to centrifugation at $400\times g$ for 5 minutes to get rid off cryoprotectant DMSO. The cell pellet obtained was again suspended in complete RPMI 1640 medium after discarding the supernatant and transferred to a T-25 cell culture flask with 10 mL of complete RPMI 1640 medium addition along with 1X non-essential amino acid solution and put in an incubator set at an ambient condition of 37°C and 5% CO_2 . Cell density was monitored every day and once

desired cell density was obtained they were transferred to the T-75 flask with 15 mL of complete RPMI 1640 medium added, and then the passaging protocol was followed as mentioned by American Type Culture Collection (ATCC) for each AML cell line.

The T-75 flask was first examined under the microscope; then THP-1, HL-60, and U937 cell suspensions were counted in a cell counter under microscope, and the suspension volume was reduced to a cell density of $2-4 \times 10^5$ cells/mL, by aspirating out 10 mL and adding 10 mL of complete RPMI-1640 to bring the total volume to 20 mL. These cell lines grow in suspension and requires passaging 3 times a week to maintain a cell density in the range of $2-4 \times 10^5$ cells/mL.

3.3.2 Cell Counting

Cell counting was performed using a "Fuchs-Rosenthal Counting Chamber" (Hausser Scientific, USA) throughout the study. The cells were repeatedly aspirated and dispensed to achieve a uniform suspension of individual cells. Subsequently, 10 μ L of trypan blue was combined with 10 μ L of the cell suspension and carefully introduced between the coverslip and the Fuchs-Rosenthal counting chamber using capillary action. Next, employing a light microscope at a magnification of 40X magnification, the mean value of the cells counted in the four squares of 16 squares divided by gridlines was selected, as depicted in figure 3.1. The depth of each square measures 0.1 mm and has a volume of 0.1 μ L (100 nL). Each of the 16 squares has a side length of 1 mm. Hence, the area will measure 1 mm² and the volume will be: 1 mm² x 0.1 mm = 0.1 mm³. As a result, the number of cells per milliliter was calculated using the following formula, considering the 1:1 dilution coefficient with trypan blue. (Formula 3.1).

Final volume / solute volume = Dilution Factor (DF)

Formula for cell concentration:

$$\text{Area} = 1 \text{ mm} \times 1 \text{ mm} = 1 \text{ mm}^2$$

$$\text{Volume} = 1 \text{ mm}^2 \times 0.1 \text{ mm} = 0.1 \text{ mm}^3$$

$$\text{Total cells/mL} = \frac{\text{Total cells counted}}{\text{No. of counted squares}} \times \text{DF} \times 0.5 \times 10^4 \quad (\text{Formula 3.1})$$

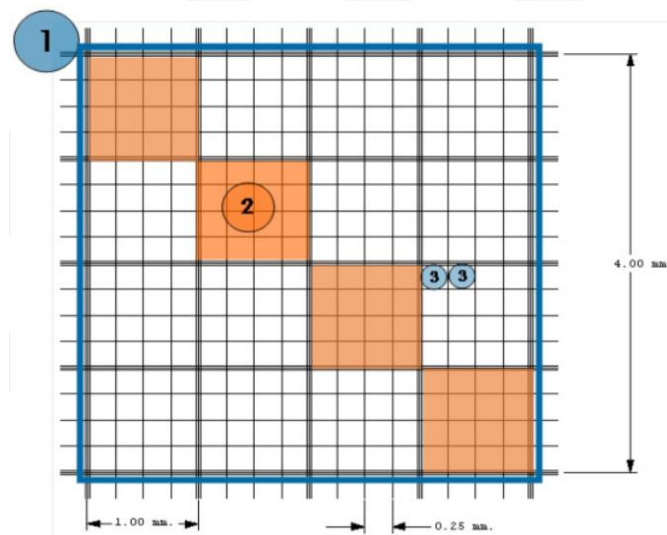


Figure 3.1. A schematic diagram for Fuchs Rosenthal Counting chamber (Hausser Scientific, USA) (190).

3.4. Isolation of Peripheral Blood Mononuclear Cells

Blood samples were obtained from healthy individuals into EDTA tubes (anticoagulant). Samples were diluted promptly v/v 1:1 with serum-free RPMI 1640 medium. Simultaneously, 3 mL of 1.077 g/mL density Ficoll solution, was transferred to a 15 mL tube and the diluted blood sample was slowly layered over it, ensuring that Ficoll and blood sample do not mix and form separate layers in the tube. Next, the sample was centrifuged at 400 g, at room temperature, for 25 minutes at the rate of 2-4 acceleration and deceleration. After 25 minutes, gradient layers were formed based on the buoyancy properties of the cells in the tube. Peripheral blood mononuclear cells (PBMCs) forms the buffy layer just above the Ficoll solution. After removing the majority of the plasma and RPMI 1640 mixture above the buffy layer (about 1-2 mL), the translucent buffy layer containing the mononuclear cells was collected in a separate tube and washed twice with 1X PBS at 1800 rpm for 5 minutes. Peripheral blood layered on Ficoll (1.077 g/mL) solution was centrifuged.

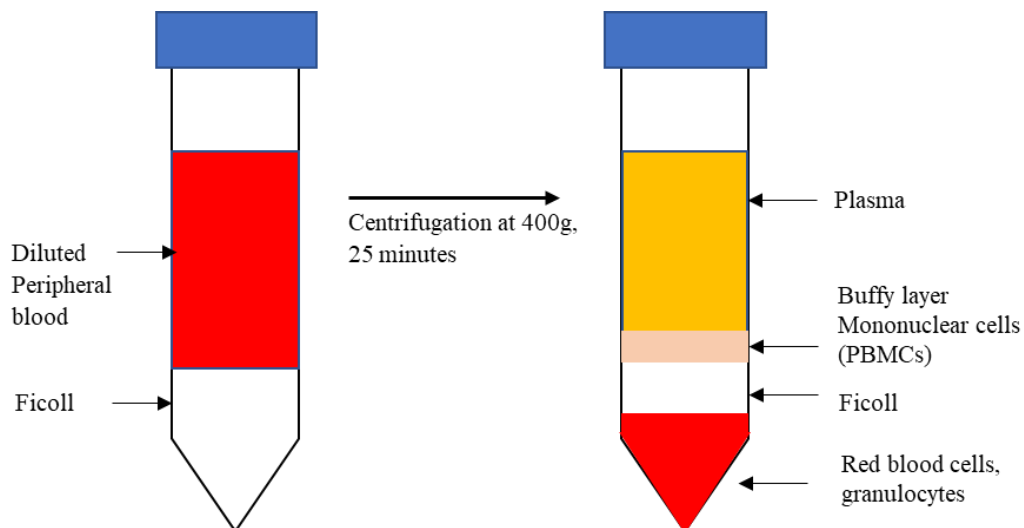


Figure 3.2. Schematic representation of the cell separation using the gradient centrifugation method. At the end of the centrifugation, the PBMC population can be isolated as a buffy layer.

3.5. Optimization of Co-Culture Ratio and Time Interval through Mixed-Leukocyte-Leukemia Cell Reactions (MLLR)

AML cell lines (125×10^3 cells/mL) and PBMCs were co-cultured at various ratios in the presence of anti-CD3 monoclonal antibody (HIT3a, 25 ng/mL). THP-1 cells were used as a prototype for determining an optimal time interval and co-culture ratio with PBMCs. AML cells and PBMCs were labelled with vital fluorescent dyes ($5 \mu\text{M}$), carboxyfluorescein succinimidyl ester (CFSE, BioLegend) and eFluor670 (Invitrogen), in order to discriminate between two cell types and to trace their proliferation activity by flow cytometry. For this cells were first washed with 1X PBS to remove the media, then 5×10^6 cells were resuspended in serum free RPMI 1640 and were stained with CFSE / eflour670 dyes at $5 \mu\text{M}$ final concentration and incubated for 10 minutes in the dark at room temperature. After incubation full RPMI was added to the tubes and were kept on ice for 5 minutes, followed by a washing step at 1800 rpm for 5 minutes. Later supernatant was discarded and cells were resuspended with complete RPMI 1640.

THP-1 cell line was used to optimize the time interval and co-culturing ratio with the immune cells to generate a mixed-leukocyte-leukemia cell reactions (MLLR) and to obtain at least 50% viable AML cells for further re-culturing

experiments with allogeneic PBMCs and other immune cells, directing AML cells to acquire resistance. For this, counted THP-1 cells and PBMCs were labeled with proliferation dye CFSE (5 μ M) and efluor670 (5 μ M) respectively, without any other molecular or biochemical manipulations on the cells prior to co-culture. Co-cultures were performed following the protocol previously optimized in our laboratory (11). According to this protocol, THP-1 cells were counted as 25×10^3 and kept constant whereas PBMC ratio was increased starting from no PBMC (1:0 to 1:0.125, 1:0.25, 1:0.5, 1:1, 1:2, 1:4) and co-cultured together with anti-CD3 stimulation (25 ng/mL, clone: HIT3a) in a U-bottom 96-well plate (Fig. 3.3). For ensuring consistency and homogeneity in each well, cells and anti-CD3 antibody were first mixed in a separate tube, before distributing them into the wells, as opposed to directly in the plate. Co-cultures were maintained for 24, 48, and 72 hours without any medium refreshment. Cells were obtained at 24, 48, and 72 hours from the co-cultures and analyzed for viability using propidium iodide (PI; 2 μ g/mL) staining and proliferation at each time point using the FACS Aria II instrument and FACS Diva software.

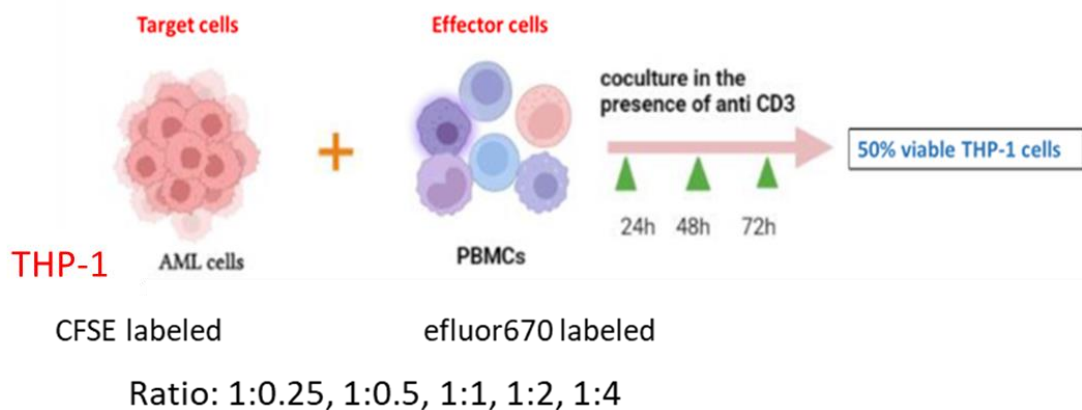


Figure 3.3. Schematic diagram of the experimental setup for MLLRs.

3.6. Selection and Purification of the AML Cell Population from the MLLRs

After the optimal ratio and time point selection at which at least 50% of cells were found to be viable next, the co-culture experimental setup was performed using PBMCs and other leukemia cell lines U937 and HL-60. AML cells counted

as 1×10^6 were co-cultured with PBMCs stained with cell division tracer CFSE at a 1:0.25 ratio at 37°C and a 5% CO₂ environment for 48 hours. To avoid any technical problems, which might occur due to fluorescent staining, the AML cells to be isolated and purified for transcriptomics and other analyses were kept unlabeled in the co-cultures. After 48 hours of co-culture with PBMC in MLLRs at a 1:0.25 ratio, and following cell staining with propidium iodide (PI, 50 µg/mL) or DRAQ7 (2 µg/mL, BioLegend) viability dyes, the viable (PI or DRAQ7-negative) AML cells were isolated by FACS. The purity and viability of the sorted AML cells were verified by flow cytometry through immunophenotyping with the pan-myeloid cell marker (anti-human mAb) CD13 (WM15), on DRAQ7-negative cells. The AML cells isolated with a purity >96% were referred as "immune-experienced AML (ieAML) cells" and used in further experiments.

The viable AML cells were sorted and purified using a FACS Aria II cell sorter installed with FACS Diva V8.0.1 software (BD Biosciences, USA). The sorter settings were set up as per the twenty-eight recommendations in the sorting manual to sort the desired cell population. FACS sorting was adjusted and finetuned to obtain the best drop delay value, drop drive frequency, and amplitude using BD FACS Accudrop Beads (BD Biosciences, USA). Following sample run and doublet exclusion, a gating strategy was designed to sort the desired cell population. The cells were scattered depending upon the granularity in an SSC plot (side scatter-area) and size in a FSC plot (forward scatter-area), respectively (Fig. 3.5). Next, the target population was selected using specific fluorochrome-labeled antibodies, and the cells (DRAQ7 negative and CD13 positive AML cells) were sorted and selected. Later, post-sort purity of the sorted cell was determined using flow cytometric analysis. Various analyses were conducted on the ieAML cells such as immunophenotyping, cell cycle analysis, and re-subjected to MLLR co-cultures with PBMCs or purified CD8⁺ and CD4⁺ T cells.

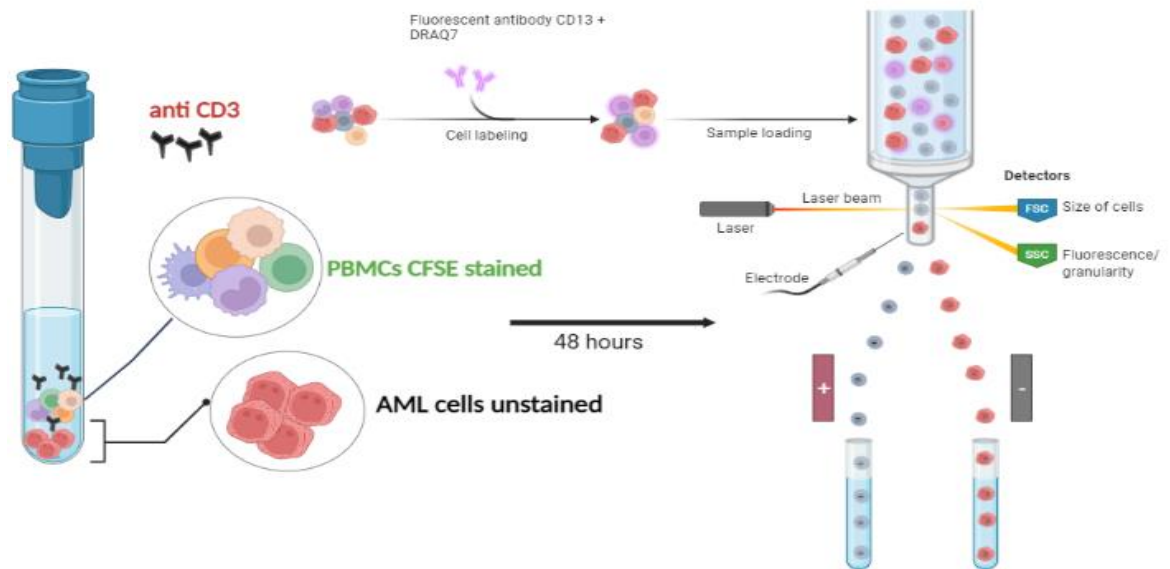


Figure 3.4. Experimental setup to purify and sort viable AML cells from the co-cultures.

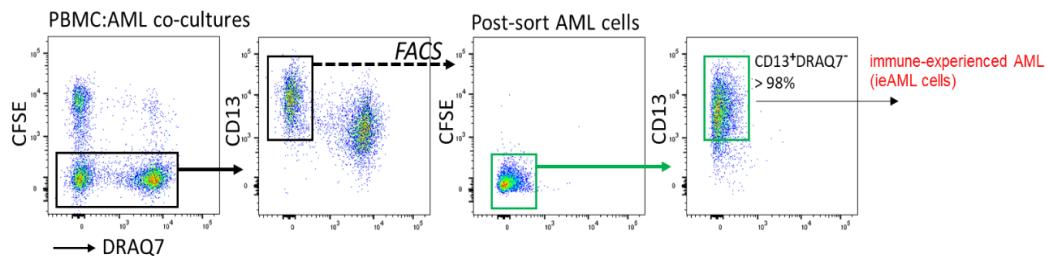


Figure 3.5. Gating strategy for the selection and isolation of immune-experienced AML sub-population from co-cultures.

3.7. Purification of CD4⁺ and CD8⁺ T-cells by FACS

T-cells were purified and sorted from PBMCs obtained through Ficoll gradient separation from healthy donors peripheral blood for subsequent re-coculturing experiments with ieAML cells. For T-cell sorting, T cells were freshly isolated from the PBMCs and purified by FACS following labeling with the monoclonal antibodies reactive against human CD16 (3G8), CD56 (MY31), CD4 (SK3), CD8 (SK1), (BioLegend) surface molecules. Next, cells were rinsed in complete RPMI 1640 at 1800 rpm for 5 minutes to remove unbound antibodies. At the end of centrifugation, the supernatant was discarded, and RPMI 1640 medium was used to

resuspend the cells and filtered through a cell strainer (40 μm) (Stem Cell Technologies, Canada) to maintain single cell suspension. Then, the cells were subjected to a FACS. Following doublet exclusion, SSC-FSC plots based on height (FSC-H) versus area (FSC-A) were created, as described below (Fig. 3.5) and cytotoxic T cells and helper T cells were sorted as $\text{CD16}^- \text{CD56}^- \text{CD4}^- \text{CD8}^+$ and $\text{CD16}^- \text{CD56}^- \text{CD4}^+ \text{CD8}^-$ populations, respectively. T-cells (CD4^+ and CD8^+) were purified by Fluorescence-activated cell sorter as per the required cell number. Next, sorted cells were subjected to purity analysis via a post-sort using a flow cytometer (See Fig. 3.5). T-cells with a purity $>96\%$ were resuspended in complete RPMI medium and were used in further co-cultures with AML cells.

3.8. Re co-culturing of ieAML Cells with T Cells and PBMCs

Three different AML cell lines (HL-60, U937, and THP-1) wildtype (wtAML) and their selected immune-experienced populations (ieAML) were labeled with cell proliferation dye CFSE (5 μM) whereas PBMCs were labeled with efluor670 (5 μM) and co-cultured at increasing PBMCs ratio (1:0.25, 1:0.5 and 1:1) for 72 hours at 37°C and 5% CO_2 environment stimulated with anti-CD3 monoclonal antibody.

Alternatively, in another setup, all the three wild type AML cell lines and their selected immune-experienced populations were labeled with cell proliferation dye CFSE (5 μM), whereas CD4^+ and CD8^+ T cells were labeled with efluor670 (5 μM) and were co-cultured for 72 hours at increasing T cell ratio (1:0.25, 1:0.5, 1:1, 1:2 and 1:4) under the stimulation of anti-CD3 mAb. At the end of the incubation, viability and proliferation were analyzed by flow cytometry.

In order to determine the consistency of immune-experienced AML populations (ieAML), the ieAML cells were rested (cultured alone) for 48 and 72 hours after purification in complete RPMI to relieve the stress they experienced during purification now designated as, rested ieAML cells. Next, efluor670-labeled CD4^+ and CD8^+ T cells were co-cultured with the 72-hour rested ieAML and wtAML cells in the presence of anti-CD3 mAb at a 1:2 ratio (AML: T cell) for 72 hours at 37°C and 5% CO_2 . Following incubation, the proliferation capacity of T cells was assessed by flow cytometry (see section 3.5).

3.9. Analysis of Cell Death by Annexin PI Labeling

Annexin V and PI double staining was carried out to determine the viable, apoptotic, and necrotic percentage of wild type (wt) AML (THP-1, HL-60, U937) and immune-experienced AML cells. The fluorescent conjugated Annexin V molecule can bind to phosphatidylserine marking it as “early apoptotic cells”. Furthermore, PI staining differentiates late apoptosis. ieAML cells purified from co-cultures (freshly sorted) or after resting in full RPMI 1640 medium for 48 and 72 hours (rested) were washed off at 1800 rpm for 5 min with 1X PBS at room temperature. After centrifugation, the cell pellet was carefully resuspended in Annexin V binding buffer (100 μ L, 1X diluted with distilled water) within a 5 mL flow tube, accommodating a maximum of 5×10^6 cells, subsequent to the removal of the supernatant. Then, the cells were incubated with 5 μ L of fluorescently conjugated Annexin V for 15 min in the dark at room temperature. At the end of the incubation period, PI was introduced to the sample, reaching a final concentration of 50 μ g/mL. The sample was then incubated for an additional 5 minutes under the same conditions. Following the incubation, 3 mL of CellWash solution was introduced to remove the PI, and the mixture was centrifuged at 1800 rpm for 5 minutes at room temperature. The cell pellet was then resuspended in CellWash solution and quickly read by flow cytometry.

3.10. Cell Cycle Analysis

Wild type AML (wtAML) cells (THP-1, HL-60, U937) and ieAML (i.e. THP-1, HL-60, U937) cells purified from co-cultures underwent a washing step with 1X PBS. The resulting cell pellets were then uniformly resuspended in 1 mL of cold 1X PBS. Then, approximately 2.5 mL of cold 99% ethanol was added dropwise with a pasteur pipette while vortexing and fixed overnight at 4°C. After fixation, a 2 mL wash with 1X PBS was performed, followed by centrifugation at 1800 rpm for 5 minutes at 4°C. Next, supernatant was removed, and RNase 40 μ L (0.1 mg/mL) and PI 40 μ L (2.5 mM) was applied to the cell pellet, mixed thoroughly with a pipette, and incubated for 20 minutes in the dark at room temperature. Post-incubation, the cells were filtered through a 40 μ m pore-sized mesh and run on a

flow cytometer. Briefly, forward scatter-height (FSC-H) and forward scatter-area (FSC-A) plots were used to eliminate clumps, doublets; then, the singlets were stringently gated on forward scatter-width (FSC-W) and forward scatter-height (FSC-H) plots (Fig. 3.6). The percentage of events in each cell cycle phases were determined based on the PI fluorescence intensity (DNA content).

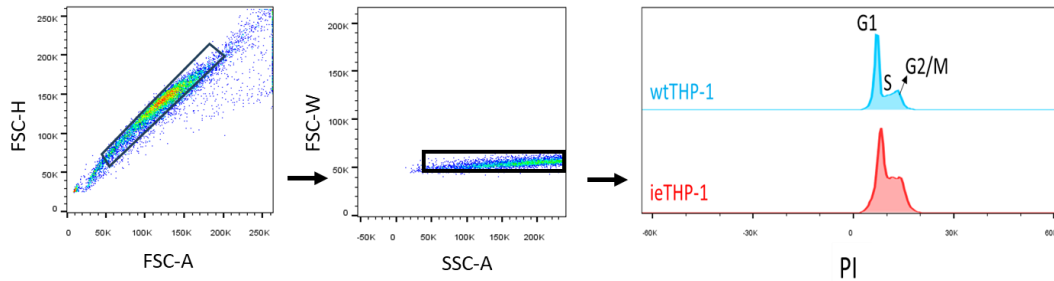


Figure 3.6. Gating strategy for cell cycle analysis.

3.11. Studies on Adhesion and Migration Dynamics of ieAML and wtAML Cells

3.11.1. Polarization Capacity of ieAML and wtAML Cells on Coated Surfaces

Immune-experienced AML cells recovered from the 48 hours of culture through FACS along with wtAML cells were incubated overnight on surface coated coverslips with Matrigel (20 mg/mL) and fibronectin (2 mg/mL) placed in a 24 well plate in an incubator in 5% CO₂ environment at 37°C. After 1 hour, cells were inspected for attachment, followed by incubation for another 16 hours. At the incubation, the medium was carefully collected with a pipette, and the coverslips were rinsed gently with 1X PBS to eliminate any remaining fibrillar protein clumps. Following the removal of PBS, the samples were treated with a 4% paraformaldehyde solution and incubated at room temperature for 15 minutes. After the incubation period, the coverslips were rinsed with 1X PBS and then incubated for 1 hour with a solution containing 1% BSA solution. For studying cell polarization, samples were next incubated with Alexa488 conjugated phalloidin (1:500 diluted in 1% BSA solution) and cell nuclei were stained with DAPI (1:1000) at room temperature in dark for 2 hours. After incubation, the cells were washed

thrice with 1X PBS, gently. Next, 100 μ L of mounting media was applied onto the slide, with the coverslips placed upside down. Next, nail polish was applied to seal the edges of the coverslip to prevent drying, and it was left undisturbed overnight in darkness at room temperature. The prepared slides can be stored for at least two months at +4°C. For fluorescent imaging, immersion oil was applied onto the coverslips and the slides were placed under an epifluorescent microscope (Olympus BX51, Japan) under a 100x objective and visualized with a cooled 5.0-megapixel CCD color camera (DC5000i, Euromex, The Netherlands). Images from polarization and adhesion experiments were processed digitally using advanced Image-J (NIH, USA) software to obtain numerical data. For this purpose, the area, perimeter, and polarity index parameters of cells growing by attaching to the relevant surfaces were assessed. The polarity index was determined using directional analysis of the cell's actin skeleton. A structural image filter applied for this process assigns directional components to each image (Directionality; Fourier Components Analysis; Nbins = 90, angle = -90; build orientation map). Subsequently, the polarity index of the cells was computed using dispersion, amount, and goodness values obtained in accordance with the specified formula (3.2)

$$\text{Polarity index} = \frac{\text{Amount} \times \text{Overlap}}{(\text{180-Scatter})/180} \quad (\text{formula 3.2})$$

3.11.2. Real-time Analysis of Cell Adhesion Dynamics

The cell adhesion dynamics were investigated in real-time using xCELLigence systems (ACEA Biosciences, USA). xCELLigence real-time cell analysis (RTCA) system consists of a station with an RTCA impedance meter, a 96-well electronic microtiter culture plate (E-plate) placed in the station, and a computer running the RTCA software. In the xCELLigence system, after adding 100 μ L of complete RPMI 1640 medium into the E-plate wells that had previously been surface coated with fibronectin and Matrigel, the E-plate was initially positioned in the RTCA station, and measurements were subsequently recorded. Next, the E-plate was taken out from the device, and the cells from different

conditions were seeded as duplicates into 64 wells. In our experiments, conducted in the xCELLigence system, ieAML cells purified from the 48 hours of co-cultures with PBMCs through FACS, and wtAML cells, were seeded into the wells of E-plate (2×10^5 cells per well). The plate was then returned to the RTCA station. Before initiating the readings, the cells were permitted to sediment at the bottom of the well for 30 minutes. In RTCA software, an E-plate figure was created, and the recording time (24 hours) and reading interval (3 minutes) were determined. The impedance change (cell index) between microelectrodes at the base of the E-plate located in the RTCA station inside the incubator was measured in real-time at 37°C and 5% CO₂ ambient condition. At the end of the experiment, the cell index data was taken from the RTCA software in .xlsx (Microsoft excel, USA) format and the analyzes were performed.

3.11.3. Migration Assay with the Boyden Chamber Reservoir

The traditional Boyden chamber reservoir employs a transwell insert, sealed at one end by a porous membrane. The insert is positioned above a large well-containing a medium which will attract the cells. The cells are loaded and permitted to traverse the membrane via the pores, which exhibit a diameter range. In our setup, we selected a 6.5 mm diameter insert with a membrane pore size 8.0 μm, at which AML cells can pass. The lower compartment of the apparatus was filled with 600 μL of RPMI 1640 solution comprising 10% FBS, whereas the purified ieAML and wtAML were suspended in 100 μL of RPMI 1640 solution with 1% FBS and placed on the upper section of the membrane. The cells were then incubated for 24 hours at a temperature of 37°C and a CO₂ concentration of 5%. The migration of ieAML and wtAML cells from the upper part of the membrane to the lower part under the influence of the serum gradient created by FBS was determined by counting the AML cells in the lower part of the membrane.

For cell counting, at the end of incubation, the upper part of the membrane was rapidly washed with 1X PBS and gently scraped with a cotton-tipped swab. The medium located at the bottom of the membrane was moved to a 1.5 mL tube and centrifuged at 400xg for 5 minutes. The resultant cell pellet was then reconstituted with 100 μL of 1X PBS, and cell counts were conducted. Additionally, 200 μL of

99% methanol was applied to the inner apparatus and allowed to fix for 2 minutes at room temperature to include the cells attached to the lower part of the inner apparatus membrane, which was removed and placed in an empty well. After fixation, the membrane was washed twice with 1X PBS at 2 minutes interval. Later, the membrane was soaked for 10 minutes in 10% Giemsa stain and quickly rinsed twice with 1X PBS. Next, the membrane was air-dried and removed by cutting from the inner apparatus. Finally, the bottom of the membrane was placed on the slide with the lower part facing up, and the rapid mounting medium (Entellan, Merck, Germany) was dripped and covered with a 0.17 mm thick coverslip. The cells adhered to the membranes were counted under a light microscope, and the overall count of migrated cells were determined.

3.12. May-Grünwald – Giemsa Staining for Morphological Analysis of the Cells

For studying changes in morphology, purified immune experienced AML cells and wild-type AML cells were washed with 1X PBS thrice at 1800 rpm, 5 minutes, room temperature to remove complete RPMI 1640 medium. Next, the supernatant was removed, cell pellets were reconstituted in 1X PBS (2 mL) and transferred into the wells of the cytopsin apparatus placed on the slide and centrifuged in a mini cytopsin device (Hettich Universal 320, Germany) at 42xg, 3 minutes at room temperature to adhere the cells on to the slides. Next, the supernatant was disposed off, and the cytopsin apparatus was removed. The samples were centrifuged at 150 xg, 1 minute, room temperature, and left overnight to allow drying. For morphological analysis of cells, cytological staining with May-Grünwald Giemsa was performed. The slides were fixed in methanol for 5 minutes. After fixation, the slides were allowed to air dry. The May-Grünwald dye diluted with distilled water (1:10) was added to the Coplin staining jar, and the slides were placed and incubated for 5 minutes at room temperature. The slides were then removed, washed with distilled water twice. Then, the slides were placed into Giemsa dye 1:10 diluted with distilled water and incubated for another 5 minutes at room temperature. The slides were rinsed twice with distilled water after the incubation period and allowed

to air dry vertically. Once dried, 2-3 drops of mounting solution (Entellan, Merck, Germany) was applied and covered with a 0.17 mm thick coverslip. Images were captured with a digital camera light microscope (DM 6000, Leica, Germany).

3.13. Immunophenotyping

For immunophenotyping, cells were resuspended in 100 μ L of CellWash solution in a 5 mL flow tube and labeled with 100 ng of the listed antibodies (see Table 3.1): anti-human CD14 (M5E2), HLA-DR (L243), CD38 (HB-7), CD63 (H5C6), CD86 (IT2.2), CD80 (2D10), PD-L1 (MIH2), CTLA-4 (L3D10), CD40 (HB14), CD206 (15-2), PD-1 (EH12.2H7) from BioLegend; CD13 (WM15), CD163 (GH1/61) from Sony Biotechnology; LAG3 (T47-530), and TIM3 (7D3) from BD Biosciences. Then, the cells were incubated in the dark at 4°C for 40 minutes or at room temperature for 25 minutes after thorough mixing with a pipette. After incubation, 1-2 mL of CellWash solution was added to the tube and centrifuged at 1800 rpm for 5 minutes to remove unbound antibodies. Subsequently, the supernatant was discarded, and the cells were resuspended in 100 μ L of CellWash. Using autofluorescence controls and isotype-matched antibodies, a flow cytometer (FACSCanto™, BD) was employed to calculate the population's median fluorescence intensity (MFI) and percentage of positive cells. The percentage of cells positive for specific immunophenotype molecules was also presented as a heat map.

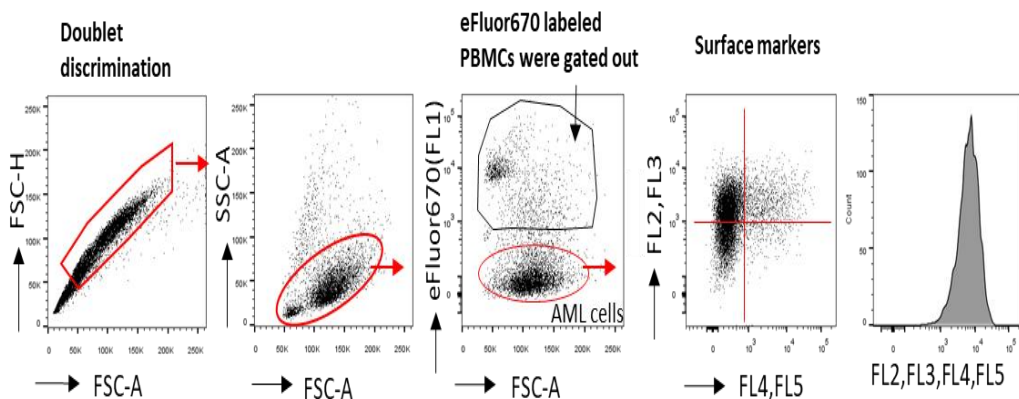


Figure 3.7: Gating strategy for immunophenotyping AML cells.

Table: 3.1 Antibodies used for Immunophenotyping

Antibody	Clone	Fluorochrome	Manufacturer
CD14	M5E2	PE/Cy7, APC/Cy7, PE	BioLegend, USA
HLA-DR	L243	PerCP	BioLegend, USA
CD38	HB-7	APC, PE/Cy7	BioLegend, USA
CD63	H5C6	Pacific Blue	BioLegend, USA
CD86	IT2.2	PE, Pacific Blue	BioLegend, USA
CD80	2D10	BV510	BioLegend, USA
PD-L1	MIH2	APC, PE	BioLegend, USA
CTLA-4	L3D10	PE, PERCP/Cy5	BioLegend, USA
CD13	WM15	APC/Cy7	Sony
CD163	GH1/61	PE	Sony
CD40	HB14	FITC	BioLegend, USA
CD206	15-2	PE/Cy7	BioLegend, USA
PD-1	EH12.2H7	APC/Cy7, BV510	BioLegend, USA
LAG3	T47-530	FITC	BD Biosciences, USA
TIM3	7D3	PE	BD Biosciences, USA

3.14. Molecular Analyses

3.14.1. Total RNA Isolation for Next Generation Sequencing (NGS)

The cells were selected and isolated from co-cultures with at least 95% purity. The RNeasy Mini Kit (Qiagen, USA), a column-based isolation kit, was utilized for total RNA isolation following the methodology advised by the manufacturer. The purified ieAML and wtAML cells were rinsed with 1X PBS at a centrifugal force of 400xg for 5 minutes at room temperature. Following washing, the cell pellet ($<5 \times 10^6$ cells) was mixed with 350 μ L of RLT buffer solution containing 1% β -mercaptoethanol RNA extraction was then carried out (per the QIAGEN, RNeasy mini kit protocol). After quantifying the isolated RNA samples' concentration and purity with an RNA spectrophotometer (NanoDrop ND1000, USA), the samples were kept in storage at -80°C .

3.14.2. Concentration and Cleaning of Isolated Total RNA Samples

If the total amount of RNA obtained was less than 10 ng, the enrichment of mRNA was performed using the universal amplification kit (SMART mRNA Amplification Kit, Ambion, USA). In spectrophotometric analysis, the OD values of RNA at A260/280 and A260/230 should be in the range of 1.8-2.1 and 2.1-2.3, respectively, to be considered pure and clean. The RNA samples obtained were cross-checked for genomic DNA contamination by PCR, and if found, the treatment with DNase was repeated, and then RNA samples were further cleaned and concentrated using an RNA concentration purification kit (Enzo, USA). After measuring the quantity and quality of RNA, a new generation sequencing system was applied for quantitative transcriptome analysis and elucidation of the mRNA profile.

3.14.3. Next Generation Sequencing (NGS)

NGS was performed at the Department of Medical Genetics at Hacettepe University Faculty of Medicine by Assoc. Prof. Dr. Ekim Z. Taşkıran and Assist.Prof. Dr. Beren Karaosmanoğlu from the Hacettepe University. RNA samples were pooled in equal amounts from at least 6 independent experiments for each time point. For transcriptome analysis, 50 ng of each RNA sample was taken, and amplification-based (ultra-multiplex PCR) libraries were prepared with the AmpliSeq Human Transcriptome kit. Each prepared library was subjected to clonal amplification by emulsion PCR (emPCR). emPCR stage was performed on the Ion One Touch device. Ion ES device was used for the purification step after emPCR. The resulting amplified libraries were loaded on Ion PI chips and sequenced in the Ion Proton device with the "semiconductor sequencing" method. In the data analysis, reads obtained after the sequencing reaction was normalized with the "Transcripts per millions" method and compared.

3.14.4. Transcriptomic Analysis

Using an Ion Torrent next-generation sequencing platform and Thermo Fisher Scientific's AmpliSeq Human Transcriptome Kit, the expression levels of

human RefSeq genes were evaluated. Integrated differential expression and pathway analysis (iDEP94) was used to build hierarchical relationships between ieAML and wtAML samples. Genes with read counts per million less than 0.5 were eliminated, and the mean expression level for each gene was deducted during pre-processing. A heat map output displayed the levels of gene expression. The read counts were subjected to the logTPM transformation, as performed in edgeR, for the purpose of cluster analysis and principal component analysis. Next, a strict criteria: i.e a fold change > 2 and an adjusted p-value ≤ 0.05 , or ii. no significant difference (a fold change < 2 with an adjusted p-value of ≤ 0.05), were used to identify differentially expressed genes (DEGs) between wtAML and ieAML. Further, we performed STRING analysis (Search Tool for the Retrieval of Interacting Genes/Protein) to find the changes in gene expression between wtAML and ieAML. In order to get list of enriched gene set, Gene Set Enrichment Analysis (GSEA) program was used to examine the DEGs in the Molecular Signature Database (MsigDB) and compare the results with publically accessible gene lists. The commonly up-regulated and down-regulated DEGs in all three immune-experienced cells were identified by comparing them with their wild-type equivalents with an adjusted p-value below 0.001 were chosen for further investigation utilizing The Cancer Genome Atlas (TCGA). This study involved accessing RNA-seq data from the TCGA-LAML database, encompassing details from 149 adult patients diagnosed with acute myeloid leukemia (AML). The TCGA data were scrutinized alongside clinical, cytogenetic, and phenotypic information, specifically categorized as "cytogenetics_risk_category." Using this information, patients were stratified into favorable, intermediate, and poor-risk groups. The expression of the identified genes was then evaluated in each patient within their respective risk category. The genes showing significant change in expression in all the three risk categories were selected and its expression was evaluated in ieAML RNA seq data.

3.14.5. RNA Isolation for Real-time PCR (RT-PCR)

RNA extraction was conducted using the Macherey-Nagel NucleoSpin® RNA purification kit as per the manufacturer's guidelines. For ieAML cells obtained through FACS sorting from co-cultures at 24, 48, and 72 hours, and wtAML cells, the procedures differed. wtAML cells were pelleted by centrifugation at 1800 rpm for 5 minutes. The cell pellet was lysed in a 2 mL Eppendorf tube using 350 μ L RL buffer supplemented with 1% β -mercaptoethanol, followed by vigorous vortexing for 30 seconds. This mixture was then applied to the NucleoSpin® Filter (violet ring), which was placed in a 2 mL collection tube and centrifuged for 1 minute at 11,000 x g to reduce lysate viscosity. After removing the filter, 350 μ L ethanol (70%) was added to the lysate, mixed by pipetting, and loaded onto the NucleoSpin® RNA Column (light blue ring). Centrifugation for 30 seconds at 11,000 x g separated the flowthrough. The remaining steps involved adding 350 μ L MDB to the column, centrifuging to dry the membrane, and preparing a DNase reaction mixture. For each isolation, 10 μ L of reconstituted rDNase was mixed with 90 μ L Reaction Buffer, and 95 μ L of this mixture was applied to the column for a 15-minute incubation at room temperature. To deactivate rDNase, 200 μ L RAW2 buffer was added, followed by centrifugation. The RNA column, placed in a new 2 mL collection tube, underwent further washing by adding 600 μ L buffer RA3 and centrifugation. A second wash involved loading 250 μ L of buffer RA3 onto the column and centrifuging for 2 minutes to ensure membrane dryness. The final step included placing the column in a nuclease-free collection tube, eluting RNA with 60 μ L RNase-free H₂O, and centrifuging at 11,000 x g for 1 minute. Following quantification, RNA samples were stored at -80 °C for future use.

The UV/VIS Spectrophotometer (NanoDrop ND-1000, USA) was employed to quantify the concentration and assess the purity of the isolated nucleic acids (RNAs) by measuring absorbance at OD260, OD280, and OD230 nm. RNA purity is commonly defined by examining the ratios of OD260/280 and OD260/230.

3.14.6. cDNA Synthesis

The isolated RNA was utilized in generating cDNA using cDNA Synthesis Kit from New England Biolabs, USA (ProtoScript® II First Strand). This kit contains ProtoScript II Enzyme Mix, featuring Reverse Transcriptase and Murine RNase Inhibitor, along with the ProtoScript II Reaction Mix containing dNTPs and an optimized buffer. The details of the cDNA synthesis reaction, including components and steps, are provided in the following table.

The first step was to prepare a mixture of RNA sample, Oligo-dT, and RNase-free dH₂O and incubate it for 5 minutes at 65°C. Subsequently, the mixture was promptly transferred to an ice-cold environment. In the second phase, both the reaction mix and enzyme mix were introduced into the mixture and allowed to incubate for one hour at 42°C, followed by a 5-minute incubation at 80°C. A thermal cycler plate (Arktik Thermal Cycler, Thermo Fisher Scientific, USA) was utilized for all the incubation steps.

Table 3.2 Reaction set-up for cDNA synthesis.

Component	Final concentration	Volume (μL)
Template RNA	Up to 1 μg	5
d(T) ₂₃ VN or Random Primer mix	50μM / 60μM	2
RNase-free water	1-8μL	1
Incubate		65°C for 5 min
M-MuLV reaction mix	2X	10
M-MuLV enzyme mix	10X	2
Final volume		20
Incubate		42°C for 1hr, 80°C for 5 min

3.14.7. Polymerase Chain Reaction (PCR)

Primer sequences for the gene of interest (KLF6, KLF2, B2M, c-MYB, SOD2, MCL1, and β-actin) designed for studying the relative mRNA expression are listed below (Table 3.3).

Table 3.3 Primer sequences for the selected genes along with the sizes in bp.

Gene	Forward (5'-3')	Reverse (5'-3')	Product size	GeneBank No.
KLF6	CCCACGGCCAAGTTTACCTC	AAGGCTTTTCTCCTGGCTTCC	202	NM_001160124.2
KLF2	GCACGCACACAGGTGAGAAG	ACCAGTCACAGTTTGGGAGG	269	NM_016270.4
B2M	AGCAGCATCATGGAGTTTG	AGCCCTCCTAGAGCTACCTG	229	NM_004048.4
c-MYB	CTCCGTTTTAATGGCACCAGC	GGTACTGCTACAAGGCTGCAA	109	NM_001161657.2
SOD2	GGCCTACGTGAACAACCTGAA	CTGTAACATCTCCCTTGCCA	71	NM_001322819.2
MCL1	ACAAAGAGGCTGGGATGGGTT	AACCAGCTCCTACTCCAGCAA	110	NM_021960.5
β -Actin	CTGGAACGGTGAAGGTGACA	AAGGGACTTCCTGTAACAATGCA	140	NM_001101.5

Table 3.4 PCR components and reaction mixture.

Component	Final concentration	Volume (μ L)
dNTP mix (2Mm)	0.2mM	2.5
Taq Buffer (10X)	1X	2.5
MgCl ₂ (25Mm)	2.5mM	2.5
Forward Primer	0.2 μ M	1
Reverse Primer	0.2 μ M	1
dH ₂ O		14.25
Taq DNA Polymerase(5U/ μ L)	0.05U/ μ L	0.25
Template cDNA		1
Total Volume		25

All the PCR components were brought to room temperature and gently spun, aside the Taq DNA Polymerase (Thermo Fisher Scientific, USA). Before the preparation of the PCR mix, all the components except cDNA were spun. The steps were performed on the ice. A reaction master mix of dNTP, Taq Buffer, forward and reverse primers, MgCl₂, and RNase/DNase free water (dH₂O) was prepared in a 2 mL tube and spun gently for the PCR reaction setup. Next, the Taq DNA polymerase was added and then 200 μ L of reaction mix was distributed equally to each PCR tube. Finally, the previously synthesized cDNA was added to each tube, and a gradient PCR program was run to determine the optimal annealing temperatures for all the targeted genes, including β actin, in the thermal cyclers (Arktik Thermal Cycler, Thermo Fisher Scientific, USA). The optimal annealing temperatures after gradient PCR mentioned in Table 3.4.

Table 3.5 Gradient PCR program for KLF6, KLF2, B2M, c-MYB, MCL1, SOD2, β -Actin.

Initial Denaturation	95°C	30 sec	} 35 cycles
Denaturation	95°C	30 sec	
Annealing	58-63°C	30 sec	
Extension	72°C	20 sec	
Final Extension	72°C	10 min	

Table 3.6 Specific annealing temperatures assessed after gradient PCR.

Genes	T_a (°C)
KLF6	61
KLF2	64
B2M	60
c-MYB	63
MCL1	63
SOD2	63
β -Actin	60

3.14.8. Semiquantitative Real-time PCR

After the optimization of annealing temperatures specific to the gene of interest, semi-quantitative RT-PCR was carried out for quantitative analysis of gene expression in the CFX Connect™ Real-Time PCR Detection System (Bio-Rad, USA) using iTaq™ SsoAdvanced universal SYBR green supermix (10X). Prior to use, all the real-time PCR components were brought to room temperature. The master mix was then prepared in a 1.5 mL tube with the required volume of forward and reverse primers, nuclease-free dH₂O, and ssoAdvanced SYBR green supermix (Biorad, USA). The mixture was then evenly distributed to each PCR tube (Biorad, USA). Finally, the cDNA template was added just before the samples were loaded into the Real-Time PCR machine (BIO-RAD CFX96 Touch Real-Time PCR Detection System, USA). The thermal cycler program for RT-PCR was prepared considering the optimized annealing temperatures (Table 3.7). The detailed

program and components for RT-PCR are discussed in the table. Gene of interest and their expression profile was analyzed after they were normalized to the relative gene expression profile of the wtAML cells according to the formula 3.3 by taking β -actin as the reference gene.

(Formula 3.3)

$$-\Delta\Delta Ct = -[(Ct \text{ target gene} - Ct \text{ reference gene} - (Ct \text{ target gene normalizer} - Ct \text{ reference gene}))]$$

Table 3.7 Semi-quantitative RT-PCR components and associated information.

Component	Final concentration	Volume (μ L)
SsoAdvanced universal SYBR green supermix (10x)	1X	5 μ L
Forward Primer	0.5 μ M	1
Reverse Primer	0.5 μ M	1
dH ₂ O		2
cDNA template		1
Total volume		10 μ L

Table 3.8 Program for the Semiquantitative Real Time-PCR.

Initial Denaturation	95°C	2 min	} 40 cycles
Denaturation	95°C	20 sec	
Annealing	58-63°C	30 sec	
Extension	72°C	30 sec	
Melting curve analysis	55-95°C 0.5 °increment	5sec/step	
Final	4°C	∞	

3.14.9. Gel Electrophoresis

For the preparation of 2 percent agarose gel (w/v), agarose was weighed and dissolved in 1% TBE solution. The prepared mixture was heated in a microwave until the agarose completely dissolved and became homogeneous. Subsequently, agarose solution was then cooled for 30 seconds by swirling the conical flask in

cold water. Next, ethidium bromide was incorporated into the mixture (10 mg/mL, final concentration), and then the agarose mixture was emptied onto a gel casting tray with a comb in place and the sides sealed. Further, a pipette tip was then used to remove bubbles, and the gel was allowed to polymerize at room temperature. After the gel polymerized, the comb was taken out and the gel casting tray was placed in a tank filled with 1X TBE buffer. After adding 1X DNA loading dye (1 μ L) to PCR samples (5 μ L), the samples were loaded along with a 50bp DNA ladder (Thermo Fisher Scientific, USA). The gel was run at 100V with a steady current for 1 hour. Finally, bands were visualized under UV light in a digital imaging system (Kodak gel Logic 1500, Carestream Health, USA).

3.15. Immunofluorescence Microscopy

For immunofluorescence analyses, the slides of patients' bone marrow aspirates and cytopsin preparations of ieAML or wtAML cells were washed with 1X PBS thrice to remove the complete RPMI 1640 medium. The method applied for fixation through cytopsin was the same as described above for May Grunwald Giemsa staining. Once cells adhered to the slides and the slides dried completely, 1X PBS was used to rinse the cells thrice. After washing, cells were incubated for 30 minutes in 1% BSA (1:10 diluted with 1X PBS) for blocking. Following blocking BSA was removed, and primary antibodies (KLF6 (1:200) and Ki67 (1:250)), KLF2 (1:200), β 2M (1:50), c-Myb (1:100) diluted in 1% BSA were added to the individual slides and allowed to sit at room temperature for 2.5 hours. Following the incubation with the primary antibody, the cells were rinsed three times with 1X PBS, and left at room temperature for 2.5 hours in the dark with DAPI nuclear dye (1:1000), Alexa488, and Alexa555 (Abcam, UK) fluorescent-conjugated secondary antibody (1:500) diluted with 1% BSA. At the end of the incubation, using 1X PBS the cells were rinsed thrice again. Finally, 100 μ L of mounting media was applied to the specimens and covered with a 0.17 mm thick coverslip. The coverslip's edges were painted with nail polish and left at room temperature in the dark overnight to prevent drying. The prepared slides were stored for more than 2 months at +4°C. For fluorescent imaging, 2-3 drops of immersion

oil, were applied to the coverslips, and the slides, were viewed under an epifluorescent microscope with a cooled 5.0-megapixel CCD color camera (Olympus BX51, Japan) (DC5000i, Euromex, The Netherlands). Image-J (NIH, USA) software was used to analyze the images.

Table 3.9. Clinical properties of AML patients.

AML PATIENTS	
NUMBER (N)	6 at initial diagnosis 5 at relapse
AGE MEDIAN (MIN-MAX)	50 (26-60)
CHEMOTHERAPY RECEIVED PRIOR TO SCT*	Idarubicin, cytarabine, mitoxantrone, venetoclax, etoposide, azacytidine, methotrexate, actinomycin
AML SUBTYPE	
M2	2
M4	5
N/A	4
BLAST % MEDIAN (MIN-MAX)	71(30-90) at initial diagnosis 40 (25-75) at relapse
TIME TO RELAPSE AFTER SCT MEDIAN (MIN-MAX)	392.5 (113-853) days

*Combination chemotherapy agents. SCT, stem cell transplantation.

3.16. Multiplex Cytometric Bead-Based Assay

Supernatants from ieAML and wtAML cells co-cultured with PBMCs and T cells were carefully collected and stored at -80°C in 1.5 mL tubes. The samples were collected from at least three independent co-culture experiments to measure the cytokines; therefore, all the samples were combined in equal amounts on ice on the day of the measurement. Cytokines (IL-10, IL-2, IL-6, IL-4, IL-17, sFAS, sFASL, TNF- α , IFN- γ , Perforin, Granulysin, GranzymeB, GranzymeA) abundantly produced by Th lymphocyte subtypes and NK cells quantification were performed using flow cytometry through a kit called "LEGENDplex™ Human CD8/NK Panel (Biolegend USA)", a fluorescently labeled microbead-based immunoassay applying manufacturer's guidelines. The microbeads in the kit consist of 13

populations with different sizes and fluorescent dye densities (in the FL4 filter) (Fig. 3.8). The surface of each microbead population is coated with an antibody that recognizes a specific cytokine. Before use, the kit was cool to RT, and the microbeads were completely suspended by vortexing for 30 seconds. Standards were prepared in accordance with the kit protocol by making serial dilutions of 10,000 pg/mL stock at a ratio of 1:4 referred to as Conc 0, Conc1, Conc2, Conc3, Conc4, Conc5, Conc6, Conc7. Following that, 25 μ L of assay buffer and 25 μ L of the sample or standard were added to the 96 well plates. Subsequently, a volume of 25 μ L of microbeads was introduced into every individual well of the plate. To avoid bead settling, the beads were vortexed intermittently as they were being added. Later, the plate was sealed with a plate sealer, covered with an aluminum foil, secured with a rubber band, and left at ambient temperature on a shaker set to 500 rpm for three hours. Following incubation, a volume of 200 μ L of 1X wash solution was introduced into each well. Excess wash buffer was removed with a multichannel pipette. Following the washing step, a volume of 25 μ L of detection antibody was introduced into each well, sealed, and covered with aluminum foil, and left to shake for 1 hour 30 minutes as described above. The analytes previously bound to the microbeads were now specifically bound by biotin-conjugated antibodies after incubation with the detection antibody cocktail. Without washing the plate, 25 μ L of SA-PE (streptavidin-phycoerythrin) solution was added at the end of the second incubation and left to shake for another half hour at 500 rpm at room temperature. SA-PE molecules bind to the biotin of the detection antibodies, generating a fluorescent signal (in the FL2 filter) proportional to the analyte concentration on the microbead. To remove the unbound antibodies, 200 μ L of 1X wash buffer solution, was added to each well of the plate at the end of the incubation. Next, the samples were resuspended, in 100 μ L of 1X wash buffer solution, analyzed by flow cytometry at a low flow rate (maximum 300 microbeads/sec), and at least 4,000 microbeads were read. The data was analyzed by transferring the files in . fcs format to the LEGENDplex online data analysis software and processing them.

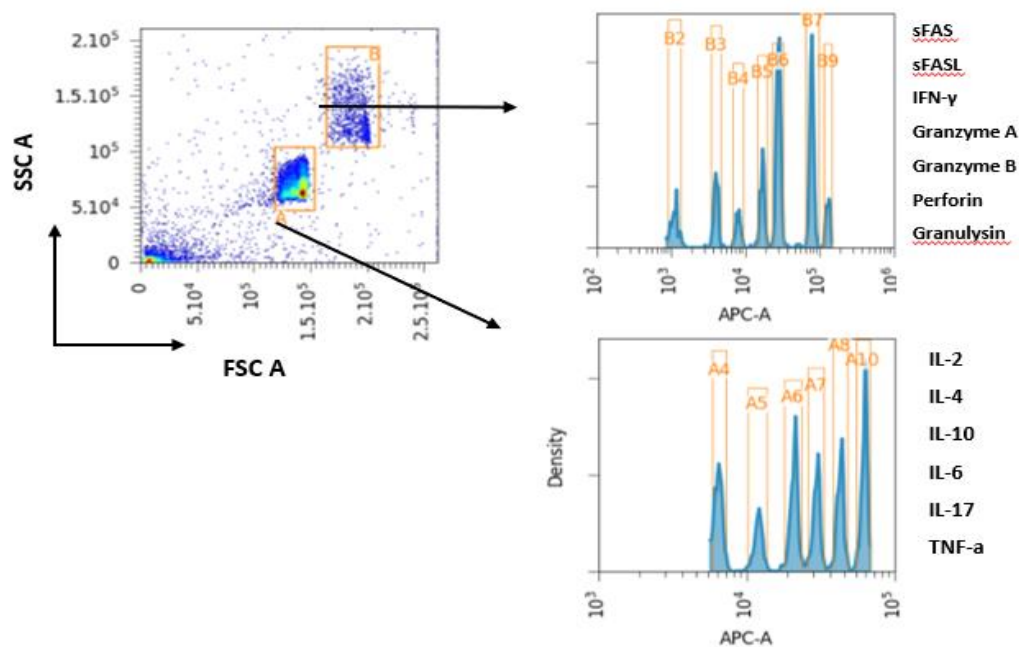


Figure 3.8. Distribution of 13 different microbeads used in cytokine determination, depending on size and internal fluorescence intensity. Microbeads are divided into 2 populations with SSC and FSC parameters and 13 populations with FL4 parameters. The amount of cytokines that each population specifically binds is measured by the FL2 parameter.

3.17. Reactive Oxygen Species and Nitric Oxide Analysis

Freshly isolated cells were rested for 48h in full media without any stimuli to check spontaneous production of ROS and NO. The cells stimulated with PMA and unstimulated cells were used for a burst response setting. ieAML cells and wtAML cells were first washed with 1X PBS to remove the complete RPMI 1640. After washing, cells were labeled with 2 μ L of 10 μ M 2',7'dichlorodihydrofluorescein diacetate (H₂DCFDA) and 1 μ L of 5 μ M 4,5-diaminofluorescein diacetate (DAF₂DA), in serum-free RPMI 1640. The tubes were gently vortexed and incubated in the dark for 25 min at 37°C. Then, 2 mL of cellwash was introduced while placed on ice, followed by centrifugation at 1800 rpm for a duration of 5 minutes. Later, cellwash was added (100 μ L) after discarding the supernatant. For PMA stimulated condition, PMA was added to the tubes after 25 minutes of incubation with H₂DCFDA and DAF₂DA, incubated for another 25 minutes at room

temperature, and immediately placed on ice, followed by washing with cellwash at 1800rpm for 5 minutes. Finally, flow cytometry was employed to quantify the mean fluorescence intensities of H₂DCFDA and DAF₂DA. The MFI of PMA-stimulated cells was normalized to the MFI of unstimulated cells using the following formula 3.3

$$\text{MFI}_{\text{PMA stimulated AML}} / \text{MFI}_{\text{unstimulated AML}} \text{ (Formula 3.3)}$$

3.18. Statistical Analysis

Each experiment was independently replicated and repeated a minimum of 3 times. All the data were statistically analyzed (ANOVA and posthoc analysis, Chi-square, and/or Student's t-tests) using the Graphpad Prism v8 software.

4. RESULTS

4.1. A subpopulation of AML cells withstands immune responses, slows down their growth, and exhibits immunomodulatory characteristics

Modifications in the immune microenvironment drive cancer cells to adopt novel characteristics, resulting in the survival of the most resilient malignant clones against immune reactions (191). However, the absence of interaction between immune cells and cancer cells in vitro creates a favourable environment for cancer cell proliferation without facing immune selection pressures. Previous research from our group demonstrated the immunogenic potential of myeloid leukemia cells through constitutive expression of costimulatory molecules (10, 11). In this thesis study, a co-culture experiment was performed wherein myeloid leukemia cell lines (THP-1, HL-60, U937) were incubated with increasing amounts of peripheral blood mononuclear cells (PBMCs) containing CD3-stimulated T cells. This setup is named as mixed-leukocyte-leukemia cell reactions (MLLRs). In MLLRs, the T cells showed strong proliferation, while the proliferation of leukemia cells was significantly inhibited (Fig. 4.1 A). In general, among the three cell lines, THP-1 was used for the optimization of ratio and time intervals, while the other two cell lines were subsequently employed for further validation and supporting experiments. Under this immunologically harsh conditions, a small population of leukemia cells managed to proliferate in the MLLRs (Fig. 4.1 A). Especially at 72h, which is long enough for proliferation of leukemia cells, the percentage of viable leukemia cells remained constant even in the co-cultures with high PBMC proportions although proportion of the immune cells was increased in the cultures (Fig. 4.1 B). This supported the observation that the percentage of dead cells being counteracted by a leukemia subpopulation capable of proliferating in the MLLRs.

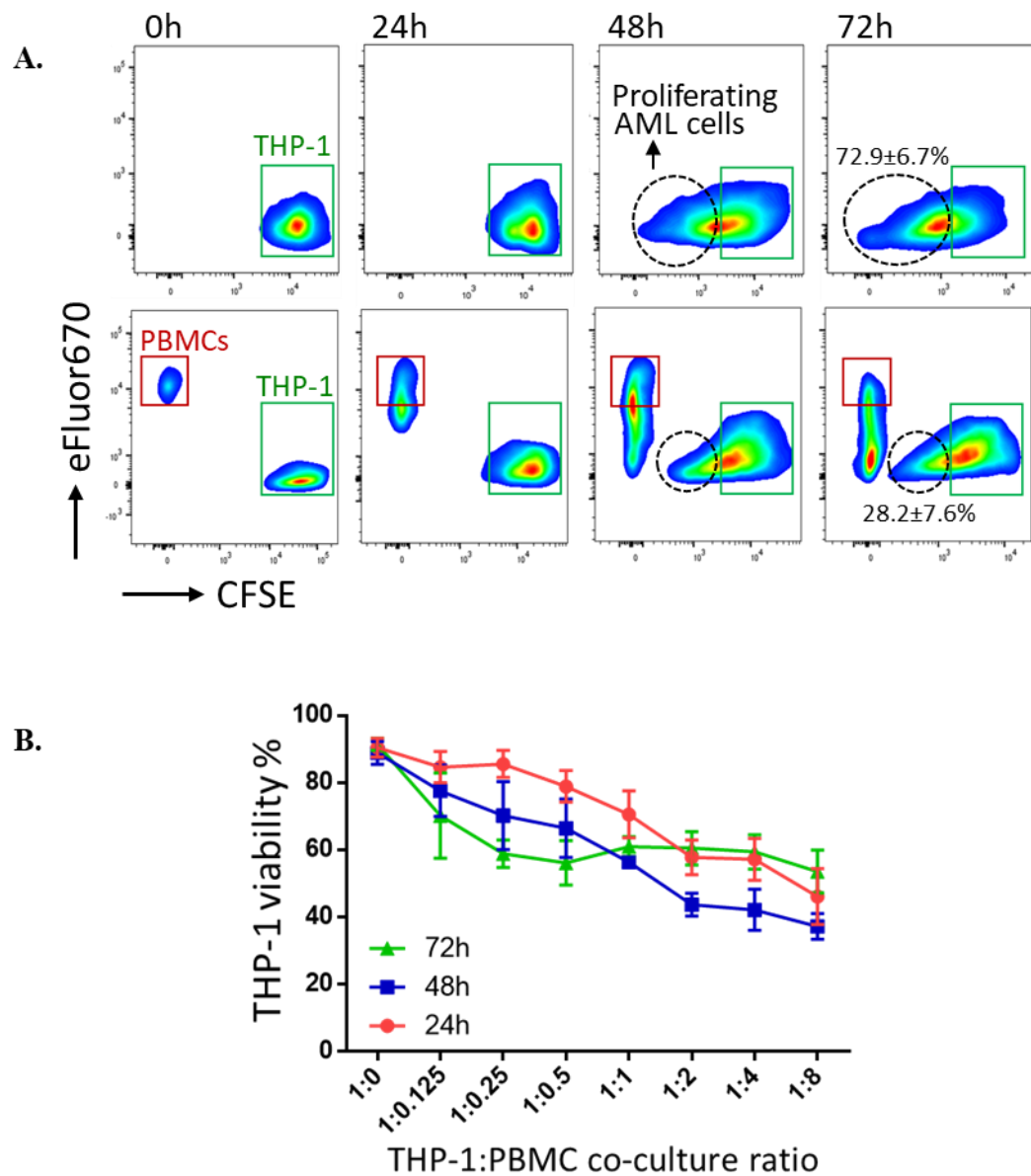


Figure 4.1. **A)** Allogenic PBMCs and AML cells were labelled with eFluor670 and CFSE proliferation tracer fluorescent dyes, respectively, and the mixed-leukocyte-leukemia cell reactions (MLLRs) were established for 72h in the presence of T cell stimulating CD3 mAbs. Representative flow cytometry plots for proliferation responses of the co-cultured PBMCs and THP-1 cells are shown. **B)** The change in viability of THP-1 cells in the MLLRs with increasing ratios of PBMCs was assayed at 24h, 48h and 72h by flow cytometry following staining with PI.

Next, using the above proliferation and viability results of the co-culture, an optimal AML cells to PBMCs ratio and incubation period was selected. The criteria

Next, for studying the after effects of MLLRs, the purified ieAML cells were maintained under standard culture conditions after the removal of immune responses and their proliferation capacity was further studied by staining with Ki67⁺. The frequency of Ki67⁺ ieAML cells was found to be less than that of wtAML following 72h incubation in culture (ieTHP-1 vs wtTHP-1 45.78±7.2% vs 80.56±5.05%, ieU937 vs wtU937 41.53±5.43% vs 79.65±3.68%, ieHL-60 vs wtHL-60 60.20±4.48% vs 86.75±4.31% (Fig.4.3 A, B).

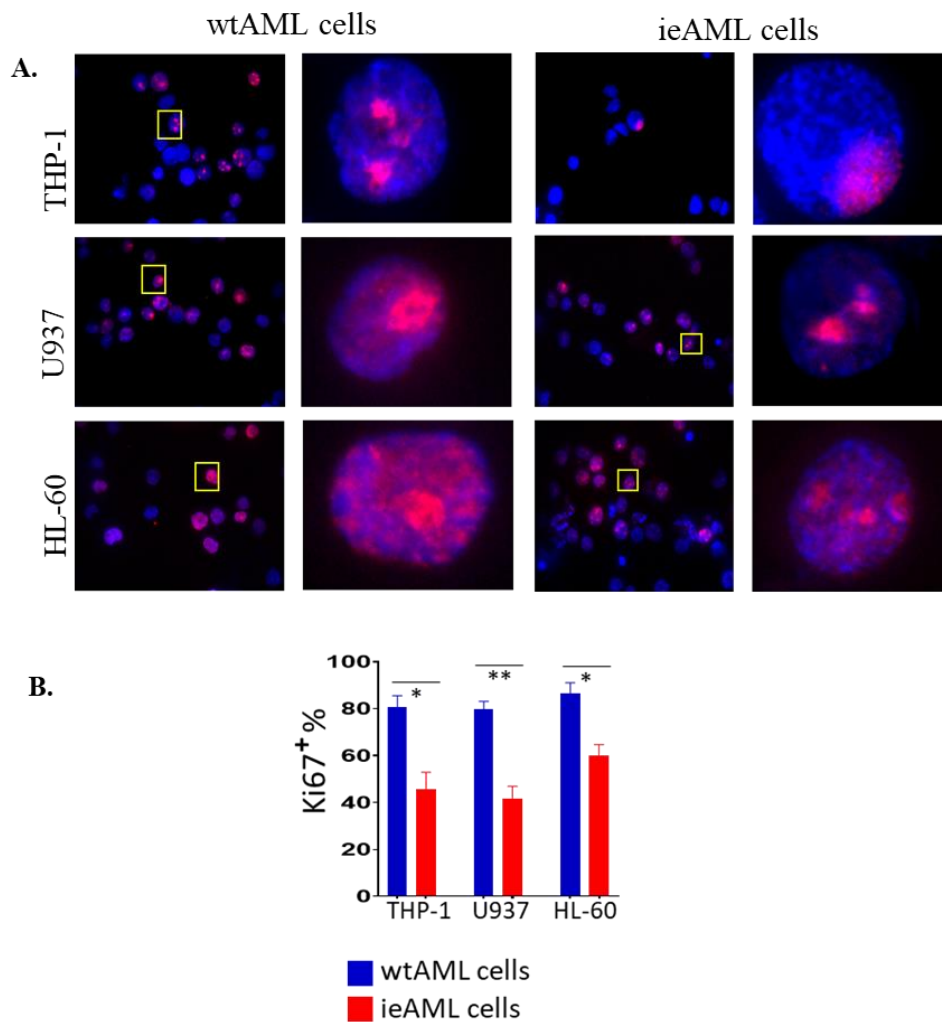


Figure 4.3. Proliferation capacities of wtAML and ieAML cells were determined by Ki67 staining. **A)** Immunofluorescence images of wtTHP-1, wtU937, wtHL-60 and ieTHP-1, ieU937, ieHL-60 are shown. **B)** Bar graphs display the mean percentage (±SEM) of Ki67-positive cells for each AML cell line that underwent the selection process. Scale bars, 10 μm. (*p ≤ 0.05, **p ≤ 0.01).

There was no significant difference in the cell cycle dynamics between these two cell populations (Fig. 4.4 A). These data were compatible with the finding that the ieAML cells continued to proliferate with a reduced pace even after removal from the MLLRs.

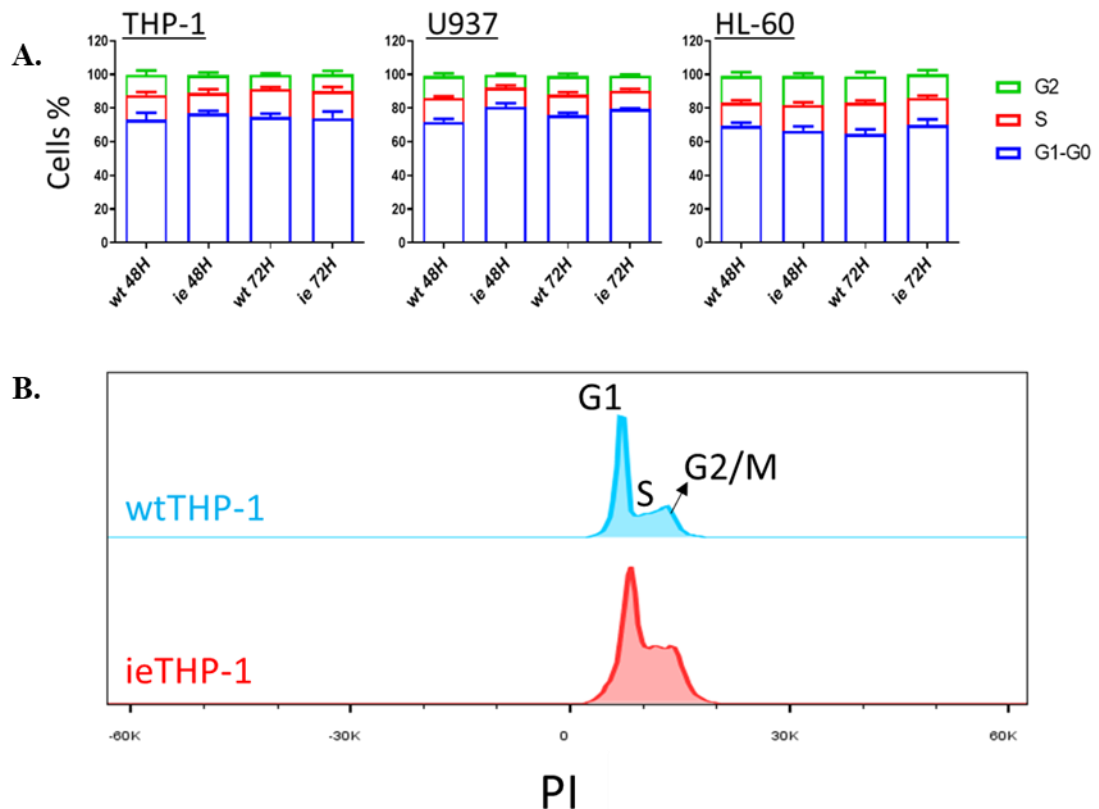


Figure 4.4. Cell cycle analysis of wtAML and ieAML cells after 48 hours and 72 hours resting in full media. **A)** Percentage distribution of the cells at G2/M, S and G1/G0 phases are shown for each cell line. **B)** A representative flow cytometry histogram showing the DNA content stained with PI in wtTHP-1 and ieTHP-1 cells.

In response to MLLRs, properties related to migration, adhesion, and polarization was also studied through Boyden chamber. In particular, the effects of immune responses on AML cell behaviour were investigated through the changes in the adhesion and migration and polarization capacities of ieAML cells. In general, AML cells were reluctant to migrate towards serum gradient. Only a small percentage of the cells migrated through 5 μm pore of the open chamber. As a result

of the Boyden chamber-mediated migration capacity analysis, the ieAML cells were able to migrate less effectively than wtAML cells at 24h displaying weaker migration capacities compared to wtAML cells with ieTHP-1 displaying less chemotaxis compares to wtTHP-1 (Fig. 4.5).

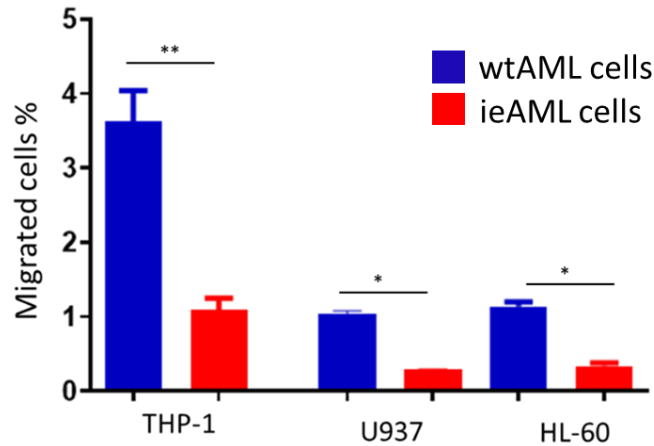


Figure 4.5. ieAML cells isolated and purified after 48 hour of co-culture with PBMCs were assessed for migration capacities compared with wtAML cells using Boyden chamber.

Next, we aimed to compare real-time changes in adhesion dynamics on surfaces coated with extracellular network proteins, namely fibronectin and Matrigel, as well as a control surface. Our findings indicated that both ieTHP-1 and ieU937 exhibited similar trends on both fibronectin and Matrigel-coated surfaces after 24 hours, showing a significant decrease in adhesion capacity compared to their wildtype counterparts. In contrast, ieHL-60 demonstrated an increase in adhesion capacity during the same time frame (Fig. 4.6 B). However, at the 48h, ieTHP-1 displayed an enhanced adhesion capacity on the fibronectin-coated surface compared to its wildtype counterpart. Meanwhile, both ieU937 and ieHL-60 still exhibited low adhesion capacity (Fig. 4.6 B).

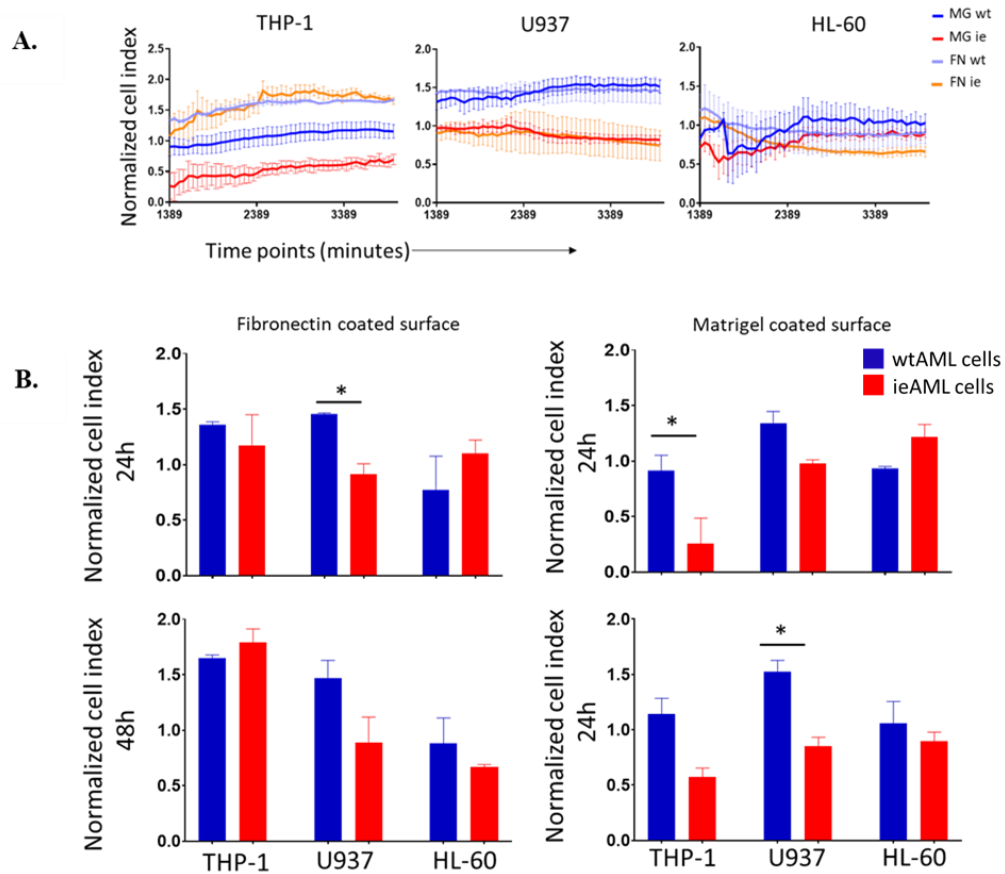


Figure 4.6. wt AML cells and ie AML isolated and purified after 48 hour of co-culture with PBMCs were assessed for adhesion. **A)** Migration assessed by Boyden chamber and XCELLigence real-time. Bar graphs showing adhesion capacities on fibronectin coated and matrigel coated surfaces at **B)** 24 hours and **C)** at 48 hours of incubation.

The polarization potential of these cells on uncoated surface and on fibronectin or Matrigel-coated surfaces for 24 hours was investigated. Directional analysis of the cell actin cytoskeleton after calculating polarity index showed that ieU937 had a distinct polarity on fibronectin-coated surfaces. Polarity of wtAML cells on fibronectin-coated surface indices were calculated as wtTHP-1, 0.07 ± 0.02 and ieTHP-1, 0.11 ± 0.07 ; wtU937, 0.03 ± 0.01 and ieU937, 0.12 ± 0.05 ; wtHL-60, 0.04 ± 0.01 and ieHL-60, 0.11 ± 0.06 . Whereas, on the Matrigel coated surface, the indices were calculated as wtTHP-1, 0.06 ± 0.03 and ieTHP-1, 0.07 ± 0.02 ; wtU937,

0.03±0.01 and ieU937, 0.08±0.02; wtHL-60, 0.05±0.01 and ieHL-60, 0.05±0.01. The ieTHP-1 cells were found to be more polarized on Matrigel coated surface compared to fibronectin, whereas ieHL-60 was found to be significantly more polarized on the fibronectin coated surface (Fig. 4.7 A).

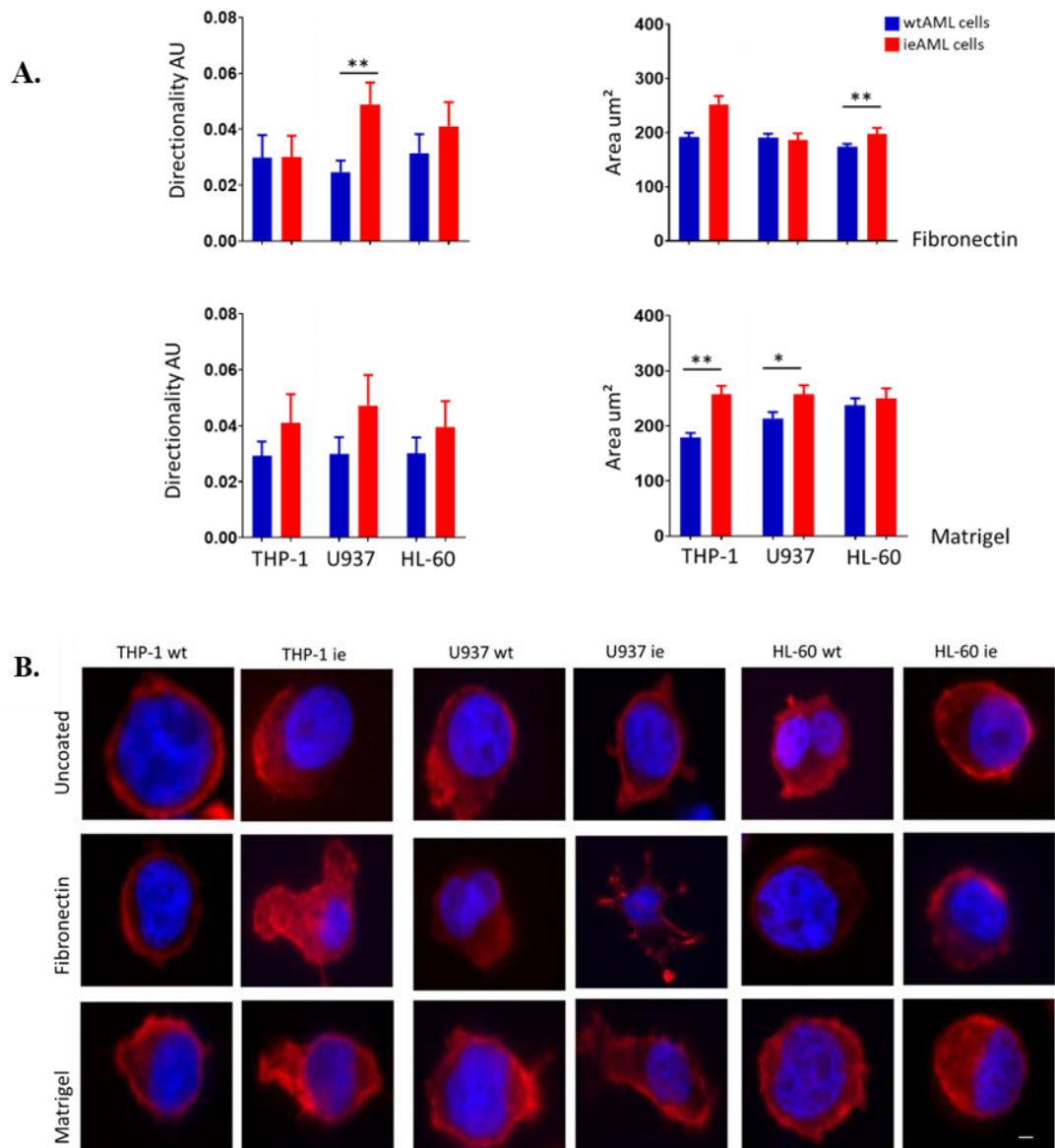


Figure 4.7. ieAML cells isolated from 48h of co-culture with PBMCs and wtAML cells were cultured on two different cell surface matrix fibronectin and matrigel for polarization. **A)** Based on cell area, cell perimeter and cell aspect ratio directionality of the actin cytoskeleton on different surfaces were calculated based on the

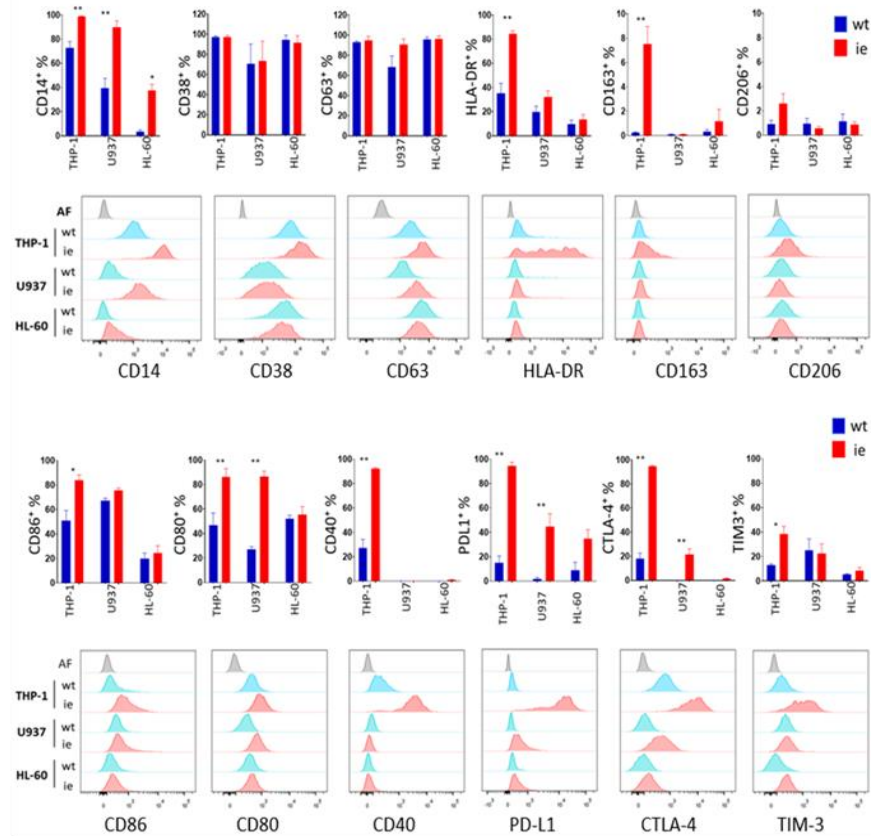
polarity index plot. **B)** Immunofluorescence staining showing cell surface representation of actin cytoskeleton orientations showing their polarity (nucleus, DAPI; actin, red). The scale bars are 10 μm . Statistical difference $p < 0,05$ * for $p < 0.01$ significance and ** for $p < 0.01$ significance.

4.2. Expression of Surface Markers Associated with Myeloid Activation and Differentiation

It has been commonly accepted that when the primary monocytes are cultured *in vitro*, they naturally undergo maturation, differentiating into cells with characteristics resembling macrophages (89). In contrast, myeloid leukemia cell lines like THP-1, U937, and HL-60 maintain their immature traits despite exposure to *in vitro* conditions. Therefore, following mixed lymphocyte leukemia reactions (MLLRs), we compared and studied the modifications in common myeloid markers associated with activation, differentiation, and maturation stages between wtAML and ieAML cells. Surface expression of different markers including CD14, CD38, CD63, HLA-DR, CD206, CD163, CD80, CD86, CD40, CTLA-4, PD-1, PD-L1 and TIM3 were studied and changes in their expression between ieAML and wtAML were determined (Fig. 4.8A). Expression of certain surface molecules, which are associated with myeloid cell activation and differentiation, tended to increase on the ieAML cells, more prominently on ieTHP-1 and ieU937 cells. The surface expression changes of various markers were assessed across three different cell lines. For CD14, the comparison between wild-type THP-1 (wtTHP-1) and its immune-experienced counterpart (ieTHP-1) revealed a substantial increase in expression from $75.68 \pm 6.73\%$ to $98.95 \pm 0.37\%$. Similarly, in the U937 cell line, CD14 expression increased notably from $39.50 \pm 8.06\%$ in the wild type to $90.08 \pm 5.23\%$ in the immune-experienced cells. In contrast, HL-60 cells exhibited a less pronounced change, with CD14 expression rising from $3.47 \pm 1.33\%$ in wtHL-60 to $37.63 \pm 5.05\%$ in ieHL-60. Regarding CD80, a significant increase in expression was observed across all ieAML cells lines upon MLLRs. For instance, in THP-1 cells, CD80 expression surged from $46.64 \pm 10.27\%$ in wildtype to $86.02 \pm 7.13\%$ in ieTHP-1 cells. Conversely, CD86 showed a more variable response, with THP-1 cells displaying an increase from $51.14 \pm 8.17\%$ in wild-type to

83.98±4.33% in ieTHP-1 cells, while U937 cells demonstrated a more modest rise from 67.13±2.29% in wtU937 to 75.73±1.83% in ieU937 cells. Additionally, HLA-DR expression increased notably in THP-1 cells from 35.33±8.21% in wild-type to 84.40±2.70% in immune-experienced THP-1 cells, while U937 and HL-60 cells showed more marginal changes. Notably, PD-L1 expression exhibited substantial increments across all ieAML cells upon MLLRs. In THP-1 cells, PD-L1 expression significantly increased from 14.84±5.77% in wild-type to 94.63±2.96% in ieTHP-1 cells. Similarly, in U937 cells, PD-L1 expression surged from a baseline of 1.68±1.30% in the wild type to 44.63±10.62% in the ieU937 cells. HL-60 cells, also showed a similar remarkable increase in PD-L1 expression pattern, rising from 2.46±0.15% in the wild type to 39.93±3.60% in the ie HL-60 counterpart (Fig. 4.8 A, B), highlighting its potential role in immune evasion mechanisms. The results were also presented as a heatmap for enabling better understanding and simultaneous comparison of distinct markers of the ieAML and wtAML cells. (Fig. 4.8 B).

A.



B.

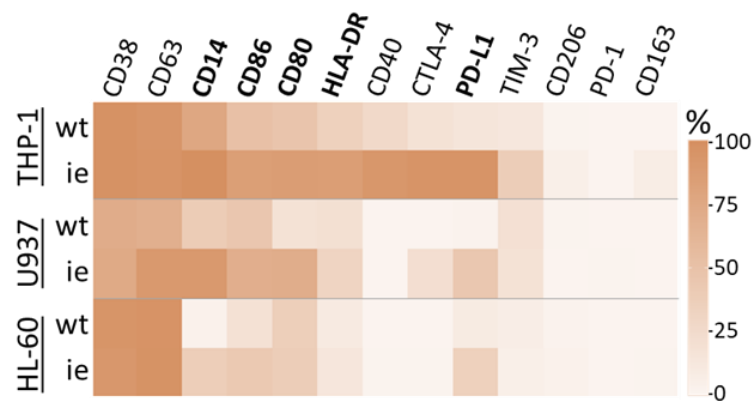


Figure 4.8. A) Immunophenotypic markers associated with myeloid activation and differentiation were analyzed by flow cytometry. B) The mean percentage results obtained from three independent analyses presented as a heatmap. The markers significantly modulated between wtAML and ieAML cells are typed in bold.

4.3. Assessment of ROS and NO Production

Freshly isolated ieAML cells were allowed to rest for 48 hours in full media without any stimuli, while wild-type AML (wtAML) cells were similarly used to assess the spontaneous production of reactive oxygen species (ROS) and nitric oxide (NO). Both cell types were subjected to PMA stimulation, and unstimulated cells were included to establish baseline levels for burst response analysis. Using mean fluorescence intensities of H_2DCFDA and DAF_2DA , the MFI of PMA-stimulated cells was normalized to that of unstimulated cells to calculate the ROS and NO indices. Despite observing no significant differences between wtAML and ieAML cells in terms of ROS and NO production, the ieAML cells exhibited a reduction in both ROS and NO production. Among the ieAML cells, ieU937 displayed a slightly more pronounced decline in ROS and NO production compared to ieTHP-1 and ieHL-60 (Fig. 4.9 A, B).

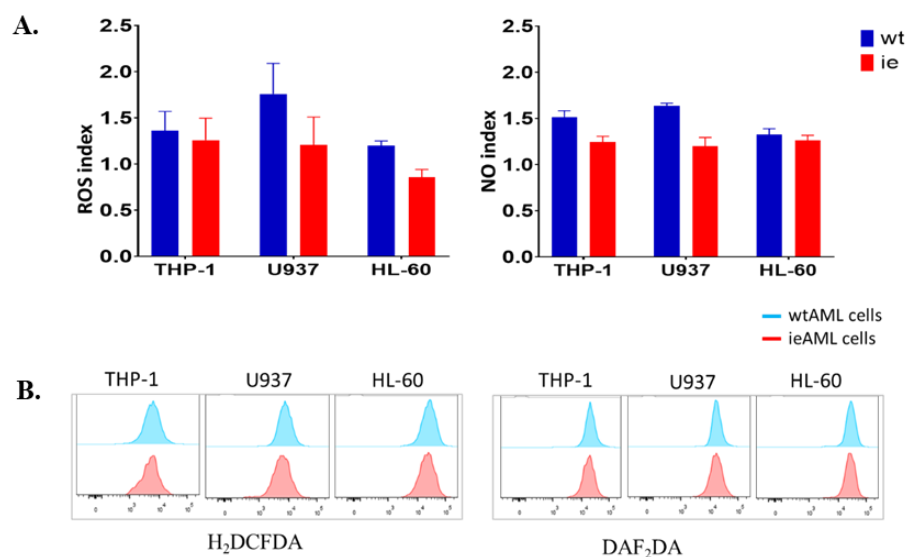


Figure 4.9. ROS and NO levels in wtAML and ieAML cells. **A)** Bar graph showing ROS and NO level between wt and ie AML cells. **B)** Representative histograms depict the fluorescence intensities of H_2DCFDA and DAF_2DA .

4.4. The Impact of ieAML Cells on T Cell Responses

The ieAML cells were resubjected to MLLRs to assess their immune modulatory capacities. Compared to the wtTHP-1 cells, the viability of ieTHP-1 remained constant in the presence of increasing numbers of the CD3-activated PBMCs proportions (at ratios of 1:0, 1:0.25, 1:0.5, 1:1, respectively: $100\pm 6.53\%$, $96\pm 6.68\%$, $93.51\pm 7.17\%$, $93.73\pm 6.99\%$). In contrast, the viability of wtTHP-1 cells decreased with rising PBMC numbers in the culture (at the same ratios: $100\pm 1.26\%$, $60.43\pm 3.41\%$, $42.73\pm 3.65\%$, $34\pm 4.76\%$) (Fig. 4.10 A).

In order to study the effect of ieAML on T cell proliferation, the ieAML cells freshly purified from the MLLRs were co-cultured with increasing amounts of CD4⁺ T cells and CD8⁺ T cells isolated from healthy individuals under CD3 stimulation for 72h. The MLLRs with wtAML cells were used as controls. CD4⁺ T cells and CD8⁺ T cells were highly proliferated when co-cultured with the wtAML with increasing numbers of T cells (e.g., at ratios of 0:1, 1:2, respectively: wtTHP-1:CD4⁺T cells, $3.5\pm 0.81\%$, $77.5\pm 3.06\%$; wtU937:CD4⁺T cells, $2.6\pm 0.63\%$, $86.1\pm 5.11\%$; wtHL-60:CD4⁺T cells, $1.9\pm 1.04\%$, $86.4\pm 4.78\%$; wtTHP-1:CD8⁺T cells, $4.1\pm 0.35\%$, $51.5\pm 8.69\%$; wtU937:CD8⁺T cells, $5.6\pm 1.50\%$, 66.9 ± 9.68). In contrast, ieAML cells did not support the proliferation of T cells at the same ratios (0:1, 1:2, respectively: ieTHP-1:CD4⁺T cells, $3.5\pm 0.81\%$, $18.5\pm 9.54\%$; ieU937:CD4⁺T cells, $3.8\pm 1.85\%$, $27.7\pm 15.66\%$; ieHL-60:CD4⁺T cells, $1.9\pm 1.04\%$, $77.0\pm 4.97\%$; ieTHP-1:CD8⁺T cells, $4.1\pm 0.35\%$, $10.4\pm 1.38\%$; ieU937:CD8⁺T cells, $3.7\pm 0.85\%$, $17.9\pm 14.28\%$) (Fig. 4.10 B).

Nevertheless, at 1:2 and 1:4 ratios of ieAML cell:T cell co-cultures, a minor increase in T cell numbers was observed. Interestingly, no significant difference was noted in CD8⁺ T cell proliferation induced by ieHL-60 and wtHL-60 cells, even with an increase in the AML:T cell ratio (0:1, 1:0.25, 1:0.5, 1:1, 1:2, 1:4, respectively for ieHL-60:CD8⁺T cells, $7.4\pm 1.40\%$, $46.1\pm 6.63\%$, $61.5\pm 6.00\%$, $74.5\pm 2.26\%$, $81.2\pm 3.73\%$, $75.1\pm 9.41\%$ and wtHL-60:CD8⁺T cells, $7.4\pm 1.40\%$, $61.1\pm 2.77\%$, $71.1\pm 0.87\%$, $72.0\pm 5.37\%$, $74.0\pm 6.35\%$, $76.3\pm 5.75\%$) (Fig. 4.10 B).

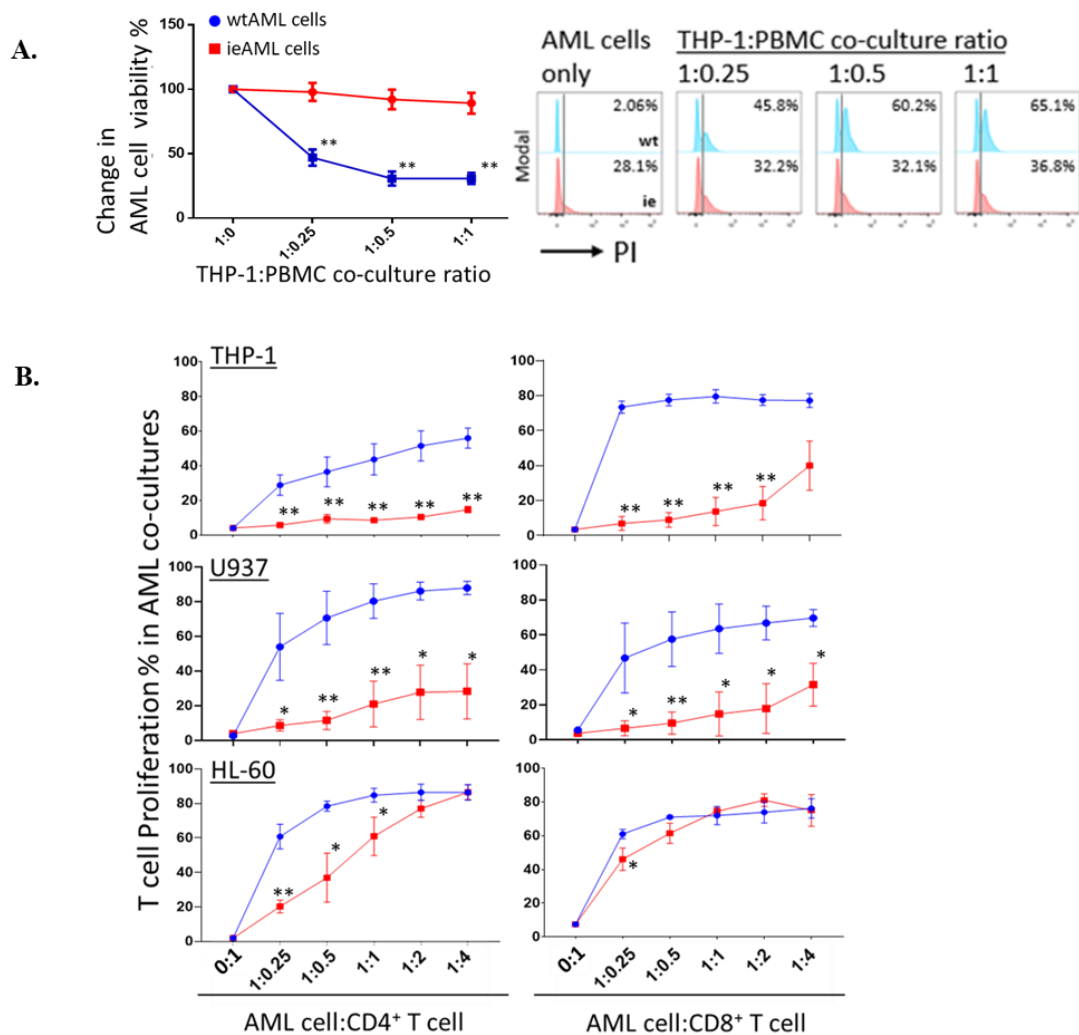
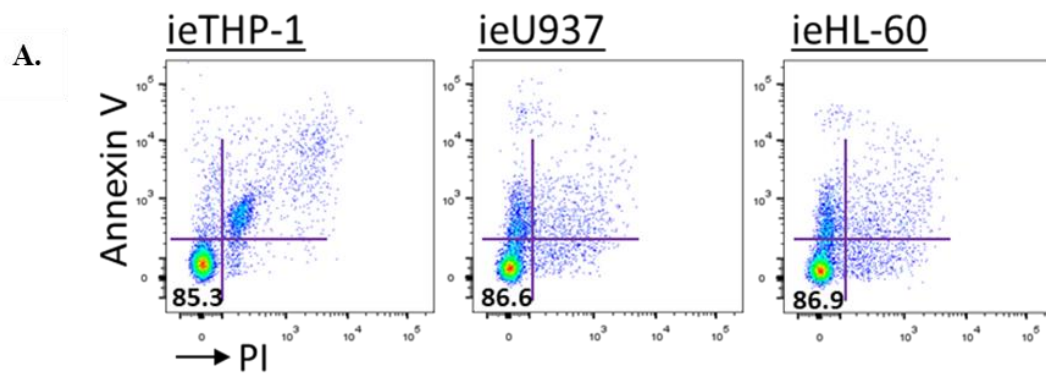


Figure 4.10. Re-exposure to immune reactions reveals functional assets of ieAML cells. **A)** The ieAML cells freshly purified from the MLLRs were co-cultured with increasing amounts of PBMCs under CD3 stimulation for 72h. The MLLRs with wtAML cells were used as controls. The change in viability of AML cells was determined by PI staining. (n=3, the data points are presented as average \pm SEM). Representative flow cytometry histograms are given below. **B)** The ieAML and wtAML cells were co-cultured with increasing ratios of CD4⁺ and CD8⁺ T cells. The percentage of proliferated T cells were calculated and plotted. Statistical difference was calculated with Student's t-test, (n=3, the data points are presented as average \pm SEM; *p \leq 0.05, **p \leq 0.01).

4.5. Transience and Heterogeneity of Immune Modulatory Capacities of ieAML Cells

Immune resistance might be transiently acquired in response to immune reactions (148, 149); therefore, the ieAML cells were established in long-term cultures and their viability, proliferation and immunomodulatory capacities were assessed. Viability of the ieAML cells was sustained upon continuous culturing (non-apoptotic cells > 85%) (Fig. 4.11 A). Nevertheless, the proliferation rates of the ieAML cells remained significantly slower than their parental wtAML cells, proliferation index of wtTHP-1 vs ieTHP-1, 3.28 ± 0.009 vs 0.31 ± 0.07 ; wtU937 vs ieU937, 3.82 ± 0.02 vs 0.43 ± 0.01 ; wtHL-60 vs ieHL-60, 5.00 vs 1.91 ± 0.05 (Fig. 4.11 B).

Next, impact of the continuously-cultured ieAML cells, hereafter termed as “ieAML (CC)” cells, on $CD4^+$ T cell and $CD8^+$ T cell responses was tested. In the presence of the ieTHP-1 (CC) cells, T cell proliferation was significantly lower than that of observed with the wtTHP cells. Nevertheless, similar percentages of T cell proliferation were induced in the co-cultures with the ieU937 (CC) or the ieHL60 (CC) and their wild-type counterparts (Fig. 4.11 C).



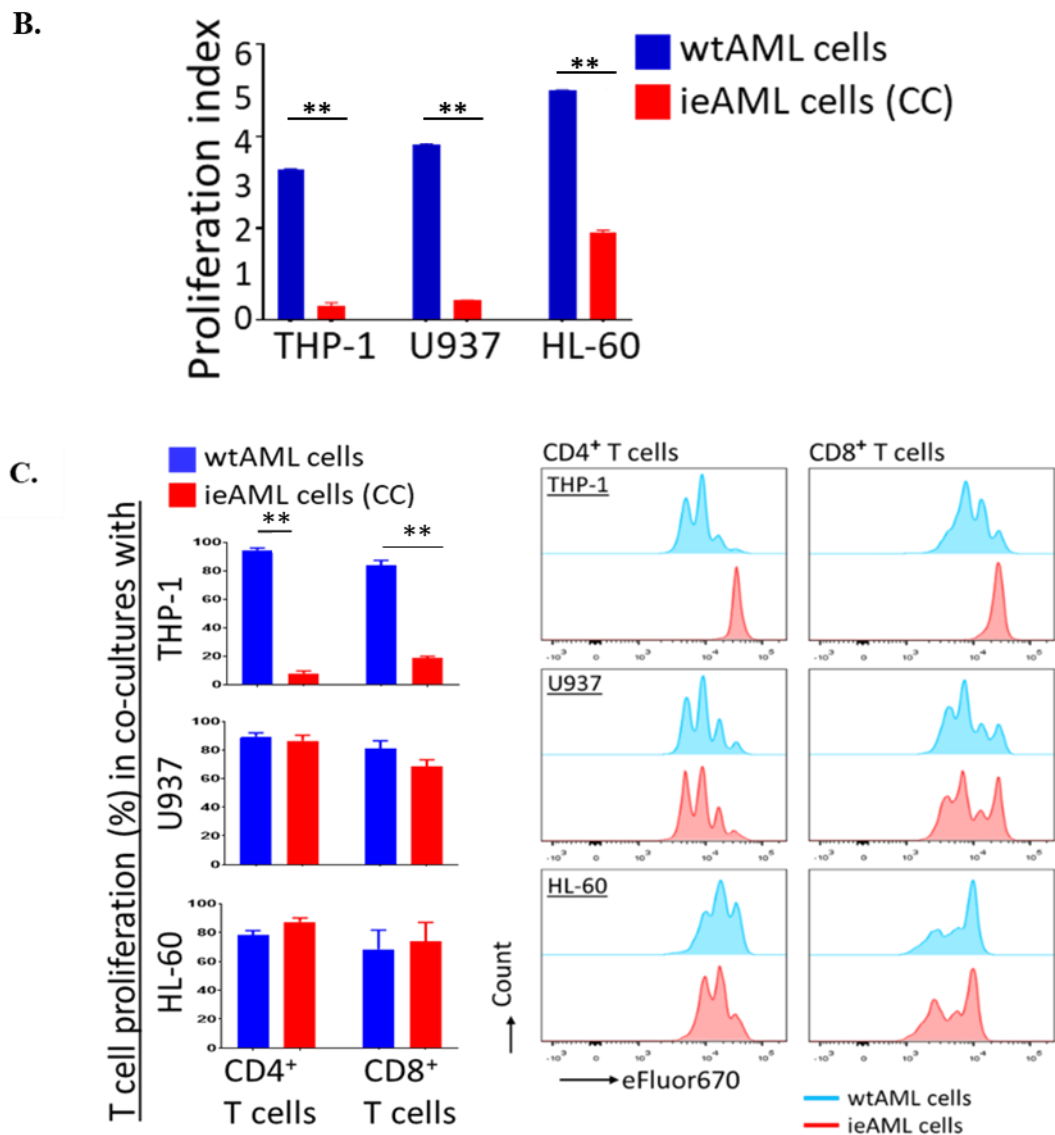


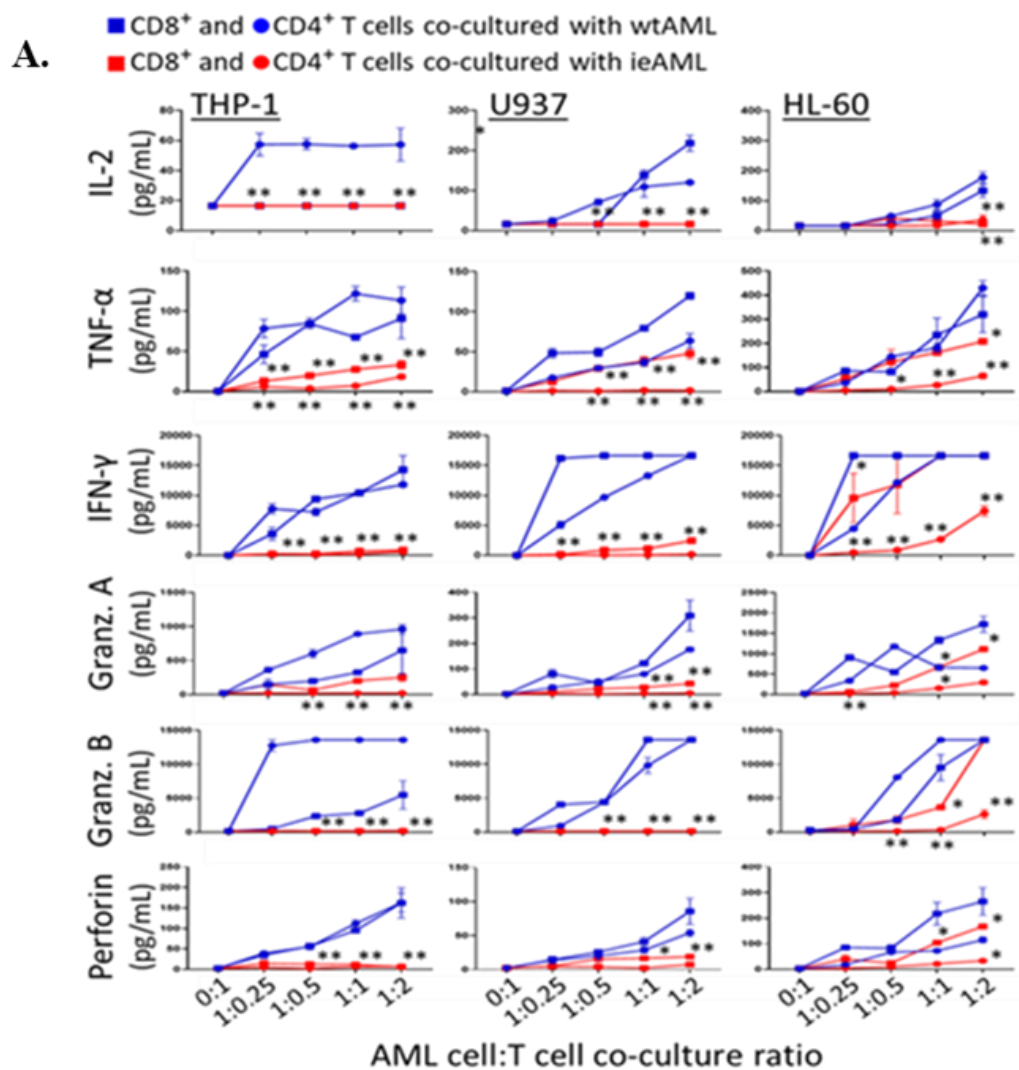
Figure 4.11. In vitro stability of acquired characters by ieAML cells. **A)** Amount of apoptotic cells upon long-term (> 96h) continuous culturing (CC) of the ieAML cells under standard conditions was assessed by annexin V and PI staining by flow cytometry. One representative image out of three independent experiments is shown. **B)** CFSE dilution assay for 72h was performed for determining the proliferation rate of continuously cultured wtAML and ieAML cells. (n=3, the data points are presented as average \pm SEM) **C)** The continuously cultured ieAML cells (CC) were re-exposed to CD3-stimulated CD4⁺ and CD8⁺ T cells. Proliferation of T cells was determined by flow cytometry for 72h. The data points are presented as average \pm SEM. Statistical difference was calculated with Student's t-test, (*p \leq 0.05, **p \leq 0.01).

While studying the T cell responses and proliferation in MLLRs with ieAML cells that are either ieAML cells and or continuously-cultured (ie AML CC) cells it was pertinent to analyze the cytokine responses. Thus, after 72h of MLLRs the supernatants collected were analyzed for the secretion of various T cell-associated cytokines. In parallel to the T cell proliferation, the secretion of IL-2, TNF- α , IFN- γ , granzyme A, granzyme B, and perforin, which are the important mediators for anti-tumor immune responses, were substantially diminished in the co-cultures of T cells and ieAML cells. Only, the levels of TNF- α , IFN- γ , and granzyme B secreted by CD8⁺ T cells in response to ieHL-60 did not significantly differ from those obtained in the presence of wtHL-60 cells (Fig. 4.12 A). In general, increasing the amount of CD4⁺ or CD8⁺ T cells in the co-cultures with wtAML cells resulted in a significant rise in the concentrations of these mediators compared to the co-cultures with ieAML cells (Fig. 4.12 A).

This reduced secretion further confirmed that, compared to wild-type AML counterparts, the ieAML subpopulation tends to be weakly immunogenic and less vulnerable to inflammation-induced cell death. Notably, continuously-cultured ieAML with CD4⁺ and CD8⁺ T cells showed an increase in T cell proliferation for ieU937 and ieHL-60 compared to freshly obtained ieAML cell co-cultures, indicating a transient or temporary acquired immune modulation capacity. Therefore, to study the dynamics of T cell-associated cytokine responses, we analyzed the supernatants from wtAML, freshly obtained ieAML cells along with continuously-cultured ieAML cells in response to CD4⁺ T cell and CD8⁺ T cell reactions. We presented the changes in cytokine release in the form of a heatmap after individual cell line normalization (Fig. 4.12 B). The co-cultures with ieU937 or ieHL-60 continuously-cultured cells resulted in a general increase in the release of cytokines involved in anti-tumor response, especially IFN- γ , which returned to the levels found in co-cultures with wild-type counterparts. Both ieU937 and ieHL-60 (CC) showed a similar trend for all cytokines, returning to almost the same levels as in wild-type AML co-cultures. On the other hand, albeit continuously-cultured ieTHP-1 cells retained low-level immunogenic properties and still exhibited reduced secretion of anti-tumor cytokines, including low levels of IL-2, TNF- α , IFN- γ , granzyme A, granzyme B, perforin, and sFASL. Among all cytokines, IFN-

γ appeared to be substantially more reduced in ieTHP-1 (CC) more than in freshly obtained ieAML co-cultures (Fig. 4.12 B).

The cytokine analysis of supernatants from T cell and ieAML co-cultures demonstrated a significant reduction in the secretion of T cell-associated cytokines that play a crucial role in promoting anti-tumor immune responses, including IL-2, TNF- α , IFN- γ , granzyme A, and granzyme B. It's worth noting that this response was transient and temporary for ieU937 and ieHL-60 (CC) cells.



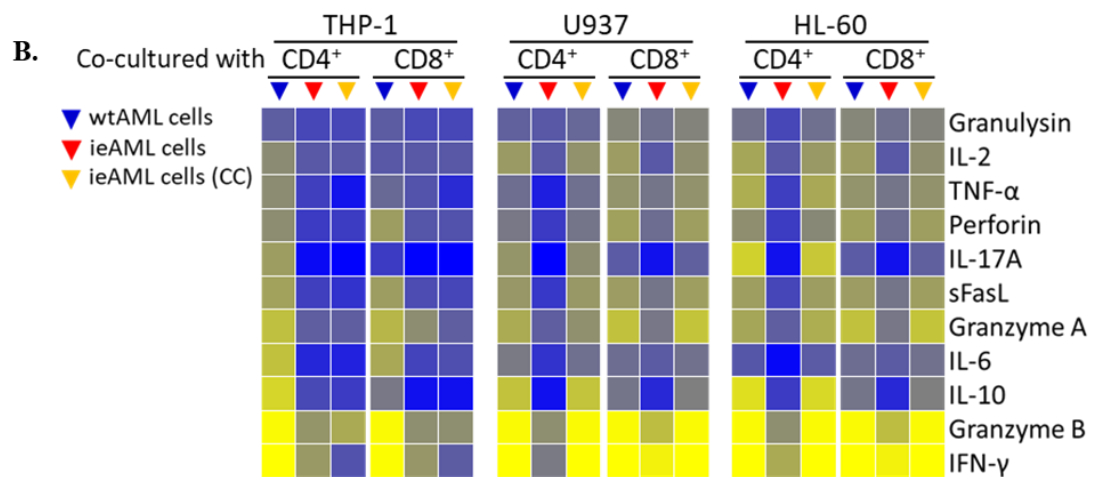


Figure 4.12. The amount of T cell-associated cytokines secreted in the co-cultures assayed by flow cytometric by multiplex bead-based cytokine assays. **A)** Graph showing major cytokines with decreased secretion in co-culture. **B)** The amount of cytokines secreted by the T cells cultured with the ieAML cells (CC) were normalized to those cultured with the freshly obtained ieAML cells was plotted as a heatmap. Statistical difference was calculated with Student's t-test, (* $p \leq 0.05$, ** $p \leq 0.01$).

4.6. Limited Number of Genes were Expressed as Common Indicators of the Immune Pressure on Myeloid Leukemia Cells

In order to reveal the molecular pathways involved in the emergence of ieAML subpopulations, transcriptomic analyses were performed. Intriguingly, the transcriptomic signatures of THP-1, U937 and HL-60 cell lines displayed restricted uniformity. Hence, the corresponding ieAML subpopulations derived from each cell line were also distinctive with specific gene expression profile, indicating the heterogeneous nature of AML (Fig. 4.13 A). Expectedly, the hierarchical clustering analysis revealed proximity between each ieAML population with its parental wtAML cell line where the ieTHP cells had the most distinguishing gene expression pattern (Fig. 4.13 B). Since our aim was to determine a common signature amongst the ieAML populations, the most differentially and commonly expressed genes in ieTHP-1, ieU937 and ieHL-60 cells were subjected to pathway analysis (Fig. 4.13 D). In terms of the gene expression changes, the ieTHP-1 cells (DEGs, total, 1483;

upregulated, 888; downregulated, 595) were the most affected from the MLLRs, followed by ieU937 (DEGs, total, 886; upregulated, 519; downregulated, 367) and ieHL-60 (DEGs, total, 287; upregulated, 208; downregulated, 79) (Fig. 4.13 C). A total of 77 genes was upregulated whereas only 7 genes were downregulated similarly in all three ieAML cells (Fig. 4.13 C, D). The genes involved in regulation of interferon signaling (*STAT1*, *IFI30*, *OAS1*, *STAT2*, *IFIT3*, *GBP1*, *GBP2*, *GBP5*, *IFI6*, *IRF1*, *IRF7*, *ISG15*), inflammatory cytokine signaling (*CXCL8*, *CXCL9*, *CXCL10*, *CCL2*, *CCL3*, *GZMB*, *IL-32*, *IL1 β* , *FCGR1A*, *S100A8*, *TNFAIP2*), antigen presentation pathways (*CD74*, *HLA-A*, *HLA-B*, *HLA-C*, *HLA-E*, *B2M*, *TAP1*, *TAPBP*, *PSMB9*, *PSMB10*, *PSME1*), apoptotic pathways (*CSRNP1*, *GADD45B*, *PIMI*, *MCL1*, *RELB*, *PPP1R15A*), cell adhesion and migration (*TUBA1A*, *RGS1*, *PRTN3*, *ICAM1*, *ITGB2*, *ITGB7*), and cellular stress response (*SOD2*, *NDRG1*, *NCF1*, *SGK1*) were regulated commonly in the ieAML cell populations when compared to their wild-type counterparts (Fig. 4.13 D and Fig. 4.14, 4.15 A).

All in all, only a limited number of differentially expressed genes were common in the ieAML cell populations which might be shared markers associated with the immune pressure on myeloid leukemia cells.

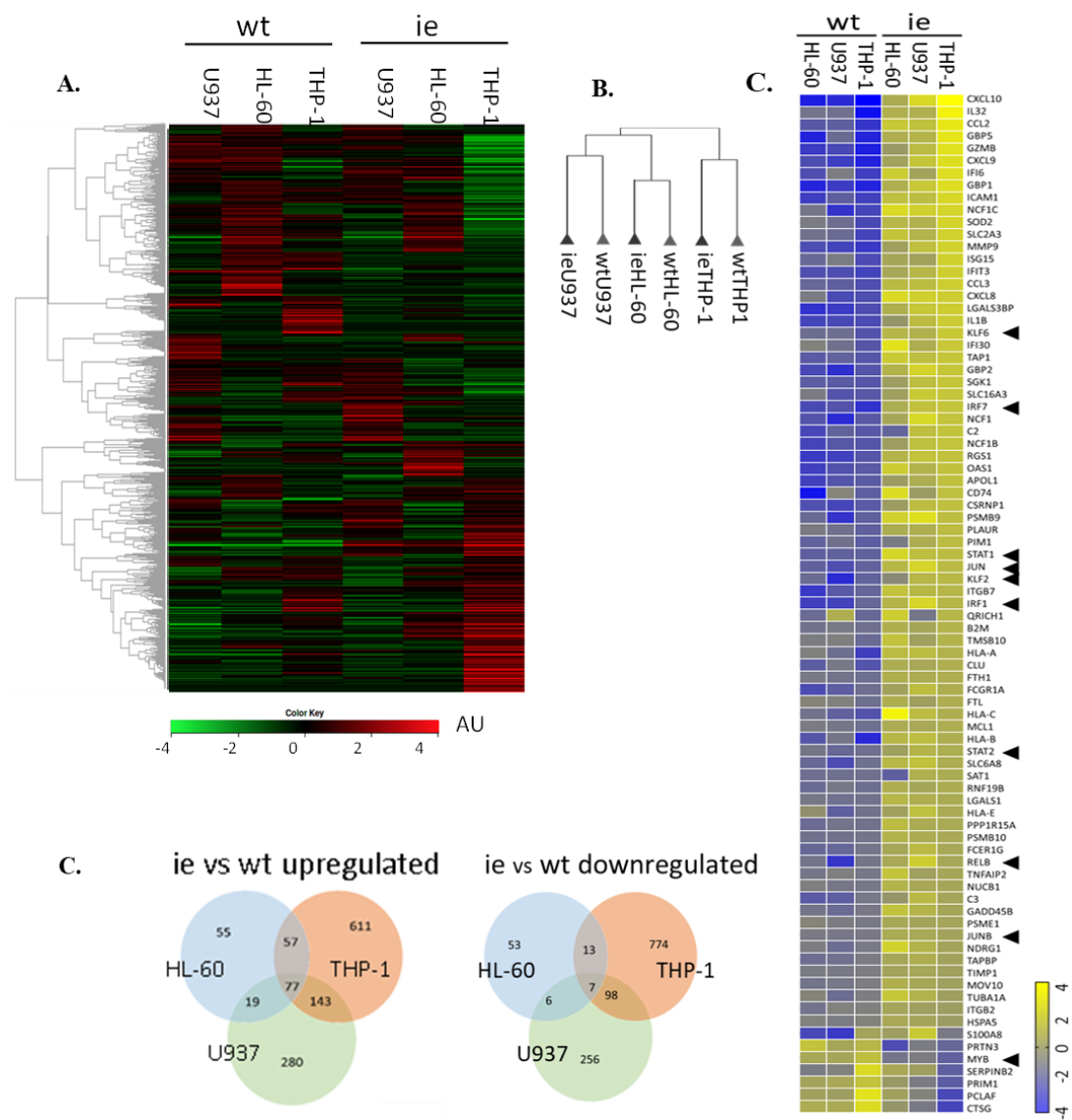


Figure 4.13. Transcriptomic analysis of the ieAML cells. **A)** RNA-seq heat maps are created and **B)** Hierarchical clustering analyses were performed on purified cells. **C)** Venn diagrams for upregulated and downregulated DEGs in the ieAML cells compared to their wtAML counterparts. **D)** Gene set enrichment heatmaps showing 84 common DEGs for all three ieAML cells.

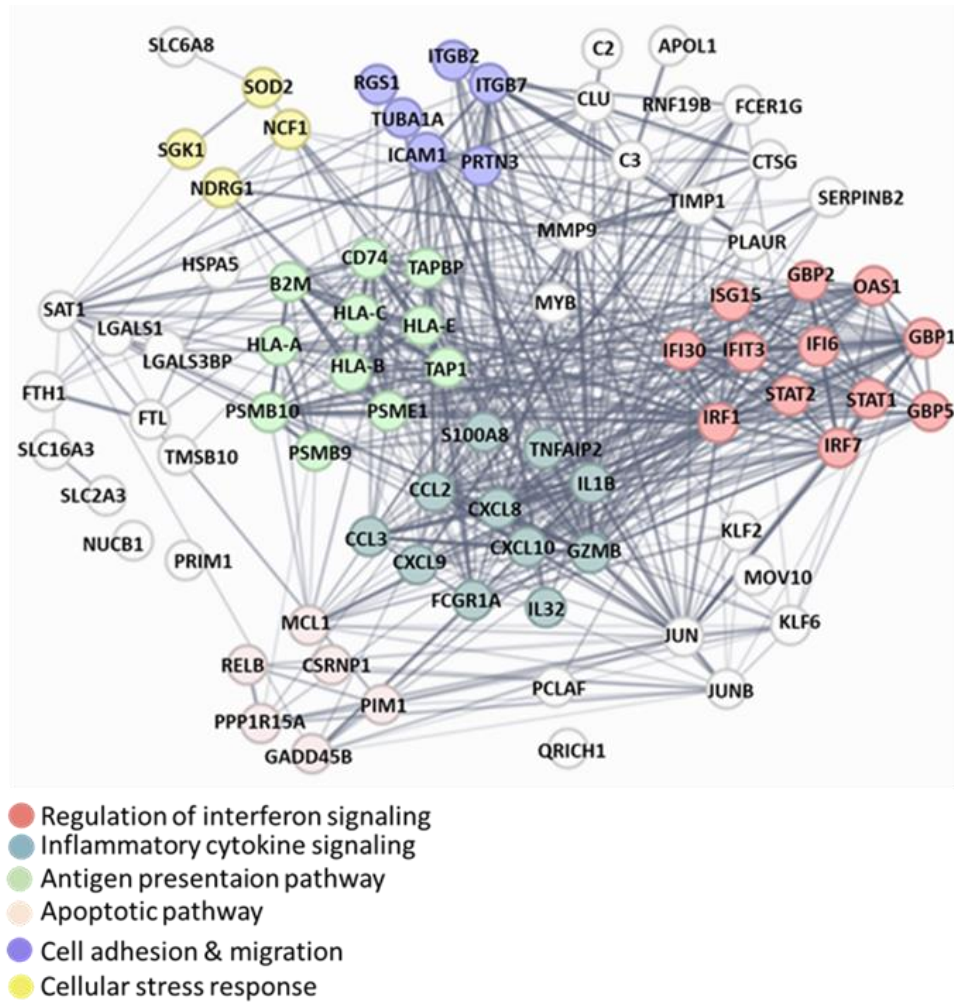


Figure 4.14. Network and pathway analyses commonly enriched in all three ieAML cells

The 84 DEGs were compared with the KEGG database to identify the major biological pathways regulated by genes common to all three cell lines. The gene set was later categorized into four groups: i. genes involved in inflammatory response, ii. apoptosis, iii. cytokine response, and iv. transcription factors (Fig. 4.15 A). Subsequently, these gene sets underwent pathway enrichment analysis. Importantly, the gene sets related to viral processes, anti-viral immunity, and viral infections, which are associated with the interferon signaling, were also upregulated (Fig. 4.15 B). Additionally, other enriched pathways included those related to antigen presentation, allograft rejection, cell-to-cell adhesion, cell migration, TNF

signaling, negative regulation of apoptosis, and pathways associated with graft-versus-host disease (Fig. 4.15 B).

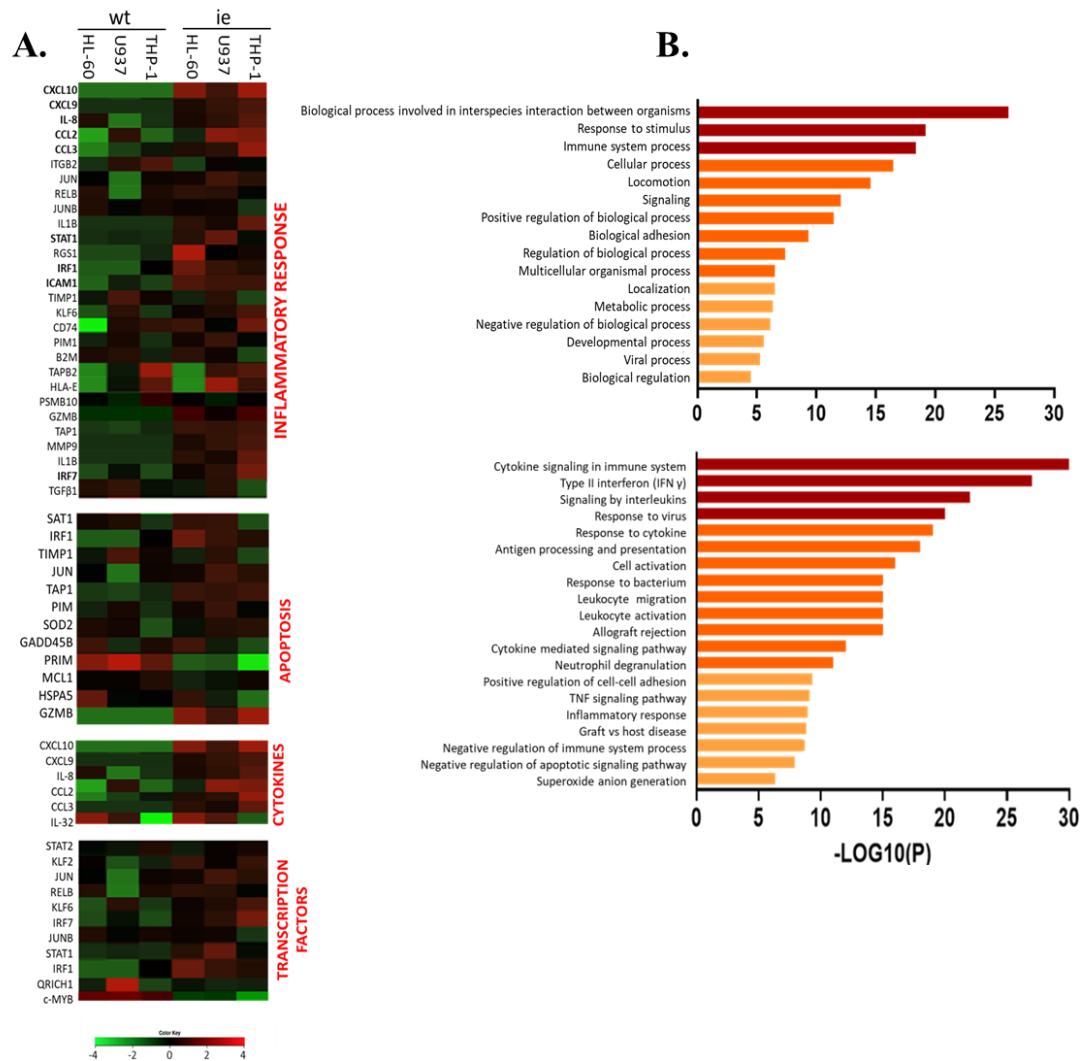
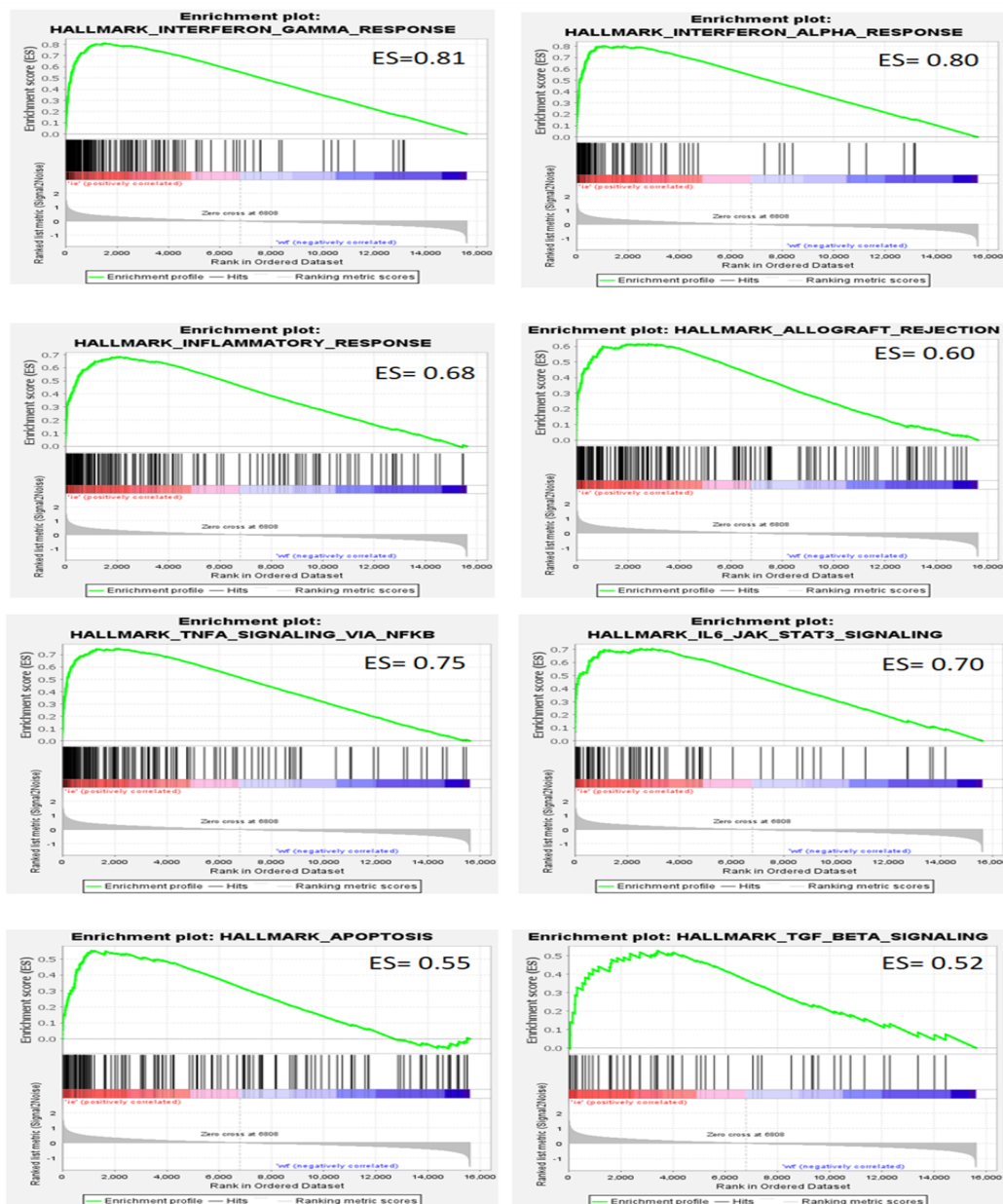


Figure 4.15. Heatmaps of the genes involved in enriched **A)** Major biological pathways from the KEGG database are plotted for the genes regulated commonly in all three cell lines studied. **B)** Enrichment of the pathways involved in biological processes and inflammatory responses are shown in the upper and the lower panels, respectively. The data from commonly regulated DEGs in all three cell lines are used for the analysis.

The gene set enrichment analysis (GSEA) revealed that the highly expressed genes which were shared by all three ieAML cells were compatible with those previously reported inflammatory response and allograft rejection response gene sets (nominal p value < 0.05) (Fig. 4.16). Hallmarks of inflammatory pathways such as IFN- γ , IFN- α , TNF- α , TGF- β , apoptosis, IL-6 and IL-2 signaling were also enriched. Reduction in the pathways related to cell proliferation including the targets of MYB transcription factor was also in accordance with the transcriptomics obtained from the ieAML cells (Fig. 4.14).



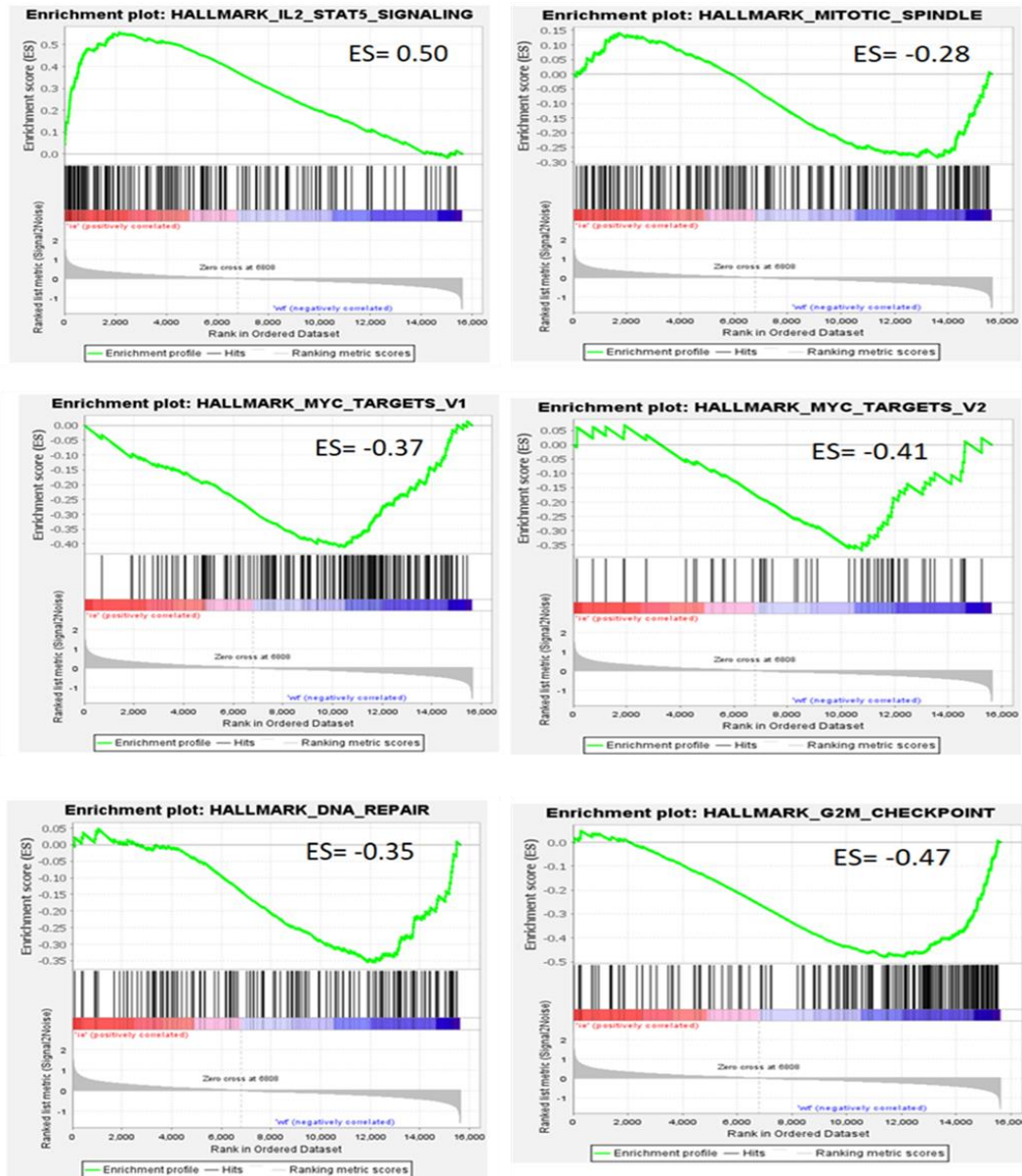
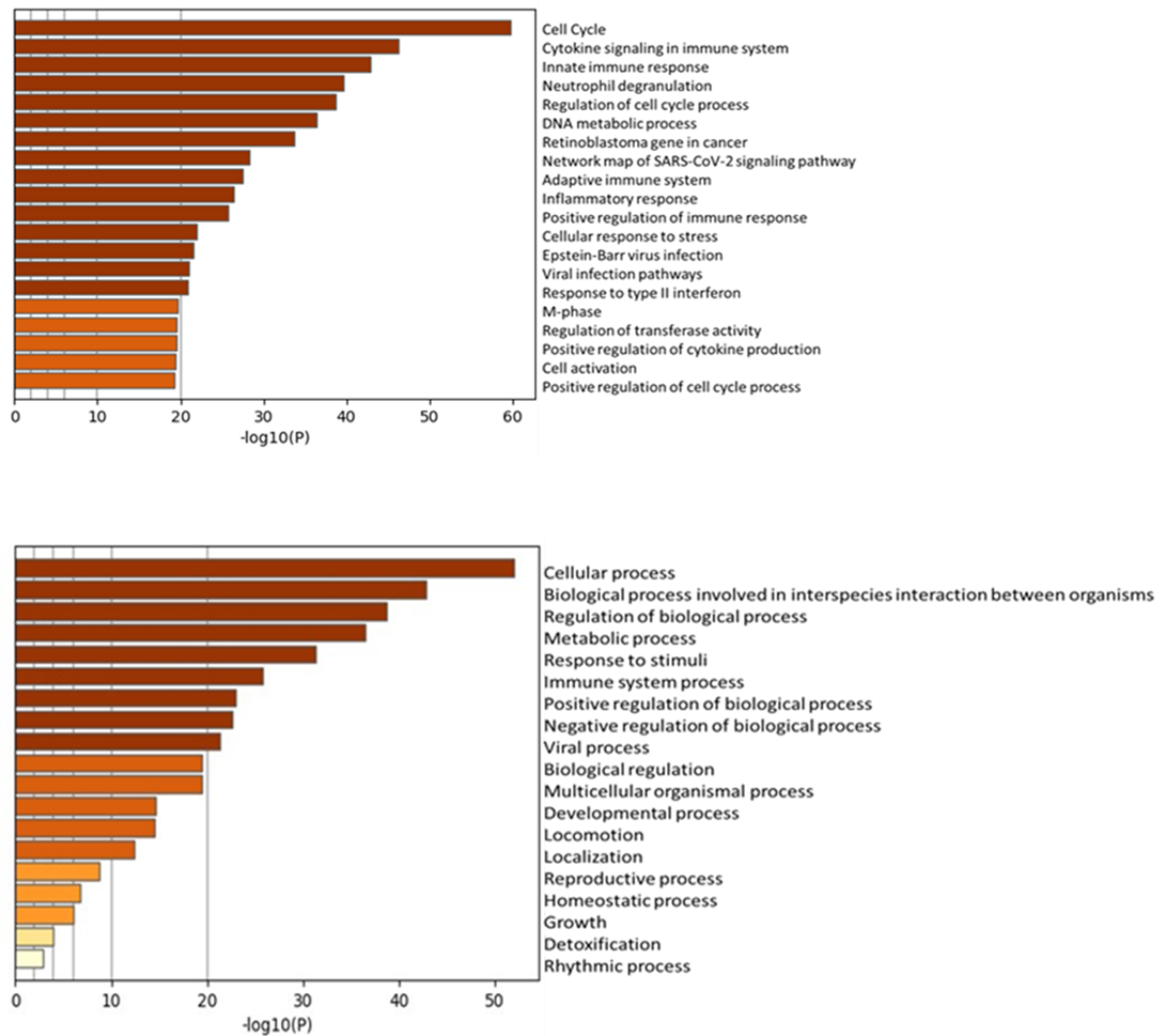


Figure 4.16. Gene set enrichment analysis (GSEA) of related gene sets. The most variable genes were ranked, and enrichment scores were calculated and plotted against the position of the genes within the rank ordered dataset using GSEA 3.0 software. The enrichment plots with the highest score are given.

AML cells are well-known for their heterogeneity. Therefore, individual AML cell lines underwent pathway analysis to reveal the differences among them, considering their distinct maturation stages (THP-1, U937, HL-60). In the previous section, we focused on commonly enriched pathways; here, we highlight the

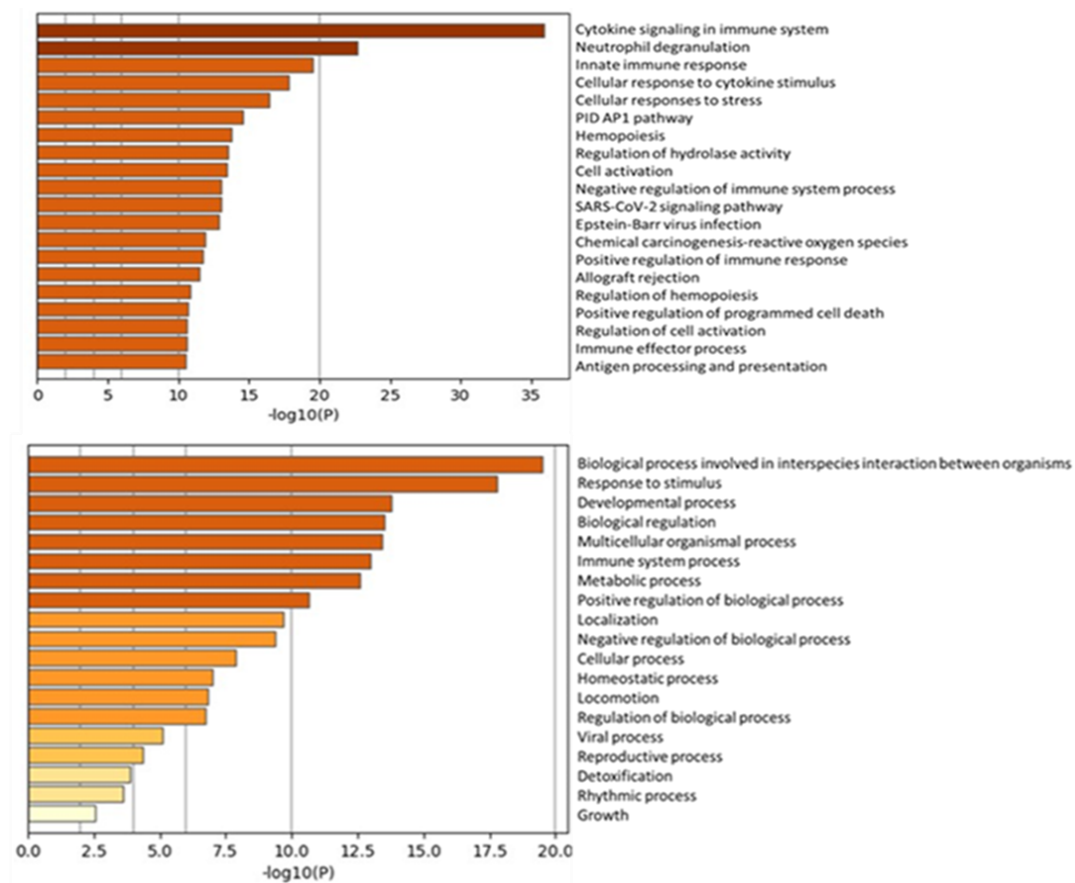
variation in pathway enrichment. In ieTHP-1 vs wtTHP-1, the most significantly enriched pathways included those involved in cell cycle regulation, cytokine signaling, neutrophil degranulation, inflammatory response, viral infection, and type II interferon pathways (Fig. 4.17 A).



A. ieTHP-1 vs THP-1

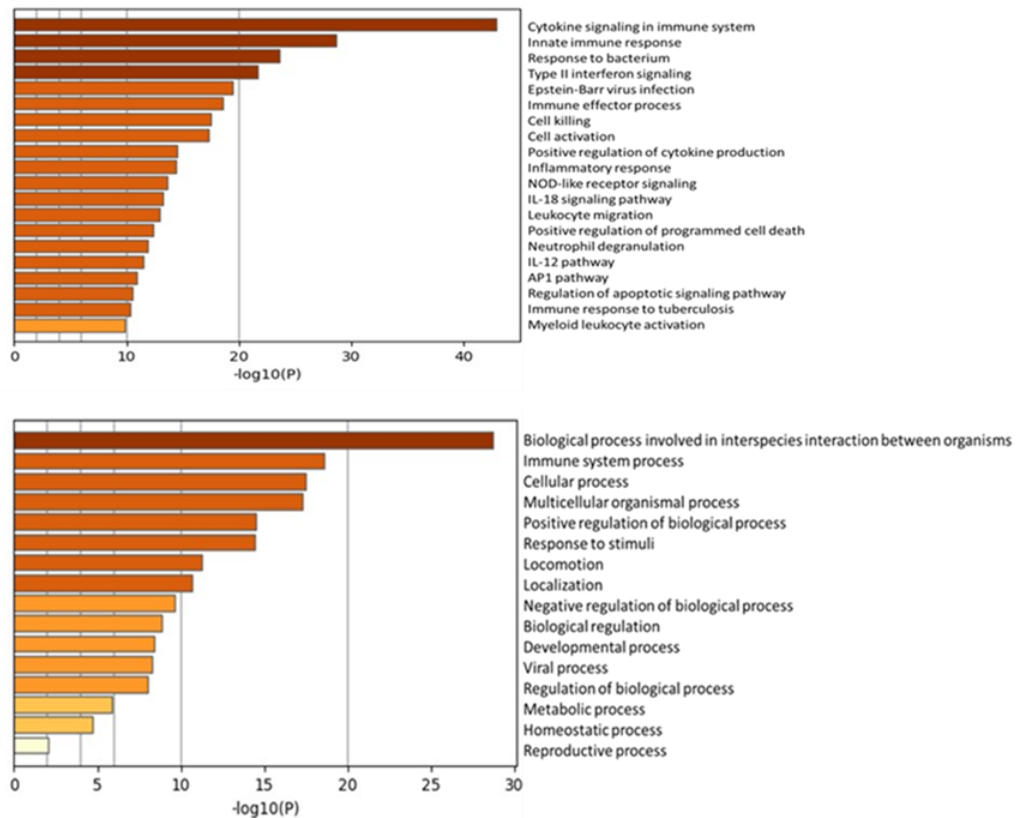
In ieU937 vs wtU937, there was enrichment in pathways related to cytokine signaling and regulation, cellular response to stress, PID/AP1 pathway, hematopoiesis and its regulation, reactive oxygen species, and pathways involved in allograft rejection (Fig. 4.17 B).

ieHL-60 also exhibited variation in enriched pathways, such as those involved in cell killing, leukocyte migration, IL-18 signaling, NOD-like receptor signaling, and pathways related to apoptosis (Fig. 4.17 C).



B. ieU937 vs wtU937

ieHL-60 and ieTHP-1 shared some common pathways, including cytokine signaling, innate immune response, type II interferon signaling, inflammatory response, and pathways related to viral response. Pathways involved in metabolic processes were enriched in all three cell lines; however, in ieTHP-1, it was one of the top-enriched pathways compared to ieU937 and ieHL-60 (Fig. 4.17 A, B, C).



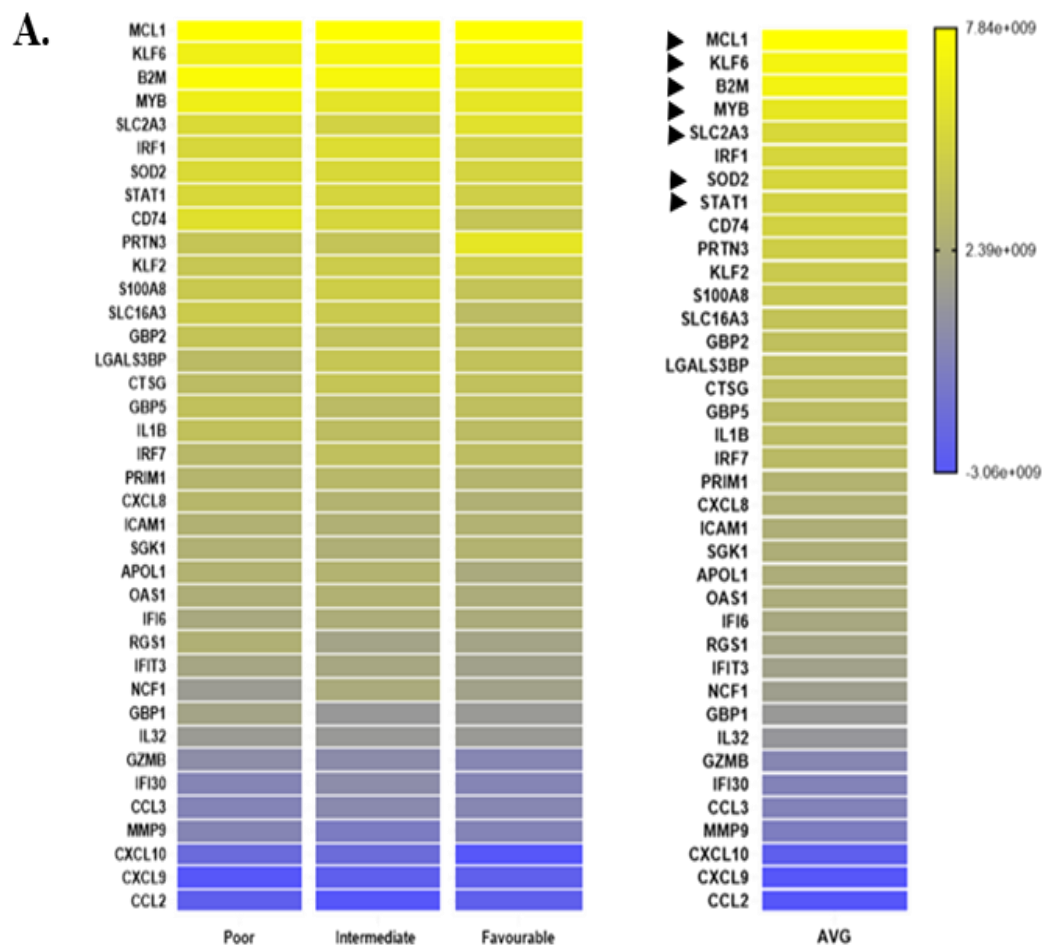
C. ieHL-60 vs HL-60

Figure 4.17. Enrichment of the pathways involved in biological processes and inflammatory responses are shown in the upper and the lower panels, respectively, for each cell line studied are given separately.

Nevertheless, the discrepancies among the transcriptomic signatures of individual ieAML cell lines indicate the heterogeneity in AML. The pathway analyses for individual ieAML lines showed the heterogeneity amongst the cells when subjected to MLLR. Of note, similar pathways were frequently regulated at distinct levels in each ieAML cell line (Fig. 4.17 A, B, C).

Next, the expression of 84 DEGs identified in the ieAML cells were evaluated through TCGA bioinformatics on AML patient data. Overall, 38 genes displayed significant expressions in AML patients' data. These 38 genes expression were evaluated in each prognosis group i.e favourable, intermediate and poor and later taking averages of each gene expression, overall expression from high to low

was presented in the form of a heatmap (Fig. 4.18 A). Out of these 38 genes the top 8 genes were selected based on the criteria that these genes have not been studied in AML immune response category : *MCL1*, *KLF6*, *B2M*, *SLC2A3*, *SOD2*, *STAT1* and *MYB* were the most regulated genes identified from the AML patient data (Fig. 4.18 A). Selected genes and their expression in individual patient's in each favourable, intermediate and poor prognosis group were evaluated and plotted in the form of dot plot (Fig. 4.18 B).



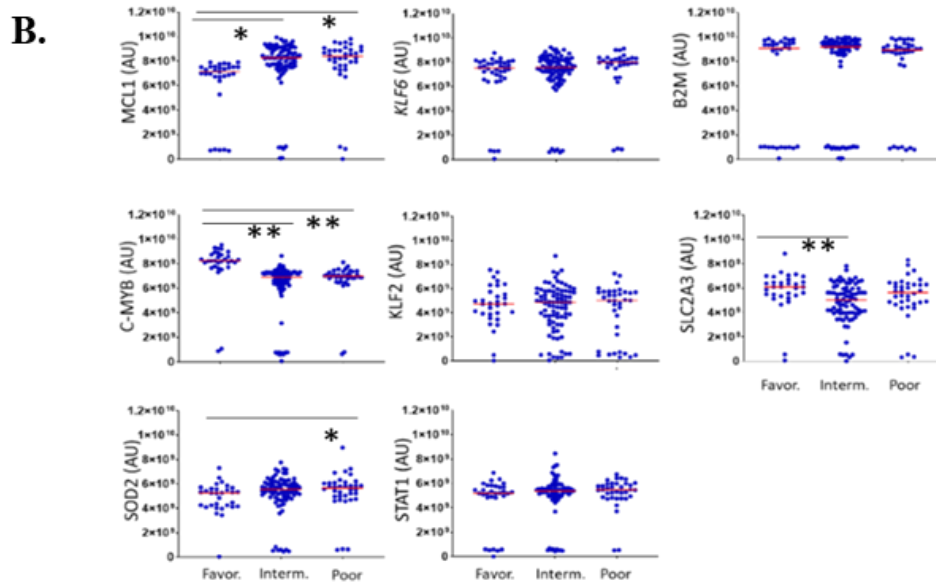


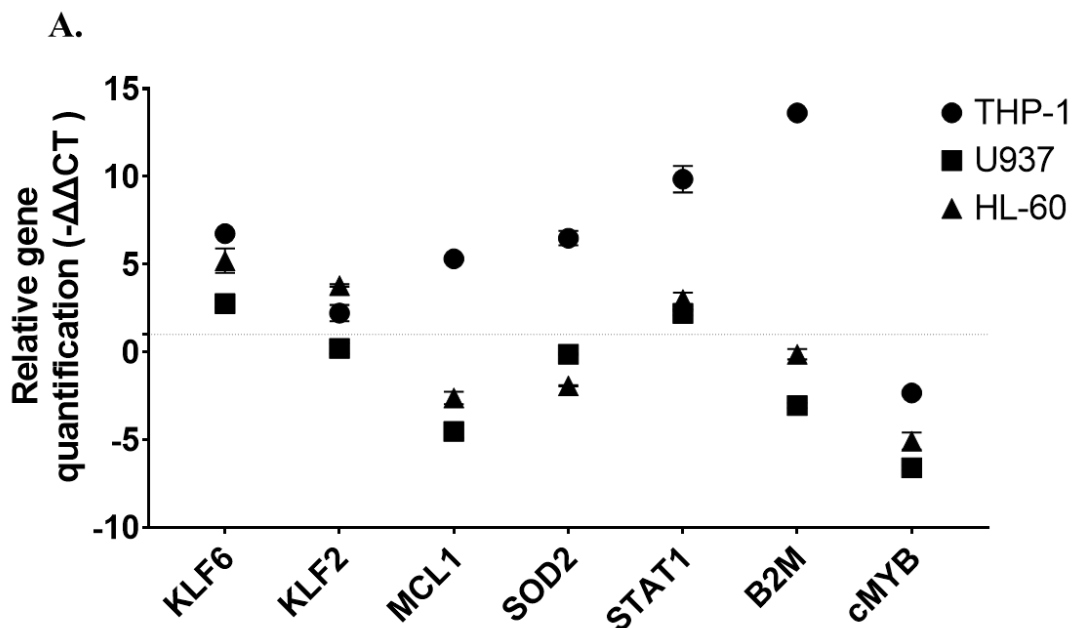
Figure 4.18. A) TCGA bioinformatics on AML patient data are analyzed for DEGs identified in the ieAML cells and presented as a heatmap. B) Selected gene expression in favor, intermediate and poor prognosis group represented as dot plot.

4.7. KLF6 and c-MYB as Transcription Factors Marking the Immune-Experienced AML Cells.

As only a limited set of genes exhibited common regulation in all three ieAML cells, our attention was directed towards those encoding transcription factors, particularly those with the capacity to influence cellular behavior. Among the 84 differentially expressed genes (DEGs), 9 were identified as transcription factors (Fig. 4.13 D, indicated by arrowheads). Notably, Kruppel-like transcription factor 6 (KLF6) and MYB genes emerged among the top two highly expressed transcription factors in AML patients based on TCGA bioinformatics analysis (Fig. 4.18 A, arrowheads). However, we investigated other genes also that occupied the top 10 spots in the patients' database, including MCL1, B2M, SLC2A3, IRF1, SOD2, STAT1, CD74, PRTN3, and KLF2. While the roles of some of these genes, such as STAT1, IRF1, CD74 and B2M, have been extensively studied in AML, our focus was on identifying a signature gene list responsible for immune resistance in

ieAML cells. To assess their expression, we conducted RT-PCR analysis. Interestingly, although the expression was high in the AML patients' database from TCGA analysis, the RT-PCR analysis yielded inconsistent results. The gene expression was elevated only in ieTHP-1 cells, while the other two cell lines, ieU937 and ieHL-60, showed variability in gene expression analyses (Fig. 4.19 A). Only KLF6 and MYB genes exhibited a consistent pattern of gene expression, as validated through quantitative gene expression analyses using RT-PCR (Fig. 4.19 A, B). Consequently, our focus shifted to KLF6 and c-MYB transcription factors, known to play crucial roles in regulating cellular processes including differentiation, maturation and proliferation (192, 193, 194).

In the ieAML cells, KLF6 exhibited a significant upregulation, while MYB was identified as one of the downregulated genes (Fig. 4.13 D). Furthermore, analysis of TCGA data revealed a significant decrease in MYB mRNA levels in patients exhibiting intermediate and poor clinical presentations. This observation prompted further exploration into the roles of KLF6 and MYB in the context of their potential implications in cellular processes and the pathogenesis of AML.



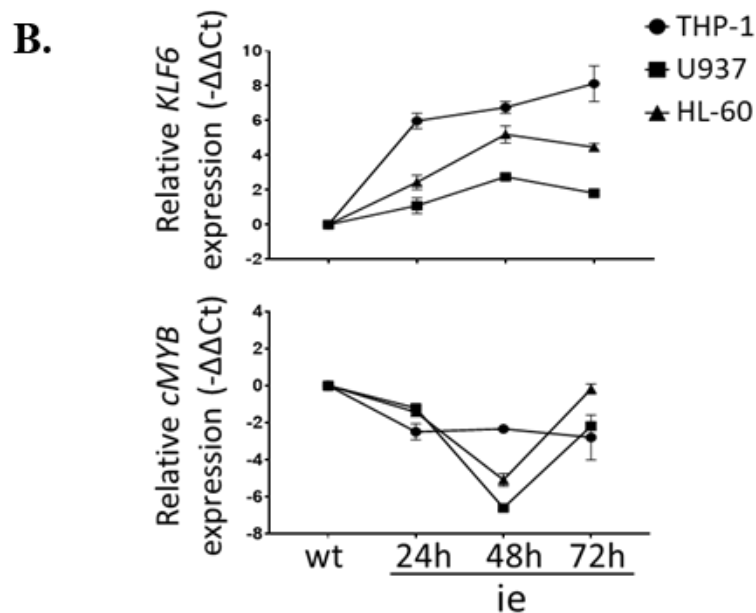


Figure 4.19. RT-PCR analyses **A)** Relative gene quantification for KLF6, KLF2, MCL1, SOD2, STAT1, B2M and c-MYB for ieAML cells. **B)** The expression dynamics of KLF6 and MYB genes were analyzed by quantitative RT-PCR in ieAML cells cultured alone for 72h. The RNA was pooled from independent experiments (n=6) and the RT-PCR analyses were done as two technical replicates.

After validating the KLF6 and c-MYB gene expression pattern in ieAML cells through q-RT PCR the next step was to study their cellular localization at the protein level by immunofluorescence. Here, we calculated the mean fluorescent intensity (MFI) of KLF6 and c-MYB between the wtAML and ieAML cells in the nuclear region of the AML blast cells. Interestingly, the nuclear localization of KLF6 was less frequently detected in wtAML blasts (Fig. 4.20 A). However, following MLLRs, the ratio of ieAML cells displaying KLF6 in the nuclei significantly increased from 60 ± 3.0 for wtTHP-1 to 79 ± 2.3 for ieTHP-1, 23 ± 2.1 for wtU937 to 53 ± 2.7 for ieU937 and 33 ± 1.59 for wtHL-60 to 67 ± 2.42 for ieHL-60 (Fig. 4.20 A, C). Conversely, the nuclear c-MYB declined upon exposure to MLLRs (wtTHP-1 120.4 ± 2.58 ; ieTHP-1 33 ± 3.2 ; wtU937 48.27 ± 1.72 ; ieU937 38.77 ± 1.87 ; wtHL-60 58.9 ± 2.8 ; ieHL-60 47.24 ± 2.54) (Fig. 4.20 A, C). Notably, a perinuclear staining pattern for these transcription factors, particularly in U937 cells, was also noted (Fig. 4.20 B, C). Furthermore, the percentage of AML cells

with KLF6 and c-MYB proteins in the nuclear region when calculated showed a decline in c-MYB in the nuclear region in ieAML cells compared to wtAML cells in all three cell lines THP-1, U937 and HL-60, respectively (80 to 30 %, 50 to 40% and 90 to 60%). Whereas, KLF6 percentage increased in ieAML cells compared to wtAML cells for THP-1, U937, HL-60 respectively (52 to 75%, 40 to 60% and 52 to 78%) (Fig. 4.20 B, C).

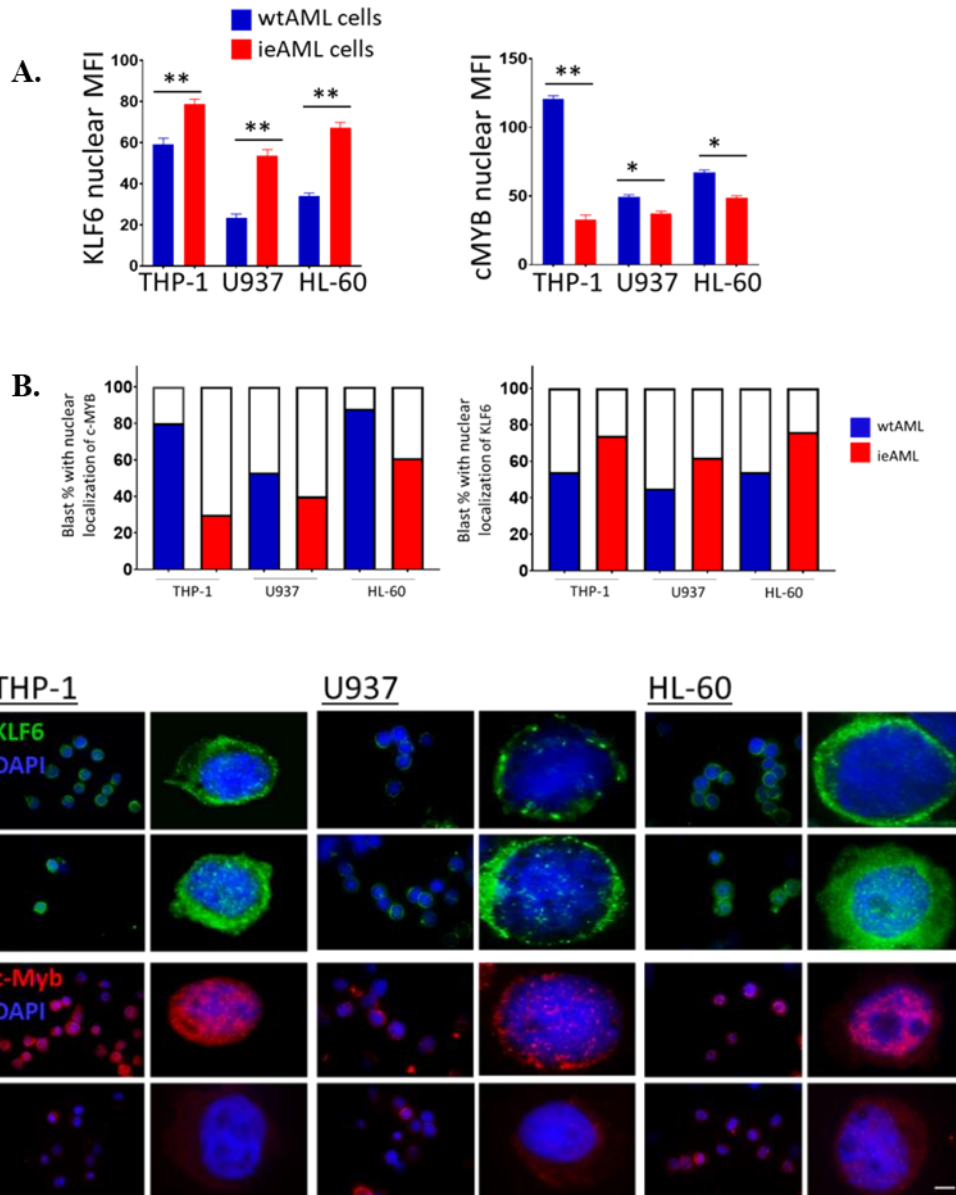


Figure 4.20. KLF6 and c-MYB expression in ieAML cells. **A)** The frequency of AML cells with KLF6 and c-MYB proteins in the nuclear region are plotted (n=3). **B)** Bar graph showing KLF6 and c-MYB nuclear MFI **C)** KLF6 and c-MYB immunofluorescence micrographs of wtAML

and ieAML cells. Higher magnification of a representative cell is shown on the right-hand side (scale bar, 1 μ m). One representative image out of three independent experiments is shown. The data points are presented as average \pm SEM. Statistical difference was calculated with one-way ANOVA, (n=11; *p \leq 0.05, **p \leq 0.01).

4.8. KLF6 and c-MYB Expression in Primary AML Blasts from Bone Marrow Aspirates of Patients

The transcription factors KLF6 and c-MYB, which were chosen from the total of 84 differentially expressed genes (DEGs) commonly identified in immune-experienced AML cells, exhibited clear differences in nuclear localization amidst wtAML and ieAML cells. Subsequently, AML patient samples were utilized to assess the nuclear localization status of KLF6 and c-MYB. In the bone marrow aspirates from newly diagnosed (n=6) or relapsed (n=5) AML patients, we observed a varied distribution of blast cells showcasing distinct nuclear levels of KLF6 and c-MYB (Fig. 4.21 A).

For each sample, the percentage of blasts exhibiting high-level nuclear localization of KLF6 (1.5 times higher KLF6 levels than the average blast population) and low-level nuclear localization of c-MYB (1.5 times lower c-MYB levels than the average blast population) was calculated. Generally, the majority of AML cells displayed low-level KLF6 (range, 62-100%) and high-level c-MYB (range, 67-100%) in the nuclear region (Fig. 4.21 A). Notably, there was an upward trend in blasts with high-level nuclear KLF6 in patients with relapsed disease (range at initial diagnosis, 0-27%; range at relapse, 20-38%). However, no discernible difference was observed between samples obtained at the initial diagnosis and those obtained at relapse for c-MYB (Fig. 4.21 A). Within the patient samples, a minority of the blast cells displayed a distinctive pattern, featuring elevated levels of KLF6 and reduced levels of c-MYB within the cell nucleus.

This observation underscores the heterogeneity in the nuclear distribution of these transcription factors among AML cells, suggesting potential implications for the disease's molecular characteristics and behavior.

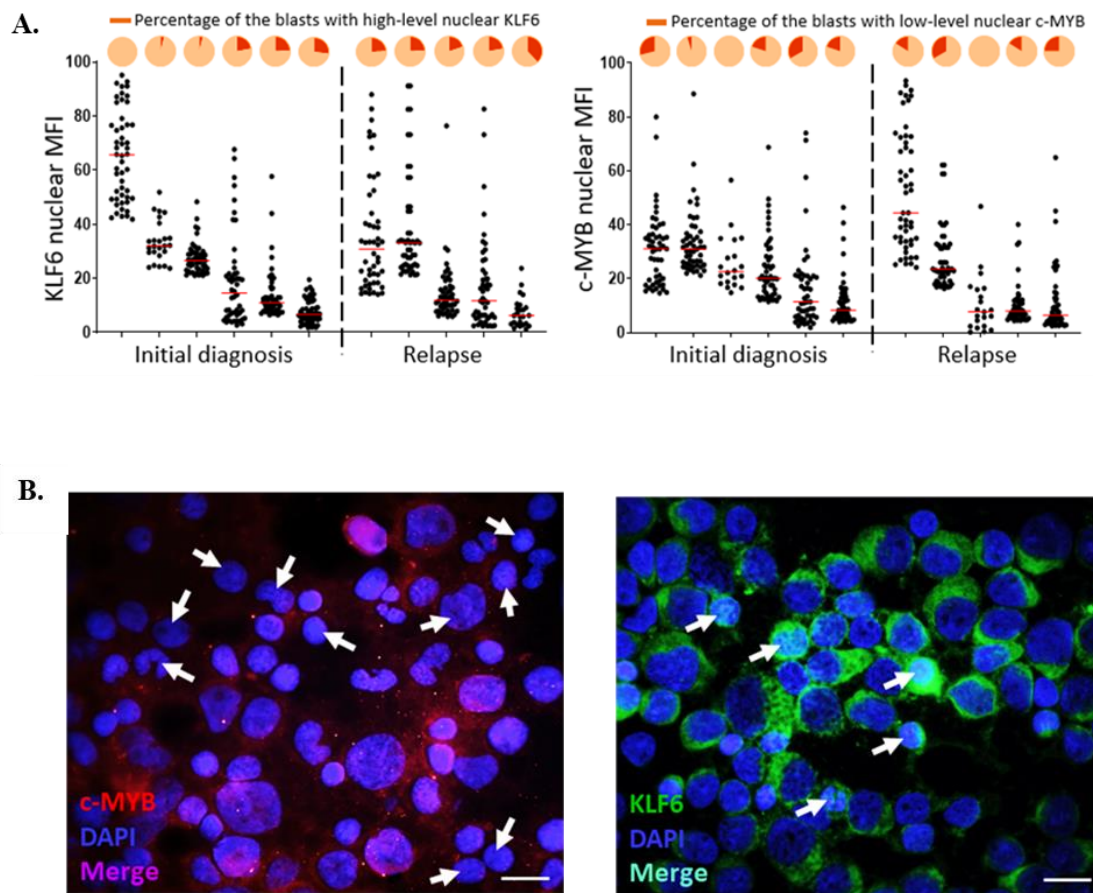


Figure 4.21. The level of nuclear KLF6 and c-MYB in the primary AML blasts from the bone marrow aspirates of patients (n=11). **A)** The pie charts given on top of the graphs show the percentage of AML blasts with 1.5 times higher levels of nuclear KLF6 or with 1.5 times lower levels of nuclear c-MYB expression than the average of the AML blasts found in each patient sample on the left-hand side and the right-hand side, respectively, each dot represents an AML blast, and the red lines represent the median values. **B)** Representative micrographs of the bone marrow aspirates, which display the heterogeneity of AML cells with nuclear localization of KLF6 and c-MYB, are given below.

5. DISCUSSION

Acute Myeloid Leukemia (AML) is a form of hematological malignancy characterized by the accumulation of immature blasts in both the bone marrow and bloodstream. These immature blasts typically inhabit niches abundant in growth factors and cytokines, fostering an environment that promotes tolerance against immune system responses. Recent advancements in genomic studies have revealed the genetic heterogeneity of AML cells, with certain subgroups displaying resistance to treatments, leading to the evolution of the tumor in response to therapeutic interventions (Turati et al., 2021). Throughout this process, marked by functional changes at both the genetic and epigenetic levels, blasts adapt by acquiring unique, temporally limited morphological, phenotypic, and genetic characteristics not observed in untreated or completely resistant cells. The removal of highly immunogenic tumor cells can lead to the emergence of malignant clones that possess enhanced abilities to withstand immune responses. This process involves the preferential survival and proliferation of tumor cell variants that exhibit superior resistance to the host immune system, potentially resulting in the development of a more aggressive and evasive tumor phenotype (163, 191, 195).

Cells derived from the myeloid lineage excel in presenting antigens and providing secondary signals crucial for eliciting T cell-mediated responses. This indicates that myeloid-origin cells play a proficient role in the immune system by effectively presenting foreign substances to T cells and facilitating the activation of immune responses. Myeloid cells, such as dendritic cells and macrophages, are essential components of the antigen-presenting cell (APC) population. They possess a unique ability to capture, process, and present antigens to T cells, initiating a cascade of immune responses. Additionally, these myeloid cells provide critical secondary signals that contribute to the proper activation and modulation of T cell-mediated immunity. This interaction, coupled with the delivery of co-stimulatory signals and other regulatory molecules, is pivotal for the effective initiation and regulation of T cell responses. The proficiency of myeloid cells in antigen presentation and secondary signaling highlights their crucial role in shaping the adaptive immune response. Understanding these processes is fundamental for

developing strategies to modulate immune reactions in various clinical contexts, including vaccine development and immunotherapy for diseases such as cancer. (196, 197). Cells associated with acute myeloid leukemia (AML) have the capability to exhibit elevated expression of costimulatory molecules. This means that AML cells can present heightened levels of proteins that play a crucial role in providing additional signals to immune cells during interactions, contributing to the modulation of immune responses. In the context of AML, the increased expression of costimulatory molecules on leukemia cells has significant implications for the interaction between these cells and the immune system. Costimulatory molecules are essential for the activation and regulation of immune responses. When AML cells express high levels of these molecules, it suggests an enhanced capacity to engage with immune cells, particularly T cells. The upregulation of costimulatory molecules on AML cells may influence the recognition and response of the immune system to the leukemia cells. It can impact the activation thresholds for immune cells and contribute to the overall immune evasion strategies employed by AML (10, 11). In the realm of acute myeloid leukemia (AML), it is common to observe the expression of major histocompatibility complex (MHC) molecules on the leukemia cells. These include both MHC class I and MHC class II, which play pivotal roles in presenting antigens to T cells, thereby influencing immune recognition and response against AML. Moreover, the activation of T cells within the bone marrow of individuals with AML implies an ongoing immune reaction. The activated state of these T cells suggests that the immune system is actively responding to the presence of AML cells in the bone marrow environment. This activation may be a reflection of the immune system's attempt to recognize and eliminate the leukemic cells, highlighting the dynamic interplay between AML and the immune response within the bone marrow microenvironment. Understanding these interactions is essential for developing targeted therapeutic strategies that harness the immune system to combat AML effectively (198). Myeloid leukemia cells have been acknowledged for their intricate strategies to evade the immune system, showcasing a notable resilience in adapting to anti-tumor immune defenses. This underscores the complex interplay between leukemia cells and the immune response, emphasizing the need for targeted therapeutic approaches that address

these adaptive immune escape mechanisms in myeloid leukemia. (8, 152, 155, 199). The dynamic interaction between the genetic and immune characteristics in acute myeloid leukemia (AML) results in significant diversity, raising the likelihood of the emergence of blast populations resistant to therapies and capable of thriving in unfavorable conditions. This complexity in the interplay between genetics and the immune response contributes to the heterogeneous nature of AML. The heterogeneity observed among leukemia cells increases the chances of certain populations developing resistance to therapeutic interventions. Moreover, these resilient blast populations can adapt and flourish even in challenging and unfavorable environments. Understanding and addressing this intricate interplay is crucial for devising more effective therapeutic strategies against AML, considering the potential for resistance and adaptability within the leukemia cell populations (148, 149, 200).

The constant evolution of leukemia cells through selection and adaptation remains active even during treatments like allogeneic bone marrow transplantation. In the context of graft-versus-leukemia (GvL) responses, where the transplanted immune cells attack the leukemia cells, the dynamic nature of selection and adaptation by the leukemia cells persists. This ongoing interplay can promote disease progression and increases the risk of relapse, emphasizing the need for comprehensive therapeutic strategies that consider and counteract the adaptive capacities of leukemia cells during various treatment modalities (6, 199, 201). The lack of substantial benefits from immunotherapy in individuals with acute myeloid leukemia (AML) underscores the need for a deeper comprehension of how leukemia cells elude the immune response. This understanding is essential for enhancing treatment options and developing more effective strategies to address the immune evasion challenges posed by AML (198, 202).

The results from our study demonstrated that within myeloid leukemia cells, there exist subpopulations that can evade the detrimental effects of the immune system. These leukemia cells, having encountered and survived immune responses, can adopt transient or enduring characteristics that aid them in navigating through anti-tumor immune reactions.

Another crucial roadblock is that the effectiveness of chemotherapy faces constraints due to multidrug resistance (MDR), a phenomenon in which cancer cells develop resistance to multiple drugs concurrently, rendering them impervious to various unrelated treatments. During multidrug resistance cancer cells, often through various mechanisms such as increased drug efflux or alterations in drug targets, develop the ability to withstand the cytotoxic effects of multiple drugs. This resistance poses a significant challenge in cancer treatment, as it reduces the effectiveness of diverse therapeutic agents intended to target the malignancy (203, 204). The mechanisms of drug resistance are frequently observed *in vivo* that the differences at genetic and epigenetic levels are demonstrated in residual disease (205). This implies that, in the context of actual biological systems, drug resistance often involves alterations at the level of both the genetic code and the epigenetic modifications of the cellular machinery. Moreover, the myeloid leukemia cells exposed to increasing concentrations of anti-cancer molecules are defined as drug-resistant subclones, *in vitro* (206, 207). This allows researchers to simulate and study the development of drug resistance in myeloid leukemia, offering insights into the mechanisms and behaviors of these resistant subpopulations. Analyzing drug-resistant subclones *in vitro* provides a controlled environment to investigate the dynamics of resistance and explore potential strategies to overcome or prevent it in the clinical treatment of myeloid leukemia. Leukemia cells employ various mechanisms to develop resistance to multiple drugs. For instance, some resistant cells exhibit diminished uptake or enhanced efflux of drugs, leading to a decrease in drug absorption or an increase in expulsion. This diminishes the amount of drug reaching its target within the cells, limiting its effectiveness. Additionally, resistance may arise from improved repair of damaged DNA, where heightened cellular mechanisms repair DNA damage caused by treatment, allowing cells to survive and proliferate. Alterations in drug targets and metabolism can also contribute to resistance by changing the molecular targets of drugs or cellular metabolic pathways, rendering them less susceptible to therapeutic effects. Furthermore, the suppression of cell death, where resistant cells evade treatment-induced apoptosis, allows these cells to persist despite therapeutic efforts, contributing to treatment resistance. These mechanisms collectively represent

major contributors to therapy resistance (208). The impact of tumor microenvironment and immune system has also been regarded as a factor contributing to MDR through various signaling pathways (209). However, resistance to immune intervention therapies such as checkpoint blockade and adoptive T cell transfer needs to be better defined (14, 210).

Therefore, in the current thesis study, a conceptual model outlining a gradual adaptation to immune responses, achieved through the acquisition of genetic and epigenetic modifications, has been suggested. In our study, we established an *in vitro* framework specifically designed to examine the biological alterations occurring in cancer cells (AML) and to assess their capacity for modulating the immune response. This approach allows for a detailed exploration of how cancer cells evolve and interact with the immune system, shedding light on potential mechanisms of adaptation and providing insights for future therapeutic strategies. Here, we used three AML cell lines with distinct maturation and differentiation properties and genetic backgrounds to model heterogeneous behavior of the AML blasts. Although not specific in nature, the T cell-mediated reactions initiated in co-cultures (MLLRs) involving myeloid leukemia cell lines and allogeneic immune cells served as a model for elucidating the molecular mechanisms underlying immune or secondary resistance. Analyzing the responses in this co-culture system helps us gain insights into the ways leukemia cells may evade immune recognition or mount resistance against immune attacks, offering a foundation for developing more targeted and effective therapeutic approaches.

The strength of T cell responses is contingent on robust costimulatory signals primarily transmitted via surface molecules from the B7 supergene family (211). The costimulatory molecules CD80, CD86 and ICOSLG are frequently expressed by leukemia blasts and may contribute to the immunogenicity of AML (11). Conversely, the regulatory implications of the costimulatory activity offered by myeloid leukemia cells may potentially contribute to immune evasion. This suggests that the interactions involving costimulatory signals from these cells could have consequences that aid in avoiding immune recognition and response (10, 11, 13).

Consistent with our present findings, various cancer types have been documented to exhibit heightened expression of checkpoint molecules, interferon response genes, and pathways associated with immune regulation in response to anti-cancer immunity (11, 13). In our study, the “immune-experienced” subclones ieAML cells were derived from three distinct AML cell lines, each possessing diverse characteristics and distinct biological attributes. This allowed us to explore a range of immune responses and evaluate variations in the underlying biological features among these subclones (212, 213) (THP-1 RRID:CVCL_0006), U-937 RRID:CVCL_0007, HL-60 RRID:CVCL_0002).

The AML cells with immune experience (ieAML) exhibited a slowdown in proliferation accompanied by heightened immune modulation capabilities, particularly during a specific timeframe. The impact of ieAML cells on T cell responses was found to be really interesting, that compared to ieAML cells, CD4⁺ T cells and CD8⁺ T cells highly proliferated when co-cultured with the wtAML with increasing numbers of T cells. However, ieAML cells retards CD4⁺ T cells and CD8⁺ T cell proliferation in the co-cultures with freshly obtained ieAML. However, this effect was transient in continuously-cultured ieU937 and ieHL-60 cells in contrast with ieTHP-1 which even in continuous culture showed impaired CD4⁺ T cells and CD8⁺ T cells proliferation. The analysis of cytokine secretion further confirmed that, in comparison to T cell-associated cytokine responses observed with wtAML, co-culturing T cells with ieAML cells led to a significant reduction in the secretion of key anti-tumor immune response mediators, such as IL-2, TNF- α , IFN- γ , granzyme A, granzyme B, and perforin during concurrent T cell proliferation. Notably, only the levels of TNF- α , IFN- γ , and granzyme B secreted by CD8⁺ T cells in response to ieHL-60 did not exhibit a significant difference compared to those observed in the presence of wtHL-60 cells. Interestingly, when using freshly obtained ieAML cells, both CD4⁺ and CD8⁺ T cell reactions with continuously-cultured ieU937 or ieHL-60 cells resulted in a general increase. Notably, the adverse impact of immune-experienced U937 and immune-experienced HL-60 cells on T cell responses appeared to be less persistent compared to that of immune-experienced THP-1 cells. The manifestation of "immune-experience" traits in THP-1 cells consistently aligned with observed

characteristics related to myeloid maturation and activation. This suggests a correlation between immune history, cellular behavior, and myeloid-related features in the context of THP-1 cells. Hence, the anti-tumor immune reactions stimulated through MLLRs, promptly induced a significant impact on leukemia blasts triggering the activation of alternative cellular programs aimed at ensuring cell survival while concurrently diminishing immunogenicity. The duration of this altered state varied among the residual populations. The persistence of this resistance is closely tied to the continuous selection pressure exerted on the cells i.e the continuum of selection pressure.

Importantly, discontinuing the therapeutic intervention could lead to a resurgence of the proliferative state in AML cells. The dynamic interplay between immune responses and leukemia cells' adaptive strategies underscores the complexity and temporality of the observed effects, with potential implications for treatment strategies and long-term outcomes. These findings carry potential implications for tailoring treatment approaches and understanding the dynamics of long-term outcomes (148, 149). In our study, THP-1 emerged as the most significantly impacted cell line following MLLRs. In comparison to ieU937 and ieHL-60, the immune-experienced THP-1 cells exhibited a more pronounced upregulation of myeloid maturation and activation markers, along with a clearer and prolonged loss of immunogenicity.

Further, our study also showed the changes in the ieAML cell surface behaviour such as adhesion, migration and polarization capacities, indicating that on encountering MLLRs, surviving AML sub-population may undergo a change in cell surface behaviour to resist immune responses. This suggests that certain subsets of myeloid leukemia cells possess mechanisms enabling them to withstand immune challenges, and the surviving cells may acquire traits that contribute to their resilience against anti-tumor immune responses.

Additionally, the transcriptomic signature of the immune-experienced THP-1 cell line was notably distinct. On the other hand, ieHL-60 cells, while being the least affected by MLLRs in terms of the tested properties, acquired substantial capabilities to impede immune reactions. Notably, the proliferation capacity of

ieHL-60 cells surpassed that of ieTHP-1 and ieU937, potentially contributing to the shorter duration of immune modulation observed in ieHL-60. Collectively, each AML cell line utilized in our study harbored a subpopulation capable of developing secondary immune resistance. However, our findings not only underscore the significance of heterogeneous subpopulations among leukemia blasts but also highlight that AML cells with diverse backgrounds can exhibit biological diversity in response to immune reactions.

According to the current understanding of tumor immunity, the cancer progression is preceded by the immune elimination, equilibrium and escape phases which continuously select the fittest malignant clones to survive despite the hostile conditions created by immune reactions (163). The signs of an active immune reaction, such as enhanced immune infiltration and increased expression of pro-inflammatory factors in the tumor microenvironment, have been associated with the success of immunotherapy (155). Nevertheless, many solid tumors and hematological malignancies are described as an immune desert and reside in an immunosuppressive niche (214). As observed with the ieAML cells, it might be hypothesized that the leukemia cells which experienced immune responses might serve as seeds for non-immunogenic clones and display resistance to immunotherapeutic interventions. As a drawback of our study, permanence of the immune resistance signatures and epigenetic changes need to be better defined and followed for prolonged periods in the ieAML cells.

Regulation and alterations in the expression of transcription factors are key elements in AML pathogenesis. One of the transcription factors that exhibited a significant upregulation in ieAML cells was KLF6 in our study. The family of the Krüppel-like factors (KLFs) proteins is intricately involved in a diverse array of cellular processes, encompassing the maintenance of stemness and pluripotency, myeloid differentiation, inflammation, proliferation, and apoptosis. A notable instance within this family is KLF6. Various functional and expression assays have indicated that the disruption of KLF6 function contributes to the development of cancer, inflammation-related diseases, and cardiovascular disorders. This underscores the versatile role of KLF6 in governing fundamental aspects of cellular function, impacting processes associated with cellular identity, immune responses,

growth, and programmed cell death. In addition, KLF6 directly upregulated HIF1 α expression in macrophages, promoting broad innate immune cell inflammatory and hypoxic response gene programming. Elaborating on these associations, the involvement of KLF6 underscores its significance in orchestrating various critical functions within the cell (193, 194, 215). This transcription factor exhibits elevated expression levels in AML and exerts detrimental effects on tumorigenesis. It achieves this by overseeing the regulation of genes involved in critical cellular processes such as the cell cycle, programmed cell death, and senescence. In essence, the heightened presence of this transcription factor in AML plays a pivotal role in influencing the molecular pathways associated with cell growth control, cell survival, and aging processes (194, 215). However, numerous studies have highlighted the involvement of KLF6 as a promoter of inflammatory diseases, including cancer. In cases of Acute Myeloid Leukemia (AML) characterized by the 8q22;21q22 translocation [t(8;21)], KLF6 plays a role in influencing the expression of downstream targets involved in leukemogenesis driven by the RUNX1-ETO fusion protein (216). The cell lines used in our study did not carry t(8;21) translocation (212, 213).

Additionally, we identified an upregulation of KLF6 in ieAML cells accompanied by alteration in the nuclear localization. Conversely, the increased translocation of KLF6 into the cell nucleus in myeloid leukemia cells following exposure to immune reactions, might imply a potential role in the attainment of a quiescent state in immune-experienced AML cells.

Another important transcription factor is the c-MYB transcriptional co-activator complex plays a crucial role in the self-renewal of hematopoietic stem cells (HSC) and the process of myelopoiesis (217, 218). In the context of AML, there is a common reliance on the disrupted functions of c-MYB (219). As hematopoietic cells undergo terminal differentiation, the expression of MYB is typically diminished (220, 221). This implies that c-MYB and its associated complex are integral components in maintaining the undifferentiated state of hematopoietic stem cells, while dysregulation of these mechanisms is frequently observed in AML, contributing to the disease's pathogenesis. Consistent with heightened myeloid maturation features and a decreased rate of proliferation, c-

MYB was excluded from the nucleus and downregulated in immune-experienced AML (ieAML) cells. This suggests that, in response to immune reactions, a MYB-independent program takes precedence in governing the cellular processes within myeloid leukemia blasts. This observation aligns with the heterogeneity observed in malignant blasts from bone marrow samples of AML patients concerning the nuclear distribution of KLF6 and c-MYB.

These observation suggests KLF6 and c-MYB transcription factors as potential indicators of the immune encounter status in myeloid leukemia blasts. The observed differences in the nuclear localization of specific transcription factors could serve as potential markers for discerning the immune encounter status in myeloid leukemia blasts, providing valuable insights for developing targeted therapeutic strategies aimed at overcoming immune evasion mechanisms in leukemia cells. However, further investigations are imperative to unravel the specific roles that KLF6 and c-MYB play in modulating the immune response within the context of AML.

Thus, the key factors contributing to relapse or resistance in Acute Myeloid Leukemia (AML) include distinctions in gene expression signatures, maturation states, and cellular plasticity (148, 149). The immune responses can create a dynamic and unstable microenvironment, compelling leukemic blasts to adapt their biological program and respond to novel conditions. Utilizing a tailored ex-vivo selection model, we identified the acquired immune resistance traits within specific subpopulations of myeloid leukemia cells.

In summary, understanding the heterogeneity, unraveling the mechanisms of immune regulation, and acknowledging the emergence of immune-resistant subpopulations are crucial facets that demand thorough investigation and attention in the context of AML. This perspective holds significant implications for advancing and refining future immune intervention therapies targeted at hematological malignancies. The intricate interplay between immune responses and leukemia cells' adaptive strategies underscores the necessity for comprehensive exploration to enhance the effectiveness of therapeutic approaches.

6. CONCLUSION AND RECOMMENDATIONS

- AML cells at different maturation stages exhibit genetic heterogeneity, leading to resistance against treatments and immune evasion. Thus, there is a need to develop targeted therapeutic strategies considering the genetic heterogeneity of AML cells to overcome resistance and adaptability.
- The dynamic interaction between heterogenous genetic background of AML subpopulation and immune cells contributes to the alteration in maturation state, activation and proliferation capacity along with modification in immune modulation potential operational at different level in different AML subpopulation.
- The constant evolution of leukemia cells during treatments, including bone marrow transplantation and chemotherapy highlights the need for comprehensive therapeutic strategies.
- AML subpopulation that survived immune attack “ieAML cells” are associated with heightened expression of costimulatory and inhibitory molecules which may impact the activation thresholds for immune cells, contributing to immune evasion strategies.
- Subpopulations of AML cells, termed "immune-experienced," can evade the immune system and acquire traits aiding in immune modulation. Thus, there is a need for strategies to investigate the permanence of immune resistance signatures and epigenetic changes in immune-experienced cells over prolonged period.
- The impact of the tumor microenvironment and immune system on immune resistance needs to be explored over a span of time where cells that survived first and second encounter with MLLRs should further undergo multiple immune cells encounters until this transience immune modulation becomes permanent.
- The biological and immune modulatory capacities of ieAML cells needs to be compared with multiple drug resistance AML cells, in order to trace a common immune signatures for enhanced understanding of myeloid cells in AML in shaping the adaptive immune response to devise strategies for

immunotherapy that can be translated into immune intervention therapies for the AML patients.

- The tumor microenvironment and immune system interactions contribute to immune resistance through various signaling pathways, particularly inflammatory pathways. Further research can be done on blocking these inflammatory pathways and studying its effect on maturation state and changes in T cell response.
- The lack of substantial benefits from immunotherapy in AML emphasizes the need for a deeper understanding of immune evasion mechanisms.
- Protein expression analysis for KLF6 through western blotting can be done in order to understand the kind of KLF6 isoform responsible for immune resistivity in ieAML cells.
- Transcription factors like KLF6 and c-MYB play a role in immune responses and may serve as potential markers for discerning the immune encounter status in myeloid leukemia blasts. Exploration of the transcription factors like KLF6 and c-MYB as therapeutic targets to modulate the immune response in AML can be further investigated by silencing/knocking out these two TFs in AML cells and studying their response on maturation state.
- KLF6 and c-MYB knockout AML cells can be introduced in mice to study the dynamics of AML immune resistivity in in-vivo studies.
- Implement long-term monitoring of KLF6 and c-MYB expression in AML patients before chemotherapy, undergoing chemotherapy, transplantation and after to understand the dynamics of immune responses, resistance, and relapse.
- Adapt treatment strategies based on the continuous evolution and adaptability of leukemia cells to immune interventions.

In conclusion, a comprehensive understanding of the interplay between genetic, immune, and adaptive characteristics in AML is crucial for advancing effective therapeutic approaches and improving long-term outcomes. The results and recommendations provide a foundation for tailoring treatments to the diverse

nature of AML, considering both genetic heterogeneity and immune evasion strategies.

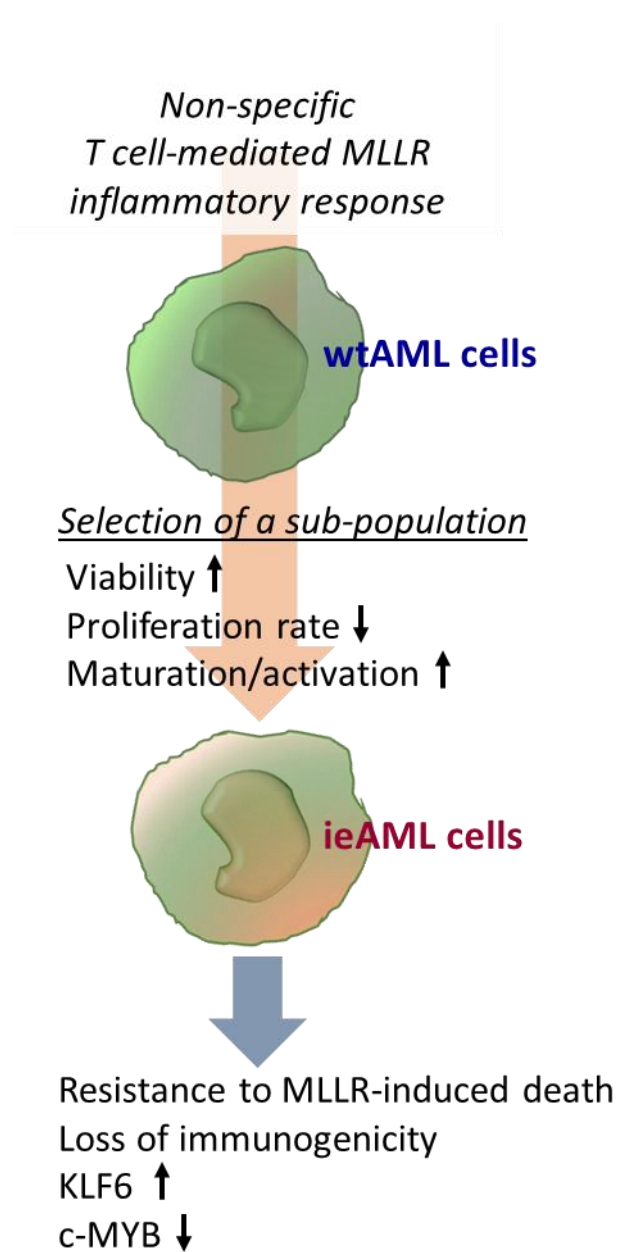


Figure 5.1. A schematical diagram showing the changes in immune experiencedAML cells (ieAML) after non-specific T cell-mediated MLLRs.

7. GENİŞ ÖZET

Anti-tümör immün yanıtların canlandırılması kanser tedavisi için umut verici bir yaklaşım haline gelmiştir (1). Konvansiyonel terapötiklerle birlikte, baskılayıcı sinyallerin bloke edilmesi veya tümöre özgü T hücrelerinin adoptif transferi hastalığın ilerlemesini sınırlar ve hasta sağkalımına katkıda bulunur (2). Lösemi tedavisi için allojenik hematopoetik kök hücre transplantasyonu (SCT), spesifik olmayan immünoterapi için bir arketip görevi görmektedir (3). Akut miyeloid lösemi (AML) riski orta ve düşük olan hastalarda, allojenik SCT, graft-versus-lösemi (GvL) etkisi yoluyla immün reaksiyonları şiddetlendirdiği için düşünülmüştür (4). Transplantasyona bağlı mortalite son yıllarda azalmış olsa da, tipik olarak tedavinin tamamlanmasından sonra veya remisyondan aylar sonra ortaya çıkan hastalığın nüksetmesi, lösemi tedavisindeki en büyük başarısızlıktır (5, 6).

İmmün seçim baskısı altında, immünojenik potansiyelini kaybeden malign hücreler hayatta kalmak için avantajlı hale gelir (7). AML'de immünojenite kaybı allojenik SCT sonrasında da gözlenmektedir ve nüks ile ilişkilendirilmiştir (7, 8). HLA-ilişkisiz nakillerde, nakilden sonra güçlü bir immünolojik baskı genellikle donörün T hücreleri tarafından desteklenir; bununla birlikte, lösemideki genomik instabilite, antijen sunum kapasiteleri azalmış blastların immün kaçışına izin veren önemli bir klonal heterojenite ile sonuçlanır (9). Alternatif olarak, lösemi antijenlerine veya lösemi hücrelerinden gelen kostimülatör sinyallere kronik maruziyet T hücre yorgunluğuna yol açabilir (10). Bu hiporesponsif durumda, yorgun T hücreleri azalmış proliferasyon, sitokin sekresyonu ve sitotoksik kapasiteleri ile karakterize edilir (10). Programlanmış hücre ölümü proteini 1 (PD-1) ve sitotoksik T-lenfosit ilişkili protein 4 (CTLA-4) gibi çoklu inhibitör reseptörlerin aşırı ekspresyonu, T hücresi inhibisyonunun bir başka yönüdür (11). Ancak AML hastalarında CTLA-4 ve PD-1 immün kontrol noktası inhibitörü (ICI) tedavilerinden elde edilen sonuçlar, immünojenik tümörlerden elde edilenlere kıyasla umut verici olmamıştır (12).

Miyeloid lösemi hücreleri, T hücre yanıtlarını güçlendirebilen CD80, CD86 ve ICOS-LG gibi kostimülatör molekül ekspresyonu ile tanımlanır (11). Bununla birlikte, daha önce grubumuz tarafından gösterildiği gibi, lösemi hücreleri özellikle aktive T hücreleri tarafından sekrete edilen interferon (IFN)- γ 'ya maruz kaldıklarında adaptif bir direnç mekanizması kullanabilirler (13). IFN- γ , lösemi hücreleri üzerinde PD-L1 ve PD-L2 moleküllerinin ekspresyonunu uyarır ve bunlar daha sonra immün reaksiyonlarla başa çıkma kapasiteleri kazanır (13). Ayrıca, AML hücreleri tarafından sürekli olarak sağlanan aşırı miktarda kostimülatör sinyal, efektör T hücresi yanıtları üzerinde olumsuz bir etkiye sahiptir ve yorgunluğa yol açabilir (10). Bu nedenle, miyeloid lösemi hücreleri T hücreleri ile etkileşime girme ve güçlü anti-tümör immün reaksiyonlarından sağ çıkmak için ayrıntılı stratejiler geliştirme potansiyeline sahiptir. Nakil sonrası nüks vakalarında da benzer gözlemler bildirilmiş ve SCT sonrası bir immün kaçınma mekanizmasına işaret edilmiştir (8). Nüks, immün reaksiyonların lösemi hücrelerini düzenlediği etkili bir GVL aralığından sonra ortaya çıkabilir (8, 14). Böylece rezidüel hastalık, immün modülatör fonksiyonları gelişmiş blastların bir seçimi olarak ortaya çıkar (15).

Bu çalışmada, AML hücre hatlarına özel bir bağışıklık baskısı uygulanmış ve hayatta kalan alt popülasyonlar (bağışıklık deneyimli AML hücreleri, ieAML olarak adlandırılmıştır) seçilerek biyolojik değişimler ve bağışıklık modülatör kapasiteleri açısından karakterize edilmiştir. Düşük hızda çoğalma, farklılaşma ve azalmış immünojenisite, miyeloid lösemide immün direnç ile ilişkilendirilmiştir. Ayrıca, iki transkripsiyon faktörü olan c-MYB ve KLF6'nın ekspresyonu ve nükleer lokalizasyonu, bağışıklık baskısı altındaki AML hücreleri için potansiyel belirteçler olarak kaydedilmiştir.

7.1. Metodoloji

Bu çalışmada, AML patogenezi ve potansiyel terapötik hedeflere odaklanarak immün deneyim kazanmış akut miyeloid lösemi (AML) hücrelerini ve immünomodülatör kapasitelerini araştırmak için çeşitli metodolojiler kullanılmıştır. AML'nin sırasıyla farklı FAB M4-5, M5 ve M3 aşamalarını temsil eden AML hücre hatları (THP-1, U937, HL-60) RPMI 1640 ortamında kültüre edilmiştir. Periferik

kan mononükleer hücreleri (PBMC'ler) sağlıklı gönüllü kişilerden taze toplanmış kan örneklerinden izole edilirken, AML tanısı konmuş hasta örnekleri hastane arşivlerinden elde edilmiştir. Çalışma için etik onay ve bilgilendirilmiş onam alınmıştır. Proliferasyonu değerlendirmek için AML hücre hatları ve PBMC'lerin anti-CD3 monoklonal antikor ile ko-kültür deneyleri yapılmış, optimal zaman aralığını ve PBMC'lerle ko-kültür oranını belirlemek için THP-1 hücreleri kullanılmıştır. AML hücreleri ve PBMC'ler, iki hücre tipini ayırtmak ve akış sitometrisi ile proliferasyon aktivitelerini izlemek için canlı floresan boyalar olan karboksiflorescein süksinimidil ester ve eFluor670 ile işaretlenmiştir. Floresan boyama nedeniyle oluşabilecek herhangi bir teknik etkiden kaçınmak için, transkriptomik ve diğer analizler için izole edilecek ve saflaştırılacak AML hücreleri ko-kültürlerde işaretlenmemiş olarak bırakılmıştır. PBMC'lerden T hücrelerini izole etmek ve ko-kültürlerden "immün deneyimli AML hücreleri" (ieAML hücreleri) olarak adlandırılan canlı AML hücrelerini saflaştırmak için FACS kullanılarak hücre ayırma işlemi gerçekleştirilmiştir. Hücre canlılığı Annexin V boyama ve akış sitometrisi kullanılarak değerlendirilirken, immünofenotipleme çeşitli yüzey belirteçlerine karşı antikorlarla hücrelerin işaretlenmesini ve akış sitometrisi analizini sağlamıştır. ieAML ve wtAML hücrelerinin yapışma ve göç dinamikleri üzerine çalışmalar Matrigel ve fibronektin ile yüzey kaplamalı lamellerde gerçekleştirilmiştir. AML hücrelerinin hücre yapışma dinamikleri xCELLigence sistemleri kullanılarak gerçek zamanlı olarak incelenmiştir. T hücreleri üzerindeki fonksiyonel deneyler, ko-kültür deneylerinde proliferasyon ve sitokin sekresyonunu değerlendirmiştir. AML hücrelerinin hücre döngüsü dağılımı akış sitometrisi kullanılarak belirlenmiştir. Taze izole edilmiş AML hücreleri, spontan ROS ve NO üretimini kontrol etmek için herhangi bir uyaran olmadan tam ortamda 48 saat dinlendirilmiştir. AML hücre popülasyonları arasındaki gen ifadesi farklılıklarını incelemek için RNA dizileme ve biyoinformatik analiz yapılmıştır. RT-PCR gen ekspresyon seviyelerini doğrularken, protein ekspresyonunu görselleştirmek için immünofloresan ve ışık mikroskopisi kullanılmıştır. Deney grupları arasındaki önemli farklılıkları belirlemek için istatistiksel testler yapılmıştır. Deney grupları arasındaki önemli farklılıkları belirlemek için istatistiksel testler yapılmıştır. Bu yöntemler birlikte, immün deneyim kazanmış

AML hücreleri ve bunların immün modülatör kapasitelerinin kapsamlı bir şekilde araştırılmasına olanak sağlayarak AML patogenezi ve potansiyel terapötik hedefler hakkında bilgiler sunmaktadır.

Burada, akut miyeloid lösemi (AML) için ex-vivo bir immün seleksiyon modeli geliştirdik ve kalan alt popülasyonları "immün-deneyimli" AML (ieAML) hücreleri olarak izole ettik.

7.2. Sonuçlar

AML hücrelerinin bir alt popülasyonunun immün reaksiyonlardan kurtulduktan sonra immün reaksiyonlara dayandığını, proliferasyonu yavaşlattığını ve immünomodülatör özellikler gösterdiğini doğruladık. İmmün mikroçevredeki değişiklikler kanser hücrelerinin yeni karakterler kazanmasına yol açmakta ve immün reaksiyonlarda hayatta kalmak için en uygun malign klonların seçilmesiyle sonuçlanmaktadır (16). Bununla birlikte, bağışıklık hücreleri ile kanser hücreleri arasındaki etkileşim in vitro ortamda yoktur ve bu da bağışıklık seçim baskısı olmadan kanser hücrelerinin büyümesini destekler. Daha önce grubumuz miyeloid lösemi hücrelerinin immünojenik potansiyelini kostimülatör moleküllerin yapısal ekspresyonu yoluyla göstermiştir (10, 11). Miyeloid lösemi hücre dizilerinin (THP-1, HL-60, U937) CD3 ile uyarılmış T hücreleri (yani karışık lökosit-lösemi hücre reaksiyonları, MLLR'ler) barındıran artan miktarlarda PBMC'lerle inkübe edildiği bir ortak kültür düzeneğinde, T hücreleri güçlü bir şekilde çoğalırken, lösemi hücresi çoğalması önemli ölçüde engellenmiştir (Şekil 4.1A). Genel olarak, THP-1 prototip hücre hattı olarak kullanılmış ve diğer iki hücre hattı doğrulama ve destekleyici deneyler için kullanılmıştır. MLLR'lerde bulunan küçük bir lösemi hücresi popülasyonu immünolojik açıdan zorlu koşullarda çoğalmayı başarmıştır (Şekil 4.1A). Özellikle THP-1 ve diğer hücre dizilerinin çoğalmasına izin veren bir süre olan 72 saatten sonra (veriler gösterilmemiştir), kültürlerde bağışıklık hücrelerinin oranı artmasına rağmen canlı lösemi hücrelerinin yüzdesi sabit kalmıştır (Şekil 4.1B). Bu da ölü hücre yüzdesinin MLLR'lerde çoğalabilen bir lösemi alt popülasyonu tarafından dengelendiği gözlemini desteklemiştir. Daha sonra, canlılığını koruyan miyeloid lösemi hücreleri MLLR'lerden yüksek saflıkta (CD13⁺DRAQ7⁻ >%98) izole edilmiş ve "immün deneyimli AML, ieAML"

hücreleri olarak adlandırılmıştır (Şekil 4.2A). İmmün deneyimli AML (ieAML) hücreleri genel olarak " wild-tip" parental AML (wtAML) hücrelerine kıyasla daha büyük çekirdek ve daha granüler sitoplazmaya sahiptir. ieU937 hücreleri daha sık olarak lobüle nükleer morfoloji göstermiştir (Şekil 4.2B). Saflaştırılmış ieAML hücreleri standart kültür koşulları altında tutulmuştur. Ki67⁺ ieAML hücrelerinin frekansının kültürde 72 saat inkübasyonun ardından wtAML'den daha az olduğu görülmektedir (Şekil 4.3 A,B). Bu iki hücre popülasyonu arasında hücre döngüsü dinamikleri açısından önemli bir fark bulunmamaktadır (Şekil 4.4A). Bu veriler, ieAML hücrelerinin MLLR'lerden çıkarıldıktan sonra bile düşük bir hızla çoğalmaya devam ettiği bulgusuyla uyumludur. MLLR'lere yanıt olarak, göç, yapışma ve polarizasyonla ilgili özellikler de Boyden odası aracılığıyla incelenmiştir. Özellikle, bağışıklık yanıtının AML hücre davranışı üzerindeki etkileri, ieAML hücrelerinin yapışma, göç ve polarizasyon kapasitelerindeki değişiklikler yoluyla değerlendirilmiştir. Genel olarak, AML hücreleri serum gradyanına doğru göç etme konusunda direnç göstermiştir. Hücrelerin sadece küçük bir yüzdesi açık bölmenin 5 µm'lik gözeneklerinden geçebilmiştir. Boyden odası aracılı göç kapasitesi analizinin bir sonucu olarak, ieAML hücreleri 24. saatte wtAML hücrelerine kıyasla daha zayıf göç kapasiteleri göstererek wtAML hücrelerinden daha az etkili bir şekilde göç edebilmiş ve ieTHP-1, wtTHP-1'e kıyasla daha az kemotaksis gözlemlenmiştir (Şekil 4.5). Daha sonra, hücre dışındaki network proteinleri, özellikle fibronektin ve Matrigel ile kaplanmış yüzeylerdeki yapışma dinamiklerindeki gerçek zamanlı değişikliklerin yanı sıra bir kontrol yüzeyini karşılaştırmayı amaçladık. Bulgularımız, hem ieTHP-1 hem de ieU937'nin 24 saat sonra fibronektin ve Matrigel kaplı yüzeylerde benzer trend gösterdiğini ve wild tipi muadillerine kıyasla yapışma kapasitesinde önemli bir düşüş olduğunu ortaya koymuştur. Buna karşılık, ieHL-60 aynı zaman sürecinde yapışma kapasitesinde bir artış göstermiştir (Şekil 4.6B). Bununla birlikte, 48. saatte, ieTHP-1 fibronektin kaplı yüzeyde wild tipi muadiline kıyasla gelişmiş bir yapışma kapasitesi göstermiştir. Bu arada, hem ieU937 hem de ieHL-60 hala düşük yapışma kapasitesi göstermektedir (Şekil 4.6B). Bu hücrelerin kaplanmamış yüzeyde ve fibronektin veya Matrigel kaplı yüzeylerde 24 saat boyunca polarizasyon potansiyeli araştırılmıştır. Polarite indeksi hesaplandıktan sonra hücre

aktin hücre iskeletinin yönlendirilmiş analizi ieU937'nin fibronektin kaplı yüzeylerde belirgin bir polariteye sahip olduğunu göstermiştir. ieTHP-1 hücrelerinin Matrigel kaplı yüzeyde fibronektine kıyasla daha polarize olduğu, ieHL-60'ın ise fibronektin kaplı yüzeyde önemli ölçüde daha polarize olduğu bulunmuştur (Şekil 4.7A).

Primer monositlerin in vitro olarak kültüre edildiklerinde doğal olarak olgunlaşmaya uğradıkları ve makrofajlara benzeyen özelliklere sahip hücrelere farklılaştıkları yaygın olarak kabul edilmektedir (89). Buna karşın, THP-1, U937 ve HL-60 gibi miyeloid lösemi hücre hatları in vitro koşullara maruz kalmalarına rağmen olgunlaşmamış özelliklerini sürdürmektedir. Bu nedenle, karışık lenfosit lösemi reaksiyonlarını (MLLR'ler) takiben, wtAML ve ieAML hücreleri arasında aktivasyon, farklılaşma ve olgunlaşma aşamalarıyla ilişkili ortak miyeloid belirteçlerdeki değişiklikleri karşılaştırdık ve inceledik. CD14, CD38, CD63, HLA-DR, CD206, CD163, CD80, CD86, CD40, CTLA-4, PD-1, PD-L1 ve TIM3 gibi farklı belirteçlerin yüzey ekspresyonu incelenmiş ve ieAML ile wtAML arasındaki ekspresyon değişiklikleri belirlenmiştir (Şekil 4.8A). Miyeloid hücre aktivasyonu ve farklılaşmasıyla ilişkili bazı yüzey moleküllerinin ekspresyonu ieAML hücrelerinde, daha belirgin olarak da ieTHP-1 ve ieU937 hücrelerinde artma eğilimindeydi. Çeşitli belirteçlerin yüzey ifadesi değişiklikleri üç farklı hücre hattında değerlendirilmiştir. Sonuçlar ayrıca ieAML ve wtAML hücrelerinin farklı belirteçlerinin daha iyi anlaşılmasını ve aynı zamanda karşılaştırılmasını sağlamak için bir ısı haritası olarak sunulmuştur (Şekil 4.8B).

Daha sonra, taze izole edilmiş ieAML hücrelerinin herhangi bir uyarandan olmadan tam ortamda 48 saat dinlenmesine izin verilirken, wild-tip AML (wtAML) hücreleri de benzer şekilde reaktif oksijen türlerinin (ROS) ve nitrik oksidin (NO) spontan üretimini değerlendirmek için kullanılmıştır. Her iki hücre tipi de PMA uyarımına maruz kalmıştır ve uyarılmamış hücreler patlama yanıtı analizi için temel seviyeleri oluşturmak üzere dahil edilmiştir. H₂DCFDA ve DAF₂DA'nın ortalama floresan yoğunlukları kullanılarak, PMA ile uyarılan hücrelerin MFI değeri, ROS ve NO endekslerini hesaplamak için uyarılmamış hücrelerinkine normalize edilmiştir. ROS ve NO üretimi açısından wtAML ve ieAML hücreleri arasında önemli bir fark gözlemlenmemesine rağmen, ieAML hücreleri hem ROS hem de

NO üretiminde bir azalma göstermiştir. İeAML hücreleri arasında ieU937, ieTHP-1 ve ieHL-60'a kıyasla ROS ve NO üretiminde biraz daha belirgin bir düşüş izlemiştir.

Ayrıca, ieAML hücreleri bağışıklık modülatör kapasitelerini değerlendirmek için MLLR'lere yeniden denenmiştir. Wild-tip THP-1 hücreleriyle karşılaştırıldığında, ieTHP-1'in canlılığı CD3 ile aktive edilmiş PBMC'lerin artan sayılarının varlığında sabit kalmıştır (Şekil 4.10A). Ayrıca, CD4⁺ T hücreleri ve CD8⁺ T hücreleri wtAML ile birlikte kültürlendiğinde yüksek oranda çoğalırken, ieAML hücreleri T hücrelerinin çoğalmasını desteklememiştir (Şekil 4.10B). Bununla birlikte, 1:2 ve 1:4 ieAML hücresi: T hücresi ko-kültür oranlarında, T hücresi sayılarında küçük bir artış gözlenmiştir. İlginç bir şekilde, ieHL-60 ve wtHL-60 hücreleri tarafından indüklenen CD8⁺ T hücresi proliferasyonu arasında bir fark bulunmamaktadır (Şekil 4.10B). İmmün direnç, immün reaksiyonlara yanıt olarak geçici olarak edinilebilir (20, 21); bu nedenle, ieAML hücreleri uzun süreli kültürlerde oluşturulmuş ve canlılıkları, çoğalmaları ve immünomodülatör kapasiteleri değerlendirilmiştir. İmmün deneyimli AML (ieAML) hücrelerinin canlılığı sürekli kültürleme ile muhafaza edilmiştir (apoptotik olmayan hücreler > %85) (Şekil 4.11A). Bununla birlikte, ieAML hücrelerinin proliferasyon oranları parental wtAML hücrelerinden önemli ölçüde daha yavaş kalmıştır (Şekil 4.11B). Daha sonra, "ieAML (CC)" hücreleri olarak adlandırılacak olan sürekli kültürlenmiş ieAML hücrelerinin CD4⁺ T hücresi ve CD8⁺ T hücresi yanıtları üzerindeki etkisi test edilmiştir. İmmün deneyimli THP-1 (CC) hücrelerinin varlığında, T hücresi çoğalması wtTHP hücrelerinde gözlenenden önemli ölçüde daha düşük bulunmuştur. Bununla birlikte, ieU937 (CC) veya ieHL60 (CC) ve bunların wild tipi muadilleriyle ko-kültürlerde benzer yüzdelerde T hücresi proliferasyonu indüklenmiştir (Şekil 4.11C).

T hücresi proliferasyonuna paralel olarak, anti-tümör immün yanıtlar için önemli araçlar olan IL-2, TNF- α , IFN- γ , granzim A, granzim B ve perforin sekresyonu, T hücreleri ve ieAML hücrelerinin ko-kültürlerinde önemli ölçüde azalmıştır. Yalnızca, ieHL-60'a yanıt olarak CD8⁺ T hücreleri tarafından sekrete edilen TNF- α , IFN- γ ve granzim B seviyeleri wtHL-60 hücrelerinin varlığında elde edilenlerden önemli ölçüde farklı değildi (Şekil 4.12A). Genel olarak, wtAML

hücreleriyle kokültürlerde CD4⁺ veya CD8⁺ T hücrelerinin miktarının artırılması, ieAML hücreleriyle ko-kültürlere kıyasla bu araçların konsantrasyonlarında önemli bir artışa neden olmuştur (Şekil 4.12A). Bu azalmış sekresyon, wild tipi AML muadillerine kıyasla, ieAML alt popülasyonunun zayıf immünojenik ve inflamasyon kaynaklı hücre ölümüne karşı daha az hassas olma eğiliminde olduğunu doğrulamıştır. T hücresi ve ieAML ko-kültürlerinden elde edilen süpernatantların sitokin analizi, IL-2, TNF- α , IFN- γ , granzim A ve granzim B dahil olmak üzere anti-tümör bağışıklık yanıtlarının desteklenmesinde önemli bir rol oynayan T hücresi ile ilişkili sitokinlerin salgılanmasında önemli bir azalma olduğunu göstermiştir. ieU937 ve ieHL-60 (CC) hücreleri için bu yanıtın geçici ve geçici olduğunu belirtmek gerekir. Bireysel hücre hattı normalizasyonundan sonra sitokin salınımindaki değişiklikleri bir ısı haritası şeklinde sunduk (Şekil 4.12B). Hem ieU937 hem de ieHL-60 (CC) tüm sitokinler için benzer bir trend göstererek wild tipi AML ko-kültürlerinde olduğu gibi neredeyse aynı seviyelere dönmüştür. Öte yandan, sürekli kültürlenmiş ieTHP-1 hücreleri düşük seviyeli immünojenik özelliklerini korusa da, düşük IL-2, TNF- α , IFN- γ , granzim A, granzim B, perforin ve sFASL seviyeleri de dahil olmak üzere anti-tümör sitokinlerinin sekresyonunda azalma görülmüştür. Tüm sitokinler arasında, IFN- γ 'nın ieTHP-1 (CC)'de yeni elde edilmiş ieAML ko-kültürlerine kıyasla önemli ölçüde daha fazla azaldığı görülmüştür (Şekil 4.12B).

Sınırlı sayıda gen, miyeloid lösemi hücreleri üzerindeki bağışıklık baskısının ortak belirteçleri olarak tanımlanmıştır. ieAML alt popülasyonlarının ortaya çıkmasında rol oynayan moleküler yolları ortaya çıkarmak için transkriptomik analizler gerçekleştirilmiştir. İlginç bir şekilde, THP-1, U937 ve HL-60 hücre hatlarının transkriptomik imzaları sınırlı bir homojenlik göstermiştir. Dolayısıyla, her bir hücre hattından elde edilen karşılık gelen ieAML alt popülasyonları da spesifik gen ekspresyon profili ile ayırt ediciydi ve bu da AML'nin heterojen doğasına işaret ediyordu (Şekil 4.13A). Beklendiği üzere, hiyerarşik sınıflandırma analizi her bir ieAML popülasyonu ile parental wtAML hücre hattı arasında yakınlık olduğunu ve ieTHP hücrelerinin en farklı gen ifade modeline sahip olduğunu ortaya çıkarmıştır (Şekil 4.13B). Amacımız ieAML popülasyonları arasında ortak bir imza belirlemek olduğundan, ieTHP-1, ieU937 ve

ieHL-60 hücrelerinde en farklı ve yaygın olarak ifade edilen genler yol analizine tabi tutulmuştur (Şekil 4.13D). Gen ifadesi değişiklikleri açısından, ieTHP-1 hücreleri (DEG'ler, toplam, 1483; yukarı düzenlenmiş, 888; aşağı düzenlenmiş, 595) MLLR'lerden en çok etkilenen hücreler olmuş, bunu ieU937 (DEG'ler, toplam, 886; yukarı düzenlenmiş, 519; aşağı düzenlenmiş, 367) ve ieHL-60 (DEG'ler, toplam, 287; yukarı düzenlenmiş, 208; aşağı düzenlenmiş, 79) izlemiştir (Şekil 4.13C). Her üç ieAML hücresinde de benzer şekilde toplam 77 gen yukarı regüle edilirken sadece 7 gen aşağı regüle edilmiştir (Şekil 4.13C,D). İnterferon sinyalinin düzenlenmesinde rol oynayan genler (STAT1, IFI30, OAS1, STAT2, IFIT3, GBP1, GBP2, GBP5, IFI6, IRF1, IRF7, ISG15), inflamatuvar sitokin sinyali (CXCL8, CXCL9, CXCL10, CCL2, CCL3, GZMB, IL-32, IL1 β , FCGR1A, S100A8, TNFAIP2), antijen sunum yolları (CD74, HLA-A, HLA-B, HLA-C, HLA-E, B2M, TAP1, TAPBP, PSMB9, PSMB10, PSME1), apoptotik yollar (CSRN1P, GADD45B, PIM1, MCL1, RELB, PPP1R15A), hücre yapışması ve göçü (TUBA1A, RGS1, PRTN3, ICAM1, ITGB2, ITGB7), ve hücrel stres yanıtı (SOD2, NDRG1, NCF1, SGK1) wild tipi karşıtlarıyla kıyaslandığında ieAML hücre popülasyonlarında yaygın olarak düzenlenmiştir (Şek. 4.13D ve Şekil 4.14, 4.15A). Sonuç olarak, miyeloid lösemi hücreleri üzerindeki immün baskıyla ilişkili ortak belirteçler olabilecek ieAML hücre popülasyonları için yalnızca sınırlı sayıda farklı şekilde ifade edilen gen ortak bulunmuştur.

84 DEG, her üç hücre hattında da ortak olan genler tarafından düzenlenen önemli biyolojik yolları belirlemek için KEGG veri tabanı ile karşılaştırılmıştır. Gen seti daha sonra dört gruba ayrılmıştır: i. inflamatuvar yanıtta rol oynayan genler, ii. apoptoz, iii. sitokin yanıtı ve iv. transkripsiyon faktörleri (Şekil 4.15A). Daha sonra, bu gen setleri yol zenginleştirme analizine dahil edilmiştir. Önemli olarak, interferon sinyali ile ilişkili olan viral süreçler, anti-viral bağışıklık ve viral enfeksiyonlarla ilgili gen setleri de yukarı doğru düzenlenmiştir (Şekil 4.15B). Ayrıca, diğer zenginleştirilmiş yollar arasında antijen sunumu, allograft rejeksiyonu, hücreden hücreye adezyon, hücre göçü, TNF sinyali, apoptozun negatif düzenlenmesi ve graft-versus-host hastalığı ile ilişkili yollar yer almaktadır (Şekil 4.15B).

Gen seti zenginleştirme analizi (GSEA), her üç ieAML hücresi tarafından paylaşılan yüksek oranda ifade edilen genlerin daha önce bildirilen enflamatuar yanıt ve allogreft rejeksiyon yanıtı gen setleriyle uyumlu olduğunu ortaya koymuştur (nominal p değeri $< 0,05$) (Şekil 4.16). IFN- γ , IFN- α , TNF- α , TGF- β , apoptoz, IL-6 ve IL-2 sinyali gibi enflamatuar yolların ayırt edici özellikleri de zenginleşmiştir. MYB transkripsiyon faktörünün hedefleri de dahil olmak üzere hücre proliferasyonu ile ilgili yollardaki azalma da ieAML hücrelerinden elde edilen transkriptomiklerle uyumluydu (Şekil 4.14).

AML hücreleri heterojenlikleri ile iyi bilinmektedir. Bu nedenle, farklı olgunlaşma aşamaları (THP-1, U937, HL-60) değerlendirilerek aralarındaki farklılıkları ortaya çıkarmak için tek tek AML hücre hatlarına yol analizi uygulanmıştır. ieTHP-1 ve wtTHP-1'de, en önemli ölçüde zenginleştirilmiş yollar arasında hücre döngüsü düzenlemesi, sitokin sinyali, nötrofil degranülasyonu, enflamatuar yanıt, viral enfeksiyon ve tip II interferon yolları yer almaktadır (Şekil 4.17A). Wild-tip U937'ye kıyasla ieU937'de, sitokin sinyali ve düzenlenmesi, strese hücre sel yanıt, PID/AP1 yolu, hematopoez ve düzenlenmesi, reaktif oksijen türleri ve allogreft rejeksiyonunda yer alan yollarla ilgili yollarda zenginleşme görülmüştür (Şekil 4.17B). ieHL-60 ayrıca hücre öldürme, lökosit migrasyonu, IL-18 sinyali, NOD benzeri reseptör sinyali ve apoptozla ilgili yollar gibi zenginleştirilmiş yollarda da farklılıklar göstermektedir (Şekil 4.17C). ieHL-60 ve ieTHP-1 sitokin sinyali, innat immün yanıt, tip II interferon sinyali, inflammatuar yanıt ve viral yanıtla ilgili yollar dahil olmak üzere bazı ortak yolları paylaşmıştır. Metabolik süreçlerle ilgili yollar her üç hücre hattında da zenginleşmiştir; ancak ieTHP-1'de ieU937 ve ieHL-60'a kıyasla en çok zenginleşen yollardan biri bulunmuştur (Şekil 4.17 A,B,C).

Sonuç olarak, miyeloid lösemi hücreleri üzerindeki immün baskıyla ilişkili ortak belirteçler olabilecek ieAML hücre popülasyonları için yalnızca sınırlı sayıda farklı şekilde ifade edilen gen ortak bulunmuştur.

Her üç ieAML hücresinde de yalnızca sınırlı sayıda gen birlikte düzenleme gösterdiği için, dikkatimiz transkripsiyon faktörlerini kodlayanlara, özellikle de hücre sel davranışı etkileme kapasitesine sahip olanlara yöneltilmiştir. Diferansiyel

olarak ifade edilen 84 gen (DEG) arasında 9 tanesi transkripsiyon faktörü olarak tanımlanmıştır (Şekil 4.13D, ok başlarıyla gösterilmiştir). Özellikle, Kruppel benzeri transkripsiyon faktörü 6 (KLF6) ve MYB genleri, TCGA biyoinformatik analizine dayalı olarak AML hastalarında yüksek oranda ifade edilen ilk iki transkripsiyon faktörü arasında ortaya çıkmıştır (Şekil 4.18A, ok başları). Bununla birlikte, MCL1, B2M, SLC2A3, IRF1, SOD2, STAT1, CD74, PRTN3 ve KLF2 dahil olmak üzere hasta veri tabanında ilk 10 sırada yer alan diğer genleri de araştırdık. STAT1, IRF1, CD74 ve B2M gibi bu genlerin bazılarının rolleri AML'de kapsamlı bir şekilde çalışılmış olsa da, odak noktamız ieAML hücrelerinde immün dirençten sorumlu bir imza gen listesi belirlemektir. Ekspresyonlarını değerlendirmek için RT-PCR analizi yaptık. İlginç bir şekilde, TCGA analizinden elde edilen AML hastalarının veritabanında ekspresyon yüksek olmasına rağmen, RT-PCR analizi tutarsız sonuçlar vermiştir. Gen ifadesi yalnızca ieTHP-1 hücrelerinde yükselirken, diğer iki hücre hattı, ieU937 ve ieHL-60, gen ifadesi analizlerinde değişkenlik göstermiştir (Şekil 4.19A). Sadece KLF6 ve MYB genleri, RT-PCR kullanılarak yapılan kantitatif gen ekspresyonu analizleri ile doğrulandığı üzere tutarlı bir gen ekspresyonu modeli göstermiştir (Şekil 4.19A,B). Sonuç olarak, odak noktamız farklılaşma, olgunlaşma ve çoğalma dahil olmak üzere hücreyel süreçlerin düzenlenmesinde önemli roller oynadığı bilinen KLF6 ve c-MYB transkripsiyon faktörlerine yönelmiştir (192, 193, 194).

İmmün deneyimli AML hücrelerinde, KLF6 önemli bir yukarı regülasyon gösterirken, MYB aşağı regüle edilen genlerden biri olarak tanımlanmıştır (Şekil 4.13D). Ayrıca, TCGA verilerinin analizi, orta ve kötü klinik tablo gösteren hastalarda MYB mRNA seviyelerinde önemli bir düşüş olduğunu ortaya göstermiştir. Bu gözlem, hücreyel süreçler ve AML patogenezindeki potansiyel etkileri bağlamında KLF6 ve MYB'nin rollerinin daha fazla araştırılmasına yol açmıştır.

İmmün deneyimli (ieAML) hücrelerinde KLF6 ve c-MYB gen ekspresyon modelini q-RT PCR ile doğruladıktan sonra, bir sonraki adım immünfloresan ile protein düzeyinde hücreyel lokalizasyonlarını incelemektir. Burada, AML blast hücrelerinin nükleer bölgesinde wtAML ve ieAML hücreleri arasında KLF6 ve c-MYB'nin ortalama floresan yoğunluğunu (MFI) hesapladık. İlginç bir şekilde,

KLF6'nın nükleer lokalizasyonu wtAML blast hücrelerinde daha az tespit edilmiştir (Şekil 4.20A). Protein düzeyinde, wtAML blastlarında KLF6'nın nükleer lokalizasyonu daha az sıklıkla tespit edilmiştir. MLLR'lerin ardından, çekirdeklerinde KLF6 taşıyan ieAML hücrelerinin oranı önemli ölçüde artmıştır. Alternatif olarak, MLLR'lere maruz bırakıldığında nükleer c-MYB içeren hücrelerin yüzdesi azalmıştır (Şekil 4.20A). Özellikle U937 hücrelerinde bu transkripsiyon faktörleri için bir perinükleer boyanma da kaydedilmiştir (Şekil 4.20B, C). Ayrıca, nükleer bölgede KLF6 ve c-MYB proteinlerine sahip AML hücrelerinin yüzdeleri hesaplandığında, her üç hücre hattında da wtAML hücrelerine kıyasla ieAML hücrelerinde nükleer bölgede c-MYB'de bir düşüş olduğu görülmüştür. KLF6 yüzdesi ise sırasıyla THP-1, U937, HL-60 için wtAML hücrelerine kıyasla ieAML hücrelerinde artmıştır (%52 ila 75, %40 ila 60 ve %52 ila 78) (Şekil 4.20 B,C). Daha sonra, KLF6 ve c-MYB'nin nükleer lokalizasyon durumunu belirlemek için AML hasta örneklerini değerlendirdik. Yeni tanı konmuş (n=6) veya nüks etmiş (n=5) AML hastalarının kemik iliği aspiratlarında, KLF6 ve c-MYB'nin farklı nükleer seviyelerine sahip blastların heterojen bir dağılımı gözlenmiştir (Şekil 4.21A). KLF6'nın yüksek seviyede nükleer lokalizasyonuna (blast popülasyonunun ortalamasından 1,5 kat daha yüksek KLF6 seviyeleri) ve c-MYB'nin düşük seviyede nükleer lokalizasyonuna (blast popülasyonunun ortalamasından 1,5 kat daha düşük c-Myb seviyeleri) sahip blastların yüzdesi her örnek için hesaplanmıştır. Genel olarak, AML hücrelerinin büyük bir çoğunluğu nükleer bölgede düşük seviyede KLF6 (aralık, %62-100) ve yüksek seviyede c-MYB (aralık, %67-100) göstermiştir (Şekil 4.21A). Nükseden hastalığı olan kişilerde yüksek seviyede nükleer KLF6 içeren blastlar için artan bir eğilim kaydedilmiştir (ilk tanıdaki aralık, %0-27; nüksdeki aralık, %20-38). Ancak, c-MYB için ilk tanıda veya nükste elde edilen örneklerde herhangi bir fark görülmemiştir (Şekil 4.21A).

Sonuç olarak, bağışıklık deneyimi olan AML hücrelerinde belirlenen 84 DEG arasından seçilen KLF6 ve c-MYB transkripsiyon faktörleri AML hücrelerinde farklı nükleer lokalizasyon göstermiştir. Hasta örneklerinde, blastların küçük bir kısmı da çekirdekte yüksek KLF6 ve düşük c-MYB ile karakterize edilmektedir.

Genel olarak, miyeloid lösemi alt popülasyonlarının ilk immün yanıtta hemen sonra kazanılmış olan immün modülatör kapasiteleri, sabit koşullarda sınırlı bir süre boyunca devam edebilir. Bununla birlikte, ieTHP-1 hücrelerinde gözlemlendiği gibi, inflamatuvar reaksiyonlar sırasında malign hücreler tarafından edinilen direnç karakterleri her zaman geçici olmayabilir.

7.3. Tartışma

Akut Miyeloid Lösemi (AML), hem kemik iliğinde hem de kan dolaşımında olgunlaşmamış blastların birikmesiyle karakterize bir hematolojik malignite formudur. Bu olgunlaşmamış blastlar genelde büyüme faktörleri ve sitokinlerin zengin olduğu nişlerde yaşar ve bağışıklık sistemi tepkilerine karşı toleransı destekleyen bir ortamı besler. Genomik çalışmalardaki son gelişmeler, AML hücrelerinin genetik heterojenliğini ortaya çıkarmış, bazı alt gruplar tedavilere direnç göstererek terapötik müdahalelere yanıt olarak tümörün evrimleşmesine yol açmıştır (Turati ve ark., 2021). Hem genetik hem de epigenetik düzeylerde işlevsel değişikliklerle işaretlenen bu süreç boyunca blastlar, tedavi edilmemiş veya tamamen dirençli hücrelerde gözlenmeyen benzersiz, zamansal olarak sınırlı morfolojik, fenotipik ve genetik özellikler edinerek adaptasyon göstermektedir. Yüksek oranda immünojenik tümör hücrelerinin ortadan kaldırılması, immün yanıtlara dayanma konusunda gelişmiş yeteneklere sahip malign klonların ortaya çıkmasına yol açabilir. Bu süreç, konakçı bağışıklık sistemine karşı üstün direnç gösteren tümör hücresi varyantlarının tercihli olarak hayatta kalmasını ve çoğalmasını içerir ve potansiyel olarak daha agresif ve kaçan bir tümör fenotipinin gelişmesine neden olur (163, 191, 195).

Miyeloid soydan gelen hücreler, antijenleri sunma ve T hücresi aracılı yanıtları ortaya çıkarmak için çok önemli olan ikincil sinyalleri sağlama konusunda mükemmeldir. Bu durum, miyeloid kökenli hücrelerin yabancı maddeleri T hücrelerine etkili bir şekilde sunarak ve bağışıklık yanıtlarının aktivasyonunu kolaylaştırarak bağışıklık sisteminde yetkin bir rol oynadığını göstermektedir. Dendritik hücreler ve makrofajlar gibi miyeloid hücreler, antijen sunan hücre (APC) popülasyonunun temel bileşenleridir. Antijenleri yakalama, işleme ve T hücrelerine sunma konusunda benzersiz bir yeteneğe sahiptirler ve bir dizi

bağışıklık tepkisi başlatırlar. Ek olarak, bu miyeloid hücreler T hücresi aracılı bağışıklığın uygun aktivasyonuna ve modülasyonuna katkıda bulunan kritik ikincil sinyaller sağlar. Bu etkileşim, ko-stimülatör sinyallerin ve diğer düzenleyici moleküllerin iletilmesiyle birleştiğinde, T hücresi yanıtlarının etkili bir şekilde başlatılması ve düzenlenmesi için çok önemlidir. Miyeloid hücrelerin antijen sunumu ve ikincil sinyalizasyondaki yeterliliği, adaptif bağışıklık yanıtının şekillendirilmesindeki önemli rollerini vurgulamaktadır. Bu süreçlerin anlaşılması, aşı geliştirme ve kanser gibi hastalıklar için immünoterapi dahil olmak üzere çeşitli klinik bağlamlarda immün reaksiyonları modüle etmek için stratejiler geliştirmek için temeldir (196, 197). Akut miyeloid lösemi (AML) ile ilişkili hücreler, kostimülatör moleküllerin yüksek ekspresyonunu gösterebilmektedir. Bu, AML hücrelerinin, etkileşimler sırasında bağışıklık hücrelerine ek sinyaller sağlamada önemli bir rol oynayan ve bağışıklık tepkilerinin modülasyonuna katkıda bulunan proteinlerin yüksek seviyelerini sunabileceği anlamına gelir. AML kapsamında, lösemi hücreleri üzerinde kostimülatör moleküllerin artan ekspresyonu, bu hücreler ile bağışıklık sistemi arasındaki etkileşim açısından önemli etkilere sahiptir. Kostimülatör moleküller, immün yanıtların aktivasyonu ve düzenlenmesi için gereklidir. AML hücreleri bu molekülleri yüksek seviyelerde ifade ettiğinde, bağışıklık hücreleri, özellikle de T hücreleri ile etkileşime girme kapasitesinin arttığını göstermektedir.

AML hücrelerinde kostimülatör moleküllerin yükseltilmesi, bağışıklık sisteminin lösemi hücrelerini tanımasını ve bunlara yanıt vermesini etkileyebilir. Bağışıklık hücreleri için aktivasyon eşiklerini etkileyebilir ve AML tarafından kullanılan genel bağışıklıktan kaçınma stratejilerine katkıda bulunabilir (10, 11). Akut miyeloid lösemi (AML) alanında, lösemi hücrelerinde majör histo-uyumluluk kompleksi (MHC) moleküllerinin ekspresyonunu gözlemlemek yaygındır. Bunlar arasında antijenlerin T hücrelerine sunulmasında önemli rol oynayan ve böylece AML'ye karşı immün tanıma ve yanıtı etkileyen hem MHC sınıf I hem de MHC sınıf II bulunmaktadır. Dahası, AML'li bireylerin kemik iliğindeki T hücrelerinin aktivasyonu devam eden bir bağışıklık reaksiyonu anlamına gelir. Bu T hücrelerinin aktive olmuş durumu, bağışıklık sisteminin kemik iliği ortamında AML hücrelerinin varlığına aktif olarak yanıt verdiğini göstermektedir. Bu aktivasyon,

bağışıklık sisteminin lösemik hücreleri tanıma ve ortadan kaldırma girişiminin bir yansıması olabilir ve AML ile kemik iliği mikroçevresindeki bağışıklık yanıtı arasındaki dinamik etkileşimi vurgular. Bu etkileşimleri anlamak, AML ile etkili bir şekilde mücadele etmek için bağışıklık sistemini kullanan hedefe yönelik terapötik stratejiler geliştirmek için gereklidir (198). Miyeloid lösemi hücreleri, bağışıklık sisteminden kaçmaya yönelik kompleks stratejileriyle tanınmakta ve anti-tümör bağışıklık savunmalarına uyum sağlamada kayda değer bir esneklik göstermektedir. Bu durum, lösemi hücreleri ile immün yanıt arasındaki karmaşık etkileşimin altını çizmekte ve miyeloid lösemide bu adaptif immün kaçış mekanizmalarını ele alan hedefe yönelik terapötik yaklaşımlara duyulan ihtiyacı vurgulamaktadır (8, 152, 155, 197). Akut miyeloid lösemide (AML) genetik ve immün özellikler arasındaki dinamik etkileşim, tedavilere dirençli ve elverişsiz koşullarda gelişebilen blast popülasyonlarının ortaya çıkma olasılığını artırarak önemli çeşitliliğe neden olur. Genetik ve immün yanıt arasındaki etkileşimdeki bu karmaşıklık, AML'nin heterojen karakteristiğine katkıda bulunur. Lösemi hücreleri arasında gözlenen heterojenlik, belirli popülasyonların terapötik müdahalelere karşı direnç geliştirme olasılığını artırmaktadır. Dahası, bu dirençli blast popülasyonları zorlu ve elverişsiz ortamlarda bile uyum sağlayabilir ve gelişebilir. Bu karmaşık etkileşimin anlaşılması ve ele alınması, lösemi hücre popülasyonları içindeki direnç ve uyarlanabilirlik potansiyeli göz önüne alındığında, AML'ye karşı daha etkili terapötik stratejiler geliştirmek için çok önemlidir (148, 149, 200). Lösemi hücrelerinin seçilim ve adaptasyon yoluyla sürekli evrimi, allojenik kemik iliği transplantasyonu gibi tedaviler sırasında bile aktif kalmaktadır. Nakledilen bağışıklık hücrelerinin lösemi hücrelerine saldırdığı graft-versus-lösemi (GvL) yanıtları bağlamında, lösemi hücreleri tarafından seçilim ve adaptasyonun dinamik doğası devam etmektedir. Devam eden bu etkileşim, hastalığın ilerlemesini teşvik edebilir ve nüks riskini artırarak, çeşitli tedavi yöntemleri sırasında lösemi hücrelerinin adaptif kapasitelerini dikkate alan ve bunlara karşı koyan kapsamlı terapötik stratejilere olan ihtiyacı vurgulamaktadır (6, 199, 201). Akut miyeloid lösemili (AML) bireylerde immünoterapiden önemli faydalar sağlanamaması, lösemi hücrelerinin immün yanıtın nasıl kaçtığına daha derinlemesine anlaşılması gerektiğinin altını çizmektedir. Bu anlayış, tedavi seçeneklerini iyileştirmek ve

AML'nin ortaya çıkardığı bağışıklıktan kaçınma zorluklarını ele almak için daha etkili stratejiler geliştirmek için gereklidir (198, 202).

Çalışmamızdan elde edilen sonuçlar, miyeloid lösemi hücreleri içinde, bağışıklık sisteminin zararlı etkilerinden kaçabilen alt popülasyonlar olduğunu göstermiştir. Bağışıklık tepkileriyle karşılaşan ve hayatta kalan bu lösemi hücreleri, anti-tümör bağışıklık tepkilerinde gezinmelerine yardımcı olan geçici veya kalıcı özellikleri benimseyebilir.

Bir diğer önemli engel ise, kemoterapinin etkinliğinin, kanser hücrelerinin aynı anda birden fazla ilaca karşı direnç geliştirdiği ve onları çeşitli ilgisiz tedavilerden etkilenmez hale getirdiği bir fenomen olan çoklu ilaç direnci (MDR) nedeniyle kısıtlamalarla karşı karşıya kalmasıdır. Çoklu ilaç direnci sırasında kanser hücreleri, genellikle artan ilaç akışı veya ilaç hedeflerindeki değişiklikler gibi çeşitli mekanizmalar yoluyla, birden fazla ilacın sitotoksik etkilerine dayanma yeteneği geliştirir. Bu direnç, maligniteyi hedef almayı amaçlayan çeşitli terapötik ajanların etkinliğini azalttığı için kanser tedavisinde önemli bir zorluk teşkil etmektedir (203, 204). İlaç direnci mekanizmaları, genetik ve epigenetik seviyelerdeki farklılıkların rezidüel hastalıkta gösterildiği in vivo ortamda sıklıkla gözlemlenmektedir (205). Bu, gerçek biyolojik sistemler bağlamında, ilaç direncinin genellikle hem genetik kod hem de hücresel mekanizmanın epigenetik modifikasyonları düzeyinde değişiklikleri içerdiği anlamına gelir. Ayrıca, anti-kanser moleküllerinin artan konsantrasyonlarına maruz kalan miyeloid lösemi hücreleri, in vitro olarak ilaca dirençli alt klonlar olarak tanımlanmaktadır (206, 207). Bu, araştırmacıların miyeloid lösemide ilaç direncinin gelişimini simüle etmelerine ve incelemelerine olanak tanıyarak, bu dirençli alt popülasyonların mekanizmaları ve davranışları hakkında bilgiler sunmaktadır. İlaça dirençli alt klonların in vitro olarak analiz edilmesi, direncin dinamiklerini araştırmak ve miyeloid löseminin klinik tedavisinde bunun üstesinden gelmek veya önlemek için potansiyel stratejileri keşfetmek için kontrollü bir ortam sağlar. Lösemi hücreleri birden fazla ilaca karşı direnç geliştirmek için çeşitli mekanizmalar kullanır. Örneğin, bazı dirençli hücreler ilaç alımında azalma veya ilaç atımında artış göstererek ilaç absorpsiyonunda azalmaya veya ilaç atımında artışa neden olur. Bu durum, hücre içindeki hedefine ulaşan ilaç miktarını azaltarak ilacın etkinliğini

sınırlandırır. Ek olarak, direnç, hücrel mekanizmaların tedavinin neden olduğu DNA hasarını onararak hücrelerin hayatta kalmasına ve çoğalmasına izin verdiği hasarlı DNA'nın gelişmiş onarımından kaynaklanabilir. İlaç hedefleri ve metabolizmasındaki değişiklikler de, ilaçların moleküler hedeflerini veya hücrel metabolik yolları değiştirerek onları terapötik etkilere daha az duyarlı hale getirerek dirence katkıda bulunabilir. Ayrıca, dirençli hücrelerin tedaviye bağlı apoptozdan kaçtığı hücre ölümünün baskılanması, bu hücrelerin terapötik çabalara rağmen devam etmesine izin vererek tedavi direncine katkıda bulunur. Bu mekanizmalar toplu olarak tedavi direncine katkıda bulunan başlıca faktörlerdir (208). Tümör mikroçevresinin ve bağışıklık sisteminin etkisi de çeşitli sinyal yolları aracılığıyla MDR'ye katkıda bulunan bir faktör olarak kabul edilmektedir (209). Bununla birlikte, kontrol noktası blokajı ve adoptif T hücre transferi gibi immün müdahale tedavilerine karşı direncin daha iyi tanımlanması gerekmektedir (14, 210).

Bu nedenle, mevcut tez çalışmasında, genetik ve epigenetik modifikasyonların kazanılmasıyla elde edilen bağışıklık yanıtına kademeli bir adaptasyonu özetleyen kavramsal bir model önerilmiştir. Çalışmamızda, kanser hücrelerinde (AML) meydana gelen biyolojik değişiklikleri incelemek ve bunların bağışıklık yanıtını modüle etme kapasitelerini değerlendirmek için özel olarak tasarlanmış bir in vitro çerçeve oluşturduk. Bu yaklaşım, kanser hücrelerinin nasıl geliştiğinin ve bağışıklık sistemiyle nasıl etkileşime girdiğinin ayrıntılı bir şekilde araştırılmasına olanak tanıyarak potansiyel adaptasyon mekanizmalarına ışık tutmakta ve gelecekteki terapötik stratejiler için bilgiler sağlamaktadır. Burada, AML blastlarının heterojen davranışını modellemek için farklı olgunlaşma ve farklılaşma özelliklerine ve genetik arka planlara sahip üç AML hücre hattı kullandık. Spesifik olmamakla birlikte, miyeloid lösemi hücre hatları ve allojenik immün hücreleri içeren ko-kültürlerde (MLLR'ler) başlatılan T hücresi aracılı reaksiyonlar, immün veya ikincil direncin altında yatan moleküler mekanizmaların aydınlatılması için bir model görevi görmüştür. Bu ko-kültür sistemindeki yanıtları analiz etmek, lösemi hücrelerinin immün tanımadan kaçma veya immün saldırılara karşı direnç oluşturma yolları hakkında bilgi edinmemize yardımcı olarak daha hedefli ve etkili terapötik yaklaşımlar geliştirmek için bir temel sunmaktadır.

T hücresi yanıtlarının gücü, öncelikle B7 süpergen ailesinden yüzey molekülleri aracılığıyla iletilen güçlü kostimülatör sinyallere bağlıdır (211). CD80, CD86 ve ICOSLG kostimülatör molekülleri lösemi blastları tarafından sıklıkla ifade edilir ve AML'nin immünojenitesine katkıda bulunabilir (11). Tersine, miyeloid lösemi hücreleri tarafından sunulan kostimülatör aktivitenin düzenleyici etkileri potansiyel olarak bağışıklıktan kaçınmaya katkıda bulunabilir. Bunun anlamı, bu hücrelerden gelen kostimülatör sinyalleri içeren etkileşimlerin immün tanıma ve yanıtta kaçınmaya yardımcı olan sonuçları olabileceğidir (10, 11, 13). Elde ettiğimiz bulgularla tutarlı olarak, çeşitli kanser tipleri, anti-kanser bağışıklığına yanıt olarak kontrol noktası moleküllerinin, interferon yanıt genlerinin ve bağışıklık düzenlemesiyle ilişkili yolakların artan ekspresyonunu gösterdiği belgelenmiştir (11, 13).

Çalışmamızda, "immün-deneyimli" alt klonlar ieAML hücreleri, her biri farklı özelliklere ve farklı biyolojik niteliklere sahip üç farklı AML hücre hattından türetilmiştir. Bu, bir dizi bağışıklık yanıtını keşfetmemize ve bu alt klonlar arasında altta yatan biyolojik özelliklerdeki varyasyonları değerlendirmemize olanak sağlamıştır (212, 213) (THP-1 RRID:CVCL_0006), U-937 RRID:CVCL_0007, HL-60 RRID:CVCL_0002).

İmmün deneyime sahip AML hücreleri (ieAML), özellikle belirli bir zaman sürecinde artan immün modülasyon kapasitelerinin beraberinde proliferasyonda bir yavaşlama göstermiştir. ieAML hücrelerinin T hücresi yanıtları üzerindeki etkisi gerçekten ilginç bulunmuştur; ieAML hücrelerine kıyasla, CD4⁺ T hücreleri ve CD8⁺ T hücreleri, artan sayıda T hücresi içeren wtAML ile birlikte kültürlendiğinde yüksek oranda çoğalmıştır. Bununla birlikte, ieAML hücreleri, yeni elde edilmiş ieAML ile ortak kültürlerde CD4⁺ T hücreleri ve CD8⁺ T hücresi çoğalmasını geciktirmektedir. Ancak bu etki, sürekli kültürde bile CD4⁺ T hücreleri ve CD8⁺ T hücreleri proliferasyonunda bozulma gösteren ieTHP-1'in aksine, sürekli kültüre alınan ieU937 ve ieHL-60 hücrelerinde geçici olmuştur. Sitokin sekresyonunun analizi, wtAML ile gözlemlenen T hücresi ile ilişkili sitokin yanıtlarına kıyasla, T hücrelerinin ieAML hücreleriyle birlikte kültürlenmesinin, aynı anda T hücresi proliferasyonu sırasında IL-2, TNF- α , IFN- γ , granzim A, granzim B ve perforin gibi önemli anti-tümör immün yanıt araçlarının sekresyonunda önemli bir azalmaya yol

açtığı da doğrulamıştır. Özellikle, sadece ieHL-60'a yanıt olarak CD8⁺ T hücreleri tarafından sekrete edilen TNF- α , IFN- γ ve granzim B seviyeleri, wtHL-60 hücrelerinin varlığında gözlenenlere kıyasla önemli bir farklılık göstermemiştir. İlginç bir şekilde, yeni elde edilmiş ieAML hücreleri kullanıldığında, sürekli kültürlenmiş ieU937 veya ieHL-60 hücreleriyle hem CD4⁺ hem de CD8⁺ T hücresi reaksiyonları genel bir artışla sonuçlanmıştır. Özellikle, immün deneyimli U937 ve immün deneyimli HL-60 hücrelerinin T hücre yanıtları üzerindeki olumsuz etkisinin, immün deneyimli THP-1 hücrelerine kıyasla daha az kalıcı olduğu görülmüştür. THP-1 hücrelerindeki "immün deneyim" özelliklerinin tezahürü, miyeloid olgunlaşma ve aktivasyonla ilgili gözlemlenen özelliklerle tutarlı bir şekilde uyumludur. Bu, THP-1 hücreleri bağlamında bağışıklık geçmişi, hücresel davranış ve miyeloid ile ilgili özellikler arasında bir korelasyon olduğunu göstermektedir. Dolayısıyla, MLLR'ler aracılığıyla uyarılan anti-tümör bağışıklık reaksiyonları, lösemi blastları üzerinde derhal önemli bir etki yaratarak hücrenin hayatta kalmasını sağlamayı ve aynı zamanda immünojeniteyi azaltmayı amaçlayan alternatif hücresel programların aktivasyonunu tetiklemiştir. Bu değişmiş durumun süresi kalıntı popülasyonlar arasında değişiklik göstermiştir. Bu direncin kalıcılığı, hücreler üzerinde uygulanan sürekli seçilim baskısına, yani seçilim baskısının sürekliliğine yakından bağlıdır.

Önemlisi, terapötik müdahalenin kesilmesi AML hücrelerinde proliferatif durumun yeniden canlanmasına yol açabilir. İmmün yanıtlar ve lösemi hücrelerinin adaptif stratejileri arasındaki dinamik etkileşim, tedavi stratejileri ve uzun vadeli sonuçlar için potansiyel çıkarımlarla birlikte, gözlemlenen etkilerin karmaşıklığının ve zamansallığının altını çizmektedir. Bu bulgular, tedavi yaklaşımlarının uyarlanması ve uzun vadeli sonuçların dinamiklerinin anlaşılması için potansiyel çıkarımlar taşımaktadır (148, 149). Çalışmamızda, THP-1, MLLR'leri takiben en önemli şekilde etkilenen hücre hattı olarak ortaya çıkmıştır. İmmün-deneyimli U937 (ieU937) ve ieHL-60 ile karşılaştırıldığında, immün deneyim olan THP-1 hücreleri, miyeloid olgunlaşma ve aktivasyon belirteçlerinde daha belirgin bir yükselme ile birlikte daha net ve uzun süreli bir immünojenite kaybı göstermiştir.

Ayrıca, çalışmamızda ieAML hücre yüzey davranışında yapışma, göç ve polarizasyon kapasiteleri gibi değişiklikler de gösterilmiştir; bu da MLLR'lerle

karşılaştığında, hayatta kalan AML alt popülasyonunun immün yanıtlara direnmek için hücre yüzey davranışında bir değişikliğe uğrayabileceğini göstermektedir. Bu durum, miyeloid lösemi hücrelerinin belirli alt popülasyonlarının immün zorluklara dayanmalarını sağlayan mekanizmalara sahip olduğunu ve hayatta kalan hücrelerin anti-tümör immün yanıtlarına karşı dirençlerine katkıda bulunan özellikler edinebileceğini düşündürmektedir.

Ek olarak, immün deneyimli THP-1 hücre hattının transkriptomik imzası belirgin şekilde farklıydı. Öte yandan, ieHL-60 hücreleri, test edilen özellikler açısından MLLR'lerden en az etkilenen hücreler olmakla birlikte, bağışıklık reaksiyonlarını engellemek için önemli yetenekler kazanmıştır. Özellikle, ieHL-60 hücrelerinin çoğalma kapasitesi ieTHP-1 ve ieU937'ninkini aşmış, bu da potansiyel olarak ieHL-60'ta gözlemlenen daha kısa süreli immün modülasyona katkıda bulunmuştur. Sonuç olarak, çalışmamızda kullanılan her AML hücre hattı ikincil immün direnç geliştirebilen bir alt popülasyon barındırmaktadır. Bununla birlikte, bulgularımız sadece lösemi patlamaları arasında heterojen alt popülasyonların önemini vurgulamakla kalmayıp, aynı zamanda farklı geçmişlere sahip AML hücrelerinin immün reaksiyonlara yanıt olarak biyolojik çeşitlilik gösterebileceğini de vurgulamaktadır.

Tümör immünesine ilişkin mevcut bilgilere göre, kanserin ilerlemesinden önce immün reaksiyonların yarattığı hostil koşullara rağmen hayatta kalmak için sürekli olarak en uygun malign klonları seçen immün eliminasyon, denge ve kaçış fazları gelmektedir (163). Tümör mikroçevresinde gelişmiş immün infiltrasyon ve pro-inflamatuar faktörlerin artan ekspresyonu gibi aktif bir immün reaksiyonun belirtileri, immünoterapinin başarısıyla ilişkilendirilmiştir (155). Bununla birlikte, birçok solid tümör ve hematolojik malignite bir immün çöl olarak tanımlanır ve immünosupresif bir niş içinde bulunur (214). İmmün-deneyimli AML (ieAML) hücrelerinde gözlemlendiği gibi, immün yanıtlara maruz kalan lösemi hücrelerinin immünojenik olmayan klonlar için tohum görevi görebileceği ve immünoterapötik müdahalelere direnç gösterebileceği varsayılabilir. Çalışmamızın bir dezavantajı olarak, immün direnç imzalarının ve epigenetik değişikliklerin kalıcılığının daha iyi tanımlanması ve ieAML hücrelerinde uzun süre takip edilmesi gerekmektedir.

Transkripsiyon faktörlerinin ekspresyonundaki düzenleme ve değişiklikler AML patogenezinde önemli faktörlerdir. Çalışmamızda ieAML hücrelerinde önemli ölçüde yukarı regülasyon gösteren transkripsiyon faktörlerinden biri KLF6 bulunmuştur. Krüppel benzeri faktörler (KLF'ler) protein ailesi, köklülük ve pluripotensinin korunması, miyeloid farklılaşma, inflamasyon, proliferasyon ve apoptozisi kapsayan çeşitli hücresel süreçlerde karmaşık bir şekilde yer almaktadır. Bu aile içinde dikkate değer bir örnek KLF6'dır. Çeşitli fonksiyonel ve ekspresyon deneyleri, KLF6 fonksiyonunun bozulmasının kanser, inflamasyonla ilgili hastalıklar ve kardiyovasküler bozuklukların gelişimine katkıda bulunduğunu göstermiştir. Bu durum, KLF6'nın hücresel fonksiyonların temel yönlerini yönetmede, hücre kimlik, bağışıklık sistemi tepkileri, büyüme ve programlanmış hücre ölümü ile ilişkili süreçleri etkilemedeki çeşitli rolünün altını çizmektedir. Buna ek olarak, KLF6 makrofajlarda HIF1 α ekspresyonunu doğrudan yükselterek, doğuştan gelen bağışıklık hücresi enflamatuar ve hipoksik yanıt gen programlamasını teşvik etmiştir. Bu ilişkileri detaylandırarak olursak, KLF6'nın katılımı, hücre içindeki çeşitli kritik fonksiyonların düzenlenmesindeki önemini altını çizmektedir (193, 194, 215). Bu transkripsiyon faktörü AML'de yüksek ekspresyon seviyeleri gösterir ve tümörigenez üzerinde zararlı etkiler uygular. Bunu, hücre döngüsü, programlanmış hücre ölümü ve yaşlanma gibi kritik hücresel süreçlerde yer alan genlerin düzenlenmesini denetleyerek başarır. Esasında, AML'de bu transkripsiyon faktörünün artan varlığı, hücre büyüme kontrolü, hücre sağkalımı ve yaşlanma süreçleriyle ilişkili moleküler yolları etkilemede çok önemli bir rol oynamaktadır (194, 215). Bununla birlikte, çok sayıda çalışma KLF6'nın kanser de dahil olmak üzere enflamatuar hastalıkların bir destekleyicisi olarak rol oynadığını vurgulamıştır. 8q22;21q22 translokasyonu [t(8;21)] ile karakterize akut miyeloid lösemi (AML) vakalarında KLF6, RUNX1-ETO füzyon proteini tarafından yönlendirilen lösemogenezde yer alan aşağı akış hedeflerinin ifadesini etkilemede rol oynar (216). Çalışmamızda kullanılan hücre hatları t(8;21) translokasyonu taşımamaktadır (212, 213).

Ayrıca, ieAML hücrelerinde KLF6'nın nükleer lokalizasyonunda değişikliklerle birlikte bir yukarı regülasyon tespit ettik. Tersine, bağışıklık reaksiyonlarına maruz kalmanın ardından miyeloid lösemi hücrelerinde KLF6'nın

hücre çekirdeğine artan translokasyonu, immün deneyimi olan AML hücrelerinde hareketsiz bir durumun elde edilmesinde potansiyel bir rol anlamına gelebilir.

Bir diğer önemli transkripsiyon faktörü olan c-MYB transkripsiyonel ko-aktivatör kompleksi, hematopoetik kök hücrelerin (HSC) kendini yenilemesinde ve miyelopoez sürecinde çok önemli bir rol oynamaktadır (217, 218). AML kapsamında, c-MYB'nin bozulmuş fonksiyonlarına yaygın bir güven söz konusudur (219). Hematopoetik hücreler terminal farklılaşmaya uğradıkça MYB ifadesi genelde azalır (220, 221). Bu durum, c-MYB ve ilişkili kompleksinin hematopoietik kök hücrelerin farklılaşmamış durumunun sürdürülmesinde entegre komponentler olduğunu, AML'de ise bu mekanizmaların düzensizliğinin sıklıkla gözlemlendiğini ve hastalığın patogeneze katkıda bulunduğunu göstermektedir. Yüksek miyeloid olgunlaşma özellikleri ve azalmış proliferasyon oranı ile tutarlı olarak, c-MYB çekirdekten çıkarılmış ve bağışıklık deneyimi olan AML (ieAML) hücrelerinde aşağı regüle edilmiştir. Bu durum, immün reaksiyonlara yanıt olarak, miyeloid lösemi blastlarındaki hücrel süreçlerin yönetilmesinde MYB'den bağımsız bir programın öncelikli olduğunu göstermektedir. Bu gözlem, KLF6 ve c-MYB'nin nükleer dağılımı ile ilgili olarak AML hastalarının kemik iliği örneklerinden elde edilen malign blastlarda gözlenen heterojenlik ile uyumludur.

Bu gözlemler KLF6 ve c-MYB transkripsiyon faktörlerinin miyeloid lösemi blastlarında immün karşılaşma durumunun potansiyel göstergeleri olduğunu göstermektedir. Spesifik transkripsiyon faktörlerinin nükleer lokalizasyonunda gözlenen farklılıklar, miyeloid lösemi blastlarında immün karşılaşma durumunu ayırt etmek için potansiyel belirteçler olarak hizmet edebilir ve lösemi hücrelerinde immün kaçınma mekanizmalarının üstesinden gelmeyi amaçlayan hedefli terapötik stratejiler geliştirmek için değerli bilgiler sağlayabilir. Bununla birlikte, KLF6 ve c-MYB'nin AML kapsamında bağışıklık yanıtının modüle edilmesinde oynadığı spesifik rolleri ortaya çıkarmak için daha fazla araştırma yapılması zorunludur.

Bu nedenle, Akut Miyeloid Lösemide (AML) nüks veya dirence katkıda bulunan temel faktörler arasında gen ekspresyonu imzalarındaki farklılıklar, olgunlaşma durumları ve hücrel plastisite yer almaktadır (148, 149). İmmün yanıtlar dinamik ve istikrarsız bir mikro çevre yaratarak lösemik blastları biyolojik

programlarını uyarlamaya ve yeni koşullara yanıt vermeye zorlayabilir. Özel bir ex-vivo seçim modeli kullanarak, miyeloid lösemi hücrelerinin belirli alt popülasyonları içinde edinilmiş immün direnç özelliklerini belirledik.

Özetle, heterojenliğin anlaşılması, immün düzenleme mekanizmalarının çözülmesi ve immün dirençli alt popülasyonların ortaya çıkışının kabul edilmesi, AML bağlamında kapsamlı araştırma ve dikkat gerektiren çok önemli yönlerdir. Bu bakış açısı, hematolojik maligniteleri hedef alan gelecekteki immün müdahale tedavilerinin ilerletilmesi ve rafine edilmesi için önemli çıkarımlara sahiptir. İmmün yanıtlar ve lösemi hücrelerinin adaptif stratejileri arasındaki kompleks etkileşim, terapötik yaklaşımların etkinliğini artırmak için kapsamlı araştırmaların gerekliliğinin altını çizmektedir.

7.4. Sonuç ve Öneriler

- Farklı olgunlaşma aşamalarındaki AML hücreleri genetik heterojenlik göstererek tedavilere karşı direnç ve bağışıklık sisteminden kaçınmaya yol açmaktadır. Bu nedenle, direnç ve uyum yeteneğinin üstesinden gelmek için AML hücrelerinin genetik heterojenliğini dikkate alan hedefe yönelik tedavi stratejilerinin geliştirilmesine ihtiyaç vardır.
- AML alt popülasyonunun heterojen genetik arka planı ile bağışıklık hücreleri arasındaki dinamik etkileşim, olgunlaşma durumu, aktivasyon ve çoğalma kapasitesindeki değişikliğin yanı sıra farklı AML alt popülasyonlarında farklı düzeyde işleyen immün modülasyon potansiyelindeki değişikliğe katkıda bulunur.
- Kemik iliği nakli ve kemoterapi dahil olmak üzere tedaviler sırasında lösemi hücrelerinin sürekli evrimi, kapsamlı terapötik stratejilere olan ihtiyacı vurgulamaktadır.
- İmmün saldırıdan kurtulan AML alt popülasyonu "ieAML hücreleri", immün hücreler için aktivasyon eşiklerini etkileyebilen ve immün kaçınma stratejilerine katkıda bulunan kostimülatör ve inhibitör moleküllerin artan ekspresyonu ile ilişkilidir.
- AML hücrelerinin "immün deneyimli" olarak adlandırılan alt popülasyonları immün sistemden kaçabilir ve immün modülasyona

yardımcı olan özellikler kazanabilir. Bu nedenle, immün direnç imzalarının ve immün deneyimli hücrelerdeki epigenetik değişikliklerin uzun süre boyunca kalıcılığını araştırmak için stratejilere ihtiyaç vardır.

- Tümör mikroçevresinin ve bağışıklık sisteminin bağışıklık direnci üzerindeki etkisinin, MLLR'lerle ilk ve ikinci karşılaşmadan kurtulan hücrelerin, bu geçici bağışıklık modülasyonu kalıcı hale gelene kadar birden fazla bağışıklık hücresiyle karşılaşması gereken bir zaman aralığında araştırılması gerekmektedir.
- AML hastaları için immün müdahale tedavilerine dönüştürülebilecek immünoterapi stratejileri geliştirmek üzere adaptif immün yanıtı şekillendirmede AML'deki miyeloid hücrelerin daha iyi anlaşılması için ortak bir immün imzanın izini sürmek amacıyla ieAML hücrelerinin biyolojik ve immün modülatör kapasitelerinin çoklu ilaç direnci AML hücreleriyle karşılaştırılması gerekmektedir.
- Tümör mikroçevresi ve immün sistem etkileşimleri, başta enflamatuar yolaklar olmak üzere çeşitli sinyal yolları aracılığıyla immün dirence katkıda bulunur. Bu enflamatuar yolları bloke etmek ve bunun olgunlaşma durumu ve T hücresi yanıtındaki değişiklikler üzerindeki etkisini incelemek için daha fazla araştırma yapılabilir.
- AML'de immünoterapiden önemli bir fayda görülmemesi, immün kaçınma mekanizmalarının daha iyi anlaşılması gerektiğini vurgulamaktadır.
- İmmün deneyimli (ieAML) hücrelerinde immün dirençten sorumlu KLF6 izoformunun türünü anlamak için western blotlama yoluyla KLF6 için protein ekspresyon analizi yapılabilir.
- KLF6 ve c-MYB gibi transkripsiyon faktörleri immün yanıtlarda rol oynar ve miyeloid lösemi blastlarında immün karşılaşma durumunu ayırt etmek için potansiyel belirteçler olarak hizmet edebilir.
- AML'de immün yanıtı modüle etmek için KLF6 ve c-MYB gibi transkripsiyon faktörlerinin terapötik hedefler olarak araştırılması, AML hücrelerinde bu iki TF'nin susturulması/kilitlenmesive olgunlaşma durumuna yanıtının incelenmesiyle daha da araştırılabilir.

- KLF6 ve c-MYB nakavt AML hücreleri, in-vivo çalışmalarda AML immün direncinin dinamiklerini incelemek için farelere yerleştirilebilir. Bağışıklık yanıtlarının, direncin ve nüksün dinamiklerini anlamak için AML hastalarında kemoterapi öncesinde, kemoterapi sırasında, nakil sırasında ve sonrasında KLF6 ve c-MYB ifadesinin uzun süreli izlenmesi.
- Tedavi stratejilerini, lösemi hücrelerinin sürekli evrimine ve bağışıklık müdahalelerine adaptasyonuna dayalı olarak uyarlayın.

Sonuç olarak, AML'de genetik, immün ve adaptif özellikler arasındaki etkileşimin kapsamlı bir şekilde anlaşılması, etkili terapötik yaklaşımların geliştirilmesi ve uzun vadeli sonuçların iyileştirilmesi için çok önemlidir. Sonuçlar ve öneriler, hem genetik heterojenite hem de bağışıklıktan kaçınma stratejileri göz önünde bulundurularak tedavilerin AML'nin çeşitli doğasına göre uyarlanması için bir temel sağlamaktadır.

8. REFERENCES

1. Lichtenegger FS, Krupka C, Haubner S, Köhnke T, Subklewe M. Recent developments in immunotherapy of acute myeloid leukemia. *Journal of hematology & oncology*. 2017;10(1):1-20.
2. Zacharakis N, Chinnasamy H, Black M, Xu H, Lu Y-C, Zheng Z, et al. Immune recognition of somatic mutations leading to complete durable regression in metastatic breast cancer. *Nature medicine*. 2018;24(6):724-30.
3. Vyas P, Appelbaum FR, Craddock C. Allogeneic hematopoietic cell transplantation for acute myeloid leukemia. *Biology of Blood and Marrow Transplantation*. 2015;21(1):8-15.
4. Cornelissen JJ, Breems D, Van Putten WL, Gratwohl AA, Passweg JR, Pabst T, et al. Comparative analysis of the value of allogeneic hematopoietic stem-cell transplantation in acute myeloid leukemia with monosomal karyotype versus other cytogenetic risk categories. *Journal of clinical oncology*. 2012;30(17):2140-6.
5. Report USTDbD. Transplant Data by Disease Report, AML - Acute myelogenous leukemia, Patient Survival 2011 - 2015. U.S: Center for International Blood and Marrow Transplant a contractor for the C.W. Bill Young Cell Transplantation Program operated through the U. S. Department of Health and Human Services, Health Resources and Services Administration, Healthcare Systems Bureau. U.S. ; 2019.
6. Christopher MJ, Petti AA, Rettig MP, Miller CA, Chendamarai E, Duncavage EJ, et al. Immune escape of relapsed AML cells after allogeneic transplantation. *New England Journal of Medicine*. 2018;379(24):2330-41.
7. Zeiser R, Vago L. Mechanisms of immune escape after allogeneic hematopoietic cell transplantation. *Blood, The Journal of the American Society of Hematology*. 2019;133(12):1290-7.
8. Toffalori C, Zito L, Gambacorta V, Riba M, Oliveira G, Bucci G, et al. Immune signature drives leukemia escape and relapse after hematopoietic cell transplantation. *Nature medicine*. 2019;25(4):603-11.
9. Jan M, Leventhal MJ, Morgan EA, Wengrod JC, Nag A, Drinan SD, et al. Recurrent genetic HLA loss in AML relapsed after matched unrelated allogeneic hematopoietic cell transplantation. *Blood Advances*. 2019;3(14):2199-204.
10. Ozkazanc D, Yoyen-Ermis D, Tavukcuoglu E, Buyukasik Y, Esendagli G. Functional exhaustion of CD4+ T cells induced by co-stimulatory signals from myeloid leukaemia cells. *Immunology*. 2016;149(4):460-71.

11. Dolen Y, Esendagli G. Myeloid leukemia cells with a B7-2+ subpopulation provoke Th-cell responses and become immuno-suppressive through the modulation of B7 ligands. *European Journal of Immunology*. 2013;43(3):747-57.
12. Stahl M, Goldberg AD. Immune checkpoint inhibitors in acute myeloid leukemia: novel combinations and therapeutic targets. *Current oncology reports*. 2019;21:1-10.
13. Yoyen-Ermis D, Tunali G, Tavukcuoglu E, Horzum U, Ozkazanc D, Sutlu T, et al. Myeloid maturation potentiates STAT3-mediated atypical IFN- γ signaling and upregulation of PD-1 ligands in AML and MDS. *Scientific reports*. 2019;9(1):1-11.
14. Alfayez M, Borthakur G. Checkpoint inhibitors and acute myelogenous leukemia: promises and challenges. *Expert review of hematology*. 2018;11(5):373-89.
15. Döhner H, Weisdorf DJ, Bloomfield CD. Acute myeloid leukemia. *New England Journal of Medicine*. 2015;373(12):1136-52.
16. Papaemmanuil E, Gerstung M, Bullinger L, Gaidzik VI, Paschka P, Roberts ND, et al. Genomic classification and prognosis in acute myeloid leukemia. *New England Journal of Medicine*. 2016;374(23):2209-21.
17. Rosen JM, Jordan CT. The increasing complexity of the cancer stem cell paradigm. *Science*. 2009;324(5935):1670-3.
18. Arber DA, Orazi A, Hasserjian R, Thiele J, Borowitz MJ, Le Beau MM, et al. The 2016 revision to the World Health Organization classification of myeloid neoplasms and acute leukemia. *Blood, The Journal of the American Society of Hematology*. 2016;127(20):2391-405.
19. Sanz MA, Fenaux P, Tallman MS, Estey EH, Löwenberg B, Naoe T, et al. Management of acute promyelocytic leukemia: updated recommendations from an expert panel of the European LeukemiaNet. *Blood, The Journal of the American Society of Hematology*. 2019;133(15):1630-43.
20. Röllig C, Kramer M, Schliemann C, Mikesch J-H, Steffen B, Krämer A, et al. Does time from diagnosis to treatment affect the prognosis of patients with newly diagnosed acute myeloid leukemia? *Blood, The Journal of the American Society of Hematology*. 2020;136(7):823-30.
21. Sasaki K, Ravandi F, Kadia TM, DiNardo CD, Short NJ, Borthakur G, et al. De novo acute myeloid leukemia: a population-based study of outcome in the United States based on the Surveillance, Epidemiology, and End Results (SEER) database, 1980 to 2017. *Cancer*. 2021;127(12):2049-61.
22. Cancer Stat Facts: Leukemia — Acute Myeloid Leukemia (AML) [Available from: (<https://seer.cancer.gov/statfacts/html/amyl.html>).

23. Foreman KJ, Marquez N, Dolgert A, Fukutaki K, Fullman N, McGaughey M, et al. Forecasting life expectancy, years of life lost, and all-cause and cause-specific mortality for 250 causes of death: reference and alternative scenarios for 2016–40 for 195 countries and territories. *The Lancet*. 2018;392(10159):2052-90.
24. Juliusson G, Hagberg O, Lazarevic VL, Ölander E, Antunovic P, Cammenga J, et al. Improved survival of men 50 to 75 years old with acute myeloid leukemia over a 20-year period. *Blood, The Journal of the American Society of Hematology*. 2019;134(18):1558-61.
25. Döhner H, Estey EH, Amadori S, Appelbaum FR, Büchner T, Burnett AK, et al. Diagnosis and management of acute myeloid leukemia in adults: recommendations from an international expert panel, on behalf of the European LeukemiaNet. *Blood, The Journal of the American Society of Hematology*. 2010;115(3):453-74.
26. Metcalf D, Moore MA, Warner NL. Colony formation in vitro by myelomonocytic leukemic cells. *Journal of the National Cancer Institute*. 1969;43(4):983-1001.
27. Moore M, Williams N, Metcalf D. In vitro colony formation by normal and leukemic human hematopoietic cells: characterization of the colony-forming cells. *Journal of the National Cancer Institute*. 1973;50(3):603-23.
28. Dick JE. Acute myeloid leukemia stem cells. *Annals of the New York Academy of Sciences*. 2005;1044(1):1-5.
29. Lapidot T, Sirard C, Vormoor J, Murdoch B, Hoang T, Caceres-Cortes J, et al. A cell initiating human acute myeloid leukaemia after transplantation into SCID mice. *Nature*. 1994;367(6464):645-8.
30. Bonnet D, Dick JE. Human acute myeloid leukemia is organized as a hierarchy that originates from a primitive hematopoietic cell. *Nature medicine*. 1997;3(7):730-7.
31. Schiffer CA, Gurbuxani S. Classification of acute myeloid leukemia (AML).
32. Pizzi M, Gurrieri C, Orazi A. What's New in the Classification, Diagnosis and Therapy of Myeloid Leukemias. *Hemato*. 2023;4(2):112-34.
33. Khoury JD, Solary E, Abla O, Akkari Y, Alaggio R, Apperley JF, et al. The 5th edition of the World Health Organization classification of haematolymphoid tumours: myeloid and histiocytic/dendritic neoplasms. *Leukemia*. 2022;36(7):1703-19.
34. Arber DA, Orazi A, Hasserjian RP, Borowitz MJ, Calvo KR, Kvasnicka H-M, et al. International Consensus Classification of Myeloid Neoplasms and Acute Leukemias: integrating morphologic, clinical, and genomic data.

- Blood, The Journal of the American Society of Hematology. 2022;140(11):1200-28.
35. Forghieri F, Nasillo V, Paolini A, Bettelli F, Pioli V, Giusti D, et al. NPM1-mutated myeloid neoplasms with < 20% blasts: a really distinct clinicopathologic entity? *International Journal of Molecular Sciences*. 2020;21(23):8975.
 36. Patel SS, Ho C, Ptashkin RN, Sadigh S, Bagg A, Geyer JT, et al. Clinicopathologic and genetic characterization of nonacute NPM1-mutated myeloid neoplasms. *Blood Advances*. 2019;3(9):1540-5.
 37. Wakita S, Sakaguchi M, Oh I, Kako S, Toya T, Najima Y, et al. Prognostic impact of CEBPA bZIP domain mutation in acute myeloid leukemia. *Blood Advances*. 2022;6(1):238-47.
 38. Taube F, Georgi JA, Kramer M, Stasik S, Middeke JM, Röllig C, et al. CEBPA mutations in 4708 patients with acute myeloid leukemia: differential impact of bZIP and TAD mutations on outcome. *Blood, The Journal of the American Society of Hematology*. 2022;139(1):87-103.
 39. Tarlock K, Lamble AJ, Wang Y-C, Gerbing RB, Ries RE, Loken MR, et al. CEBPA-bZip mutations are associated with favorable prognosis in de novo AML: a report from the Children's Oncology Group. *Blood, The Journal of the American Society of Hematology*. 2021;138(13):1137-47.
 40. Estey E, Hasserjian RP, Döhner H. Distinguishing AML from MDS: a fixed blast percentage may no longer be optimal. *Blood, The Journal of the American Society of Hematology*. 2022;139(3):323-32.
 41. DiNardo CD, Garcia-Manero G, Pierce S, Nazha A, Bueso-Ramos C, Jabbour E, et al. Interactions and relevance of blast percentage and treatment strategy among younger and older patients with acute myeloid leukemia (AML) and myelodysplastic syndrome (MDS). *American journal of hematology*. 2016;91(2):227-32.
 42. Estey E, Thall P, Beran M, Kantarjian H, Pierce S, Keating M. Effect of diagnosis (refractory anemia with excess blasts, refractory anemia with excess blasts in transformation, or acute myeloid leukemia [AML]) on outcome of AML-type chemotherapy. *Blood, The Journal of the American Society of Hematology*. 1997;90(8):2969-77.
 43. DiNardo CD, Garcia-Manero G, Kantarjian HM. Time to blur the blast boundaries. *Wiley Online Library*; 2022. p. 1568-70.
 44. Trottier AM, Godley LA. Inherited predisposition to haematopoietic malignancies: overcoming barriers and exploring opportunities. *British Journal of Haematology*. 2021;194(4):663-76.

45. Godley LA, Shimamura A. Genetic predisposition to hematologic malignancies: management and surveillance. *Blood, The Journal of the American Society of Hematology*. 2017;130(4):424-32.
46. Rafei H, DiNardo CD. Hereditary myeloid malignancies. *Best Practice & Research Clinical Haematology*. 2019;32(2):163-76.
47. Yang F, Long N, Anekpuritanang T, Bottomly D, Savage JC, Lee T, et al. Identification and prioritization of myeloid malignancy germline variants in a large cohort of adult patients with AML. *Blood, The Journal of the American Society of Hematology*. 2022;139(8):1208-21.
48. Li P, Brown S, Williams M, White T, Xie W, Cui W, et al. The genetic landscape of germline DDX41 variants predisposing to myeloid neoplasms. *Blood, The Journal of the American Society of Hematology*. 2022;140(7):716-55.
49. Polprasert C, Schulze I, Sekeres MA, Makishima H, Przychodzen B, Hosono N, et al. Inherited and somatic defects in DDX41 in myeloid neoplasms. *Cancer cell*. 2015;27(5):658-70.
50. Duployez N, Largeaud L, Duchmann M, Kim R, Rieunier J, Lambert J, et al. Prognostic impact of DDX41 germline mutations in intensively treated acute myeloid leukemia patients: an ALFA-FILO study. *Blood, The Journal of the American Society of Hematology*. 2022;140(7):756-68.
51. Döhner H, Wei AH, Appelbaum FR, Craddock C, DiNardo CD, Dombret H, et al. Diagnosis and management of AML in adults: 2022 recommendations from an international expert panel on behalf of the ELN. *Blood, The Journal of the American Society of Hematology*. 2022;140(12):1345-77.
52. Yates J, Wallace Jr H, Ellison R, Holland J. Cytosine arabinoside (NSC-63878) and daunorubicin (NSC-83142) therapy in acute nonlymphocytic leukemia. *Cancer chemotherapy reports*. 1973;57(4):485-8.
53. Rai KR, Holland JF, Glidewell OJ, Weinberg V, Brunner K, Obrecht J, et al. Treatment of acute myelocytic leukemia: a study by cancer and leukemia group B. 1981.
54. Ho MM, Hogge DE, Ling V. MDR1 and BCRP1 expression in leukemic progenitors correlates with chemotherapy response in acute myeloid leukemia. *Experimental hematology*. 2008;36(4):433-42.
55. Wulf GG, Wang R-Y, Kuehnle I, Weidner D, Marini F, Brenner MK, et al. A leukemic stem cell with intrinsic drug efflux capacity in acute myeloid leukemia. *Blood, The Journal of the American Society of Hematology*. 2001;98(4):1166-73.

56. Shlush LI, Mitchell A, Heisler L, Abelson S, Ng SW, Trotman-Grant A, et al. Tracing the origins of relapse in acute myeloid leukaemia to stem cells. *Nature*. 2017;547(7661):104-8.
57. Saito Y, Kitamura H, Hijikata A, Tomizawa-Murasawa M, Tanaka S, Takagi S, et al. Identification of therapeutic targets for quiescent, chemotherapy-resistant human leukemia stem cells. *Science translational medicine*. 2010;2(17):17ra9-ra9.
58. Mitchell K, Steidl U. Targeting immunophenotypic markers on leukemic stem cells: how lessons from current approaches and advances in the leukemia stem cell (LSC) model can inform better strategies for treating acute myeloid leukemia (AML). *Cold Spring Harbor Perspectives in Medicine*. 2020;10(1).
59. Mattes K, Vellenga E, Schepers H. Differential redox-regulation and mitochondrial dynamics in normal and leukemic hematopoietic stem cells: A potential window for leukemia therapy. *Critical Reviews in Oncology/Hematology*. 2019;144:102814.
60. Chan W-I, Huntly BJ, editors. *Leukemia stem cells in acute myeloid leukemia*. Seminars in oncology; 2008: Elsevier.
61. Goardon N, Marchi E, Atzberger A, Quek L, Schuh A, Soneji S, et al. Coexistence of LMPP-like and GMP-like leukemia stem cells in acute myeloid leukemia. *Cancer cell*. 2011;19(1):138-52.
62. Quek L, Otto GW, Garnett C, Lhermitte L, Karamitros D, Stoilova B, et al. Genetically distinct leukemic stem cells in human CD34⁻ acute myeloid leukemia are arrested at a hemopoietic precursor-like stage. *Journal of Experimental Medicine*. 2016;213(8):1513-35.
63. Haubner S, Perna F, Köhnke T, Schmidt C, Berman S, Augsberger C, et al. Coexpression profile of leukemic stem cell markers for combinatorial targeted therapy in AML. *Leukemia*. 2019;33(1):64-74.
64. Appelbaum FR, Bernstein ID. Gemtuzumab ozogamicin for acute myeloid leukemia. *Blood, The Journal of the American Society of Hematology*. 2017;130(22):2373-6.
65. Stelmach P, Trumpp A. Leukemic stem cells and therapy resistance in acute myeloid leukemia. *Haematologica*. 2023;108(2):353.
66. Konopleva MY, Jordan CT. Leukemia stem cells and microenvironment: biology and therapeutic targeting. *Journal of clinical oncology*. 2011;29(5):591.
67. Quail DF, Joyce JA. Microenvironmental regulation of tumor progression and metastasis. *Nature medicine*. 2013;19(11):1423-37.

68. Sendker S, Reinhardt D, Niktoreh N. Redirecting the immune microenvironment in acute myeloid leukemia. *Cancers*. 2021;13(6):1423.
69. Barakos GP, Hatzimichael E. Microenvironmental Features Driving Immune Evasion in Myelodysplastic Syndromes and Acute Myeloid Leukemia. *Diseases*. 2022;10(2):33.
70. Taussig DC, Vargaftig J, Miraki-Moud F, Griessinger E, Sharrock K, Luke T, et al. Leukemia-initiating cells from some acute myeloid leukemia patients with mutated nucleophosmin reside in the CD34⁻ fraction. *Blood, The Journal of the American Society of Hematology*. 2010;115(10):1976-84.
71. Falini B, Mecucci C, Tiacci E, Alcalay M, Rosati R, Pasqualucci L, et al. Cytoplasmic nucleophosmin in acute myelogenous leukemia with a normal karyotype. *New England Journal of Medicine*. 2005;352(3):254-66.
72. Chan SM, Majeti R. Role of DNMT3A, TET2, and IDH1/2 mutations in pre-leukemic stem cells in acute myeloid leukemia. *International journal of hematology*. 2013;98:648-57.
73. Sarry J-E, Murphy K, Perry R, Sanchez PV, Secreto A, Keefer C, et al. Human acute myelogenous leukemia stem cells are rare and heterogeneous when assayed in NOD/SCID/IL2R γ -deficient mice. *The Journal of clinical investigation*. 2011;121(1):384-95.
74. Eppert K, Takenaka K, Lechman ER, Waldron L, Nilsson B, Van Galen P, et al. Stem cell gene expression programs influence clinical outcome in human leukemia. *Nature medicine*. 2011;17(9):1086-93.
75. Gentles AJ, Plevritis SK, Majeti R, Alizadeh AA. Association of a leukemic stem cell gene expression signature with clinical outcomes in acute myeloid leukemia. *Jama*. 2010;304(24):2706-15.
76. Zhou H-S, Carter BZ, Andreeff M. Bone marrow niche-mediated survival of leukemia stem cells in acute myeloid leukemia: Yin and Yang. *Cancer biology & medicine*. 2016;13(2):248.
77. Shlush LI, Zandi S, Mitchell A, Chen WC, Brandwein JM, Gupta V, et al. Identification of pre-leukaemic haematopoietic stem cells in acute leukaemia. *Nature*. 2014;506(7488):328-33.
78. Lara-Astiaso D, Weiner A, Lorenzo-Vivas E, Zaretzky I, Jaitin DA, David E, et al. Chromatin state dynamics during blood formation. *science*. 2014;345(6199):943-9.
79. Schenk T, Chen WC, Göllner S, Howell L, Jin L, Hebestreit K, et al. Inhibition of the LSD1 (KDM1A) demethylase reactivates the all-trans-retinoic acid differentiation pathway in acute myeloid leukemia. *Nature medicine*. 2012;18(4):605-11.

80. Wong SH, Goode DL, Iwasaki M, Wei MC, Kuo H-P, Zhu L, et al. The H3K4-methyl epigenome regulates leukemia stem cell oncogenic potential. *Cancer cell*. 2015;28(2):198-209.
81. Krawczyk J, O'Dwyer M, Swords R, Freeman C, Giles FJ. The role of inflammation in leukaemia. *Inflammation and Cancer*. 2014:335-60.
82. Cerrano M, Duchmann M, Kim R, Vasseur L, Hirsch P, Thomas X, et al. Clonal dominance is an adverse prognostic factor in acute myeloid leukemia treated with intensive chemotherapy. *Leukemia*. 2021;35(3):712-23.
83. Duchmann M, Laplane L, Itzykson R. Clonal architecture and evolutionary dynamics in acute myeloid leukemias. *Cancers*. 2021;13(19):4887.
84. Binder S, Luciano M, Horejs-Hoeck J. The cytokine network in acute myeloid leukemia (AML): A focus on pro-and anti-inflammatory mediators. *Cytokine & growth factor reviews*. 2018;43:8-15.
85. Boissel N, Leroy H, Brethon B, Philippe N, de Botton S, Auvrignon A, et al. Incidence and prognostic impact of c-Kit, FLT3, and Ras gene mutations in core binding factor acute myeloid leukemia (CBF-AML). *Leukemia*. 2006;20(6):965-70.
86. Goemans B, Zwaan CM, Miller M, Zimmermann M, Harlow A, Meshinchi S, et al. Mutations in KIT and RAS are frequent events in pediatric core-binding factor acute myeloid leukemia. *Leukemia*. 2005;19(9):1536-42.
87. Park SH, Chi H-S, Min S-K, Park BG, Jang S, Park C-J. Prognostic impact of c-KIT mutations in core binding factor acute myeloid leukemia. *Leukemia research*. 2011;35(10):1376-83.
88. Tsai F-Y, Keller G, Kuo FC, Weiss M, Chen J, Rosenblatt M, et al. An early haematopoietic defect in mice lacking the transcription factor GATA-2. *Nature*. 1994;371(6494):221-6.
89. Wlodarski MW, Hirabayashi S, Pastor V, Starý J, Hasle H, Masetti R, et al. Prevalence, clinical characteristics, and prognosis of GATA2-related myelodysplastic syndromes in children and adolescents. *Blood, The Journal of the American Society of Hematology*. 2016;127(11):1387-97.
90. Katsumura KR, Yang C, Boyer ME, Li L, Bresnick EH. Molecular basis of crosstalk between oncogenic Ras and the master regulator of hematopoiesis GATA-2. *EMBO reports*. 2014;15(9):938-47.
91. Katsumura KR, Ong IM, DeVilbiss AW, Sanalkumar R, Bresnick EH. GATA factor-dependent positive-feedback circuit in acute myeloid leukemia cells. *Cell reports*. 2016;16(9):2428-41.
92. Wu L, Amarachintha S, Xu J, Oley Jr F, Du W. Mesenchymal COX 2-PG secretome engages NR 4A-WNT signalling axis in haematopoietic

- progenitors to suppress anti-leukaemia immunity. *British journal of haematology*. 2018;183(3):445-56.
93. Imbert V, Peyron J-F. NF- κ B in hematological malignancies. *Biomedicines*. 2017;5(2):27.
 94. Mi G. Nuclear factor-kappaB is constitutively activated in primitive human acute myelogenous leukemia cells. *Blood*. 2001;98:2301-7.
 95. Nakagawa M, Shimabe M, Watanabe-Okochi N, Arai S, Yoshimi A, Shinohara A, et al. AML1/RUNX1 functions as a cytoplasmic attenuator of NF- κ B signaling in the repression of myeloid tumors. *Blood, The Journal of the American Society of Hematology*. 2011;118(25):6626-37.
 96. Bosman MCJ, Schuringa JJ, Vellenga E. Constitutive NF- κ B activation in AML: Causes and treatment strategies. *Critical reviews in oncology/hematology*. 2016;98:35-44.
 97. Gasparini C, Celeghini C, Monasta L, Zauli G. NF- κ B pathways in hematological malignancies. *Cellular and Molecular Life Sciences*. 2014;71:2083-102.
 98. Brandão MM, Soares E, Salles TSI, Saad STO. Expression of Inducible Nitric Oxide Synthase Is Increased in Acute Myeloid Leukaemia. *Acta Haematologica*. 2001;106(3):95-9.
 99. Rushworth SA, MacEwan DJ. HO-1 underlies resistance of AML cells to TNF-induced apoptosis. *Blood*. 2008;111(7):3793-801.
 100. Heasman S-A, Zaitseva L, Bowles KM, Rushworth SA, MacEwan DJ. Protection of acute myeloid leukaemia cells from apoptosis induced by front-line chemotherapeutics is mediated by haem oxygenase-1. *Oncotarget*. 2011;2(9):658.
 101. Rushworth SA, Bowles KM, Raninga P, MacEwan DJ. NF- κ B-inhibited acute myeloid leukemia cells are rescued from apoptosis by heme oxygenase-1 induction. *Cancer research*. 2010;70(7):2973-83.
 102. Kagoya Y, Yoshimi A, Kataoka K, Nakagawa M, Kumano K, Arai S, et al. Positive feedback between NF- κ B and TNF- α promotes leukemia-initiating cell capacity. *The Journal of clinical investigation*. 2014;124(2):528-42.
 103. Reckzeh K, Cammenga J. Molecular mechanisms underlying deregulation of C/EBP α in acute myeloid leukemia. *International journal of hematology*. 2010;91:557-68.
 104. Tolomeo M, Grimaudo S. The “Janus” role of C/EBPs family members in cancer progression. *International journal of molecular sciences*. 2020;21(12):4308.

105. Alberich-Jordà M, Wouters B, Balastik M, Shapiro-Koss C, Zhang H, DiRuscio A, et al. C/EBP γ deregulation results in differentiation arrest in acute myeloid leukemia. *The Journal of clinical investigation*. 2012;122(12):4490-504.
106. Preudhomme C, Sagot C, Boissel N, Cayuela J-M, Tigaud I, de Botton S, et al. Favorable prognostic significance of CEBPA mutations in patients with de novo acute myeloid leukemia: a study from the Acute Leukemia French Association (ALFA). *Blood, The Journal of the American Society of Hematology*. 2002;100(8):2717-23.
107. Paz-Priel I, Ghosal A, Kowalski J, Friedman A. C/EBP α or C/EBP β oncoproteins regulate the intrinsic and extrinsic apoptotic pathways by direct interaction with NF- κ B p50 bound to the bcl-2 and FLIP gene promoters. *Leukemia*. 2009;23(2):365-74.
108. Vogt M, Domszalai T, Kleshchanok D, Lehmann S, Schmitt A, Poli V, et al. The role of the N-terminal domain in dimerization and nucleocytoplasmic shuttling of latent STAT3. *Journal of cell science*. 2011;124(6):900-9.
109. Redell MS, Ruiz MJ, Gerbing RB, Alonzo TA, Lange BJ, Tweardy DJ, et al. FACS analysis of Stat3/5 signaling reveals sensitivity to G-CSF and IL-6 as a significant prognostic factor in pediatric AML: a Children's Oncology Group report. *Blood, The Journal of the American Society of Hematology*. 2013;121(7):1083-93.
110. Panopoulos AD, Zhang L, Snow JW, Jones DM, Smith AM, El Kasmi KC, et al. STAT3 governs distinct pathways in emergency granulopoiesis and mature neutrophils. *Blood*. 2006;108(12):3682-90.
111. Bowman T, Garcia R, Turkson J, Jove R. STATs in oncogenesis. *Oncogene*. 2000;19(21):2474-88.
112. Stevens AM, Ruiz MJ, Gerbing RB, Alonzo TA, Gamis AS, Redell MS. Ligand-induced STAT3 signaling increases at relapse and is associated with outcome in pediatric acute myeloid leukemia: a report from the Children's Oncology Group. *haematologica*. 2015;100(12):e496.
113. Asano Y, Shibata S, Kobayashi S, Okamura S, Niho Y. Interleukin-10 inhibits the autocrine growth of leukemic blast cells from patients with acute myeloblastic leukemia. *International journal of hematology*. 1997;66(4):445-50.
114. Benekli M, Xia Z, Donohue KA, Ford LA, Pixley LA, Baer MR, et al. Constitutive activity of signal transducer and activator of transcription 3 protein in acute myeloid leukemia blasts is associated with short disease-free survival. *Blood, The Journal of the American Society of Hematology*. 2002;99(1):252-7.

115. Zhang H-F, Lai R. STAT3 in cancer—friend or foe? *Cancers*. 2014;6(3):1408-40.
116. Arnould C, Philippe C, Bourdon V, Grégoire MJ, Berger R, Jonveaux P. The signal transducer and activator of transcription STAT5b gene is a new partner of retinoic acid receptor α in acute promyelocytic-like leukaemia. *Human molecular genetics*. 1999;8(9):1741-9.
117. Dong S, Tweardy DJ. Interactions of STAT5b-RAR α , a novel acute promyelocytic leukemia fusion protein, with retinoic acid receptor and STAT3 signaling pathways. *Blood, The Journal of the American Society of Hematology*. 2002;99(8):2637-46.
118. Arranz L, del Mar Arriero M, Villatoro A. Interleukin-1 β as emerging therapeutic target in hematological malignancies and potentially in their complications. *Blood Reviews*. 2017;31(5):306-17.
119. Weber A, Wasiliew P, Kracht M. Interleukin-1 (IL-1) pathway. *Science signaling*. 2010;3(105):cm1-cm.
120. Martinon F, Burns K, Tschopp J. The inflammasome: a molecular platform triggering activation of inflammatory caspases and processing of proIL- β . *Molecular cell*. 2002;10(2):417-26.
121. Yang C-A, Chiang B-L. Inflammasomes and human autoimmunity: a comprehensive review. *Journal of autoimmunity*. 2015;61:1-8.
122. Freeman LC, Ting JPY. The pathogenic role of the inflammasome in neurodegenerative diseases. *Journal of neurochemistry*. 2016;136:29-38.
123. Song L, Pei L, Yao S, Wu Y, Shang Y. NLRP3 inflammasome in neurological diseases, from functions to therapies. *Frontiers in cellular neuroscience*. 2017;11:63.
124. Chen L, Huang C-F, Li Y-C, Deng W-W, Mao L, Wu L, et al. Blockage of the NLRP3 inflammasome by MCC950 improves anti-tumor immune responses in head and neck squamous cell carcinoma. *Cellular and Molecular Life Sciences*. 2018;75:2045-58.
125. Liu W, Luo Y, Dunn JH, Norris DA, Dinarello CA, Fujita M. Dual role of apoptosis-associated speck-like protein containing a CARD (ASC) in tumorigenesis of human melanoma. *Journal of Investigative Dermatology*. 2013;133(2):518-27.
126. Dinarello CA. Interleukin-1 in the pathogenesis and treatment of inflammatory diseases. *Blood, The Journal of the American Society of Hematology*. 2011;117(14):3720-32.
127. Carey A, Edwards DK, Eide CA, Newell L, Traer E, Medeiros BC, et al. Identification of interleukin-1 by functional screening as a key mediator of

- cellular expansion and disease progression in acute myeloid leukemia. *Cell reports*. 2017;18(13):3204-18.
128. Lo Y-H, Huang Y-W, Wu Y-H, Tsai C-S, Lin Y-C, Mo S-T, et al. Selective inhibition of the NLRP3 inflammasome by targeting to promyelocytic leukemia protein in mouse and human. *Blood, The Journal of the American Society of Hematology*. 2013;121(16):3185-94.
 129. Hamarsheh Sa, Osswald L, Saller BS, Unger S, De Feo D, Vinnakota JM, et al. Oncogenic KrasG12D causes myeloproliferation via NLRP3 inflammasome activation. *Nature communications*. 2020;11(1):1659.
 130. Zhong C, Wang R, Hua M, Zhang C, Han F, Xu M, et al. NLRP3 inflammasome promotes the progression of acute myeloid leukemia via IL-1 β pathway. *Frontiers in Immunology*. 2021;12:661939.
 131. Mitchell K, Barreyro L, Todorova TI, Taylor SJ, Antony-Debré I, Narayanagari S-R, et al. IL1RAP potentiates multiple oncogenic signaling pathways in AML. *Journal of Experimental Medicine*. 2018;215(6):1709-27.
 132. Yasinska IM, Gonçalves Silva I, Sakhnevych SS, Ruegg L, Hussain R, Siligardi G, et al. High mobility group box 1 (HMGB1) acts as an “alarmin” to promote acute myeloid leukaemia progression. *Oncoimmunology*. 2018;7(6):e1438109.
 133. Zhou X, Zhou S, Li B, Li Q, Gao L, Li D, et al. Transmembrane TNF- α preferentially expressed by leukemia stem cells and blasts is a potent target for antibody therapy. *Blood, The Journal of the American Society of Hematology*. 2015;126(12):1433-42.
 134. Saultz JN, Garzon R. Acute myeloid leukemia: a concise review. *Journal of clinical medicine*. 2016;5(3):33.
 135. Assi SA, Imperato MR, Coleman DJ, Pickin A, Potluri S, Ptasinska A, et al. Subtype-specific regulatory network rewiring in acute myeloid leukemia. *Nature genetics*. 2019;51(1):151-62.
 136. Olsson I, Bergh G, Ehinger M, Gullberg U. Cell differentiation in acute myeloid leukemia. *European journal of haematology*. 1996;57(1):1-16.
 137. Breitman T, Selonick SE, Collins SJ. Induction of differentiation of the human promyelocytic leukemia cell line (HL-60) by retinoic acid. *Proceedings of the National Academy of Sciences*. 1980;77(5):2936-40.
 138. Sun G. Treatment of acute promyelocytic leukemia (APL) with all-trans retinoic acid (ATRA): a report of five-year experience. *Zhonghua zhong liu za zhi [Chinese journal of oncology]*. 1993;15(2):125-9.

139. Chim C, Kwong Y, Liang R, Chu Y, Chan C, Chan L, et al. All-trans retinoic acid (ATRA) in the treatment of acute promyelocytic leukemia (APL). *Hematological oncology*. 1996;14(3):147-54.
140. Stein EM, Dinardo CD, Pollyea DA, Fathi AT, Roboz GJ, Altman JK, et al. Enasidenib in mutant-IDH2 relapsed or refractory acute myeloid leukemia (R/R AML): Results of a phase I dose-escalation and expansion study. *American Society of Clinical Oncology*; 2017.
141. DiNardo CD, Stein EM, de Botton S, Roboz GJ, Altman JK, Mims AS, et al. Durable remissions with ivosidenib in IDH1-mutated relapsed or refractory AML. *New England Journal of Medicine*. 2018;378(25):2386-98.
142. Bower H, Andersson TM, Björkholm M, Dickman P, Lambert PC, Derolf ÅR. Continued improvement in survival of acute myeloid leukemia patients: an application of the loss in expectation of life. *Blood cancer journal*. 2016;6(2):e390-e.
143. Burnett A, Wetzler M, Lowenberg B. Therapeutic advances in acute myeloid leukemia. *J Clin Oncol*. 2011;29(5):487-94.
144. Goyal G, Gundabolu K, Vallabhajosyula S, Silberstein PT, Bhatt VR. Reduced-intensity conditioning allogeneic hematopoietic-cell transplantation for older patients with acute myeloid leukemia. *Therapeutic advances in hematology*. 2016;7(3):131-41.
145. de Thé H. Differentiation therapy revisited. *Nature Reviews Cancer*. 2018;18(2):117-27.
146. Thomas D, Majeti R. Biology and relevance of human acute myeloid leukemia stem cells. *Blood, The Journal of the American Society of Hematology*. 2017;129(12):1577-85.
147. Bamezai S, Buske C. Cutting off leukemogenesis: hydra-like plasticity of mature leukemic cells. *Cell Stem Cell*. 2019;25(2):167-8.
148. McKenzie MD, Ghisi M, Oxley EP, Ngo S, Cimmino L, Esnault C, et al. Interconversion between tumorigenic and differentiated states in acute myeloid leukemia. *Cell stem cell*. 2019;25(2):258-72. e9.
149. Ngo S, Oxley EP, Ghisi M, Garwood MM, McKenzie MD, Mitchell HL, et al. Acute myeloid leukemia maturation lineage influences residual disease and relapse following differentiation therapy. *Nature Communications*. 2021;12(1):6546.
150. Ferrara JL, Levine JE, Reddy P, Holler E. Graft-versus-host disease. *The Lancet*. 2009;373(9674):1550-61.

151. Rowe JM. Graft-versus-disease effect following allogeneic transplantation for acute leukaemia. *Best Practice & Research Clinical Haematology*. 2008;21(3):485-502.
152. Hattori N, Nakamaki T. Natural killer immunotherapy for minimal residual disease eradication following allogeneic hematopoietic stem cell transplantation in acute myeloid leukemia. *International Journal of Molecular Sciences*. 2019;20(9):2057.
153. Davidson-Moncada J, Viboch E, Church SE, Warren SE, Rutella S. Dissecting the immune landscape of acute myeloid leukemia. *Biomedicines*. 2018;6(4):110.
154. Reichel J, Chadburn A, Rubinstein PG, Giulino-Roth L, Tam W, Liu Y, et al. Flow sorting and exome sequencing reveal the oncogenome of primary Hodgkin and Reed-Sternberg cells. *Blood, The Journal of the American Society of Hematology*. 2015;125(7):1061-72.
155. Vago L, Gojo I. Immune escape and immunotherapy of acute myeloid leukemia. *The Journal of clinical investigation*. 2020;130(4):1552-64.
156. Chen DS, Mellman I. Oncology meets immunology: the cancer-immunity cycle. *immunity*. 2013;39(1):1-10.
157. Gide TN, Wilmott JS, Scolyer RA, Long GV. Primary and acquired resistance to immune checkpoint inhibitors in metastatic melanoma. *Clinical Cancer Research*. 2018;24(6):1260-70.
158. Dunn GP, Old LJ, Schreiber RD. The three Es of cancer immunoediting. *Annu Rev Immunol*. 2004;22:329-60.
159. Dunn GP, Old LJ, Schreiber RD. The immunobiology of cancer immunosurveillance and immunoediting. *Immunity*. 2004;21(2):137-48.
160. Chester C, Fritsch K, Kohrt HE. Natural killer cell immunomodulation: targeting activating, inhibitory, and co-stimulatory receptor signaling for cancer immunotherapy. *Frontiers in immunology*. 2015;6:601.
161. Janelle V, Rulleau C, Del Testa S, Carli C, Delisle J-S. T-cell immunotherapies targeting histocompatibility and tumor antigens in hematological malignancies. *Frontiers in immunology*. 2020;11:276.
162. Vesely MD, Kershaw MH, Schreiber RD, Smyth MJ. Natural innate and adaptive immunity to cancer. *Annual review of immunology*. 2011;29:235-71.
163. Kim R. Cancer immunoediting: from immune surveillance to immune escape. *Cancer Immunotherapy*. 2007:9-27.

164. Khong HT, Restifo NP. Natural selection of tumor variants in the generation of “tumor escape” phenotypes. *Nature immunology*. 2002;3(11):999-1005.
165. Pitt J, Marabelle A, Eggermont A, Soria J-C, Kroemer G, Zitvogel L. Targeting the tumor microenvironment: removing obstruction to anticancer immune responses and immunotherapy. *Annals of Oncology*. 2016;27(8):1482-92.
166. Fleming V, Hu X, Weber R, Nagibin V, Groth C, Altevogt P, et al. Targeting myeloid-derived suppressor cells to bypass tumor-induced immunosuppression. *Frontiers in immunology*. 2018;9:398.
167. Park S-M, Youn J-I. Role of myeloid-derived suppressor cells in immune checkpoint inhibitor therapy in cancer. *Archives of pharmacal research*. 2019;42:560-6.
168. Chen Y, Song Y, Du W, Gong L, Chang H, Zou Z. Tumor-associated macrophages: an accomplice in solid tumor progression. *Journal of biomedical science*. 2019;26(1):1-13.
169. Yoshimura A, Wakabayashi Y, Mori T. Cellular and molecular basis for the regulation of inflammation by TGF- β . *The journal of biochemistry*. 2010;147(6):781-92.
170. Chow MT, Luster AD. Chemokines in cancer. *Cancer immunology research*. 2014;2(12):1125-31.
171. JMurphy KM, & Weaver, C. . *Janeway's immunobiology*. 9th ed.2017.
172. Jiang X, Wang J, Deng X, Xiong F, Ge J, Xiang B, et al. Role of the tumor microenvironment in PD-L1/PD-1-mediated tumor immune escape. *Molecular cancer*. 2019;18(1):1-17.
173. Lastwika KJ, Wilson III W, Li QK, Norris J, Xu H, Ghazarian SR, et al. Control of PD-L1 expression by oncogenic activation of the AKT–mTOR pathway in non–small cell lung cancer. *Cancer research*. 2016;76(2):227-38.
174. McGowan M, Hoven AS, Lund-Iversen M, Solberg S, Helland Å, Hirsch FR, et al. PIK3CA mutations as prognostic factor in squamous cell lung carcinoma. *Lung Cancer*. 2017;103:52-7.
175. He Y, Sun MM, Zhang GG, Yang J, Chen KS, Xu WW, et al. Targeting PI3K/Akt signal transduction for cancer therapy. *Signal transduction and targeted therapy*. 2021;6(1):425.
176. Bai J, Gao Z, Li X, Dong L, Han W, Nie J. Regulation of PD-1/PD-L1 pathway and resistance to PD-1/PD-L1 blockade. *Oncotarget*. 2017;8(66):110693.

177. Song M, Chen D, Lu B, Wang C, Zhang J, Huang L, et al. PTEN loss increases PD-L1 protein expression and affects the correlation between PD-L1 expression and clinical parameters in colorectal cancer. *PloS one*. 2013;8(6):e65821.
178. Chen J, Jiang C, Jin L, Zhang X. Regulation of PD-L1: a novel role of pro-survival signalling in cancer. *Annals of oncology*. 2016;27(3):409-16.
179. Zerdes I, Wallerius M, Sifakis EG, Wallmann T, Betts S, Bartish M, et al. STAT3 activity promotes programmed-death ligand 1 expression and suppresses immune responses in breast cancer. *Cancers*. 2019;11(10):1479.
180. Curran EK, Godfrey J, Kline J. Mechanisms of immune tolerance in leukemia and lymphoma. *Trends in immunology*. 2017;38(7):513-25.
181. Mussai F, De Santo C, Abu-Dayyeh I, Booth S, Quek L, McEwen-Smith RM, et al. Acute myeloid leukemia creates an arginase-dependent immunosuppressive microenvironment. *Blood, The Journal of the American Society of Hematology*. 2013;122(5):749-58.
182. Wang X, Zheng J, Liu J, Yao J, He Y, Li X, et al. Increased population of CD4⁺ CD25^{high} regulatory T cells with their higher apoptotic and proliferating status in peripheral blood of acute myeloid leukemia patients. *European journal of haematology*. 2005;75(6):468-76.
183. Zhang L, Gajewski TF, Kline J. PD-1/PD-L1 interactions inhibit antitumor immune responses in a murine acute myeloid leukemia model. *Blood, The Journal of the American Society of Hematology*. 2009;114(8):1545-52.
184. Zhou Q, Munger ME, Veenstra RG, Weigel BJ, Hirashima M, Munn DH, et al. Coexpression of Tim-3 and PD-1 identifies a CD8⁺ T-cell exhaustion phenotype in mice with disseminated acute myelogenous leukemia. *Blood, The Journal of the American Society of Hematology*. 2011;117(17):4501-10.
185. Zhang L, Chen X, Liu X, Kline DE, Teague RM, Gajewski TF, et al. CD40 ligation reverses T cell tolerance in acute myeloid leukemia. *The Journal of clinical investigation*. 2013;123(5):1999-2010.
186. Melvold RW, Sticca RP. Basic and tumor immunology: a review. *Surgical oncology clinics of North America*. 2007;16(4):711-35.
187. Benci JL, Xu B, Qiu Y, Wu TJ, Dada H, Twyman-Saint Victor C, et al. Tumor interferon signaling regulates a multigenic resistance program to immune checkpoint blockade. *Cell*. 2016;167(6):1540-54. e12.
188. Mittal D, Gubin MM, Schreiber RD, Smyth MJ. New insights into cancer immunoediting and its three component phases—elimination, equilibrium and escape. *Current opinion in immunology*. 2014;27:16-25.

189. Turati VA, Guerra-Assunção JA, Potter NE, Gupta R, Ecker S, Daneviciute A, et al. Chemotherapy induces canalization of cell state in childhood B-cell precursor acute lymphoblastic leukemia. *Nature cancer*. 2021;2(8):835-52.
190. Ncardia. Pluricyte® Cardiomyocytes & Hamamatsu FDSS/μCell kinetic plate reader 2018 2018 [Available from: https://www.ncardia.com/files/documents/user%20guides/User%20Guide_Pluricyte].
191. Greaves M, Maley CC. Clonal evolution in cancer. *Nature*. 2012;481(7381):306-13.
192. Humbert M, Halter V, Shan D, Laedrach J, Leibundgut EO, Baerlocher GM, et al. Deregulated expression of Kruppel-like factors in acute myeloid leukemia. *Leukemia Research*. 2011;35(7):909-13.
193. Syafruddin SE, Mohtar MA, Wan Mohamad Nazarie WF, Low TY. Two sides of the same coin: the roles of KLF6 in physiology and pathophysiology. *Biomolecules*. 2020;10(10):1378.
194. Sabatino ME, Castellaro A, Racca AC, Carbajosa González S, Pansa MF, Soria G, et al. Krüppel-like factor 6 is required for oxidative and oncogene-induced cellular senescence. *Frontiers in Cell and Developmental Biology*. 2019;7:297.
195. Blankenstein T, Coulie PG, Gilboa E, Jaffee EM. The determinants of tumour immunogenicity. *Nature Reviews Cancer*. 2012;12(4):307-13.
196. Rasaiyaah J, Yong K, Katz DR, Kellam P, Chain BM. Dendritic cells and myeloid leukaemias: plasticity and commitment in cell differentiation. *British Journal of Haematology*. 2007;138(3):281-90.
197. Miao E. Significance of Myeloid Antigen-Presenting Cells. *Immunome Research*. 2022;18(1):1-.
198. Daver N, Garcia-Manero G, Basu S, Boddu PC, Alfayez M, Cortes JE, et al. Efficacy, Safety, and Biomarkers of Response to Azacitidine and Nivolumab in Relapsed/Refractory Acute Myeloid Leukemia: A Nonrandomized, Open-Label, Phase II Study. *Cancer Discovery*. 2019;9(3):370-83.
199. Norde WJ, Maas F, Hobo W, Korman A, Quigley M, Kester MG, et al. PD-1/PD-L1 interactions contribute to functional T-cell impairment in patients who relapse with cancer after allogeneic stem cell transplantation. *Cancer research*. 2011;71(15):5111-22.
200. Vadakekolathu J, Minden MD, Hood T, Church SE, Reeder S, Altmann H, et al. Immune landscapes predict chemotherapy resistance and immunotherapy response in acute myeloid leukemia. *Science Translational Medicine*. 2020;12(546):eaaz0463.

201. Noviello M, Manfredi F, Ruggiero E, Perini T, Oliveira G, Cortesi F, et al. Bone marrow central memory and memory stem T-cell exhaustion in AML patients relapsing after HSCT. *Nature Communications*. 2019;10(1):1065.
202. Goswami M, Gui G, Dillon LW, Lindblad KE, Thompson J, Valdez J, et al. Pembrolizumab and decitabine for refractory or relapsed acute myeloid leukemia. *Journal for immunotherapy of cancer*. 2022;10(1).
203. Goodman LS, Wintrobe MM, Dameshek W, Goodman MJ, Gilman A, McLennan MT. Nitrogen mustard therapy: Use of methyl-bis (beta-chloroethyl) amine hydrochloride and tris (beta-chloroethyl) amine hydrochloride for hodgkin's disease, lymphosarcoma, leukemia and certain allied and miscellaneous disorders. *Journal of the American Medical Association*. 1946;132(3):126-32.
204. Emran TB, Shahriar A, Mahmud AR, Rahman T, Abir MH, Faijanur-Rob-Siddiquee M, et al. Multidrug Resistance in Cancer: Understanding Molecular Mechanisms, Immunoprevention, and Therapeutic Approaches. *Frontiers in Oncology*. 2022:2581.
205. Lo Y-L, Liu Y, Tsai J-C. Overcoming multidrug resistance using liposomal epirubicin and antisense oligonucleotides targeting pump and nonpump resistances in vitro and in vivo. *Biomedicine & Pharmacotherapy*. 2013;67(4):261-7.
206. Watson MB, Lind MJ, Cawkwell L. Establishment of in-vitro models of chemotherapy resistance. *Anti-Cancer Drugs*. 2007;18(7):749-54.
207. Takemura Y, Kobayashi H, Gibson W, Kimbell R, Miyachi H, Jackman AL. The influence of drug-exposure conditions on the development of resistance to methotrexate or ZD1694 in cultured human leukaemia cells. *International journal of cancer*. 1996;66(1):29-36.
208. Oh KT, Baik HJ, Lee AH, Oh YT, Youn YS, Lee ES. The reversal of drug-resistance in tumors using a drug-carrying nanoparticulate system. *International journal of molecular sciences*. 2009;10(9):3776-92.
209. Curiel TJ. Immunotherapy: A useful strategy to help combat multidrug resistance. *Drug Resistance Updates*. 2012;15(1):106-13.
210. O'Donnell JS, Teng MW, Smyth MJ. Cancer immunoediting and resistance to T cell-based immunotherapy. *Nature reviews Clinical oncology*. 2019;16(3):151-67.
211. Collins M, Ling V, Carreno BM. The B7 family of immune-regulatory ligands. *Genome Biology*. 2005;6(6):223.
212. Koeffler HP, Golde DW. Human Myeloid Leukemia Cell Lines: A Review. *Blood*. 1980;56(3):344-50.

213. Chanput W, Peters V, Wichers H. THP-1 and U937 Cells. In: Verhoeckx K, Cotter P, López-Expósito I, Kleiveland C, Lea T, Mackie A, et al., editors. *The Impact of Food Bioactives on Health: in vitro and ex vivo models*. Cham: Springer International Publishing; 2015. p. 147-59.
214. Ferraro F, Miller CA, Christensen KA, Helton NM, O’Laughlin M, Fronick CC, et al. Immunosuppression and outcomes in adult patients with de novo acute myeloid leukemia with normal karyotypes. *Proceedings of the National Academy of Sciences*. 2021;118(49):e2116427118.
215. Chen P-Y, Yen J-H, Kao R-H, Chen J-H. Down-Regulation of the Oncogene PTTG1 via the KLF6 Tumor Suppressor during Induction of Myeloid Differentiation. *PLOS ONE*. 2013;8(8):e71282.
216. DeKelder RC, Lewin B, Lam K, Komeno Y, Yan M, Rundle C, et al. Cooperation between RUNX1-ETO9a and Novel Transcriptional Partner KLF6 in Upregulation of Alox5 in Acute Myeloid Leukemia. *PLOS Genetics*. 2013;9(10):e1003765.
217. Mucenski ML, McLain K, Kier AB, Swerdlow SH, Schreiner CM, Miller TA, et al. A functional c-myb gene is required for normal murine fetal hepatic hematopoiesis. *Cell*. 1991;65(4):677-89.
218. Sumner R, Crawford A, Mucenski M, Frampton J. Initiation of adult myelopoiesis can occur in the absence of c-Myb whereas subsequent development is strictly dependent on the transcription factor. *Oncogene*. 2000;19(30):3335-42.
219. Takao S, Forbes L, Uni M, Cheng S, Pineda JMB, Tarumoto Y, et al. Convergent organization of aberrant MYB complex controls oncogenic gene expression in acute myeloid leukemia. *eLife*. 2021;10:e65905.
220. Ramsay RG, Gonda TJ. MYB function in normal and cancer cells. *Nature Reviews Cancer*. 2008;8(7):523-34.
221. Hoffman-Liebermann B, Liebermann D. Suppression of c-myc and c-myb is tightly linked to terminal differentiation induced by IL6 or LIF and not growth inhibition in myeloid leukemia cells. *Oncogene*. 1991;6(6):903-9.

9. APPENDICES

Appendix 1: Ethics Committee Approval



T.C.
HACETTEPE ÜNİVERSİTESİ
Girişimsel Olmayan Klinik Araştırmalar Etik Kurulu

Sayı : 16969557-2215

Konu : ARAŞTIRMA PROJESİ DEĞERLENDİRME RAPORU

Toplantı Tarihi : 03 ARALIK 2019 SALI
Toplantı No : 2019/28
Proje No : GO 19/1142 (Değerlendirme Tarihi: 03.12.2019)
Karar No : 2019/28-12

Üniversitemiz Kanser Enstitüsü Temel Onkoloji Anabilim Dalı öğretim üyelerinden Prof. Dr. Güneş ESENDAĞLI'nın sorumlu araştırmacı olduğu, Uzm. Bio. Mubaida PARVEEN'in doktora tezi olan, GO 19/1142 kayıt numaralı, "*İmmün-Dirençli Akut Miyeloid Lösemi Hücrelerinin Seçilimi ve Karakterizasyonu- Selection and Characterization of Immune-Resistant Acute Myeloid Leukemia Cells*" başlıklı proje önerisi araştırmacının gerekece, amaç, yaklaşım ve yöntemleri dikkate alınarak incelenmiş olup, 04 Aralık 2019-04 Aralık 2022 tarihleri arasında geçerli olmak üzere etik açıdan **uygun bulunmuştur**. Çalışma tamamlandığında sonuçlarını içeren bir rapor örneğinin Etik Kurulumuza gönderilmesi gerekmektedir.

1. Prof. Dr. Ayşe Lale DOĞAN	(Başkan)	9. Doç. Dr. Fatma Visal OKUR	(Üye)
2. Prof. Dr. Sevdâ F. MÜFTÜOĞLU	(Üye)	İZİNLİ 10. Doç. Dr. Can Ebru KURT	(Üye)
3. Prof. Dr. M. Yıldırım SARI	(Üye)	11. Doç. Dr. H. Hüseyin TURNAGÖL	(Üye)
4. Prof. Dr. Nedret SAULAM	(Üye)	12. Dr. Öğr. Üyesi Özay GÖKÖZ	(Üye)
İZİNLİ			
5. Prof. Dr. Mintaze Kerem GÜNEL	(Üye)	13. Dr. Öğr. Üyesi Müge DEMİR	(Üye)
6. Prof. Dr. Oya Nuran EMİROĞLU	(Üye)	14. Öğr. Gör. Dr. Meltem ŞENGELEN	
7. Prof. Dr. M. Özgür UYANIK	(Üye)	15. Av. Meltem ONURLU	(Üye)
8. Doç. Dr. Gözde GİRGİN	(Üye)		

Tarih: 14/02/2023 14:21
Sayı: E-16969/23-000/01/34
0000265094



0000265094

HACETTEPE ÜNİVERSİTESİ
GİRİŞİMSEL OLMAYAN KLİNİK ARAŞTIRMALAR ETİK KURULU

KURUL KARARI

OTURUM TARİHİ	OTURUM SAYISI	KARAR SAYISI
07.02.2023	2023/02	2023/02-02
Araştırma Numarası : GO 23/52		Değerlendirme Tarihi : 07.02.2023

Üniversitemiz Tıp Fakültesi Temel Onkoloji Anabilim Dalı öğretim üyelerinden Prof. Dr. Güneş ESENDAĞLI'nın sorumlu araştırmacı olduğu, Prof. Dr. Ayşegül ÜNER, Uzm. Bio. Mubaida PARVEEN ile birlikte çalışacakları, GO 23/52 kayıt numaralı "*Akut Lösemide Transkripsiyon Faktörlerinin Nükleer Translokasyon Düzeyinin Araştırılması*" başlıklı araştırma önerisi gerekçe, amaç, yaklaşım ve yöntemleri dikkate alınarak incelenmiş olup, 01 Ocak 2010 – 31 Aralık 2016 tarihleri arasındaki arşiv kayıtlarının 08 Şubat 2023 – 08 Şubat 2024 tarihleri arasında geçerli olmak üzere etik açıdan **uygun bulunmuştur**.

Çalışma tamamlandığında sonuçlarını içeren bir rapor örneğinin Etik Kurulumuza gönderilmesi gerekmektedir.

İZİNLİ

Prof. Dr. Nüket
PAKSOY ERBAYDAR
Kurul Başkanı

Prof. Dr. Güzide Burça
AYDIN
Kurul Üyesi

Prof. Dr. Mehmet Özgür
UYANIK
Kurul Üyesi

Prof. Dr. Ayşe KİN
İŞLER
Kurul Üyesi

Prof. Dr. Sibel
PEHLİVAN
Kurul Üyesi

Prof. Dr. Burcu Balam
DOĞU
Kurul Üyesi

Prof. Dr. Tolga
YILDIRIM
Kurul Üyesi

Prof. Dr. Hande GÜNEY
DENİZ
Kurul Üyesi

Doç. Dr. Betül ÇELEBİ
SALTİK
Kurul Üyesi

Doç. Dr. Merve BATUK
Kurul Üyesi

Doç. Dr. Gülten IŞIK
KOÇ
Kurul Üyesi

Dr. Öğr. Üyesi Müge
DEMİR
Kurul Üyesi

Dr. Öğr. Üyesi Burcu
Ersöz ALAN
Kurul Üyesi

Av. Buket ÇINAR
Kurul Üyesi

Evrakın elektronik imzalı suretine <https://www.turkiye.gov.tr/hu-ebys> adresinden e84d40bd-e0e7-4250-bc6d-f7a1bba624d9 k
Bu belge 5070 sayılı Elektronik İmza Kanunu'na uygun olarak Güvenli Elektronik İmza ile imzalanmıştır.

Appendix 2: Scientific meetings where the data of this thesis were presented

Poster Presentation:

Parveen M., Esendagli G. (2019). Repeated encounter with activated PBMC mediates the progression of Immune resistance in THP-1 myeloid leukemia cells. **International Molecular Immunology & Immunogenetics Congress (MIMIC-IV)**. Bursa/ Türkiye. **P-A59**.

Parveen M., Esendagli G. (2020). Immunoresistance in AML. **6th Black Sea International Immunology School. Teteven/Bulgaria**.

Parveen M., Esendagli G. (2020). Periferik kan mononükleer hücreleri ile ko-kültür edilen AML hücrelerinde immün direnç mekanizmasının uyarılması ve t lenfositler üzerine etkisi. **XXV Ulusal İmmunoloji kongresi**. İstanbul/ Türkiye. **PS-079**.

Parveen M., Esendagli G. (2021). Invoking immune resistance in acute myeloid leukemia (AML) cells through ex-vivo allogeneic immune reactions. **6th European Congress of Immunology**. Belgrade/ Serbia. **P-0467**.

Parveen M., Esendagli G., Karaosmanoglu B., Taskiran Z E., Sucularli C. (2022). Immune- resistance patterns in Acute Myeloid Leukemia. **5th International Molecular Immunology & Immunogenetics Congress (MIMIC-V)**. İzmir/Türkiye. **PP-24**.

Parveen M., Esendagli G., Karaosmanoglu B., Taskiran Z E. (2023). Beta-2-microglobulin (β 2M): A prognostic marker for immune responsiveness in Acute Myeloid Leukemia. **XXVI. Ulusal İmmunoloji kongresi**. Ankara/Türkiye. **P-026**.

Appendix 3: Thesis Originality Report

Full title of thesis: Selection and Charaterization of Immune- Resistant Acute Myeloid Leukemia Cells

Student's name and surname: Mubaida Parveen

Total number of pages of the file:174

THESIS FINAL

ORIGINALITY REPORT

5%

SIMILARITY INDEX

2%

INTERNET SOURCES

4%

PUBLICATIONS

1%

STUDENT PAPERS

PRIMARY SOURCES

1

coek.info

Internet Source

<1 %

2

www.frontiersin.org

Internet Source

<1 %

3

www.science.gov

Internet Source

<1 %

4

Submitted to Grand Canyon University

Student Paper

<1 %

5

Mohsen Alizadeh, Ali Safarzadeh, Seyed Ali Hoseini, Reza Piryaee et al. "The potentials of immune checkpoints for the treatment of blood malignancies", Critical Reviews in Oncology/Hematology, 2020

Publication

<1 %

6

T Braun, G Carvalho, C Fabre, J Grosjean, P Fenaux, G Kroemer. "Targeting NF-κB in hematologic malignancies", Cell Death & Differentiation, 2006

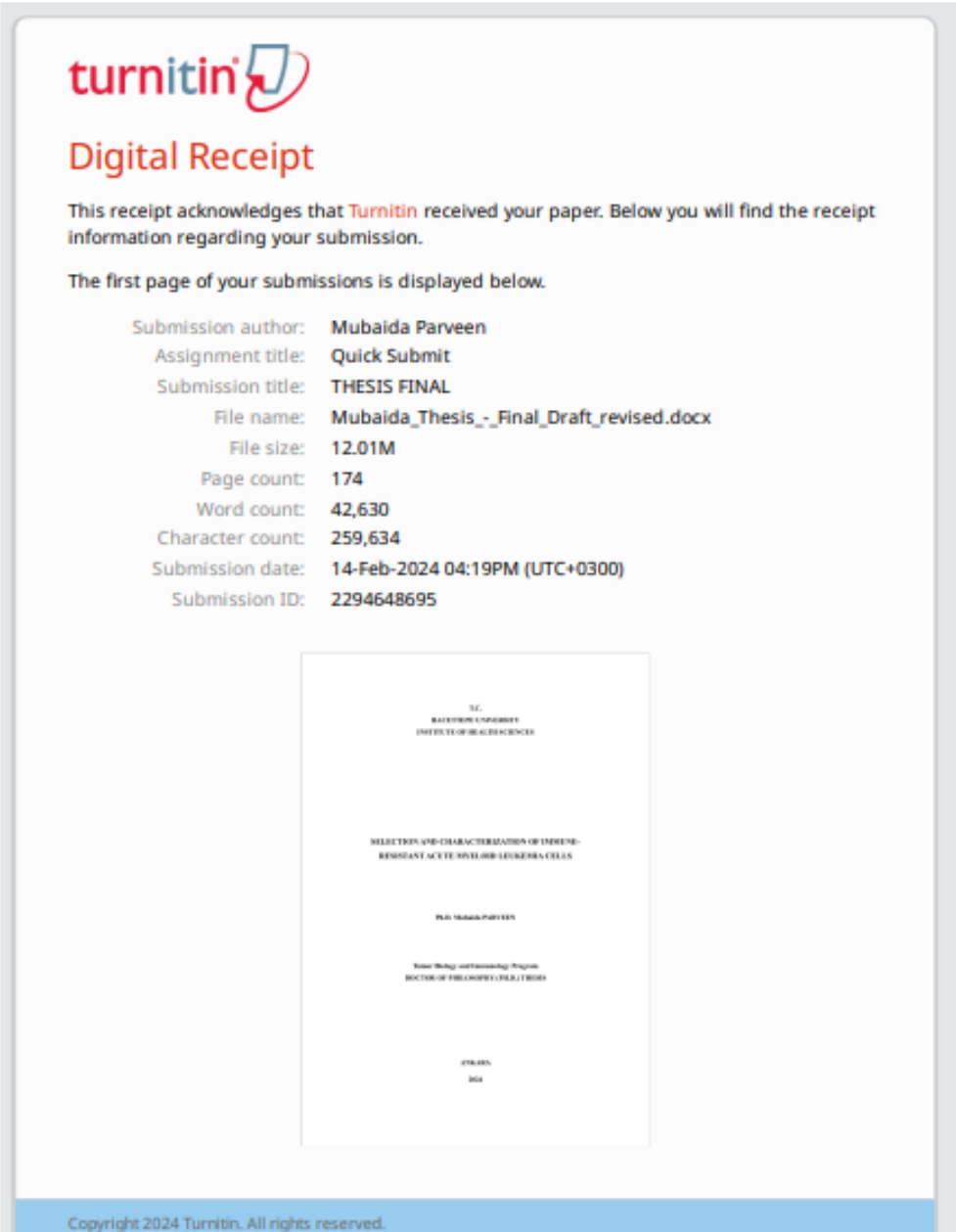
Publication

<1 %

7

Submitted to Universiti Putra Malaysia

Appendix 4: Digital Receipt



The image shows a digital receipt from Turnitin. At the top left is the Turnitin logo. Below it is the title "Digital Receipt" in a large, bold, orange font. A paragraph of text explains that the receipt acknowledges the submission of a paper and that submission information is provided below. Another paragraph states that the first page of the submission is displayed. This is followed by a list of submission details: author (Mubaida Parveen), assignment title (Quick Submit), submission title (THESIS FINAL), file name (Mubaida_Thesis_-_Final_Draft_revised.docx), file size (12.01M), page count (174), word count (42,630), character count (259,634), submission date (14-Feb-2024 04:19PM (UTC+0300)), and submission ID (2294648695). Below this list is a preview of the first page of the document, which is a title page for a thesis. The title page text includes the author's name, the title "SELECTION AND CHARACTERIZATION OF IMMUNE-RESISTANT ACUTE MYELOID LEUKEMIA CELLS", the author's name "MUBAIDA PARVEEN", the department "Bioscience and Technology Program", and the institution "UNIVERSITY OF CALicut". At the bottom of the receipt, there is a blue bar with the text "Copyright 2024 Turnitin. All rights reserved."

turnitin

Digital Receipt

This receipt acknowledges that Turnitin received your paper. Below you will find the receipt information regarding your submission.

The first page of your submissions is displayed below.

Submission author: **Mubaida Parveen**
Assignment title: **Quick Submit**
Submission title: **THESIS FINAL**
File name: **Mubaida_Thesis_-_Final_Draft_revised.docx**
File size: **12.01M**
Page count: **174**
Word count: **42,630**
Character count: **259,634**
Submission date: **14-Feb-2024 04:19PM (UTC+0300)**
Submission ID: **2294648695**

SE
BIO SCIENCE PROGRAM
UNIVERSITY OF CALICUT

SELECTION AND CHARACTERIZATION OF IMMUNE-
RESISTANT ACUTE MYELOID LEUKEMIA CELLS

MUBAIDA PARVEEN

Bioscience and Technology Program
UNIVERSITY OF CALICUT

UNIVERSITY OF CALICUT

2024

Copyright 2024 Turnitin. All rights reserved.

10. CURRICULAM VITAE

Name: Mubaida Parveen